frontiers | Research Topics

Interaction between marine invertebrates and symbiotic microbes in a changing environment: Community structure and ecological functions

Edited by
Jie Li, Yang Zhang, Jin Sun, Fabiano Thompson and Yanying Zhang

Published in
Frontiers in Marine Science
Frontiers in Microbiology

ISSN 1664-8714
ISBN 978-2-83251-464-1
DOI 10.3389/978-2-83251-464-1

About Frontiers

Frontiers is more than just an open access publisher of scholarly articles: it is a pioneering approach to the world of academia, radically improving the way scholarly research is managed. The grand vision of Frontiers is a world where all people have an equal opportunity to seek, share and generate knowledge. Frontiers provides immediate and permanent online open access to all its publications, but this alone is not enough to realize our grand goals.

Frontiers journal series

The Frontiers journal series is a multi-tier and interdisciplinary set of open-access, online journals, promising a paradigm shift from the current review, selection and dissemination processes in academic publishing. All Frontiers journals are driven by researchers for researchers; therefore, they constitute a service to the scholarly community. At the same time, the *Frontiers journal series* operates on a revolutionary invention, the tiered publishing system, initially addressing specific communities of scholars, and gradually climbing up to broader public understanding, thus serving the interests of the lay society, too.

Dedication to quality

Each Frontiers article is a landmark of the highest quality, thanks to genuinely collaborative interactions between authors and review editors, who include some of the world's best academicians. Research must be certified by peers before entering a stream of knowledge that may eventually reach the public - and shape society; therefore, Frontiers only applies the most rigorous and unbiased reviews. Frontiers revolutionizes research publishing by freely delivering the most outstanding research, evaluated with no bias from both the academic and social point of view. By applying the most advanced information technologies, Frontiers is catapulting scholarly publishing into a new generation.

What are Frontiers Research Topics?

Frontiers Research Topics are very popular trademarks of the *Frontiers journals series*: they are collections of at least ten articles, all centered on a particular subject. With their unique mix of varied contributions from Original Research to Review Articles, Frontiers Research Topics unify the most influential researchers, the latest key findings and historical advances in a hot research area.

Find out more on how to host your own Frontiers Research Topic or contribute to one as an author by contacting the Frontiers editorial office: frontiersin.org/about/contact

Interaction between marine invertebrates and symbiotic microbes in a changing environment: Community structure and ecological functions

Topic editors

Jie Li — South China Sea Institute of Oceanology, Chinese Academy of Sciences (CAS), China

Yang Zhang — South China Sea Institute of Oceanology, Chinese Academy of Sciences (CAS), China

Jin Sun — Ocean University of China, China

Fabiano Thompson — Federal University of Rio de Janeiro, Brazil

Yanying Zhang — Yantai University, China

Citation

Li, J., Zhang, Y., Sun, J., Thompson, F., Zhang, Y., eds. (2023). *Interaction between marine invertebrates and symbiotic microbes in a changing environment: Community structure and ecological functions*. Lausanne: Frontiers Media SA. doi: 10.3389/978-2-83251-464-1

Table of contents

frontiers | Frontiers in Marine Science

TYPE Editorial
PUBLISHED 12 January 2023
DOI 10.3389/fmars.2022.1128906

OPEN ACCESS

EDITED AND REVIEWED BY
M Pilar Francino,
Fundación para el Fomento de la Investigación Sanitaria y Biomédica de la Comunitat Valenciana (FISABIO), Spain

*CORRESPONDENCE
Jie Li
lijietaren@scsio.ac.cn

SPECIALTY SECTION
This article was submitted to Microbial Symbioses, a section of the journal Frontiers in Marine Science

RECEIVED 21 December 2022
ACCEPTED 29 December 2022
PUBLISHED 12 January 2023

CITATION
Li J, Zhang Y, Sun J, Thompson F and Zhang Y (2023) Editorial: Interaction between marine invertebrates and symbiotic microbes in a changing environment: Community structure and ecological functions.
Front. Mar. Sci. 9:1128906.
doi: 10.3389/fmars.2022.1128906

Editorial: Interaction between marine invertebrates and symbiotic microbes in a changing environment: Community structure and ecological functions

Jie Li[1]*, Yang Zhang[1], Jin Sun[2], Fabiano Thompson[3] and Yanying Zhang[4]

[1]CAS Key Laboratory of Tropical Marine Bio-resources and Ecology, South China Sea Institute of Oceanology, Chinese Academy of Sciences, Guangzhou, China, [2]Institute of Evolution & Marine Biodiversity, Ocean University of China, Qingdao, China, [3]Institute of Biology and COPPE, Federal University of Rio de Janeiro, Rio de Janeiro, Brazil, [4]School of Ocean, Yantai University, Yantai, China

KEYWORDS

marine invertebrates, symbiotic microbes, microbial community structure, environmental disturbance, co-evolution

Editorial on the Research Topic
Interaction between marine invertebrates and symbiotic microbes in a changing environment: Community structure and ecological functions

Symbiotic associations between marine invertebrates and microbes have been found in various ecosystems ranging from coral reefs (Figure 1) in shallow coastal waters to hydrothermal vents and cold seeps in the deep sea. Marine organisms surviving in diverse environments depend to a large extent or completely on symbiotic microbes (Dubilier et al., 2008). Symbiotic relationships between microorganisms and their marine invertebrate hosts are continuously formed and co-evolved with a long-term history that impacts morphology, behavior, development, metabolism, and even evolution (McFall-Ngai et al., 2013; Gould et al., 2018). In addition to organismal adaptation and evolution, symbioses between marine invertebrates and microbes underpin the health of marine ecosystems, especially the most threatened ecosystems (Wilkins et al., 2019). In the face of global climate change and the Anthropocene, it is essential to understand the interaction between marine invertebrates and symbiotic microbes in a changing environment to predict whether symbiosis will allow marine life to cope with future threats to the biosphere (Li et al., 2022). Given the significance of symbiosis between marine invertebrates and microbes, this Research Topic aims to contribute to a better understanding of the community structure and function of marine invertebrate-associated microbes and the interaction between marine invertebrates and their symbiotic microbes in a changing environment.

Dynamic marine invertebrate-associated microbial communities have been largely observed in response to environmental disturbance as well as the physiological and developmental status of their hosts (Webster and Taylor, 2012; Apprill; van Oppen and

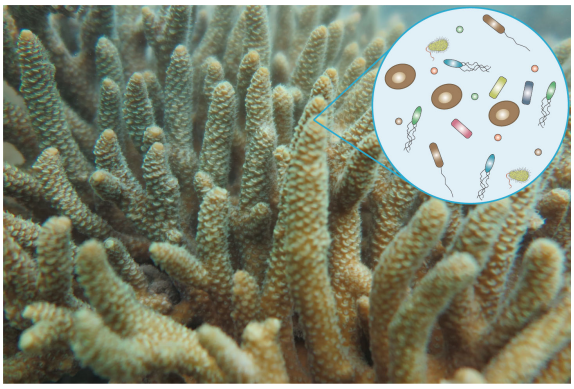

FIGURE 1
A typical case of symbioses between marine invertebrates and microbes: Coral and its associated microorganisms.

Blackall, 2019; Carrier and Bosch, 2022). The flexibility of symbioses between marine invertebrates and microbes has been considered to be crucial for host health and fitness (Reshef et al., 2006; Apprill, 2020). To explore how plastic coral-associated microbial communities are in response to environmental variation, Haydon et al. reciprocally transplanted the coral *Pocillopora acuta* between a mangrove lagoon and an adjacent reef crest-slope on the northern Great Barrier Reef and investigated the bacterial and Symbiodiniaceae communities associated with the transplanted coral specimens. The results demonstrated obvious changes in the bacterial communities. These shifts were distinct between the reef-to-mangrove and mangrove-to-reef transplanted corals. The Symbiodiniaceae communities remain highly stable. Scleractinian corals, whose food source mainly comes from the photosynthesis of algal symbionts, are principal coral reef-builders. Scientists recently found that sponges are the major reef epifauna in a newly recognized biogenic reef system, the Great Amazon Reef System, which stays under a plume layer (Moura et al., 2016; Francini-Filho et al.; de Menezes et al., 2022). Pinto et al. found that plume-associated dissolved and particulate organic carbon (originating from the Amazon forest) and the heterotrophic microbiota associated with sponges may support host survival in an environment with attenuated light availability.

Salinity is one of the important drivers of microbial distribution (Lozupone and Knight, 2007). To explore the effects of changes in salinity on host-protected microbiomes, Kivistik et al. investigated the bacterial communities within the gastrointestinal tract of *Ampullaceana balthica* in different salinities. The results showed a high mortality rate of *A. balthica* after a shift from freshwater to salinity 6, along with altered gastrointestinal bacterial communities. There was a substantial difference between the bacterial communities in aquaria and *in situ* at salinity 6. Kivistik et al. further suggested that the intestinal microbiome needs long-term adaptation to higher salinity. Microbiomes associated with aquatic animals have received increasing attention. Haditomo et al. found alterations in the gut bacterial composition of sea urchins *Mesocentrotus nudus* and *Strongylocentrotus intermedius* after rearing in an aquarium with circulating and running water. In addition, the results of the transplanting experiment further revealed that these gut microbiota were affected by diet rather than rearing environment and host species. Furthermore, Haditomo et al. proposed that the gut microbiome reduces nitrates to ammonium to promote sea urchin growth. Increasing evidence supports the importance of pioneer microbes in early life stages in host biology (Korpela and de Vos, 2018; Fallet et al., 2022). To understand the pioneer microbiota of sea cucumber, Yu et al. investigated the bacterial communities in the early life stages of *Apostichopus japonicus*. The results demonstrated significant changes in the microbiota in the late auricularia stage and possible first colonizers in the gut affiliated with *Rhodobacterales* and *Flavobacterales*. On the basis of the dynamic changes in the bacterial community alongside the developmental stages and feeding time, Yu et al. suggested that organogenesis and feeding are major drivers of variation in early life microbiota in sea cucumber.

Exploring the evolution of the physiological and genomic properties of microbes associated with marine invertebrates is helpful for understanding their roles in symbioses. Jiang et al. compared the genomes of type strains of Halioticoli clade species in Vibrionaceae with different lifestyles and found more carbohydrate metabolism-related genes in the genome of free-living *Vibrio ishigakensis* compared to host-associated lineages. Guo et al. demonstrated a more complex antagonistic network among coral-associated bacteria at 32°C than at 25°C and proposed that the trade-off between antagonism and resource exploitation shifted in the antagonistic interactions under varied environmental temperatures.

A phylosymbiotic signal, i.e., the degree of similarity between microbial communities reflecting the evolutionary history of their hosts, has been observed in many hosts and their symbiotic microbiomes (Lim and Bordenstein, 2020). On the basis of the differential bacterial communities associated with two *Aurelia* polyp species, Li et al. proposed a correlation between the symbiotic microbial community and their host genetic background though they did not refer to the concept of phylosymbiosis. Co-evolutionary patterns may be affected by both horizontally and vertically transmitted microbes. Wale et al. summarized the vertical and horizontal transmission of the microbiome in crab larval stages and speculated that symbiotic microbiomes facilitate the transition of crabs from living in water to land. The authors further proposed that the integration of the early life history stages of crabs and their microbiomes is a crucial paradigm for the evolution of terrestrialization in crabs.

This Research Topic provides a glimpse of host-microbe interactions and possible examples of co-evolution that demonstrate the immense potential of the global marine biodiversity for discoveries. In addition, studies have shown the dynamic microbiomes associated with the developmental stages of marine invertebrates, e.g., in the case of the sea cucumber *A. japonicus* and its associated microbiome. Moreover, the impacts of altered environments because of both local and global changes are possibly altering microbial communities associated with marine invertebrates and the potential functions of microbial symbionts. We advocate that the phylosymbiosis and co-evolution of marine invertebrate hosts and their symbiotic microbiome are worth further investigation. Currently, we know much about the community compositions of microbial symbionts under various environmental conditions. However, we know far less regarding the mechanistic connections between the microbiome and its host at micro-spatial and short-term

time scales, as well as *in situ* microbial activities and interactions within holobionts. Approaches that combine imaging technologies with metabolic activity detection and single-cell and (meta)genomic/transcriptomic sequencing will facilitate addressing these questions in the not-too-distant future.

Author contributions

JL drafted the editorial. All authors reviewed and edited the editorial. All authors contributed to the article and approved the submitted version.

Acknowledgments

The authors are grateful to the Frontiers in Microbiology and Frontiers in Marine Science editorial staff, especially Nina Hall, Talitha Gray, Chao Xiao, Alice Lickley and Emily Keynton, for their initial invitation and professional support.

Conflict of interest

The authors declare that the research was conducted in the absence of any commercial or financial relationships that could be construed as a potential conflict of interest.

Publisher's note

References

Apprill, A. (2020). The role of symbioses in the adaptation and stress responses of marine organisms. *Annu. Rev. Mar. Sci.* 12, 291–314. doi: 10.1146/annurev-marine-010419-010641

Carrier, T. J., and Bosch, T. C. G. (2022). Symbiosis: The other cells in development. *Development* 149, dev200797. doi: 10.1242/dev.200797

de Menezes, T. A., de Freitas, M. A. M., Lima, M. S., Soares, A. C., Leal, C., Busch, M. S., et al. (2022). Fluxes of the Amazon river plume nutrients and microbes into marine sponges. *Sci. Total. Environ.* 847, 157474. doi: 10.1016/j.scitotenv.2022.157474

Dubilier, N., Bergin, C., and Lott, C. (2008). Symbiotic diversity in marine animals: The art of harnessing chemosynthesis. *Nat. Rev. Microbiol.* 6, 725–740. doi: 10.1038/nrmicro1992

Fallet, M., Montagnani, C., Petton, B., Dantan, L., de Lorgeril, J., Comarmond, S., et al. (2022). Early life microbial exposures shape the crassostrea gigas immune system for lifelong and intergenerational disease protection. *Microbiome* 10, 1–21. doi: 10.1186/s40168-022-01280-5

Gould, A. L., Zhang, V., Lamberti, L., Jones, E. W., Obadia, B., Korasidis, N., et al. (2018). Microbiome interactions shape host fitness. *Proc. Natl. Acad. Sci. U.S.A.* 115, 11951–11960. doi: 10.1073/pnas.1809349115

Korpela, K., and de Vos, W. M. (2018). Early life colonization of the human gut: Microbes matter everywhere. *Curr. Opin. Microbiol.* 44, 70–78. doi: 10.1016/j.mib.2018.06.003

Lim, S. J., and Bordenstein, S. R. (2020). An introduction to phylosymbiosis. *Proc. R. Soc B* 287, 20192900. doi: 10.1098/rspb.2019.2900

Li, J., Yang, Q., Dong, J., Sweet, M., Zhang, Y., Liu, C., et al. (2022). Microbiome engineering: A promising approach to improve coral health. *Engineering* doi: 10.1016/j.eng.2022.07.010

Lozupone, C. A., and Knight, R. (2007). Global patterns in bacterial diversity. *Proc. Natl. Acad. Sci. U.S.A.* 104, 11436–11440. doi: 10.1073/pnas.0611525104

McFall-Ngai, M., Hadfield, M. G., Bosch, T. C. G., Carey, H. V., Domazet-Lošo, T., Douglas, A. E., et al. (2013). Animals in a bacterial world, a new imperative for the life sciences. *Proc. Natl. Acad. Sci. U.S.A.* 110, 3229–3236. doi: 10.1073/pnas.1218525110

Moura, R. L., Amado-Filho, G. M., Moraes, F. C., Brasileiro, P. S., Salomon, P. S., Mahiques, M. M., et al. (2016). An extensive reef system at the amazon river mouth. *Sci. Adv.* 2, e1501252. doi: 10.1126/sciadv.1501252

Reshef, L., Koren, O., Loya, Y., Zilber-Rosenberg, I., and Rosenberg, E. (2006). The coral probiotic hypothesis. *Environ. Microbiol.* 8, 2068–2073. doi: 10.1111/j.1462-2920.2006.01148.x

van Oppen, M. J. H., and Blackall, L. L. (2019). Coral microbiome dynamics, functions and design in a changing world. *Nat. Rev. Microbiol.* 17, 557–567. doi: 10.1038/s41579-019-0223-4

Webster, N. S., and Taylor, M. W. (2012). Marine sponges and their microbial symbionts: Love and other relationships. *Environ. Microbiol.* 14, 335–346. doi: 10.1111/j.1462-2920.2011.02460.x

Wilkins, L. G. E., Leray, M., O'Dea, A., Yuen, B., Peixoto, R. S., Pereira, T. J., et al. (2019). Host-associated microbiomes drive structure and function of marine ecosystems. *PloS Biol.* 17, e3000533. doi: 10.1371/journal.pbio.3000533

frontiers in Microbiology

OPINION
published: 15 October 2021
doi: 10.3389/fmicb.2021.770245

The Importance of Larval Stages for Considering Crab Microbiomes as a Paradigm for the Evolution of Terrestrialization

Matthew Wale[1]*, *Daniele Daffonchio*[2], *Marco Fusi*[1], *Ramona Marasco*[2], *Elisa Garuglieri*[2] *and Karen Diele*[1]*

[1] School of Applied Sciences, Edinburgh Napier University, Edinburgh, United Kingdom, [2] Red Sea Research Center, King Abdullah University of Science and Technology, Thuwal, Saudi Arabia

Keywords: terrestrial crabs, symbiotic microbiota, hologenome theory, microbiome transmission, larval development

OPEN ACCESS

Edited by:
Jin Sun,
Ocean University of China, China

Reviewed by:
Tyler J. Carrier,
GEOMAR Helmholtz Center for Ocean Research Kiel, Germany
Ariadne Hernández-Pérez,
National Autonomous University of Mexico, Mexico

***Correspondence:**
Matthew Wale
m.wale@napier.ac.uk
Karen Diele
k.diele@napier.ac.uk

Specialty section:
This article was submitted to Microbial Symbioses, a section of the journal Frontiers in Microbiology

Received: *03 September 2021*
Accepted: *15 September 2021*
Published: *15 October 2021*

Citation:
Wale M, Daffonchio D, Fusi M, Marasco R, Garuglieri E and Diele K (2021) The Importance of Larval Stages for Considering Crab Microbiomes as a Paradigm for the Evolution of Terrestrialization. Front. Microbiol. 12:770245. doi: 10.3389/fmicb.2021.770245

INTRODUCTION

The transition from an aquatic to a terrestrial lifestyle has evolved multiple times, and in numerous different phyla, in earth's history. In many crab species, this process is still underway (Bliss and Mantel, 1968), providing a unique opportunity to study the evolution of terrestrialization, as well as the role of associated microbiomes during this process (Cannicci et al., 2020). Recently, Cannicci et al. (2020) reported on the potential importance of microbiomes in the transition of crabs, formally wholly aquatic species, to life, fully or in part, in terrestrial environments. The authors argue that symbiotic bacteria, such as those of gill and gut microbiomes, may play a key role in easing this transition, by helping crabs to overcome physiological and morphological challenges associated with conquering the terrestrial environment, such as impaired respiration and osmotic regulation, and a new, often primary plant-based low nitrogen diet. Here we focus on the microbiomes of crab larvae and their potential role for the evolution of terrestrialization.

Crabs that are transitioning to life on land fall into two broad categories: terrestrial species that spend their whole adult life (except for larval release) on land independent of tidal inundation or freshwater bodies, and semi-terrestrial species that spend their adult life on land but are dependent on tidal inundation or freshwater (Burggren and McMahon, 1988; Anger, 1995). Many marine organisms form symbiotic relationships with microorganisms to aid life in extreme environments (Sogin et al., 2020). In line with the hologenome theory, this suggests that host-microbe interactions play an important role in an organism's evolution, where the genes of both the host and its microbes co-evolve in the collective "holobiont" (Zilber-Rosenberg and Rosenberg, 2008), potentially allowing the colonization of formerly hostile environments (Bang et al., 2018). Microbial symbionts, as individual species or in mixed-species assemblages, are present in many crustaceans, such as the marine isopod *Idotea balthica* (diet-specific gut microbiomes, Mattila et al., 2014), the intertidal brachyuran crab *Eriocheir sinensis* (gill and gut microbiomes, Zhang et al., 2016), and the freshwater signal crayfish *Pacifastacus leniusculus* (intestinal bacteria, Hernández-Pérez et al., 2021). Given that microbial assemblages are often specific to certain organs of their hosts (Chomicki et al., 2020), symbioses have likely evolved in support of a specific function.

The microbial assemblages associated with the guts of semi-terrestrial crabs have been proposed to aid in the adaptation of a low nitrogen, herbivorous diet during terrestrialization (Bui and Lee, 2015), like microbial assemblages of other aquatic invertebrates, e.g., isopods, where they enable the digestion of cellulose (Zimmer et al., 2002; O'Connor et al., 2014). The bacteria specifically associated with crab gills (Zhang et al., 2016, 2017) may facilitate ammonia excretion

(Weihrauch et al., 2004), utilize gaseous CO_2 (Morris, 2001), and buffer exposure to oxygen, which occurs at a concentration 30 times higher (Hsia et al., 2013) in the terrestrial compared to the marine environment where the host organism evolved. The microbiomes of both gut and gills could therefore provide terrestrial and semi-terrestrial crabs (here collectively called semi-/terrestrial) with means to cope with life in marine as well as in terrestrial environments. Whilst the presence of microbiomes and their role in buffering the stresses imposed on crabs by terrestrialization is beginning to be discussed (Bui and Lee, 2015; Cannicci et al., 2020), there are many unknowns. For example, the mode of bacterial acquisition, bacterial diversity, topological association, and the precise functions of their organ-specific microbial assemblages are still poorly understood, both for adult semi-/terrestrial crabs and their early life stages.

Most semi-/terrestrial crab species, like their aquatic counterparts, have a biphasic life cycle including fully aquatic larvae, via which they transition to semi-/terrestrial juvenile/adult life (Anger, 1995; Hartnoll et al., 2014). Understanding microbial colonization of the larvae would likely provide critical insights into how these crabs have been able to move from water to land, and whether the bacteria themselves facilitate this transition.

LARVAE, THE VECTOR BETWEEN WATER AND LAND, AND THEIR POTENTIAL MICROBIOME ACQUISITION PATHWAYS

Most semi-/terrestrial crab species are broadcast spawners with pelagic larvae that develop for 3–6 weeks in the marine environment (Bliss and Mantel, 1968; Anger, 1995), undergoing multiple zoeal stages and one megalopal stage, mirroring the life history characteristics of fully aquatic crabs. In some semi-/terrestrial species, larval development is abbreviated (Anger, 1995; González-Gordillo et al., 2010; Vogt, 2013) and/or maternal brood care increased. For example, the larvae of the fiddler crab *Uca subcylindrica*, a species adapted to semiarid habitats, develop inside non-permanent water bodies to megalopae within as little as 2.5 days (Rabalais and Cameron, 1983). The Jamaican freshwater bromeliad crab *Metopaulias depressus* also undergoes abbreviated development; its larvae are released into phytothelmes and are actively guarded by their mothers (Diesel, 1989; Diesel and Schuh, 1993). Semi-/terrestrial crabs with larvae that (still) need to develop in the sea act as vectors at the marine-terrestrial interface. Some species travel considerable distances over land from their inland habitats to the coast, e.g., the inland forest-dwelling Christmas Island crab *Gecarcoidea natalis* travels up to 4 km (Adamczewska and Morris, 2001) to release its larvae into the sea. In the sea, the offspring of semi-/terrestrial crabs are preyed upon by aquatic predators and consume plankton to acquire biomass that is brought back to the land when the megalopae settle and metamorphose into the benthic juvenile stage. Hence, semi-/terrestrial crab larvae are couplers of nutrients, and likely microbiomes, between aquatic and terrestrial ecosystems, with each successive generation having to make the transition from a life in water to a life on land. If, as recently suggested (Cannicci et al., 2020), symbiotic microbiomes facilitate the evolution from an aquatic to a terrestrial life, then these larval stages provide a unique opportunity to explore this transition firsthand.

Bacterial colonization of marine invertebrate larvae has been evidenced as an essential step in their adaptation to specific, often extreme, environments. For example, once settled, the larvae and juveniles of the gutless giant tube worm *Riftia* spp. are colonized by sulfur-oxidizing bacteria (Nussbaumer et al., 2006). Their acquisition promotes developmental changes in the juvenile worm, including the growth of specific tissues for the bacteria to colonize. The endosymbiotic bacteria within these tissues facilitate sulfur-oxidation (Minic and Hervé, 2004), allowing the worms to survive in hydrothermal vent ecosystems. In some species, such as the sponge *Amphimedon queenslandica*, settlement and metamorphosis to benthic juvenile stage are facilitated by the larvae's microbiota (Song et al., 2021). These vertically acquired symbiotic bacteria produce arginine, the substrate needed for nitric oxide synthesis and the signal that regulates settlement and metamorphosis in many invertebrate species. Bacterial colonization plays a key role in the larvae of the intertidal barnacle *Semibalanus balanoides,* which are colonized during the settlement phase of the cyprid stage. The cypris' microbiome composition changes upon settlement, with potential implications for growth and survival during the barnacle's benthic life stage (Aldred and Nelson, 2019). In other marine crustacean species embryos and larvae are colonized by specific symbiotic bacteria that increase protection from pathogenic fungi and bacteria (Gil-Turnes et al., 1989—*Palaemon macrodactylus*; Gil-Turnes and Fenical, 1992—*Homarus americanus*), and in Bryozoa bacteria reduce larval predation risk through the production of cytotoxins (Lopanik et al., 2004—*Bugula neritina*).

While microbiomes have not been found in all animal species studied (including crustacean larvae) (Hammer et al., 2019; Martin et al., 2020), there is evidence that when present in marine invertebrate larvae, symbiotic relationships are often formed. It is important to comprehend at which developmental stage these microbes are acquired if we are to understand whether and how these relationships aid the transition between life stages and contribute to the evolution toward terrestrialization.

Larval microbiomes of semi-/terrestrial crabs may be obtained horizontally from the surrounding environment, or vertically, through their parents (**Figure 1**). Horizontal bacterial transmission can occur either during the pelagic stages from the surrounding water (Lopanik et al., 2004; Hadfield, 2021) or upon first settlement (Nussbaumer et al., 2006; Aldred and Nelson, 2019) e.g., at the megalopa stage. Megalopae of many semi-/terrestrial crabs spend considerable time on the sediment surface, ahead of their metamorphosis into benthic juveniles (Anger, 2001; Hamasaki et al., 2015) and settlement is often driven by specific environmental and conspecific cues present in the sediment or the water layer above (Diele and Simith, 2007; Simith et al., 2013), possibly

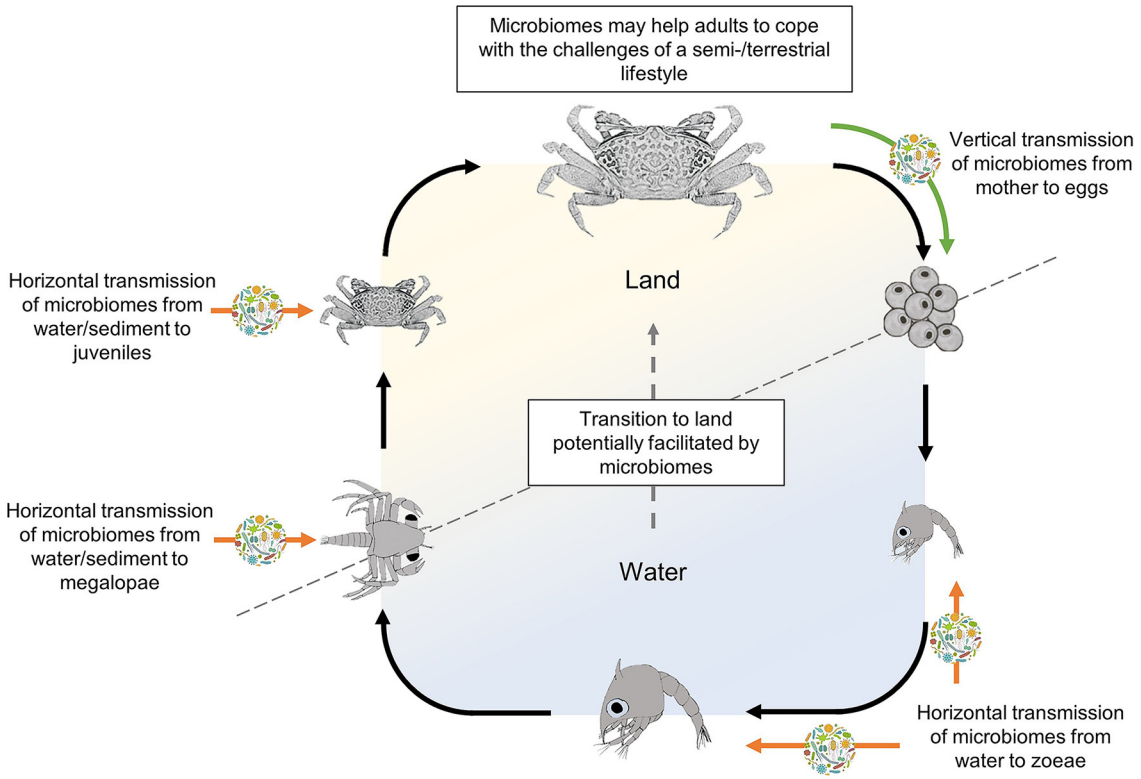

FIGURE 1 | Life cycle of a semi-terrestrial crab (here represented as a female fiddler crab; subfamily Gelasiminae, taken as a model species; adapted after Peer et al., 2015) indicating the potential time points of vertical and horizontal acquisition of symbiotic microbiomes that may facilitate the transition from a life in water to one on land. Green and orange arrows indicate potential vertical and horizontal transmission routes of symbiotic microorganisms, respectively. Black arrows indicate the model life cycle from egg, through larvae, to adult crab.

including substances emitted by bacterial biofilms (Simith et al., 2017). The period that the megalopae spend on the sediment before metamorphosing to the first juvenile crab stage may therefore provide an ideal time for the acquisition of bacteria from this substrate (Lim et al., 2019). Evidence of sediment bacteria transfer has been shown in adult fiddler crabs, *Uca panacea*, where the crabs' microbiome is populated by bacteria from their burrows (carapace microbiome) and the sediment surface (carapace and gut microbiome) (Cuellar-Gempeler and Leibold, 2019).

Alternatively, vertical transmission of a larva's microbiome is generally through the mother, either from her microbiota or that received from the father during mating (Damiani et al., 2008). Given the conservative broadcast spawning and pelagic larval stages of most semi-/terrestrial crabs, vertical transmission would have to occur through symbiont association with adult gametes (Russell et al., 2018) or through an association between the microbes and the females' ovaries. Egg associated microbiomes that act as the vertical transmission point for symbionts (Nyholm, 2020) have been evidenced for the deep-sea yeti crab, *Kiwa puravida* (Goffredi et al., 2014), and the hydrothermal vent shrimp, *Rimicaris exoculata* (Methou et al., 2019). In semi-/terrestrial crabs, microbes that are transmitted through the mother's eggs would colonize their target organ upon hatching or, if such organ has not yet developed at this developmental stage (e.g., gills), persist internally or on the larvae's carapace until formed. If vertical transmission is occurring in semi-/terrestrial crabs, it would indicate a complex symbiotic relationship where the crabs' entire life cycles are intertwined with their microbiome.

Given the large number of crab species that have conquered the land but retained pelagic larvae that develop in the oceans, we advocate the importance of integrating the early life history stages into future studies on microbiomes as a paradigm for the evolution of terrestrialization in crabs. Identifying whether, when, and under which acquisition pathway microbiome transmission is occurring in the early life history of species with biphasic life cycles has the potential to significantly enhance our understanding of the contribution of animal-microbiome interactions in the crabs' transition from a life in water onto land.

AUTHOR CONTRIBUTIONS

MW and KD conceived the idea for the paper. MW led the manuscript drafting, with input from all co-authors.

FUNDING

This work received funding from King Abdullah University of Science and Technology Competitive Research Grant Program 2018—OSR-CRG 2018-3739.

ACKNOWLEDGMENTS

The authors would like to acknowledge the support of their host institutions and colleagues from the Extreme Systems Microbiology lab for helpful discussion.

REFERENCES

Adamczewska, A. M., and Morris, S. (2001). Metabolic status and respiratory physiology of *Gecarcoidea natalis*, the Christmas Island red crab, during the annual breeding migration. *Biol. Bull.* 200, 321–335. doi: 10.2307/1543513

Aldred, N., and Nelson, A. (2019). Microbiome acquisition during larval settlement of the barnacle *Semibalanus balanoides*. *Biol. Lett.* 15:20180763. doi: 10.1098/rsbl.2018.0763

Anger, K. (1995). The conquest of freshwater and land by marine crabs: adaptations in life-history patterns and larval bioenergetics. *J. Exp. Mar. Bio. Ecol.* 193, 119–145. doi: 10.1016/0022-0981(95)00114-X

Anger, K. (2001). *The Biology of Decapod Crustacean Larvae*. Lisse: A.A. Balkema, 1–420.

Bang, C., Dagan, T., Deines, P., Dubilier, N., Duschl, W. J., Fraune, S., et al. (2018). Metaorganisms in extreme environments: do microbes play a role in organismal adaptation? *Zoology* 127, 1–19. doi: 10.1016/j.zool.2018.02.004

Bliss, D. E., and Mantel, L. H. (1968). Adaptations of crustaceans to land: a summary and analysis of new findings. *Integr. Comp. Biol.* 8, 673–685. doi: 10.1093/icb/8.3.673

Bui, T. H. H., and Lee, S. Y. (2015). Potential contributions of gut microbiota to the nutrition of the detritivorous sesarmid crab *Parasesarma erythodactyla*. *Mar. Biol.* 162, 1969–1981. doi: 10.1007/s00227-015-2723-8

Burggren, W. W., and McMahon, B. R. (1988). *Biology of Land Crabs*. Cambridge: Cambridge University Press.

Cannicci, S., Fratini, S., Meriggi, N., Bacci, G., Iannucci, A., Mengoni, A., et al. (2020). To the land and beyond: crab microbiomes as a paradigm for the evolution of terrestrialization. *Front. Microbiol.* 11:575372. doi: 10.3389/fmicb.2020.575372

Chomicki, G., Werner, G. D. A., West, S. A., and Kiers, E. T. (2020). Compartmentalization drives the evolution of symbiotic cooperation. *Philos. Trans. R. Soc. B* 375: 20190602. doi: 10.1098/rstb.2019.0602

Cuellar-Gempeler, C., and Leibold, M. A. (2019). Key colonist pools and habitat filters mediate the composition of fiddler crab–associated bacterial communities. *Ecology* 100, 1–14. doi: 10.1002/ecy.2628

Damiani, C., Ricci, I., Crotti, E., Rossi, P., Rizzi, A., Scuppa, P., et al. (2008). Paternal transmission of symbiotic bacteria in malaria vectors. *Curr. Biol.* 18, 1087–1088. doi: 10.1016/j.cub.2008.10.040

Diele, K., and Simith, D. J. B. (2007). Effects of substrata and conspecific odour on the metamorphosis of mangrove crab megalopae, *Ucides cordatus* (Ocypodidae). *J. Exp. Mar. Bio. Ecol.* 348, 174–182. doi: 10.1016/j.jembe.2007.04.008

Diesel, R. (1989). Parental care in an unusual environment: *Metopaulias depressus* (Decapoda: Grapsidae), a crab that lives in epiphytic bromeliads. *Anim. Behav.* 38, 561–575. doi: 10.1016/S0003-3472(89)80001-6

Diesel, R., and Schuh, M. (1993). Maternal care in the bromeliad crab *Metopaulias depressus* (Decapoda): maintaining oxygen, pH and calcium levels optimal for the larvae. *Behav. Ecol. Sociobiol.* 32, 11–15. doi: 10.1007/BF00172218

Gil-Turnes, M. S., and Fenical, W. (1992). Embryos of *Homarus americanus* are protected by epibiotic bacteria. *Biol. Bull.* 182, 105–108. doi: 10.2307/1542184

Gil-Turnes, M. S., Hay, M. E., and Fenical, W. (1989). Symbiotic marine bacteria chemically defend crustacean embryos from a pathogenic fungus. *Science* 246, 116–118. doi: 10.1126/science.2781297

Goffredi, S. K., Gregory, A., Jones, W. J., Morella, N. M., and Sakamoto, R. I. (2014). Ontogenetic variation in epibiont community structure in the deep-sea yeti crab, *Kiwa puravida*: convergence among crustaceans. *Mol. Ecol.* 23, 1457–1472. doi: 10.1111/mec.12439

González-Gordillo, J. I., Anger, K., and Schubart, C. D. (2010). Morphology of the larval and first juvenile stages of two Jamaican endemic crab species with abbreviated development, *Sesarma windsor* and *Metopaulias depressus* (Decapoda: Brachyura: Sesarmidae). *J. Crustac. Biol.* 30, 101–121. doi: 10.1651/08-3110.1

Hadfield, M. G. (2021). Developmental symbiosis: a sponge larva needs symbiotic bacteria to succeed on the benthos. *Curr. Biol.* 31, R88–R90. doi: 10.1016/j.cub.2020.11.007

Hamasaki, K., Ishiyama, N., and Kitada, S. (2015). Settlement behavior and substrate preference of the coconut crab *Birgus latro* megalopae on natural substrata in the laboratory. *J. Exp. Mar. Bio. Ecol.* 468, 21–28. doi: 10.1016/j.jembe.2015.03.011

Hammer, T. J., Sanders, J. G., and Fierer, N. (2019). Not all animals need a microbiome. *FEMS Microbiol. Lett.* 366, 1–11. doi: 10.1093/femsle/fnz117

Hartnoll, R. G., Weber, N., Régnier-Mckellar, C., and Weber, S. B. (2014). Return to the land; the stages of terrestrial recruitment in land crabs. *Crustaceana* 87, 531–539. doi: 10.1163/15685403-00003294

Hernández-Pérez, A., Zamora-briseño, J. A., Söderhäll, K., and Söderhäll, I. (2021). Gut microbiome alterations in the crustacean *Pacifastacus leniusculus* exposed to environmental concentrations of antibiotics and effects on susceptibility to bacteria challenges. *Dev. Comp. Immunol.* 126:104181. doi: 10.1016/j.dci.2021.104181

Hsia, C. C. W., Schmitz, A., Lambertz, M., Perry, S. F., and Maina, J. N. (2013). Evolution of air breathing: oxygen homeostasis and the transitions from water to land and sky. *Compr. Physiol.* 3, 849–915. doi: 10.1002/cphy.c120003

Lim, S. J., Davis, B. G., Gill, D. E., Walton, J., Nachman, E., Engel, A. S., et al. (2019). Taxonomic and functional heterogeneity of the gill microbiome in a symbiotic coastal mangrove lucinid species. *ISME J.* 13, 902–920. doi: 10.1038/s41396-018-0318-3

Lopanik, N., Lindquist, N., and Targett, N. (2004). Potent cytotoxins produced by a microbial symbiont protect host larvae from predation. *Oecologia* 139, 131–139. doi: 10.1007/s00442-004-1487-5

Martin, G. G., Natha, Z., Henderson, N., Bang, S., Hendry, H., and Loera, Y. (2020). Absence of a microbiome in the midgut trunk of six representative Crustacea. *Crustac. Biol.* 40, 122–130. doi: 10.1093/jcbiol/ruz087

Mattila, J. M., Zimmer, M., Vesakoski, O., and Jormalainen, V. (2014). Habitat-specific gut microbiota of the marine herbivore *Idotea balthica* (Isopoda). *J. Exp. Mar. Bio. Ecol.* 455, 22–28. doi: 10.1016/j.jembe.2014.02.010

Methou, P., Hernández-Ávila, I., Aube, J., Cueff-Gauchard, V., Gayet, N., Amand, L., et al. (2019). Is it first the egg or the shrimp? – Diversity and variation in microbial communities colonizing broods of the vent shrimp *Rimicaris exoculata* during embryonic development. *Front. Microbiol.* 10:808. doi: 10.3389/fmicb.2019.00808

Minic, Z., and Hervé, G. (2004). Biochemical and enzymological aspects of the symbiosis between the deep-sea tubeworm *Riftia pachyptila* and its bacterial endosymbiont. *Eur. J. Biochem.* 271, 3093–3102. doi: 10.1111/j.1432-1033.2004.04248.x

Morris, S. (2001). Neuroendocrine regulation of osmoregulation and the evolution of air-breathing in decapod crustaceans. *J. Exp. Biol.* 204, 979–989. doi: 10.1242/jeb.204.5.979

Nussbaumer, A. D., Fisher, C. R., and Bright, M. (2006). Horizontal endosymbiont transmission in hydrothermal vent tubeworms. *Nature* 441, 345–348. doi: 10.1038/nature04793

Nyholm, S. V. (2020). In the beginning: egg-microbe interactions and consequences for animal hosts. *Philos. Trans. R. Soc. B Biol. Sci.* 375:20190593. doi: 10.1098/rstb.2019.0593

O'Connor, R. M., Fung, J. M., Sharp, K. H., Benner, J. S., McClung, C., Cushing, S., et al. (2014). Gill bacteria enable a novel digestive strategy in a wood-feeding mollusk. *Proc. Natl. Acad. Sci. U.S.A.* 111, E5096–E5104. doi: 10.1073/pnas.1413110111

Peer, N., Miranda, N. A. F., and Perissinotto, R. (2015). A review of fiddler crabs (genus *Uca* Leach, 1814) in South Africa. *African Zool.* 50, 187–204. doi: 10.1080/15627020.2015.1055700

Rabalais, N. N., and Cameron, J. N. (1983). Abbreviated development of *Uca subcylindrica* (Stimpson, 1859) (Crustacea, Decapoda, Ocypodidae) reared in the laboratory. *J. Crustac. Biol.* 3, 519–541. doi: 10.2307/1547948

Russell, S. L., McCartney, E., and Cavanaugh, C. M. (2018). Transmission strategies in a chemosynthetic symbiosis: detection and quantification of symbionts in host tissues and their environment. *Proc. R. Soc. B Biol. Sci.* 285:20182157. doi: 10.1098/rspb.2018.2157

Simith, D. D. J. D. B., Abrunhosa, F. A., and Diele, K. (2013). Chemical induction in mangrove crab megalopae, *Ucides cordatus* (Ucididae): do young recruits emit metamorphosis-triggering odours as do conspecific adults? *Estuar. Coast. Shelf Sci.* 131, 264–270. doi: 10.1016/j.ecss.2013.07.015

Simith, D. D. J. D. B., Abrunhosa, F. A., and Diele, K. (2017). Metamorphosis of the edible mangrove crab *Ucides cordatus* (Ucididae) in response to benthic microbial biofilms. *J. Exp. Mar. Bio. Ecol.* 492, 132–140. doi: 10.1016/j.jembe.2017.01.022

Sogin, E. M., Leisch, N., and Dubilier, N. (2020). Chemosynthetic symbioses. *Curr. Biol.* 30, R1137–R1142. doi: 10.1016/j.cub.2020.07.050

Song, H., Hewitt, O. H., and Degnan, S. M. (2021). Arginine biosynthesis by a bacterial symbiont enables nitric oxide production and facilitates larval settlement in the marine-sponge host. *Curr. Biol.* 31, 433–437.e3. doi: 10.1016/j.cub.2020.10.051

Vogt, G. (2013). Abbreviation of larval development and extension of brood care as key features of the evolution of freshwater Decapoda. *Biol. Rev.* 88, 81–116. doi: 10.1111/j.1469-185X.2012.00241.x

Weihrauch, D., Morris, S., and Towle, D. W. (2004). Ammonia excretion in aquatic and terrestrial crabs. *J. Exp. Biol.* 207, 4491–4504. doi: 10.1242/jeb.01308

Zhang, M., Sun, Y., Chen, L., Cai, C., Qiao, F., Du, Z., et al. (2016). Symbiotic bacteria in gills and guts of Chinese mitten crab (*Eriocheir sinensis*) differ from the free-living bacteria in water. *PLoS ONE* 11:e0148135. doi: 10.1371/journal.pone.0148135

Zhang, N., Song, C., Wang, M., Liu, Y., Hui, M., and Cui, Z. (2017). Diversity and characterization of bacteria associated with the deep-sea hydrothermal vent crab *Austinograea* sp. comparing with those of two shallow-water crabs by 16S ribosomal DNA analysis. *PLoS ONE* 12:e0187842. doi: 10.1371/journal.pone.0187842

Zilber-Rosenberg, I., and Rosenberg, E. (2008). Role of microorganisms in the evolution of animals and plants: the hologenome theory of evolution. *FEMS Microbiol. Rev.* 32, 723–735. doi: 10.1111/j.1574-6976.2008.00123.x

Zimmer, M., Danko, J. P., Pennings, S. C., Danford, A. R., Carefoot, T. H., Ziegler, A., et al. (2002). Cellulose digestion and phenol oxidation in coastal isopods (Crustacea: Isopoda). *Mar. Biol.* 140, 1207–1213. doi: 10.1007/s00227-002-0800-2

Conflict of Interest: The authors declare that the research was conducted in the absence of any commercial or financial relationships that could be construed as a potential conflict of interest.

Publisher's Note: All claims expressed in this article are solely those of the authors and do not necessarily represent those of their affiliated organizations, or those of the publisher, the editors and the reviewers. Any product that may be evaluated in this article, or claim that may be made by its manufacturer, is not guaranteed or endorsed by the publisher.

frontiers in Microbiology

ORIGINAL RESEARCH
published: 25 October 2021
doi: 10.3389/fmicb.2021.756091

Rapid Shifts in Bacterial Communities and Homogeneity of Symbiodiniaceae in Colonies of *Pocillopora acuta* Transplanted Between Reef and Mangrove Environments

Trent D. Haydon[1], Justin R. Seymour[1], Jean-Baptiste Raina[1], John Edmondson[2], Nachshon Siboni[1], Jennifer L. Matthews[1], Emma F. Camp[1] and David J. Suggett[1]*

[1] Climate Change Cluster, University of Technology, Ultimo, NSW, Australia, [2] Wavelength Reef Cruises, Port Douglas, QLD, Australia

OPEN ACCESS

Edited by:
Fabiano Thompson, Alberto Luiz Coimbra Institute for Graduate Studies and Engineering Research, Federal University of Rio de Janeiro, Brazil

Reviewed by:
Guowei Zhou, Key Laboratory of Tropical Marine Bio-resources and Ecology, South China Sea Institute of Oceanology, Chinese Academy of Sciences (CAS), China
Julie L. Meyer, University of Florida, United States

***Correspondence:**
Trent D. Haydon
Trent.Haydon@uts.edu.au

Specialty section:
This article was submitted to Microbial Symbioses, a section of the journal Frontiers in Microbiology

Received: *10 August 2021*
Accepted: *24 September 2021*
Published: *25 October 2021*

Citation:
Haydon TD, Seymour JR, Raina J-B, Edmondson J, Siboni N, Matthews JL, Camp EF and Suggett DJ (2021) Rapid Shifts in Bacterial Communities and Homogeneity of Symbiodiniaceae in Colonies of Pocillopora acuta Transplanted Between Reef and Mangrove Environments. Front. Microbiol. 12:756091. doi: 10.3389/fmicb.2021.756091

It has been proposed that an effective approach for predicting whether and how reef-forming corals persist under future climate change is to examine populations thriving in present day extreme environments, such as mangrove lagoons, where water temperatures can exceed those of reef environments by more than 3°C, pH levels are more acidic (pH < 7.9, often below 7.6) and O_2 concentrations are regularly considered hypoxic (<2 mg/L). Defining the physiological features of these "extreme" corals, as well as their relationships with the, often symbiotic, organisms within their microbiome, could increase our understanding of how corals will persist into the future. To better understand coral-microbe relationships that potentially underpin coral persistence within extreme mangrove environments, we therefore conducted a 9-month reciprocal transplant experiment, whereby specimens of the coral *Pocillopora acuta* were transplanted between adjacent mangrove and reef sites on the northern Great Barrier Reef. Bacterial communities associated with *P. acuta* specimens native to the reef environment were dominated by *Endozoicomonas*, while Symbiodiniaceae communities were dominated by members of the *Cladocopium* genus. In contrast, *P. acuta* colonies native to the mangrove site exhibited highly diverse bacterial communities with no dominating members, and Symbiodiniaceae communities dominated by *Durusdinium.* All corals survived for 9 months after being transplanted from reef-to-mangrove, mangrove-to-reef environments (as well as control within environment transplants), and during this time there were significant changes in the bacterial communities, but not in the Symbiodiniaceae communities or their photo-physiological functioning. In reef-to-mangrove transplanted corals, there were varied, but sometimes rapid shifts in the associated bacterial communities, including a loss of "core" bacterial members after 9 months where coral bacterial communities began to resemble those of the native mangrove corals. Bacterial communities associated

with mangrove-to-reef *P. acuta* colonies also changed from their original composition, but remained different to the native reef corals. Our data demonstrates that *P. acuta* associated bacterial communities are strongly influenced by changes in environmental conditions, whereas Symbiodiniaceae associated communities remain highly stable.

Keywords: coral microbiome, 16S rRNA gene, *Pocillopora acuta*, mangrove coral, *Endozoicomonas*, transplant, extreme environment

INTRODUCTION

Coral reefs worldwide are rapidly deteriorating as a consequence of increasingly frequent and severe marine heatwaves (e.g., Hughes et al., 2018), chronic ocean warming, acidification and deoxygenation (Altieri et al., 2017; Cornwall et al., 2021). Climate change projections indicate that by 2030, most coral reef environments will exceed the current temperature, pH and/or O_2 thresholds that govern optimal coral reef functioning (Hoegh-Guldberg et al., 2017; Hughes et al., 2018, 2020), threatening reef survival. Understanding whether, and if so how, corals can acclimatise or adapt to these various stressors has therefore become a global research priority in recent years (Howells et al., 2016; Torda et al., 2017; van Oppen and Blackall, 2019; Cropp and Norbury, 2020). One approach has been to study corals already thriving under present-day natural extremes, in reef or reef-adjacent habitats where daily pH, O_2 and temperature already reach or exceed levels predicted to occur by the end of the century (reviewed by Camp et al., 2018). Such extreme environments include tidal pools (Palumbi et al., 2014; Klepac and Barshis, 2020) and macrotidal reefs (Schoepf et al., 2015, 2020), where corals exhibit exceptional thermal tolerance. Corals in these extreme environments can provide important insights into the future of conspecific reef populations under continued ocean warming.

Extreme systems recently identified as ideal sites for studying coral resilience to complex stressor regimes are reef adjacent mangrove lagoons (Camp et al., 2018), which can be inhabited by species of reef-building corals commonly found on nearby reefs (Macintyre et al., 2000; Rogers, 2009, 2017; Camp et al., 2017, 2019; Lord et al., 2020). Mangroves can reduce thermal stress by shading corals, but these shallow environments also expose corals to hotter, more acidic and deoxygenated conditions (Rogers and Herlan, 2012; Camp et al., 2017; Rogers, 2017; Maggioni et al., 2021). Compared to adjacent reefs, where pH levels fluctuate between 8.1 and 8.2, mangrove lagoons can exhibit consistently low pH (below 7.8), with daily drops to below 7.3 (Camp et al., 2017, 2019). These environments are also on average 2°C warmer than nearby reefs and contain lower dissolved O_2 concentrations (<1 mg L^{-1}) relative to adjacent reefs (Camp et al., 2017, 2020). As a result, corals thriving in mangrove lagoons exhibit very different physiological and metabolic signatures, such as enhanced respiration and reduced photosynthesis (Camp et al., 2017; Ros et al., 2021), which likely facilitate their survival within these relatively hostile environments. However, other underlying factors, such as shifts in the coral microbiome, might also contribute to the persistence of corals in these extreme environments.

Microorganisms are central to healthy coral function (Bourne et al., 2016; Putnam et al., 2017), but their role in coral stress responses has mostly been characterised for the endosymbiotic dinoflagellates (Symbiodiniaceae) (Howells et al., 2012; Cunning et al., 2015a; Lewis et al., 2019; Rosset et al., 2019; Rädecker et al., 2021). Coral hosts closely associated with specific Symbiodiniaceae taxa (Howells et al., 2020; Osman et al., 2020), except when exposed to atypical ("stressful") conditions (Cunning et al., 2015b; Lewis et al., 2019; Thomas et al., 2019). For example, coral populations persisting across changing environmental gradients experience shifts in dominant Symbiodiniaceae types (Innis et al., 2018; Wall et al., 2020), likely as a host response to retain metabolic compatibility as external resource availability shifts (Suggett et al., 2017). Similarly, corals exhibit ecological associations with diverse and abundant communities of prokaryotes, which play important roles in nutrient cycling (e.g., nitrogen, carbon, sulphur) and protection from pathogens (Ritchie, 2006; Raina et al., 2009; Rädecker et al., 2015; Glasl et al., 2016). The composition of bacterial assemblages associated with corals is rarely static and often displays seasonal (Roder et al., 2015; Sharp et al., 2017) and spatial (McDevitt-Irwin et al., 2017; Ziegler et al., 2019; Osman et al., 2020) heterogeneity governed by changing environmental conditions. There is evidence that these bacterial communities can also facilitate coral acclimation under environmental stress, enhancing coral resilience (Ziegler et al., 2017, 2019; Yu et al., 2020), and recent microbiome manipulation experiments have led to altered levels of stress susceptibility (Fragoso Ados Santos et al., 2015; Damjanovic et al., 2017; Rosado et al., 2019; Doering et al., 2021; Zhang et al., 2021). However, the specific metabolic advantages that beneficial bacteria provide to corals remain to be elucidated.

Recent work in New Caledonia has revealed that conspecific corals inhabiting reef and mangrove habitats harbour different bacterial and Symbiodiniaceae communities (Camp et al., 2020). However, it is unclear whether these contrasting communities are a direct consequence of these different environments, and how plastic these communities might be to environmental variation. Transplantation experiments have been used in reef studies to resolve how corals can adjust to environmental change (and/or populate diverse conditions), demonstrating capacity for corals to acclimatise to depth ranges (Cohen and Dubinsky, 2015; Tamir et al., 2020), temperature regimes (Barshis et al., 2010; Dixon et al., 2018), turbidity gradients (Padilla-Gamiño et al., 2012), and heat stress exposure (Palumbi et al., 2014). Such studies have

begun to examine the possible roles that microbial associates play in facilitating acclimation, demonstrating clear shifts in microbial communities when corals are introduced to non-native environments (Ziegler et al., 2019; Chapron et al., 2020; Roitman et al., 2020). For example, when transplanted to a hotter and more thermally variable environment, heat sensitive corals acquired a microbiome similar to that of heat tolerant corals (Ziegler et al., 2017). However, such reshuffling of the microbiome under stress does not appear to be a conserved trait across all coral species because the microbiome of some species remain unchanged when transplanted from unpolluted to polluted environments (Ziegler et al., 2019).

Following recent observations that coral species found on the northern Great Barrier Reef in both mangrove lagoon and adjacent reef sites are inhabited by different communities of Symbiodiniaceae (Low Isles; Camp et al., 2019; Ros et al., 2021), we conducted a 9-month reciprocal transplant experiment, using the common coral species *Pocillopora acuta*, to identify whether: (i) bacterial communities differ between sites, and (ii) bacterial and Symbiodiniaceae community composition changes to resemble that of native corals when moved across the contrasting environments. Given previous observations of rapid adjustments in bacterial assemblages (Sharp et al., 2017; Sweet et al., 2017; Pootakham et al., 2019), we hypothesised that the microbiome of *P. acuta* would shift after 9 months of reciprocal transplantation into non-native sites and would mirror that of native non-transplanted corals. Understanding if the microbiomes of transplanted corals have the capacity to resemble those of native corals is important to decipher some of the possible mechanisms involved of how corals will adapt to changing future conditions.

MATERIALS AND METHODS

Site Description

Two sites, situated ∼500 m apart and located on the northern Great Barrier Reef (GBR), were selected for our reciprocal transplant experiment: a mangrove lagoon (Woody Isles) and an adjacent reef crest-slope (Low Isles reef) (**Figure 1**). The Woody Isles mangrove lagoon is semi-enclosed by a mangrove forest and undergoes daily tidal flushing, but does not appear to have freshwater inputs from the surrounding catchment. Corals inhabiting this mangrove environment undergo dynamic diurnal changes in temperature (range 7.7°C), pH (1.3), oxygen (7.33 mg l^{-1}), and salinity (15.5) (see Camp et al., 2019). In comparison, the Low Isles reef site has considerably more stable physiochemical conditions.

Experimental Design and Sample Collection

To characterise daily and seasonal temperature shifts, we deployed HOBO Pendant data loggers (Onset, MA, United States) at both sites (Woody Isles mangrove; Low Isles reef), which recorded data for the 9-month duration of the experiment. In addition, spot measurements were periodically taken for temperature, salinity and oxygen using a multi-meter (3430, WTW) and pH using a pH meter (913, Metrohm). Environmental data series (temperature, salinity, O_2, and pH) were tested using independent samples *t* tests with Welch's corrections to test for any differences between reef and mangrove environments (GraphPad Prism v.7).

Five colonies of *P. acuta* were selected for transplantation from each habitat. Colonies were sampled from a depth of ca. 0.25–0.5 m (mangrove, $n = 5$) and <1 m (reef crest-slope, $n = 5$) on the lowest astronomical tide to ensure consistency across the two sites. All colonies were subsampled to yield a partial colony fragment, which was then split in half (ca. 10 cm diameter). The two resulting fragments subsequently served as either a native (remaining within site) or non-native (transplanted between sites) specimen, where colonies were either retained within their native mangrove (mangrove-mangrove), or reef (reef-reef), or were moved from the mangrove to the reef (mangrove-reef), or reef to mangrove (reef-mangrove). All split colonies were attached onto one of five aluminium racks with cable ties within each location, such that each rack contained either a replicate mangrove-mangrove or reef-mangrove coral colony within the mangrove lagoon, or replicate reef-reef or mangrove-reef coral colony on the reef (total $n = 20$). Two small fragments (<5 cm each) of *P. acuta* were collected from each of the 20 split colonies at the start of the transplantation (May 2018, t_0) for characterisation of the Symbiodiniaceae and bacterial communities, and Symbiodiniaceae photo-physiology *via* Pulse Amplitude Modulation (PAM) fluorometry. All fragments were collected using sterile pliers and placed in zip lock bags filled with seawater from the respective location before being returned to the sampling vessel within 30 min for immediate processing. One fragment was used for microbiome characterisation and rinsed with sterile artificial seawater before immediate flash freezing in liquid N_2, while the second fragment was analysed using PAM fluorometry. Further samples were collected using this approach three days after transplantation (t_{3d}) to determine any immediate transplant effects on the coral microbiome or photophysiology. The experiment continued with samples collected 2 months (t_{2M}), 3 months (t_{3M}), 6 months (t_{6M}), and 9 months (t_{9M}) after transplantation, which were all immediately processed for microbiome and PAM fluorometry analysis.

Photophysiological Data

Photophysiology was characterised using a diving PAM set to conduct a fluorescence-light response curve as previously detailed (e.g., Nitschke et al., 2018; Camp et al., 2019), where the actinic light source intensity was verified against a factory-calibrated quantum sensor (Li-COR, United States). Briefly, samples were low light acclimated (ca. 5–10 mol photons m^{-2} s^{-1}) for 20 min and then exposed to an increasing light gradient of ca. 0, 180, 210, 360, 450, 670, 1070, 1550, and 1980 μmol photons m^{-2} s^{-1}. Minimum (F_0, F_0', F') and maximum (F_m, F_m') fluorescence yields were obtained to calculate the excitation energy dissipation terms [1-C] and [1-Q], which are the photochemical and dynamic non-photochemical coefficients, respectively (see Suggett et al., 2015). To assess the differences of photosynthetic strategies between reef and

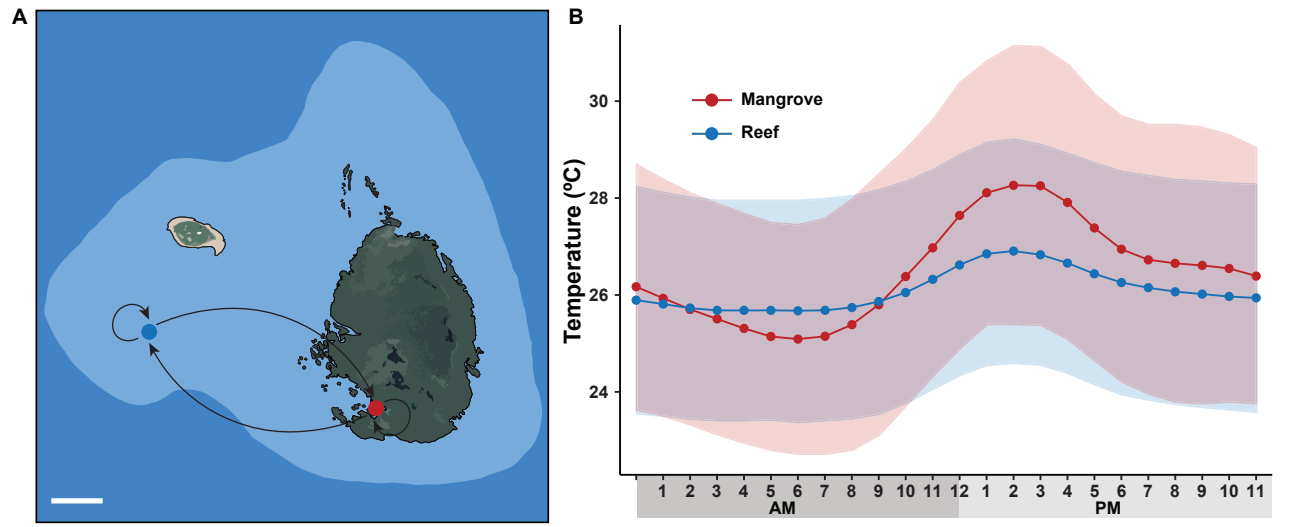

FIGURE 1 | Long-term reciprocal transplantation experiment. **(A)** Map of sampling sites on Low Isles reef crest (blue dot) and adjacent Woody Isles mangrove lagoons (red dot) with different environmental regimes. Five coral colonies were transplanted to each adjacent site (mangrove-reef and reef-mangrove) and five coral colonies remained in their natural environments (mangrove-mangrove and reef-reef). White line (lower left) represents 100 m distance. **(B)** Mean hourly temperature (°C) measured over a 9-month period between May 2018 and February 2019. Data was collected from HOBO sensors deployed on Woody Isles mangrove lagoon (red) and Low Isles reef (blue). Shading represents SD for $n = 269$ per time point.

mangrove corals, data series were confirmed for normality (Shapiro-Wilk) and then tested using independent samples *t* tests (GraphPad Prism v.7).

Sample Processing and DNA Extractions

Total genomic DNA (gDNA) was extracted using a modified phenol-chloroform protocol. Coral tissue was initially removed from frozen fragments by air-blasting tissue into zip lock bags containing 5 ml of sterile artificial seawater. Coral slurry was then centrifuged at 8,000 *g* for 10 min, the supernatant was discarded, and pellets were frozen at −80°C prior to subsequent analysis. Pellets were later resuspended in 0.5 mL of extraction buffer (0.75 M Sucrose, 40 mM EDTA, 50 mM Tris-base pH 8.3) with the addition of 75 µL of Lysozyme (100 mg/ml stock), incubated at 37°C for 1 h and shaken every 15 min, followed by three freeze/thaw cycles in liquid N_2 and incubation at 70°C on a heat block. Sodium dodecyl sulphate (SDS; 100 µL of a 25% solution) was added to samples and then incubated at 70°C for 10 min. Samples were cooled to room temperature before adding proteinase K (20 µL of 20 mg/mL stock) and further incubated for 1 h at 37°C, followed by three additional freeze/thaw cycles. Samples were then added to an equal volume of phenol:chloroform:isoamyl alcohol (25:24:1, pH 8), mixed by inversion for ten min at room temperature, followed by centrifugation for 15 min at 13,000 *g*. For each sample, the aqueous phase containing the DNA was transferred into a clean tube and equal volumes of chloroform:isoamyl alcohol (24:1) was added. Samples were mixed by inversion for 10 min and centrifuged for 10 min at 16,000 *g*. The aqueous layer was transferred to a new tube and mixed with sodium acetate (50 µl of 3M solution), then an equal volume of ice-cold molecular-grade isopropanol was added to precipitate the extracted DNA. Tubes were then centrifuged at 20,000 *g* for 30 min at 4°C and the supernatant was discarded. The DNA pellets were washed with 500 µL of molecular grade ethanol (70%) and centrifuged for 10 min 20,000 *g*. Ethanol was removed and samples were air dried for 15 min in the dark, before DNA pellets were resuspended in 30 µL of nuclease free water.

Host Identification

To confirm the identity of the coral species, extracted DNA was amplified using the Pdam-F (5′-AAGAAGATTCGGGCTCG TTT-′3) and Pdam-R (5′-CGCCTCCTCTACCAAGACAG-′3) primers, which provide species delineation in pocilloporids (Flot and Tillier, 2007). The PCR conditions involved a denaturing cycle at 95°C for 10 min, followed by 25 cycles at 95°C for 30 s, 58.5°C for 30 s, and 72°C for 30 s, and a final extension step at 72°C for 10 min. Amplification efficiency was confirmed using 1% agarose gels with 3 µL of PCR product. Amplicons were then sequenced in both directions using Sanger Sequencing (Australian Genomic Research Facility, NSW, Australia). Sequences were aligned in Geneious V R6 against reference sequences for *Pocillopora* from NCBI. All sequences matched with reference sequences for *P. acuta* (Schmidt-Roach et al., 2014) and confirmed initial classification based on visual identification in the field.

Prokaryote Community Composition

For characterisation of the bacteria associated with *P. acuta*, the V3-V4 region of the 16S rRNA gene was amplified using the 341F (5′-TCGTCGGCAGCGTCAGATGTGTATAAGAGACAG CCTAYGGGRBGCASCAG-′3) and 805R (5′-GTCTCGTGGG CTCGGAGATGTGTATAAGAGACAGGGACTACNNGGGTAT CTAAT-′3) primers (Klindworth et al., 2013) (underlined

segments represent adapter sequences; Illumina, San Diego, CA, United States). PCR reactions consisted of 1 μL of template DNA, 12 μL of Velocity high fidelity master mix (Bioline, United Kingdom) and 1 μL of each primer. The PCR cycling conditions involved an initial denaturation step at 95°C for 10 min, then 25 cycles at 95°C for 30 s, 50°C for 30 s and 72°C for 30 s, followed by a final extension at 72°C for 5 min. Amplicons were sequenced using the Illumina MiSeq platform (2 × 300 bp) at the Ramaciotti Centre for Genomics (University of New South Wales, Sydney, Australia). Raw FASTQ format files obtained from the 16S rRNA gene amplicon sequencing were processed using the Quantitative Insights into Microbial Ecology (QIIME2) pipeline (Bolyen et al., 2019). The DADA2 plugin (version 2019.1.0) was subsequently applied to remove chimeras, denoise and trim paired-end sequences (Callahan et al., 2016). Sequences were examined at the amplicon sequence variants (ASVs) level. ASVs with reads below 0.005% relative abundance and corresponding to chloroplast or mitochondria were removed (Gonzalez et al., 2019) along with any extraction kit contaminants found in sequenced negative controls. Taxonomy was assigned using *classify-sklearn* (Pedregosa et al., 2011) against the SILVA v138 database. Rarefaction curves were produced to determine differences in sequencing depth between samples, with data then rarefied to 5,250 reads per sample. Alpha-diversity indices were produced in QIIME2 (Shannon's diversity and Chao1 species richness).

To visualise differences in bacterial community composition among locations and treatments, non-metric multidimensional scaling ordinations (nMDS) were carried out using Bray-Curtis dissimilarity matrices. Differences in alpha diversity and community structure (beta diversity) were analysed using permutational multivariate analysis of variance (PERMANOVA) on square-root transformed data in PRIMER-E + PERMANOVA package v1.0.6. One-factorial PERMANOVA was run with 999 permutations to test for differences between sites (mangrove vs reef). Two-factorial PERMANOVAs were run with 999 permutations to test for differences between sites at different timepoints, and differences within sites between timepoints (fixed factors time and site). To identify differentially abundant bacterial taxa across sites and between timepoints, we used MetagenomeSeq (Paulson et al., 2013) at the ASV and family levels. Additionally, to identify the core microbiome of both mangrove and reef environments, we used the panbiom python script (Kahlke, 2018), which detect ASVs present in at least 0.1% relative abundance in more than 80% of samples tested.

Symbiodiniaceae Community Composition

Symbiodiniaceae community characterisation among *P. acuta* colonies was assessed at t_0 ($n = 19$) and t_{9M} ($n = 13$) to characterise any changes over time. Specifically, the ITS2 region of the Symbiodiniaceae communities associated with experimental coral colonies was targeted using the ITSintfor2 (5′- TCGTCGGCAGCGTCAGATGTGTATAAGAGACAGGAA TTGCAGAACTCCGTG-′3) and ITS2-reverse (5′-GTCTCGTG GGCTCGGAGATGTGTATAAGAGACAGGGGATCCATATGC TTAAGTTCAGCGGGT-′3) primer pairs (Coleman et al., 1994; LaJeunesse, 2002) (attached Illumina adapters underlined). PCR reactions and sequencing were carried out as described for the 16S rRNA sequencing, except that the annealing temperature used was 55°C. Resulting amplicons were sequenced using the Illumina MiSeq platform (2 × 300 bp) (Australian Genomic Research Facility, Victoria, Australia). Demultiplexed FASTQ files from the Illumina sequencing were analysed using the SymPortal analytical framework (Hume et al., 2019), which predicts ITS2-type profiles from specific sets of defining intragenomic ITS2 sequence variants (DIVs) based on genetically differentiated Symbiodiniaceae taxa. Sequences were submitted directly to the SymPortal pipeline, where they were quality controlled using Mother 1.39.5 (Schloss et al., 2009), BLAST+ suite of executables (Camacho et al., 2009) and minimum entropy decomposition (Eren et al., 2014) to predict Symbiodiniaceae taxa from the ITS2 marker. Differences in Symbiodiniaceae communities were visualised using nMDS and tested using PERMANOVA as described for the prokaryote data analysis above.

RESULTS

Environmental Characterisation

Reef and mangrove sites had distinct environmental regimes. Specifically, throughout the 9-month study period, average diel (day-night) temperature variation for the mangroves (28°C) was ∼2°C higher ($p < 0.001$) than for the reef (26°C). Similarly, peak temperature (15:00) was on average 1.5°C higher ($p < 0.001$) in the mangrove (28.2°C) compared to the reef (26.7°) (**Figure 1**). Over each sampling timepoint (t_0, t_{3D}, t_{t2M}, t_{3M}, t_{6M}, and t_{9M}), pH, salinity and oxygen were lower in the mangrove (7.74–7.81, 33.9–34.2, 2.5–4.1 mg/L) compared to the reef (8.08–8.11, 35.0–35.2, 6.2–6.8 mg/L) ($p < 0.0001$) (**Supplementary Table 1**).

Symbiodiniaceae Associations Are Site-Specific Yet Do Not Change After Transplantation

Symbiodiniaceae communities associated with *P. acuta* exhibited site-specific ITS2 profiles ($p < 0.005$; **Figure 2** and **Supplementary Table 2**). The Symbiodiniaceae assemblage within mangrove corals was dominated by species from the *Durusdinium* genus (ITS2 type profile D1bt_D6_D1_D4_D1bs and D4_D1_D6_D1bu_D2.2_D1h), while reef corals were dominated by members of the *Cladocopium* genus (ITS2 type profile C1d_C42.2_C1, C1d_C42.2_C1bl_C1_C3cg_C1b and C1d_C1_C42.2_C3cg_C1b_C3), whereby each genus represented >95% of the ITS2 relative abundance at each site. Notably, transplantation to adjacent sites had no effect on coral associated Symbiodiniaceae communities, which remained stable within transplanted corals (**Figure 2**). After 9 months (t_{9M}), ITS2 profiles of the transplants (either within or between sites) were indistinguishable from those at the beginning of the experiment (t_0) ($p > 0.05$; **Supplementary Table 3**). Photo-physiological assessments revealed strong seasonal signatures

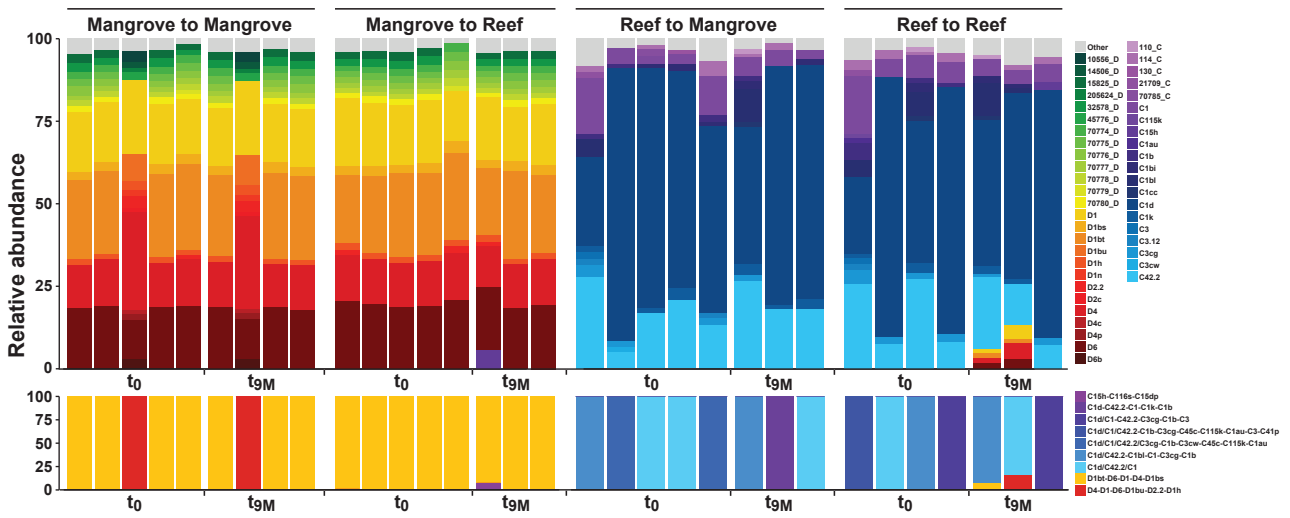

FIGURE 2 | Relative abundance (%) of ITS2 sequence types (upper section) and predicted major ITS2 type profiles (lower section) for *Pocillopora acuta* across both the mangrove lagoons and reef habitats on the Great Barrier Reef over transplantation treatments; mangrove-mangrove (MM), mangrove-reef (MR), reef-mangrove (RM), and reef-reef (RR). t_0 represents samples taken prior to transplantation and t_{9M} 9 months after transplantation. Only sequence types above 1% relative abundance are shown, anything below 1% relative abundance is represented by top grey bars. Designated names (e.g., D1) represent sequences previously characterised in the literature or that have been previously run through the SymPortal analytical framework (Hume et al., 2019). Other less common sequences designated to a unique database ID and their associated clade/genera (e.g., 10566_D) represent sequences that have not been previously used to characterise ITS2 type profiles. C refers to *Cladocopium* species (clade C) and D refers to *Durusdinium* species (clade D).

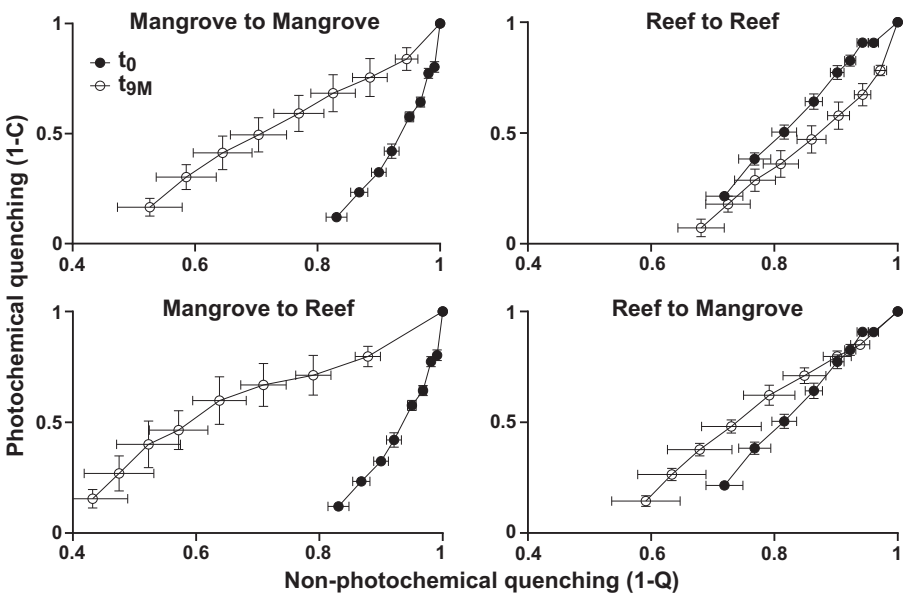

FIGURE 3 | Photophysiology of *Pocillopora acuta* (mean, $n = 3$–5) showing photochemical quenching (1-C) versus non-photochemical quenching (1-Q) from Rapid Light Curves for each transplantation treatment; mangrove-mangrove, mangrove-reef, reef-reef, and reef to mangrove at each sampling timepoint; t_0 (prior to transplantation) and t_{9M} (after 9 months of transplantation).

in the dissipation of excitation energy for the mangrove corals, which were retained independently of transplanted location (i.e., mangrove-mangrove and mangrove-reef) (**Figure 3**). Specifically, much greater non-photochemical quenching [lower values of (1-Q)] occurred at t_{9M} when water was the warmest, compared to t_0 ($p < 0.001$). In contrast, reef populations exhibited no significant change in quenching dynamics through time, a pattern that was conserved whether colonies were located in native (reef-reef) or non-native (reef-mangrove) habitats (**Figure 3**). Thus, Symbiodiniaceae communities also retained their initial physiological signatures regardless of location over the 9-month period following transplantation.

Sequencing Overview

In total, 113 samples of *P. acuta* (t_0; $n = 20$, t_{3D}; $n = 19$, t_{2M}; $n = 20$, t_{3M}; $n = 18$, t_{6M}; $n = 19$, t_{9M}; $n = 14$) and 3 negative controls were characterised using 16S rRNA amplicon sequencing, which yielded 10,745,579 sequences (**Supplementary Table 4**). Following quality control and removal of unwanted sequences, we retained 3,241,809 sequences (mean ± SE, 28,688 ± 7951 per sample). After Subsampling to 5250 sequences per sample, there were 110 samples retained with a total of 13,380 ASVs in the dataset.

Coral-Associated Bacterial Communities Are Site-Specific

Bacterial alpha diversity analysis revealed statistically significant patterns between environments (PERMANOVA, $p < 0.001$; **Supplementary Table 5**). Specifically, bacterial community richness at t_0 was significantly higher in the mangrove corals relative to corals located on the reef (ASV richness of 469 ± 66 SE and 149 ± 31, respectively; **Figure 4A**), and more diverse than in the reef (Shannon diversity of 8.2 ± 0.23 and 5.9 ± 0.40, respectively; **Figure 4B**).

The composition of the bacterial communities was also site-specific (PERMANOVA, $P < 0.001$; **Figure 5**, **Supplementary Figure 1**, and **Supplementary Table 6**). This was further confirmed visually by ordination analysis (**Figure 4C**). These inter-site differences at t_0 were driven by 79 differentially abundant ASVs, however, each of these ASVs was generally rare (<1% relative abundance). Therefore, we further analysed these differences at the family level using metagenomeSeq. Overall, we identified 60 differentially abundant bacterial families between the two sites (**Supplementary Table 7**), but only five of these represented at least 2% relative abundance in samples of either habitat (mangrove or reef). Specifically, Endozoicomonadaceae (33% ± 8.7), Cyanobiaceae (6% ± 1.7), and Bacillaceae (2.8% ± 0.78) were relatively more abundant in the reef corals at t_0, whereas Rhizobiaceae (2.6% ± 0.2) and Desulfocapsaceae (2.5% ± 0.3) were relatively more abundant in the mangrove corals at t_0 (**Figure 6C**).

Coral Core Microbiome

At t_0, a core microbiome was not conserved across *P. acuta* colonies in the mangrove environment. In contrast, 5 ASVs were identified as core members of the microbiomes in reef colonies. These 5 ASVs all belonged to the genus *Endozoicomonas*, on average they accounted for 26.3% of the microbiome in reef colonies and were all present in 9 out of the 10 replicates at t_0.

Bacterial Communities Rapidly Shift When Corals Are Transplanted

Transplantation of *P. acuta* colonies from the reef to the mangrove lagoon (reef-mangrove) resulted in no significant changes in alpha diversity over time (PERMANOVA, $p > 0.05$; **Supplementary Figure 2**, **Supplementary Table 8**). However, comparisons of beta diversity revealed a significant interactive effect between sites and timepoints (PERMANOVA, $p < 0.005$; **Supplementary Table 9**). Composition of bacterial communities in reef-mangrove corals shifted after 3 months of transplantation (t_{3M}), where these samples as well as those from subsequent time points, became highly dissimilar compared to t_0 samples

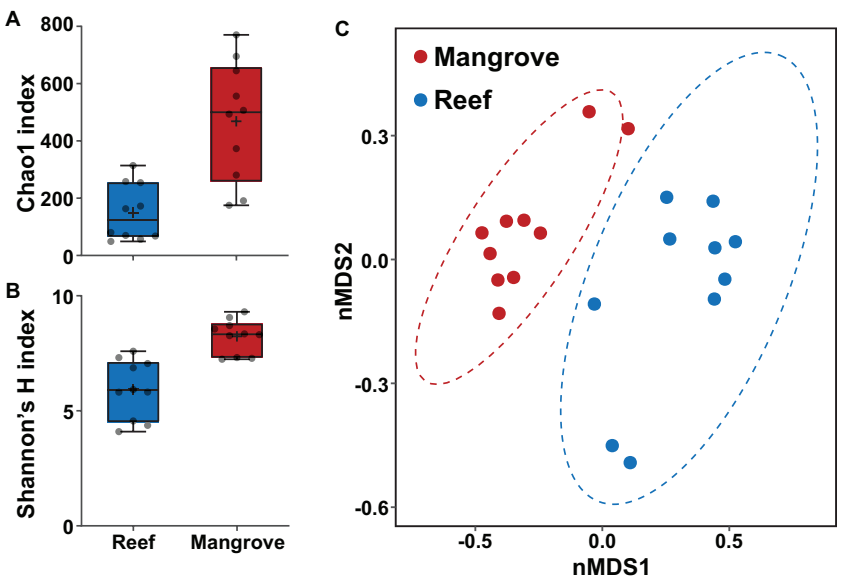

FIGURE 4 | Bacterial diversity of ASVs associated with *Pocillopora acuta* in the mangrove lagoons and the reef environments prior to transplantation of corals (t_0), based on **(A)** Chao1 and **(B)** Shannon's diversity index. Box plots represent 25th–75th percentile range, lines show medians, error bars represent IQR and + represent the mean, $n = 10$ coral colonies. **(C)** Bacterial community structure at the ASV level within the coral *Pocillopora acuta* between mangrove lagoon ($n = 10$) and reef environments ($n = 10$) at t_0. Plot is based on non-metric multidimensional scaling (nMDS) of Bray-Curtis distances with corals prior to transplantation. Ellipses denote 95% confidence intervals. 2D stress: 0.10.

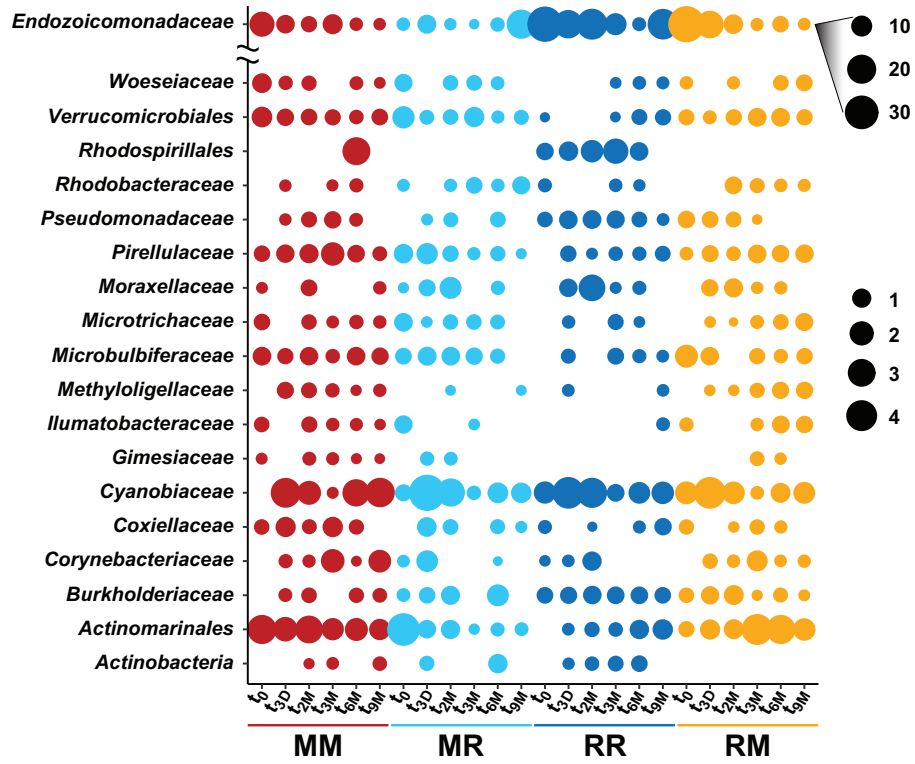

FIGURE 5 | Bubble plot of the highest abundant bacterial families associated with the coral *Pocillopora acuta* across different collection timepoints (t_0; 0 days, t_{3D}; 3 days, t_{2M}; 2 months, t_{3M}; 3 months, t_{6M}; 6 months, t_{9M}; 9 months) and transplant treatments (MM; mangrove-mangrove, MR; mangrove-reef, RR; reef-reef and RM; reef-mangrove). Size of the bubble represents the relative abundance. Note: Due to their abundance, bubble sizes of Endozoicomonadaceae were scaled separately.

(PERMANOVA, $p < 0.05$; **Figure 5** and **Supplementary Table 9**). In addition, communities between t_0 and t_{9M} were clearly partitioned (nMDS; **Figure 6B**). These changes in bacterial communities from t_0 to t_{9M} were primarily driven by statistically significant shifts in the relative abundance of 17 bacterial families (**Supplementary Table 10**). Notably, the proportion of Endozoicomonadaceae dramatically decreased from an average of 35 to 0.7%, while the relative abundance of members of the Rhizobiaceae significantly increased over time (1.3–4.5%) (**Figures 6D**, **7**).

Coral-associated bacterial communities in corals transplanted from mangrove to reef (mangrove-reef) were significantly altered after only three days (t_{3D}) of transplantation (PERMANOVA, $p < 0.05$; **Supplementary Table 9**). Overall ASV diversity (Shannon diversity) decreased over time (t_0; 7.9 and t_{9M}; 5.1, $p < 0.05$; **Supplementary Figure 2** and **Supplementary Table 8**), but no significant changes were observed in bacterial richness. Changes in bacterial community structure were observed between t_0 and t_{9M} (nMDS; **Figure 6A**) along with overall changes in community composition (PERMANOVA, $p < 0.05$, **Figure 5** and **Supplementary Table 9**). Among mangrove-reef colonies, nine bacterial families were differentially abundant over time (t_0–t_{9M}) (**Supplementary Table 11**), specifically significant increases in the relative abundance of Endozoicomonadaceae (0.96–19%) and Cyanobiaceae (2.5–4.5%), and a decrease in Desulfocapsaceae (2.7–0.24%) occurred (**Figures 6D**, **7**). Each individual mangrove-reef replicate became highly dominated by one or two different bacterial families following 9 months of transplantation to the reef. For example, one of the replicates was characterised by a high relative abundance of Rhodobacteraceae (79%), whereas another was dominated by Endozoicomonaceae (56%) (**Supplementary Figure 1**). This pattern contrasts with the lack of many highly relatively abundant bacterial families (>5%) among mangrove-reef samples prior to transplantation (t_0).

Coral Microbiomes of Transplanted Corals Resemble Those of Native Corals

Transplantation of coral colonies between habitats indicated the rate with which coral microbial communities adjusted to their new sites (environmental regime). The bacterial assemblages associated with the corals transplanted from the reef to mangrove (reef-mangrove) became indistinguishable to those of the native mangrove corals (mangrove-mangrove) by t_{9M} (PERMANOVA, $p > 0.05$; nMDS; **Figure 6B**). In contrast, the bacterial communities associated with corals that remained in the reef environment (reef-reef) did not change significantly over the course of the experiment. Bacterial communities of the mangrove-reef corals changed over time

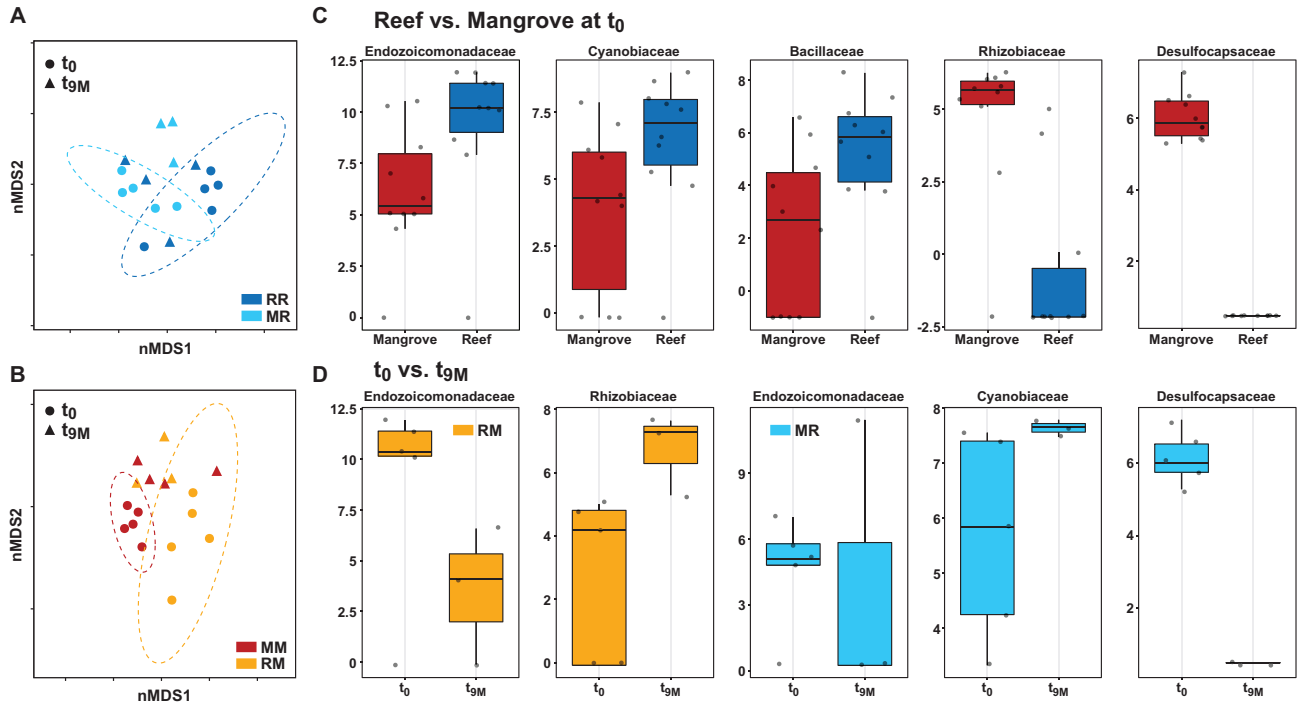

FIGURE 6 | Bacterial community structure at the amplicon sequence variant (ASV) level and differential abundance of bacterial families associated with the coral *Pocillopora acuta*. Non-metric multidimensional scaling (nMDS) of Bray-Curtis distances between timepoints (t_0 and t_{9M}) and treatments; **(A)** reef-reef (RR) and mangrove-reef (MR) (2D stress: 0.18), **(B)** mangrove-mangrove (MM) and reef-mangrove (RM) (2D stress: 0.13). MetagenomeSeq analysis of significantly differentially abundant bacterial families ($p < 0.05$ following FDR corrections) between **(C)** native reef and mangrove corals (t_0), **(D)** timepoints in mangrove-reef (MR) corals (t_0 vs t_{9M}) and reef-mangrove (RM) corals (t_0 vs t_{9M}). Bacteria family names are provided above each box, box plots represent log transformed count.

but showed little resemblance to the bacterial communities of the native reef corals (reef-reef) by t_{9M} (nMDS; **Figure 6A**). Additionally, the bacterial communities in the native mangrove corals (mangrove-mangrove) shifted between t_0 and t_{9M} ($p < 0.05$), which was characterised partly by the loss of *Endozoicomonas* ASVs (**Figure 7**). In fact, bacterial communities within the mangrove–mangrove native colonies were highly dynamic and shifted significantly at every timepoint measured (PERMANOVA, $p < 0.05$; **Figure 5** and **Supplementary Table 9**). The major distinction between bacterial communities from t_0 to t_{9M} for the native mangrove corals was the loss of highly abundant bacterial families, which contrasted with the corals translocated from mangrove to the reef (**Figure 5**).

DISCUSSION

Coral microbiomes are sensitive to environmental stressors and can dramatically differ across colonies of the same coral species inhabiting dissimilar environments (McDevitt-Irwin et al., 2017). Within this context, there is evidence that corals tolerant of the often hot, acidic and deoxygenated conditions within "extreme" mangrove lagoons harbour different microbial communities relative to colonies of the same species on nearby reefs (Camp et al., 2020). However, whether corals from mangrove environments retain such microbial characteristics when transplanted to a more stable reef environment is currently unknown. Here, we performed the first reciprocal transplant experiment of corals between a mangrove lagoon and adjacent reef, to identify the influence of environmental extremes on the structure of the coral microbiome. Our results show that a rapid shift in the bacterial communities occurred after translocation, whereas the Symbiodiniaceae communities – and associated physiological performance – remained remarkably stable. Bacterial communities associated with corals translocated from the reef environment into mangrove habitats became statistically indistinguishable from native mangrove corals. In contrast, bacterial communities of corals moved from the mangrove to reef environment did not begin to resemble the native reef corals, even 9 months after transplantation. Our experiment demonstrates that the bacterial communities of *P. acuta* strongly respond to changing environmental conditions, but the pressure exerted on the bacterial community is greater in mangrove environments.

Reef Versus Mangrove Environmental Conditions Influence Coral-Microbial Associations

Symbiodiniaceae taxa profoundly influence the physiology and stress resilience of their coral hosts (Oliver and Palumbi, 2011; Howells et al., 2012; Suggett et al., 2017). We found

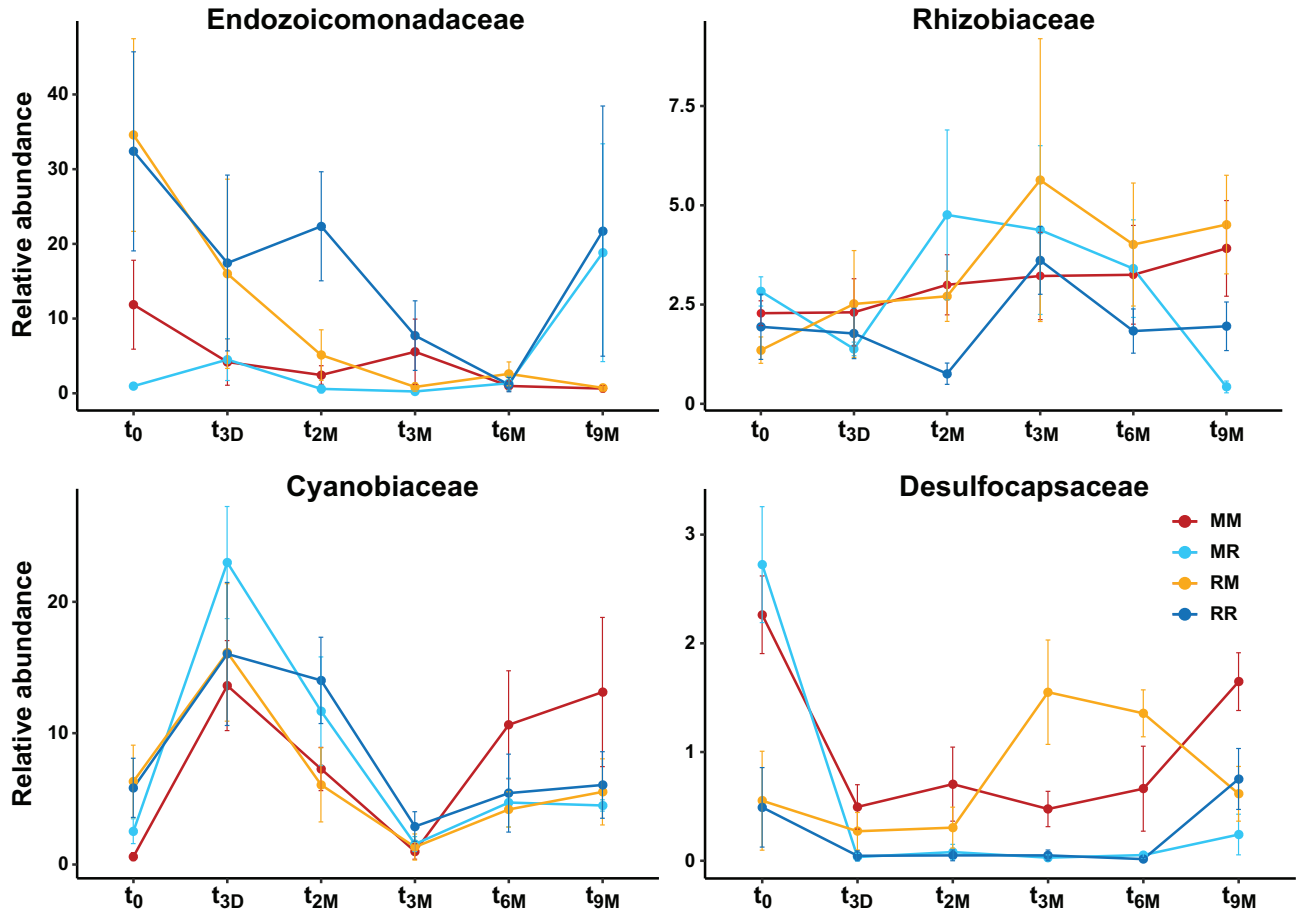

FIGURE 7 | Changes in relative abundance of dominant bacterial families over time (t_0; 0 days, t_{3D}; 3 days, t_{2M}; 2 months, t_{3M}; 3 months, t_{6M}; 6 months, t_{9M}; 9 months) and between transplant treatments (MM; mangrove-mangrove, MR; mangrove-reef, RM; reef-mangrove, and reef-reef; RR). Error bars represent standard error.

distinct communities of Symbiodiniaceae associated with *P. acuta* between the reef and mangrove environments, which is in line with previous observations at this field site (Ros et al., 2021). *P. acuta* colonies on the reef were largely dominated by the genus *Cladocopium*, whereas the mangrove colonies were dominated by the genus *Durusdinium*. Whilst *Durusdinium* is often observed in corals with enhanced stress tolerance, in particular to increased temperature (Berkelmans and Van Oppen, 2006; Lajeunesse et al., 2014; Hoadley et al., 2019), this genus is also often abundant with corals inhabiting turbid reefs and shallow high-light environments (Hoadley et al., 2019; Wall et al., 2020). However, it appears that other coral species in mangrove lagoons are not predominately associated with *Durusdinium*, but instead with ITS2 types corresponding to *Cladocopium* [e.g., *Porites lutea* (Woody Isles; Camp et al., 2019), *Acropora muricata* and *Acropora pulchra* (New Caledonia; Camp et al., 2020)]. Our contrasting findings for *P. acuta* suggest that Symbiodiniaceae-coral associations in multi-stress mangrove environments is species specific.

Symbiodiniaceae communities remained stable over time in both the reef and mangrove corals, which is consistent with previous studies in reef environments (Klepac et al., 2015; Cai et al., 2018; Epstein et al., 2019). However, it is perhaps surprising that after 9 months of reciprocal-transplantation, the seasonally dependent photo-physiological signatures of these Symbiodiniaceae communities remained unchanged from their native state. Corals have been known to shift their dominant Symbiodiniaceae compositions from *Cladocopium* to *Durusdinium* following changes in environmental conditions (Jones et al., 2008; Cunning et al., 2018). However, the conserved association observed after transplantation in this study reveals a high capacity to tolerate the new environmental regimes over 9 months. Transplantation began during the beginning of winter (t_0, May 2018) when the various environmental conditions between the two sites were more similar than towards the end of the experiment in summer (t_{6-9M}, December 2018–February 2019) (**Supplementary Table 1**), suggesting the change in conditions were slow enough for acclimatisation of the inherent Symbiodiniaceae-host association.

Similar to the Symbiodiniaceae communities, coral-associated bacterial communities differed between *P. acuta* colonies inhabiting mangrove and reef environments. Such difference among sites is consistent with previous studies that have identified highly divergent bacterial communities in *P. acuta*

over small spatial scales (Wainwright et al., 2019; Deignan and McDougald, 2021). However, despite the dynamic nature of *P. acuta* microbiomes over small geographical scales, *P. acuta* microbiomes appear to remain relatively stable under thermal stress (Epstein et al., 2019). One notable feature among mangrove *P. acuta* colonies was the exceptionally high diversity of bacteria observed at both the ASV and genus levels. Compared to other reported values (Shannon's index 1.5–3.5) in previous *P. acuta* studies (Epstein et al., 2019; Wainwright et al., 2019), alpha diversity values in our study were more than twofold higher. High bacterial diversity (Simpson's index 75) has also been observed in some mangrove corals in New Caledonia, but these patterns are not consistent across all mangrove coral species, with some exhibiting much lower values (Simpson's index 1–4) (Camp et al., 2020). Additionally, the *P. acuta* colonies within the mangroves lacked a core microbiome and only a few members of the bacterial assemblage exceeded 5% average relative abundance. Compared to the oligotrophic and often stable conditions of tropical reefs, mangrove environments are highly heterogeneous, with dynamic physiochemical shifts, and impacts from higher nutrient loads and organic content (Huxham et al., 2010; Camp et al., 2017; De Valck and Rolfe, 2018). These more heterogenous conditions likely favour a more diverse microbial community that would conceivably harbour greater responsiveness to changing environmental conditions than a microbiome dominated by only a few species (Roder et al., 2015).

In contrast to the lack of a core microbiome among *P. acuta* colonies inhabiting the mangrove environment, five ASVs belonging to the *Endozoicomonas* genus were identified as members of a core microbiome in the reef colonies. *Endozoicomonas* was also the most relatively abundant bacterial genus in reef corals, a common observation in *P. acuta* (Epstein et al., 2019; Damjanovic et al., 2020a,b) and many other coral microbiome studies (Bayer et al., 2013; Neave et al., 2017; Pogoreutz et al., 2018; Glasl et al., 2019; Ziegler et al., 2019; Haydon et al., 2021). While *Endozoicomonas* was also present in mangrove corals, there was a large difference in the total relative abundance of this genus between the two environments (reef 40%, mangrove 7%). This is consistent with previous reports from corals in mangroves and adjacent reefs in New Caledonia (Camp et al., 2020).

Transplanted Corals Undergo Rapid Shifts in Bacterial Community Composition and Loss of Core Communities Over Time

After 9 months of transplantation (t_{9M}), coral associated bacterial communities in the native transplants (reef-reef) underwent very little change in composition, suggesting there had been little to no effect of transplantation on the bacterial communities associated with these corals. In contrast, the bacterial communities associated with the mangrove-mangrove corals differed significantly over all six timepoints sampled, highlighting a dynamic relationship between bacterial communities and the environment.

The bacteria communities associated with both groups of cross-habitat transplanted colonies (reef-mangrove, mangrove-reef) underwent strong shifts over the 9-month duration of the experiment. This pattern is in contrast to previous studies, that have shown that the bacterial communities associated with *Pocillopora* corals (*P. acuta* or the closely related *Pocillopora verrucosa*) remain relatively stable even when subjected to dramatic changes in environmental conditions, including temperature or pollution (Sawall et al., 2015; Pogoreutz et al., 2018; Epstein et al., 2019; Ziegler et al., 2019). Changes in bacterial communities were apparent after only 3 days in the mangrove-reef corals. Such rapid changes in bacterial community structure indicates plasticity among mangrove corals but also outlines the presence of strong environmental pressure on the microbiome.

Extreme fluctuations over diel and tidal cycles at Woody Isles (Camp et al., 2019) and other mangrove lagoon systems (Camp et al., 2017), as well as the enriched nutrient conditions present in mangrove environments compared to adjacent reefs (De Valck and Rolfe, 2018), are likely underlying factors for the profound changes observed in reef-mangrove *P. acuta* associated bacterial communities. Coral microbiomes can be altered by shifting environmental conditions such as nutrient availability (Zaneveld et al., 2016; Ziegler et al., 2019), temperature (Wang et al., 2018; Gardner et al., 2019), pH (Webster et al., 2016; Grottoli et al., 2018), and salinity (Röthig et al., 2016). In addition, internal physiochemical conditions of corals with thin tissue (e.g., *Pocillopora*) are more influenced by the external environment compared to those with thicker tissue (Putnam et al., 2017). Therefore, given the short generation times of bacteria and their ability to respond to changes in environmental conditions and physiochemical gradients at a rapid rate, we propose that the inherently high environmental variations in mangrove lagoons promotes changes in the bacterial composition of transplanted corals as well as in the native mangrove colonies.

Changes in bacterial communities in reef-mangrove corals after transplantation were largely characterised by a rapid decrease in relative abundance, and potential loss, of *Endozoicomonas*. These patterns are notable, given the prominence, and potentially important function, of members of this genus in coral microbiomes (Neave et al., 2016, 2017). Our findings are consistent to other studies that have observed significant reductions in the relative abundance of *Endozoicomonas* under changing environmental conditions that promote coral stress (Bourne et al., 2008; Roder et al., 2015; Ziegler et al., 2016; Gignoux-Wolfsohn et al., 2017). While a range of changing environmental conditions may be responsible for the decreased abundance of this bacteria in reef-mangrove colonies, *Endozoicomonas* is thought to be particularly sensitive to changes in pH (Morrow et al., 2015). One study found that coral-associated *Endozoicomonas* were significantly reduced at low pH (7.9), suggesting that a decrease in pH could even result in the loss of *Endozoicomonas* (Webster et al., 2016). Following 3 months of transplantation (t_{3M}), when we observed a significant shift in the bacterial communities of Reef-mangrove colonies from their original state, the pH in the mangrove environment (pH 7.8) was 0.3 units lower than in the reef environment (pH 8.1). The acidic conditions of the mangrove environment are likely responsible for the loss of other coral-associated bacteria among reef corals.

Corals Transplanted From the Reef to the Mangrove Develop Bacterial Communities That Resemble Native Mangrove Corals

In line with recent studies in thermally variable habitats (in *Acropora hyacinthus*) and polluted sites (in *Acropora hemprichii*) (Ziegler et al., 2017, 2019), transplanted coral-associated bacteria communities (reef-mangrove) became similar to those of the native transplanted corals (mangrove-mangrove) by the end of the experiment. Besides the observed shifts in the relative abundance of bacterial communities in reef-mangrove colonies there was also an acquisition of many new low abundant bacteria (<1%) that were not present prior to transplantation. An increase in bacterial diversity is thought to be indicative of a holobiont stress response (Thurber et al., 2009; Zaneveld et al., 2017), whereby opportunists shift species dominance away from symbiotic bacterial members. However, considering the high bacterial diversity of the native mangrove corals (mangrove-mangrove), this is perhaps more suggestive of local environmental conditions selecting for a more metabolically diverse community of bacteria (Kelly et al., 2014), which may be beneficial to the host under variable environmental conditions. In contrast to the patterns seen in the reef-mangrove transplants, the bacterial communities of mangrove-reef transplanted corals did not resemble the native reef-reef colonies by the end of the experiment. We did observe a significant decrease in bacterial diversity in mangrove-reef corals between the beginning of the experiment and 9 months later, characterised with a divergence from their original state, but no resemblance to the native reef corals. However, each individual replicate was dominated by different bacteria, suggesting an acclimation response and stabilised microbial community function in each coral colony. Thus, the relatively stable conditions on the reef may have played an important role in selecting for the increased abundance of specific bacteria.

CONCLUSION

Here we examined the microbial (Symbiodiniaceae and bacterial) communities associated with *P. acuta* in mangrove lagoon and adjacent reef, and characterised the effect of the surrounding environment on the structure of the microbiome by transplanting corals between the sites. We show that corals living in extreme mangrove environments support highly diverse and transient bacterial communities, which could be beneficial and allow them to cope under environmental variability. In comparison, reef corals maintained more consistent bacterial communities with highly dominant members. Transplantation of corals induced major shifts in bacterial composition, but had little to no effect on the Symbiodiniaceae communities. Our results reveal that coral-associated Symbiodiniaceae communities are initially shaped by divergent environmental conditions, but appeared unaffected by longer term (9 month) changes to these conditions. Bacterial communities changed rapidly following transplantation, suggesting strong selective pressure from the environment. The dynamic nature of the bacterial communities in resident mangrove corals reflects that of the microbiomes of corals persisting in other extreme environments – such as *A. hemprichii*, *A. hyacinthus*, and *P. verrucosa* – which have exhibited acclimation and adaptation potential (Ziegler et al., 2017, 2019). This research demonstrated the dynamic nature of *P. acuta* bacterial communities and highlights the strong influence of changing environmental conditions on their community structure.

DATA AVAILABILITY STATEMENT

The datasets presented in this study can be found in online repositories. Raw fastq read files were deposited in the NCBI Sequence Read Archive (SRA), accession number: PRJNA764039.

AUTHOR CONTRIBUTIONS

DS and EC designed the experiments. EC, TH, DS, and JE collected and processed the samples. TH performed all laboratory work and data analysis. TH and J-BR produced the figures. TH, JS, J-BR, DS, and EC wrote the manuscript. All authors edited the manuscript.

FUNDING

This research was funded by the AMP Foundation (Tomorrow Maker Award "Future-proofing the Great Barrier Reef through climate change-resilient super corals") to DS. Additional support was provided through ARC Discovery Project DP180100074 (DS), and the contribution to manuscript writing and final preparation was through the University of Technology Sydney Chancellor's Post-doctoral Research Fellowship and ARC Discovery Early Career Research Award (DE190100142) to EC, and Human Frontier Science Programme Long-term Post-doctoral Fellowship LT000625/2018-L to JM. All field activities were conducted under Great Barrier Reef Marine Park Authority Permit number G19/42553 to EC and DS.

ACKNOWLEDGMENTS

We would like to thank Lorna Howlett, Mickael Ros, David Hughes, Jenny Edmondson, and the Wavelength crew for their assistance with fieldwork. We would also like to thank Benjamin Hume for his assistance with the SymPortal, Sebastian Schmidt-Roach for his support with matching the reference sequences for *P. acuta*, and Emmanuelle Botté for her help with the figures.

SUPPLEMENTARY MATERIAL

The Supplementary Material for this article can be found online at: https://www.frontiersin.org/articles/10.3389/fmicb.2021.756091/full#supplementary-material

REFERENCES

Altieri, A. H., Harrison, S. B., Seemann, J., Collin, R., Diaz, R. J., and Knowlton, N. (2017). Tropical dead zones and mass mortalities on coral reefs. *Proc. Natl. Acad. Sci. U. S. A.* 114, 3660–3665. doi: 10.1073/pnas.1621517114

Barshis, D. J., Stillman, J. H., Gates, R. D., Toonen, R. J., Smith, L. W., and Birkeland, C. (2010). Protein expression and genetic structure of the coral Porites lobata in an environmentally extreme Samoan back reef: does host genotype limit phenotypic plasticity? *Mol. Ecol.* 19, 1705–1720. doi: 10.1111/j.1365-294X.2010.04574.x

Bayer, T., Neave, M. J., Alsheikh-Hussain, A., Aranda, M., Yum, L. K., Mincer, T., et al. (2013). The microbiome of the red sea coral stylophora pistillata is dominated by tissue-associated endozoicomonas bacteria. *Appl. Environ. Microbiol.* 79, 4759–4762. doi: 10.1128/AEM.00695-13

Berkelmans, R., and Van Oppen, M. J. H. (2006). The role of zooxanthellae in the thermal tolerance of corals: a "nugget of hope" for coral reefs in an era of climate change. *Proc. R. Soc. B Biol. Sci.* 273, 2305–2312. doi: 10.1098/rspb.2006.3567

Bolyen, E., Rideout, J. R., Dillon, M. R., Bokulich, N. A., Abnet, C. C., Al-Ghalith, G. A., et al. (2019). Reproducible, interactive, scalable and extensible microbiome data science using QIIME 2. *Nat. Biotechnol.* 37, 852–857. doi: 10.1038/s41587-019-0209-9

Bourne, D., Iida, Y., Uthicke, S., and Smith-Keune, C. (2008). Changes in coral-associated microbial communities during a bleaching event. *ISME J.* 2, 350–363. doi: 10.1038/ismej.2007.112

Bourne, D. G., Morrow, K. M., and Webster, N. S. (2016). Insights into the Coral Microbiome: underpinning the Health and Resilience of Reef Ecosystems. *Annu. Rev. Microbiol.* 70, 317–340. doi: 10.1146/annurev-micro-102215-095440

Cai, L., Zhou, G., Tong, H., Tian, R. M., Zhang, W., Ding, W., et al. (2018). Season structures prokaryotic partners but not algal symbionts in subtropical hard corals. *Appl. Microbiol. Biotechnol.* 102, 4963–4973. doi: 10.1007/s00253-018-8909-5

Callahan, B. J., McMurdie, P. J., Rosen, M. J., Han, A. W., Johnson, A. J. A., and Holmes, S. P. (2016). DADA2: high-resolution sample inference from Illumina amplicon data. *Nat. Methods* 13, 581–583. doi: 10.1038/nmeth.3869

Camacho, C., Coulouris, G., Avagyan, V., Ma, N., Papadopoulos, J., Bealer, K., et al. (2009). BLAST+: architecture and applications. *BMC Bioinformatics* 101:421. doi: 10.1186/1471-2105-10-421

Camp, E., Edmondson, J., Doheny, A., Rumney, J., Grima, A., Huete, A., et al. (2019). Mangrove lagoons of the Great Barrier Reef support coral populations persisting under extreme environmental conditions. *Mar. Ecol. Prog. Ser.* 625, 1–14. doi: 10.3354/meps13073

Camp, E. F., Nitschke, M. R., Rodolfo-Metalpa, R., Houlbreque, F., Gardner, S. G., Smith, D. J., et al. (2017). Reef-building corals thrive within hot-acidified and deoxygenated waters. *Sci. Rep.* 7:2434. doi: 10.1038/s41598-017-02383-y

Camp, E. F., Schoepf, V., Mumby, P. J., Hardtke, L. A., Rodolfo-Metalpa, R., Smith, D. J., et al. (2018). The future of coral reefs subject to rapid climate change: lessons from natural extreme environments. *Front. Mar. Sci.* 5:4. doi: 10.3389/fmars.2018.00004

Camp, E. F., Suggett, D. J., Pogoreutz, C., Nitschke, M. R., Houlbreque, F., Hume, B. C. C., et al. (2020). Corals exhibit distinct patterns of microbial reorganisation to thrive in an extreme inshore environment. *Coral Reefs* 39, 701–716. doi: 10.1007/s00338-019-01889-3

Chapron, L., Lartaud, F., Le Bris, N., Peru, E., and Galand, P. E. (2020). Local Variability in Microbiome Composition and Growth Suggests Habitat Preferences for Two Reef-Building Cold-Water Coral Species. *Front. Microbiol.* 11:275. doi: 10.3389/fmicb.2020.00275

Cohen, I., and Dubinsky, Z. (2015). Long term photoacclimation responses of the coral Stylophora pistillata to reciprocal deep to shallow transplantation: photosynthesis and calcification. *Front. Mar. Sci.* 2:45. doi: 10.3389/fmars.2015.00045

Coleman, A. W., Suarez, A., and Goff, L. J. (1994). Molecular deliniation of species and syngens in volvocacean green algae (*Chlorophyta*)1. *J. Phycol.* 30, 80–90. doi: 10.1111/J.0022-3646.1994.00080.X

Cornwall, C. E., Comeau, S., Kornder, N. A., Perry, C. T., van Hooidonk, R., DeCarlo, T. M., et al. (2021). Global declines in coral reef calcium carbonate production under ocean acidification and warming. *Proc. Natl. Acad. Sci. U. S. A.* 118:e2015265118. doi: 10.1073/pnas.2015265118

Cropp, R., and Norbury, J. (2020). The potential for coral reefs to adapt to a changing climate - an eco-evolutionary modelling perspective. *Ecol. Modell.* 426:109038. doi: 10.1016/j.ecolmodel.2020.109038

Cunning, R., Gillette, P., Capo, T., Galvez, K., and Baker, A. C. (2015a). Growth tradeoffs associated with thermotolerant symbionts in the coral Pocillopora damicornis are lost in warmer oceans. *Coral Reefs* 34, 155–160. doi: 10.1007/s00338-014-1216-4

Cunning, R., Silverstein, R. N., and Baker, A. C. (2015b). Investigating the causes and consequences of symbiont shuffling in a multi-partner reef coral symbiosis under environmental change. *Proc. R. Soc. B Biol. Sci.* 282:20141725. doi: 10.1098/rspb.2014.1725

Cunning, R., Silverstein, R. N., and Baker, A. C. (2018). Symbiont shuffling linked to differential photochemical dynamics of Symbiodinium in three Caribbean reef corals. *Coral Reefs* 37, 145–152. doi: 10.1007/s00338-017-1640-3

Damjanovic, K., Menéndez, P., Blackall, L. L., and van Oppen, M. J. H. (2020b). Mixed-mode bacterial transmission in the common brooding coral Pocillopora acuta. *Environ. Microbiol.* 22, 397–412. doi: 10.1111/1462-2920.14856

Damjanovic, K., Blackall, L. L., Menéndez, P., and van Oppen, M. J. H. (2020a). Bacterial and algal symbiont dynamics in early recruits exposed to two adult coral species. *Coral Reefs* 39, 189–202. doi: 10.1007/s00338-019-01871-z

Damjanovic, K., Blackall, L. L., Webster, N. S., and van Oppen, M. J. H. (2017). The contribution of microbial biotechnology to mitigating coral reef degradation. *Microb. Biotechnol.* 10, 1236–1243. doi: 10.1111/1751-7915.12769

De Valck, J., and Rolfe, J. (2018). Linking water quality impacts and benefits of ecosystem services in the Great Barrier Reef. *Mar. Pollut. Bull.* 130, 55–66. doi: 10.1016/j.marpolbul.2018.03.017

Deignan, L. K., and McDougald, D. (2021). Differential Response of the Microbiome of Pocillopora acuta to Reciprocal Transplantation Within Singapore. *Microb. Ecol.* doi: 10.1007/s00248-021-01793-w [Epub Online ahead of print].

Dixon, G., Liao, Y., Bay, L. K., and Matz, M. V. (2018). Role of gene body methylation in acclimatization and adaptation in a basal metazoan. *Proc. Natl. Acad. Sci. U. S. A.* 115, 13342–13346. doi: 10.1073/pnas.1813749115

Doering, T., Wall, M., Putchim, L., Rattanawongwan, T., Schroeder, R., Hentschel, U., et al. (2021). Towards enhancing coral heat tolerance: a "microbiome transplantation" treatment using inoculations of homogenized coral tissues. *Microbiome* 9:102. doi: 10.1186/s40168-021-01053-6

Epstein, H. E., Torda, G., and van Oppen, M. J. H. (2019). Relative stability of the Pocillopora acuta microbiome throughout a thermal stress event. *Coral Reefs* 38, 373–386. doi: 10.1007/s00338-019-01783-y

Eren, A. M., Morrison, H. G., Lescault, P. J., Reveillaud, J., Vineis, J. H., and Sogin, M. L. (2014). Minimum entropy decomposition: unsupervised oligotyping for sensitive partitioning of high-throughput marker gene sequences. *ISME J.* 94, 968–979. doi: 10.1038/ismej.2014.195

Flot, J. F., and Tillier, S. (2007). The mitochondrial genome of Pocillopora (*Cnidaria*: *scleractinia*) contains two variable regions: the putative D-loop and a novel ORF of unknown function. *Gene* 401, 80–87. doi: 10.1016/j.gene.2007.07.006

Fragoso Ados Santos, H., Duarte, G. A. S., Rachid, C. T. D. C., Chaloub, R. M., Calderon, E. N., Marangoni, L. F. D. B., et al. (2015). Impact of oil spills on coral reefs can be reduced by bioremediation using probiotic microbiota. *Sci. Rep.* 5:18268. doi: 10.1038/srep18268

Gardner, S. G., Camp, E. F., Smith, D. J., Kahlke, T., Osman, E. O., Gendron, G., et al. (2019). Coral microbiome diversity reflects mass coral bleaching susceptibility during the 2016 El Niño heat wave. *Ecol. Evol.* 9, 938–956. doi: 10.1002/ece3.4662

Gignoux-Wolfsohn, S. A., Aronson, F. M., and Vollmer, S. V. (2017). Complex interactions between potentially pathogenic, opportunistic, and resident bacteria emerge during infection on a reef-building coral. *FEMS Microbiol. Ecol.* 93:80. doi: 10.1093/femsec/fix080

Glasl, B., Herndl, G. J., and Frade, P. R. (2016). The microbiome of coral surface mucus has a key role in mediating holobiont health and survival upon disturbance. *ISME J.* 10, 2280–2292. doi: 10.1038/ismej.2016.9

Glasl, B., Smith, C. E., Bourne, D. G., and Webster, N. S. (2019). Disentangling the effect of host-genotype and environment on the microbiome of the coral Acropora tenuis. *PeerJ* 7:e6377. doi: 10.7717/peerj.6377

Gonzalez, E., Pitre, F. E., and Brereton, N. J. B. (2019). ANCHOR: a 16S rRNA gene amplicon pipeline for microbial analysis of multiple environmental samples. *Environ. Microbiol.* 21, 2440–2468. doi: 10.1111/1462-2920.14632

Grottoli, A. G., Dalcin Martins, P., Wilkins, M. J., Johnston, M. D., Warner, M. E., Cai, W.-J., et al. (2018). Coral physiology and microbiome dynamics under combined warming and ocean acidification. *PLoS One* 13:e0191156. doi: 10.1371/journal.pone.0191156

Haydon, T. D., Suggett, D. J., Siboni, N., Kahlke, T., Camp, E. F., and Seymour, J. R. (2021). Temporal Variation in the Microbiome of Tropical and Temperate Octocorals. *Microb. Ecol.* doi: 10.1007/S00248-021-01823-7 [Epub Online ahead of print].

Hoadley, K. D., Lewis, A. M., Wham, D. C., Pettay, D. T., Grasso, C., Smith, R., et al. (2019). Host–symbiont combinations dictate the photo-physiological response of reef-building corals to thermal stress. *Sci. Rep.* 9:9985. doi: 10.1038/s41598-019-46412-4

Hoegh-Guldberg, O., Poloczanska, E. S., Skirving, W., and Dove, S. (2017). Coral reef ecosystems under climate change and ocean acidification. *Front. Mar. Sci.* 4:158. doi: 10.3389/fmars.2017.00158

Howells, E. J., Abrego, D., Meyer, E., Kirk, N. L., and Burt, J. A. (2016). Host adaptation and unexpected symbiont partners enable reef-building corals to tolerate extreme temperatures. *Glob. Chang. Biol.* 22, 2702–2714. doi: 10.1111/gcb.13250

Howells, E. J., Bauman, A. G., Vaughan, G. O., Hume, B. C. C., Voolstra, C. R., and Burt, J. A. (2020). Corals in the hottest reefs in the world exhibit symbiont fidelity not flexibility. *Mol. Ecol.* 29, 899–911. doi: 10.1111/mec.15372

Howells, E. J., Beltran, V. H., Larsen, N. W., Bay, L. K., Willis, B. L., and Van Oppen, M. J. H. (2012). Coral thermal tolerance shaped by local adaptation of photosymbionts. *Nat. Clim. Chang.* 2, 116–120. doi: 10.1038/nclimate1330

Hughes, D. J., Alderdice, R., Cooney, C., Kühl, M., Pernice, M., Voolstra, C. R., et al. (2020). Coral reef survival under accelerating ocean deoxygenation. *Nat. Clim. Chang.* 10, 296–307. doi: 10.1038/s41558-020-0737-9

Hughes, T. P., Kerry, J. T., Baird, A. H., Connolly, S. R., Dietzel, A., Eakin, C. M., et al. (2018). Global warming transforms coral reef assemblages. *Nature* 556, 492–496. doi: 10.1038/s41586-018-0041-2

Hume, B. C. C., Smith, E. G., Ziegler, M., Warrington, H. J. M., Burt, J. A., LaJeunesse, T. C., et al. (2019). SymPortal: a novel analytical framework and platform for coral algal symbiont next-generation sequencing *ITS2* profiling. *Mol. Ecol. Resour.* 19, 1063–1080. doi: 10.1111/1755-0998.13004

Huxham, M., Langat, J., Tamooh, F., Kennedy, H., Mencuccini, M., Skov, M. W., et al. (2010). Decomposition of mangrove roots: effects of location, nutrients, species identity and mix in a Kenyan forest. *Estuar. Coast. Shelf Sci.* 88, 135–142. doi: 10.1016/j.ecss.2010.03.021

Innis, T., Cunning, R., Ritson-Williams, R., Wall, C. B., and Gates, R. D. (2018). Coral color and depth drive symbiosis ecology of Montipora capitata in Kāneʻohe Bay, Oʻahu, Hawaiʻi. *Coral Reefs* 37, 423–430. doi: 10.1007/s00338-018-1667-0

Jones, A. M., Berkelmans, R., Van Oppen, M. J. H., Mieog, J. C., and Sinclair, W. (2008). A community change in the algal endosymbionts of a *scleractinian coral* following a natural bleaching event: field evidence of acclimatization. *Proc. R. Soc. B Biol. Sci.* 275, 1359–1365. doi: 10.1098/rspb.2008.0069

Kahlke, T. (2018). *timkahlke/panbiom 1.0 (Version 1.0)*. European: Zenodo. doi: 10.5281/zenodo.1137875

Kelly, L. W., Williams, G. J., Barott, K. L., Carlson, C. A., Dinsdale, E. A., Edwards, R. A., et al. (2014). Local genomic adaptation of coral reef-associated microbiomes to gradients of natural variability and anthropogenic stressors. *Proc. Natl. Acad. Sci. U. S. A.* 111, 10227–10232. doi: 10.1073/pnas.1403319111

Klepac, C., Beal, J., Kenkel, C., Sproles, A., Polinski, J., Williams, M., et al. (2015). Seasonal stability of coral-Symbiodinium associations in the subtropical coral habitat of St. Lucie Reef, Florida. *Mar. Ecol. Prog. Ser.* 532, 137–151. doi: 10.3354/meps11369

Klepac, C. N., and Barshis, D. J. (2020). Reduced thermal tolerance of massive coral species in a highly variable environment. *Proc. Biol. Sci.* 287:20201379. doi: 10.1098/rspb.2020.1379

Klindworth, A., Pruesse, E., Schweer, T., Peplies, J., Quast, C., Horn, M., et al. (2013). Evaluation of general 16S ribosomal RNA gene PCR primers for classical and next-generation sequencing-based diversity studies. *Nucleic Acids Res.* 41:e1. doi: 10.1093/NAR/GKS808

LaJeunesse, T. (2002). Diversity and community structure of symbiotic dinoflagellates from Caribbean coral reefs. *Mar. Biol.* 1412, 387–400. doi: 10.1007/S00227-002-0829-2

Lajeunesse, T. C., Wham, D. C., Pettay, D. T., Parkinson, J. E., Keshavmurthy, S., and Chen, C. A. (2014). Ecologically differentiated stress-tolerant endosymbionts in the dinoflagellate genus Symbiodinium (*Dinophyceae*) Clade D are different species. *Phycologia* 53, 305–319. doi: 10.2216/13-186.1

Lewis, C., Neely, K., and Rodriguez-Lanetty, M. (2019). Recurring episodes of thermal stress shift the balance from a dominant host-specialist to a background host-generalist zooxanthella in the threatened pillar coral, Dendrogyra cylindrus. *Front. Mar. Sci.* 6:5. doi: 10.3389/fmars.2019.00005

Lord, K. S., Lesneski, K., and Kuhn, K. M. (2020). Multi-Year Viability of a Reef Coral Population Living on Mangrove Roots Suggests an Important Role for Mangroves in the Broader Habitat Mosaic of Corals. *Front. Mar. Sci.* 7:377. doi: 10.3389/fmars.2020.00377

Macintyre, I. G., Goodbody, I., Rutzler, K., Littler, D. S., and Littler, M. M. (2000). A general biological and geological survey of the rims of ponds in the major Mangrove Islands of the Pelican Cays, Belize. *Atoll Res. Bull.* 15–44. doi: 10.5479/si.00775630.467.15

Maggioni, F., Pujo-Pay, M., Aucan, J., Cerrano, C., Calcinai, B., Payri, C., et al. (2021). The Bouraké semi-enclosed lagoon (New Caledonia) – a natural laboratory to study the lifelong adaptation of a coral reef ecosystem to extreme environmental conditions. *Biogeosciences* 18, 5117–5140. doi: 10.5194/BG-18-5117-2021

McDevitt-Irwin, J. M., Baum, J. K., Garren, M., and Vega Thurber, R. L. (2017). Responses of coral-associated bacterial communities to local and global stressors. *Front. Mar. Sci.* 4:262. doi: 10.3389/fmars.2017.00262

Morrow, K. M., Bourne, D. G., Humphrey, C., Botté, E. S., Laffy, P., Zaneveld, J., et al. (2015). Natural volcanic CO2 seeps reveal future trajectories for host-microbial associations in corals and sponges. *ISME J.* 9, 894–908. doi: 10.1038/ismej.2014.188

Neave, M. J., Apprill, A., Ferrier-Pagès, C., and Voolstra, C. R. (2016). Diversity and function of prevalent symbiotic marine bacteria in the genus Endozoicomonas. *Appl. Microbiol. Biotechnol.* 100, 8315–8324. doi: 10.1007/s00253-016-7777-0

Neave, M. J., Rachmawati, R., Xun, L., Michell, C. T., Bourne, D. G., Apprill, A., et al. (2017). Differential specificity between closely related corals and abundant Endozoicomonas endosymbionts across global scales. *ISME J.* 11, 186–200. doi: 10.1038/ismej.2016.95

Nitschke, M. R., Gardner, S. G., Goyen, S., Fujise, L., Camp, E. F., Ralph, P. J., et al. (2018). Utility of photochemical traits as diagnostics of thermal tolerance amongst great barrier reef corals. *Front. Mar. Sci.* 5:45. doi: 10.3389/FMARS.2018.00045

Oliver, T. A., and Palumbi, S. R. (2011). Many corals host thermally resistant symbionts in high-temperature habitat. *Coral Reefs* 30, 241–250. doi: 10.1007/s00338-010-0696-0

Osman, E. O., Suggett, D. J., Voolstra, C. R., Pettay, D. T., Clark, D. R., Pogoreutz, C., et al. (2020). Coral microbiome composition along the northern Red Sea suggests high plasticity of bacterial and specificity of endosymbiotic dinoflagellate communities. *Microbiome* 8, 1–16. doi: 10.1186/s40168-019-0776-5

Padilla-Gamiño, J. L., Hanson, K. M., Stat, M., and Gates, R. D. (2012). Phenotypic plasticity of the coral Porites rus: acclimatization responses to a turbid environment. *J. Exp. Mar. Bio. Ecol.* 434–435, 71–80. doi: 10.1016/j.jembe.2012.08.006

Palumbi, S. R., Barshis, D. J., Traylor-Knowles, N., and Bay, R. A. (2014). Mechanisms of reef coral resistance to future climate change. *Science* 344, 895–898. doi: 10.1126/science.1251336

Paulson, J. N., Colin Stine, O., Bravo, H. C., and Pop, M. (2013). Differential abundance analysis for microbial marker-gene surveys. *Nat. Methods* 10, 1200–1202. doi: 10.1038/nmeth.2658

Pedregosa, F., Varoquaux, G., Gramfort, A., Michel, V., Thirion, B., Grisel, O., et al. (2011). Scikit-learn: machine Learning in Python. *J. Mach. Learn. Res.* 12, 2825–2830.

Pogoreutz, C., Rädecker, N., Cárdenas, A., Gärdes, A., Wild, C., and Voolstra, C. R. (2018). Dominance of Endozoicomonas bacteria throughout coral bleaching and mortality suggests structural inflexibility of the Pocillopora verrucosa microbiome. *Ecol. Evol.* 8, 2240–2252. doi: 10.1002/ece3.3830

Pootakham, W., Mhuantong, W., Yoocha, T., Putchim, L., Jomchai, N., Sonthirod, C., et al. (2019). Heat-induced shift in coral microbiome reveals several members of the Rhodobacteraceae family as indicator species for thermal stress in Porites lutea. *Microbiologyopen* 8:e935. doi: 10.1002/mbo3.935

Putnam, H. M., Barott, K. L., Ainsworth, T. D., and Gates, R. D. (2017). The Vulnerability and Resilience of Reef-Building Corals. *Curr. Biol.* 27, R528–R540. doi: 10.1016/j.cub.2017.04.047

Rädecker, N., Pogoreutz, C., Gegner, H. M., Cárdenas, A., Roth, F., Bougoure, J., et al. (2021). Heat stress destabilizes symbiotic nutrient cycling in corals. *Proc. Natl. Acad. Sci. U. S. A.* 118:e2022653118. doi: 10.1073/PNAS.2022653118

Rädecker, N., Pogoreutz, C., Voolstra, C. R., Wiedenmann, J., and Wild, C. (2015). Nitrogen cycling in corals: the key to understanding holobiont functioning? *Trends Microbiol.* 23, 490–497. doi: 10.1016/j.tim.2015.03.008

Raina, J. B., Tapiolas, D., Willis, B. L., and Bourne, D. G. (2009). Coral-associated bacteria and their role in the biogeochemical cycling of sulfur. *Appl. Environ. Microbiol.* 75, 3492–3501. doi: 10.1128/AEM.02567-08

Ritchie, K. (2006). Regulation of microbial populations by coral surface mucus and mucus-associated bacteria. *Mar. Ecol. Prog. Ser.* 322, 1–14. doi: 10.3354/meps322001

Roder, C., Bayer, T., Aranda, M., Kruse, M., and Voolstra, C. R. (2015). Microbiome structure of the fungid coral C tenactis echinata aligns with environmental differences. *Mol. Ecol.* 24, 3501–3511.

Rogers, C. S. (2009). High diversity and abundance of *scleractinian corals* growing on and near mangrove prop roots. *Coral Reefs* 28:909. doi: 10.1007/s00338-009-0526-4

Rogers, C. S. (2017). *diversity A Unique Coral Community in the Mangroves of Hurricane Hole*. US Virgin Islands: St. John

Rogers, C. S., and Herlan, J. J. (2012). "Life on the edge: corals in mangroves and climate change," in *Proceedings of the 12th International Coral Reef Symposium*, (Cairns QLD: James Cook University).

Roitman, S., López-Londoño, T., Joseph Pollock, F., Ritchie, K. B., Galindo-Martínez, C. T., Gómez-Campo, K., et al. (2020). Surviving marginalized reefs: assessing the implications of the microbiome on coral physiology and survivorship. *Coral Reefs* 39, 795–807. doi: 10.1007/s00338-020-01951-5

Ros, M., Suggett, D. J., Edmondson, J., Haydon, T., Hughes, D. J., Kim, M., et al. (2021). Symbiont shuffling across environmental gradients aligns with changes in carbon uptake and translocation in the reef-building coral Pocillopora acuta. *Coral Reefs* 40, 595–607. doi: 10.1007/s00338-021-02066-1

Rosado, P. M., Leite, D. C. A., Duarte, G. A. S., Chaloub, R. M., Jospin, G., Nunes da Rocha, U., et al. (2019). Marine probiotics: increasing coral resistance to bleaching through microbiome manipulation. *ISME J.* 13, 921–936. doi: 10.1038/s41396-018-0323-6

Rosset, S., Koster, G., Brandsma, J., Hunt, A. N., Postle, A. D., and D'Angelo, C. (2019). Lipidome analysis of Symbiodiniaceae reveals possible mechanisms of heat stress tolerance in reef coral symbionts. *Coral Reefs* 38, 1241–1253. doi: 10.1007/s00338-019-01865-x

Röthig, T., Ochsenkühn, M. A., Roik, A., van der Merwe, R., and Voolstra, C. R. (2016). Long-term salinity tolerance is accompanied by major restructuring of the coral bacterial microbiome. *Mol. Ecol.* 25, 1308–1323. doi: 10.1111/mec.13567

Sawall, Y., Al-Sofyani, A., Hohn, S., Banguera-Hinestroza, E., Voolstra, C. R., and Wahl, M. (2015). Extensive phenotypic plasticity of a Red Sea coral over a strong latitudinal temperature gradient suggests limited acclimatization potential to warming. *Sci. Rep.* 5:8940. doi: 10.1038/srep08940

Schloss, P. D., Westcott, S. L., Ryabin, T., Hall, J. R., Hartmann, M., Hollister, E. B., et al. (2009). Introducing mothur: open-Source, Platform-Independent, Community-Supported Software for Describing and Comparing Microbial Communities. *Appl. Environ. Microbiol.* 75, 7537–7541. doi: 10.1128/AEM.01541-09

Schmidt-Roach, S., Miller, K. J., Lundgren, P., and Andreakis, N. (2014). With eyes wide open: a revision of species within and closely related to the Pocillopora damicornis species complex (*Scleractinia*; *Pocilloporidae*) using morphology and genetics. *Zool. J. Linn. Soc.* 170, 1–33. doi: 10.1111/ZOJ12092

Schoepf, V., Jung, M. U., McCulloch, M. T., White, N. E., Stat, M., and Thomas, L. (2020). Thermally Variable, Macrotidal Reef Habitats Promote Rapid Recovery From Mass Coral Bleaching. *Front. Mar. Sci.* 7:245. doi: 10.3389/fmars.2020.00245

Schoepf, V., Stat, M., Falter, J. L., and McCulloch, M. T. (2015). Limits to the thermal tolerance of corals adapted to a highly fluctuating, naturally extreme temperature environment. *Sci. Rep.* 5:17639. doi: 10.1038/srep17639

Sharp, K. H., Pratte, Z. A., Kerwin, A. H., Rotjan, R. D., and Stewart, F. J. (2017). Season, but not symbiont state, drives microbiome structure in the temperate coral Astrangia poculata. *Microbiome* 5:120. doi: 10.1186/s40168-017-0329-8

Suggett, D. J., Goyen, S., Evenhuis, C., Szabó, M., Pettay, D. T., Warner, M. E., et al. (2015). Functional diversity of photobiological traits within the genus *Symbiodinium* appears to be governed by the interaction of cell size with cladal designation. *New Phytol.* 208, 370–381. doi: 10.1111/nph.13483

Suggett, D. J., Warner, M. E., and Leggat, W. (2017). Symbiotic Dinoflagellate Functional Diversity Mediates Coral Survival under Ecological Crisis. *Trends Ecol. Evol.* 32, 735–745. doi: 10.1016/j.tree.2017.07.013

Sweet, M. J., Brown, B. E., Dunne, R. P., Singleton, I., and Bulling, M. (2017). Evidence for rapid, tide-related shifts in the microbiome of the coral Coelastrea aspera. *Coral Reefs* 36, 815–828. doi: 10.1007/s00338-017-1572-y

Tamir, R., Ben-Zvi, O., Eyal, G., Kramer, N., and Loya, Y. (2020). Reciprocal-transplantation between shallow and mesophotic stony corals. *Mar. Environ. Res.* 161:105035. doi: 10.1016/j.marenvres.2020.105035

Thomas, L., López, E. H., Morikawa, M. K., and Palumbi, S. R. (2019). Transcriptomic resilience, symbiont shuffling, and vulnerability to recurrent bleaching in reef-building corals. *Mol. Ecol.* 28, 3371–3382. doi: 10.1111/mec.15143

Thurber, R. V., Willner-Hall, D., Rodriguez-Mueller, B., Desnues, C., Edwards, R. A., Angly, F., et al. (2009). Metagenomic analysis of stressed coral holobionts. *Environ. Microbiol.* 11, 2148–2163. doi: 10.1111/j.1462-2920.2009.01935.x

Torda, G., Donelson, J. M., Aranda, M., Barshis, D. J., Bay, L., Berumen, M. L., et al. (2017). Rapid adaptive responses to climate change in corals. *Nat. Clim. Chang.* 7, 627–636. doi: 10.1038/nclimate3374

van Oppen, M. J. H., and Blackall, L. L. (2019). Coral microbiome dynamics, functions and design in a changing world. *Nat. Rev. Microbiol.* 17, 557–567. doi: 10.1038/s41579-019-0223-4

Wainwright, B. J., Afiq-Rosli, L., Zahn, G. L., and Huang, D. (2019). Characterisation of coral-associated bacterial communities in an urbanised marine environment shows strong divergence over small geographic scales. *Coral Reefs* 38, 1097–1106. doi: 10.1007/s00338-019-01837-1

Wall, C. B., Kaluhiokalani, M., Popp, B. N., Donahue, M. J., and Gates, R. D. (2020). Divergent symbiont communities determine the physiology and nutrition of a reef coral across a light-availability gradient. *ISME J.* 14, 945–958. doi: 10.1038/s41396-019-0570-1

Wang, L., Shantz, A. A., Payet, J. P., Sharpton, T. J., Foster, A., Burkepile, D. E., et al. (2018). Corals and Their Microbiomes Are Differentially Affected by Exposure to Elevated Nutrients and a Natural Thermal Anomaly. *Front. Mar. Sci.* 5:101. doi: 10.3389/fmars.2018.00101

Webster, N. S., Negri, A. P., Botté, E. S., Laffy, P. W., Flores, F., Noonan, S., et al. (2016). Host-associated coral reef microbes respond to the cumulative pressures of ocean warming and ocean acidification. *Sci. Rep.* 6:19324. doi: 10.1038/srep19324

Yu, X., Yu, K., Huang, W., Liang, J., Qin, Z., Chen, B., et al. (2020). Thermal acclimation increases heat tolerance of the *scleractinian coral* Acropora pruinosa. *Sci. Total Environ.* 733:139319. doi: 10.1016/j.scitotenv.2020.139319

Zaneveld, J. R., Burkepile, D. E., Shantz, A. A., Pritchard, C. E., McMinds, R., Payet, J. P., et al. (2016). Overfishing and nutrient pollution interact with temperature to disrupt coral reefs down to microbial scales. *Nat. Commun.* 7:11833. doi: 10.1038/ncomms11833

Zaneveld, J. R., McMinds, R., and Thurber, R. V. (2017). Stress and stability: applying the Anna Karenina principle to animal microbiomes. *Nat. Microbiol.* 2:17121. doi: 10.1038/nmicrobiol.2017.121

Zhang, Y., Yang, Q., Ling, J., Long, L., Huang, H., Yin, J., et al. (2021). Shifting the microbiome of a coral holobiont and improving host physiology by inoculation with a potentially beneficial bacterial consortium. *BMC Microbiol.* 21:130. doi: 10.1186/s12866-021-02167-5

Ziegler, M., Grupstra, C. G. B., Barreto, M. M., Eaton, M., BaOmar, J., Zubier, K., et al. (2019). Coral bacterial community structure responds to environmental change in a host-specific manner. *Nat. Commun.* 10:3092. doi: 10.1038/s41467-019-10969-5

Ziegler, M., Roik, A., Porter, A., Zubier, K., Mudarris, M. S., Ormond, R., et al. (2016). Coral microbial community dynamics in response to anthropogenic impacts near a major city in the central Red Sea. *Mar. Pollut. Bull.* 105, 629–640. doi: 10.1016/j.marpolbul.2015.12.045

Ziegler, M., Seneca, F. O., Yum, L. K., Palumbi, S. R., and Voolstra, C. R. (2017). Bacterial community dynamics are linked to patterns of coral heat tolerance. *Nat. Commun.* 8:4213. doi: 10.1038/ncomms14213

Conflict of Interest: The authors declare that the research was conducted in the absence of any commercial or financial relationships that could be construed as a potential conflict of interest.

Publisher's Note: All claims expressed in this article are solely those of the authors and do not necessarily represent those of their affiliated organizations, or those of the publisher, the editors and the reviewers. Any product that may be evaluated in this article, or claim that may be made by its manufacturer, is not guaranteed or endorsed by the publisher.

frontiers in Marine Science

ORIGINAL RESEARCH
published: 22 December 2021
doi: 10.3389/fmars.2021.802754

The Structure and Function of Gut Microbiomes of Two Species of Sea Urchins, *Mesocentrotus nudus* and *Strongylocentrotus intermedius*, in Japan

*Alfabetian Harjuno Condro Haditomo[1,2], Masanori Yonezawa[1], Juanwen Yu[1], Sayaka Mino[1], Yuichi Sakai[3] and Tomoo Sawabe[1]**

[1] *Laboratory of Microbiology, Faculty of Fisheries Sciences, Hokkaido University, Hakodate, Japan,* [2] *Aquaculture Department, Faculty of Fisheries and Marine Sciences, Universitas Diponegoro, Semarang, Indonesia,* [3] *Hakodate Fisheries Research, Hokkaido Research Organization, Local Independent Administrative Agency, Hakodate, Japan*

OPEN ACCESS

Edited by:
Fabiano Thompson, Federal University of Rio de Janeiro, Brazil

Reviewed by:
Reiji Tanaka, Mie University, Japan
Adam Michael Reitzel, University of North Carolina at Charlotte, United States

***Correspondence:**
Tomoo Sawabe
sawabe@fish.hokudai.ac.jp

Specialty section:
This article was submitted to Microbial Symbioses, a section of the journal Frontiers in Marine Science

Received: *27 October 2021*
Accepted: *25 November 2021*
Published: *22 December 2021*

Citation:
Haditomo AHC, Yonezawa M, Yu J, Mino S, Sakai Y and Sawabe T (2021) The Structure and Function of Gut Microbiomes of Two Species of Sea Urchins, Mesocentrotus nudus and Strongylocentrotus intermedius, in Japan. Front. Mar. Sci. 8:802754. doi: 10.3389/fmars.2021.802754

Sea urchin is an indicator of coastal environmental changes in the global warming era, and is also a model organism in developmental biology and evolution. Due to the depletion of wild resources, new aquaculture techniques for improving stocks have been well studied. The gut microbiome shapes various aspects of a host's physiology. However, these microbiome structures and functions on sea urchins, particularly *Mesocentrotus nudus* and *Strongylocentrotus intermedius* which are important marine bioresources commonly found in Japan, have not been fully investigated yet. Using metagenomic approaches including meta16S and shotgun metagenome sequencings, the structures, functions, and dynamics of the gut microbiome of *M. nudus* and *S. intermedius*, related to both habitat environment and host growth, were studied. Firstly, a broad meta16S analysis revealed that at the family level, *Psychromonadaceae* and *Flavobacteriaceae* reads (38–71%) dominated in these sea urchins, which is a unique feature observed in species in Japan. *Flavobacteriaceae* reads were more abundant in individuals after rearing in an aquarium with circulating compared to one with running water. *Campylobacteraceae* and *Vibrionaceae* abundances increased in both kinds of laboratory-reared sea urchins in both types of experiments. 2-weeks feeding experiments of *M. nudus* and *S. intermedius* transplanted from the farm to laboratory revealed that these gut microbial structures were affected by diet rather than rearing environments and host species. Secondly, further meta16S analysis of microbial reads related to *M. nudus* growth revealed that at least four Amplicon Sequence Variant (ASV) affiliated to *Saccharicrinis fermentans*, which is known to be a nitrogen (N_2) fixing bacterium, showed a significant positive correlation to the body weight and test diameter. Interestingly, gut microbiome comparisons using shotgun metagenome sequencing of individuals showing higher and lower growth rates revealed a significant abundance of "Nitrate and nitrite ammonification" genes in the higher-grown individuals

under the circulating water rearing. These findings provide new insights on the structure-function relationship of sea urchin gut microbiomes beyond previously reported nitrogen fixation function in sea urchin in 1950s; we discovered a nitrate reduction function into ammonium for the growth promotion of sea urchin.

Keywords: sea urchin, gut, microbiome, *Mesocentrotus nudus*, *Strongylocentrotus intermedius*

INTRODUCTION

Sea urchin is an important aquatic resource worldwide. However, its global production has been decreasing since the 1990s (Stefánsson et al., 2017). *Strongylocentrotus intermedius* and *Mesocentrotus nudus* are important fishery resources in many Asian countries. *S. intermedius* is found on the intertidal and subtidal rocky seabed in the northern region in the Pacific Ocean, the Sea of Japan, the Korean peninsula, northeastern China, Sakhalin, and Vladivostok (Agatsuma, 2013). *M. nudus* is found on the intertidal and subtidal seabed and is distributed from Dalian in China to Primorskyi Kray in Russia and Japan (Agatsuma, 2013; Takagi et al., 2019; Ding et al., 2020). As a result of the great efforts of pioneer biologists, seed production of both species has been established, currently on a practical level in Japan. Sea urchin has been used for over a hundred years as a model organism in developmental biology research (Wilson, 1895). Knowledge of sea urchins in the field of biology has expanded to include (1) the effects of toxic substances on their immune system, reproduction, and development (Nobre et al., 2015; Brown et al., 2020; Pikula et al., 2020; Rendell-Bhatti et al., 2021), (2) the gene expression involved in sea urchin fertilization and development stages (Li et al., 2020; Wessel et al., 2021; Cui et al., 2022), (3) the nervous system (Wood et al., 2018; Martín-Durán and Hejnol, 2021; Formery et al., 2021), and (4) sea urchin genomes (Sodergren et al., 2006; Kudtarkar and Cameron, 2017; Kinjo et al., 2018; Warner et al., 2021). Sea urchins have also been studied in various aspects related to the impact of current changing environments, such as ocean acidification and global warming to their development and growth (Dworjanyn and Byrne, 2018; García et al., 2018; Zhao et al., 2018; Houlihan et al., 2020).

Sea urchin has been studied for a long time as fisheries resources and model organisms of biology. However, there have been a few studies on general views of their gut microbes' structure, function, and dynamics, particularly using individual-level metagenome approaches (Hakim et al., 2015, 2016, 2019, Yao et al., 2019; Faddetta et al., 2020; Miller et al., 2021). The abundances of reads assigned to phyla *Bacteroidetes* and *Proteobacteria* were observed in the gut of *Tripneustes gratilla*, and those assigned to phyla *Fusobacteria* and *Proteobacteria* in *Diadema setosum* and *Stomopneustes variolaris* (Yao et al., 2019), and the order *Vibrionales* was abundant in wild American green sea urchin (Hakim et al., 2016). Compared to the important roles of gut microbiota in various animals, including humans (Sharma et al., 2019; Youngblut et al., 2019; Fong et al., 2020; Fan and Pedersen, 2021; Morais et al., 2021; Tang et al., 2021), knowledge of gut microbes of sea urchin is behind that of other animals. Only the roles of nitrogen-fixing microbes in the gut of sea urchins have been discussed since the 1950s to answer why C/N rich diet provides nutrition to sea urchins (Mann, 1977).

In this study, we applied a non-destructive individual methodology (Yamazaki et al., 2016) to sea urchin species, *S. intemedius* and *M. nudus*, in Japan for the first time, (1) to examine the external factors, e.g., environments and diets, affecting the structure of the sea urchin gut microbiome, and (2) to explore the function of those gut microbiomes and specific microbes contributing to host growth by monitoring fecal microbiome changes. Here, we report new insights into the gut microbiome's structure, function, and dynamics of two sea urchin species in Japan.

MATERIALS AND METHODS

Samples Collection

M. nudus (n = 13) cultured at the Esan Seedling Center (ESC), Hakodate, and *S. intermedius* (n = 4) cultured at the Toi Seedling Center (TSC), Hakodate, in 2014 and 2015, were used in these individual microbiome studies. Both ESC and TSC were also designated to be Farm below. The procedure for rearing the two species of sea urchin larvae was carried out based on Sakai et al. (2003). Wild individuals of *M. nudus* (n = 4) and *S. intermedius* (n = 4) collected at Menagawa, Hakodate, in 2015 were also used as a comparison. We did not need a specific authorization to handle wild animals' feces. The seawater samples taken from sea urchin rearing in both running and circulation-water system experiments were also used.

Rearing Experiments

Two types of rearing experiments were performed to understand (1) factors affecting the shape of the gut microbiome (Experiment 1; Exp. 1) and (2) microbiome functions affecting the host growth (Experiment 2; Exp. 2) (**Supplementary Figure 1**).

Experiment 1 (Exp. 1)

Nine individuals, including the two species *M. nudus* and *S. intermedius* were used for this experiment. Five specimens of *M. nudus* (test diameter 24.43 ± 6.69 mm, weight 8.67 ± 5.91 g) were collected at the farm ESC. They were fed with microalgae throughout the larval stage and subsequently a brown alga, *Saccharina japonicus*, at juvenile stage until collection time. Four *S. intermedius* (weight 2.88 ± 0.76 g) were obtained from the farm TSC, and were fed with microalgae until that collection. After feces collection on these farms, the sea urchins were transplanted to the laboratory of Hakodate

Fisheries Experiment Station (HFES), which is equipped with a running-water rearing system and reared for 2-weeks. At the HFES laboratory, an ambient natural seawater temperature of approximately 15°C was used to feed sea urchins individually in a caged 2 L polyethylene terephthalate (PET) aquarium created with water exchange holes with full feeding of fresh *S. japonicus* thalli. After 2 weeks of rearing at the laboratory, feces samples were collected. Seawater samples from farm and laboratory aquarium were collected and used for microbiome analyses.

Experiment 2 (Exp. 2)

Eight specimens of *M. nudus* (test diameter 22.25 ± 4.47 mm, weight 4.77 ± 2.13 g) were taken from ESC, and they were transplanted to the laboratory of Hokkaido University, and fed with a fine slice of boiled frozen *S. japonicus* thalli. They were fed for 6 weeks in a circulating-water rearing system maintained at an optimal temperature of 18°C. Every day, half of the water was replaced with fresh artificial seawater. Artificial seawater (SEALIFE, Marine Tech, Japan) was used. Feces and seawater samples were collected at the farm ESC. They were also collected bi-weekly after start rearing in the laboratory.

Collection of Feces and Seawater

Feces and seawater samples for microbiome analyses were collected according to Yamazaki et al. (2016). In brief, feces collections on-site and at the farm HFES were performed inside an instant clean booth, illuminated by ultraviolet light for 15 min (GL-15, Panasonic, Japan). Sea urchin individuals were cleaned using filter-sterilized seawater and moved individually into sterile beakers with filter-sterilized seawater until feces were released. The filter-sterilized seawater was prepared as follows; the natural seawater taken from a coastal area at a depth of 3–4 m was transferred to pressure tanks and filtered through a 0.22 μm Sterivex filter (Sterivex-GV Sterile Vented Filter Unit 0.22 μm, EMD, Millipore, United States) under positive pressure using filtered (0.22 μm) high purity N_2 gas. Feces was collected into 1.5 mL tubes using adopted 5 mL pipette tips. Feces collected on-site and at the farm HFES were immediately frozen in a sterilized 1.5 mL tube on dry ice, transferred to our lab, and kept at –80°C until the DNA extraction was performed. A total of 5 L of the seawater was collected and filtered through a 0.22 μm Sterivex filter. The Sterivex filter was filled with a SET buffer (sucrose 20%, EDTA 50 mM, Tris-HCl 50 mM) and rapidly frozen on dry ice, and kept at –80°C until the DNA extraction was performed.

Microbial DNA Extraction

According to the manufacture's protocol, the microbial DNA extraction of sea urchin feces was performed using the NucleoSpin Soil Kit (MACHEREY-NAGEL, Germany). According to the modified manufacture's protocol, the microbial DNA extraction from seawater was performed using the NucleoSpin Tissue Kit (MACHEREY-NAGEL) (Yamazaki et al., 2016). We used 20% SDS and proteinase K (20 mg/mL) for pre-lysis instead of buffer T1 and proteinase K. We also used 1 mL buffer B3 instead of 200 μ L.

Meta16S Sequencing and Downstream Analyses

PCR amplification and amplicon sequencing of the V1-V2 region on 16S rRNA gene were also performed according to Yamazaki et al. (2016) with minor modifications. Amplified PCR products using 27Fmod with barcode sequences and 338R primers were sequenced using MiSeq (Illumina, United States). Data was further qualified by the removal of reads with average quality values below 25. Filter-passed reads were filed as FASTA for downstream analysis after trimming off both primer sequences.

The sequence data of 16S rRNA genes was analyzed using the Quantitative Insights Into Microbial Ecology 2 (QIIME2) (Bolyen et al., 2019) version 2019.1. Sequence denoise, dereplication, and chimeras filtering were performed using the DADA2 pipeline (Callahan et al., 2016). During the "dada2" pipelines, the representative Amplicon Sequence Variant (ASV) sequences, consist of reads with 100% similarity, were constructed. ASVs were assigned taxonomic status through the "q2-feature-classifier" plugin (Bokulich et al., 2018) with the Greengeenes (version 13.8) database trained by Naïve Bayes methods. ASVs assigned to chloroplast or mitochondria were removed from the dataset through the "filter-features" plugin. Using this dataset, further analyses were conducted. For beta diversity, we performed weighted and unweighted UniFrac analysis (Lozupone et al., 2011) and visualized them in a PCoA plot based on a phylogenetic tree generated from the Greengenes database through the FastTree pipeline. To verify if specific ASVs abundance correlated to sea urchin body weight, we performed multiple Person correlations, and p-values were adjusted using the Holm (1979) method. We searched for highly ($r > 0.6$) and significantly (correlated $p < 0.05$) correlated ASVs against the bodyweight and test diameter of the sea urchins. ASVs that occurred in only one sample were removed from this analysis. Growth rate was calculated by Excel software. Meta16S sequences retrieved from the public database were also included in understanding the overview structure of the gut microbiome of sea urchin worldwide; SRP062365 (Hakim et al., 2015), SRP076869 (Hakim et al., 2016), and PRJNA504890 (Hakim et al., 2019).

Shotgun Metagenomic Sequencing and Analysis

Shotgun metagenome sequencing using the Illumina platform was performed on the high and low growth individuals based on their growth rate. Analysis of correlation coefficient used Excel software using the standardized number of leads and the body weight and test diameter of *M. nudus* was performed. The ASVs with an absolute correlation coefficient greater than 0.6 were defined as bacterial communities that correlated with sea urchin growth.

Individuals of *M. nudus* with high growth rates and low growth rates were selected, and the DNAs from fecal samples at both 4th and 6th weeks of rearing were metagenomically sequenced. The shotgun metagenome sequencing was performed on the HiSeq platform by Hokkaido System Science, Co., Ltd., Sapporo, Japan. The DNA quality and quantity were

estimated using NanoDrop, Qubit Fluorometer, and Agilent 2200 TapeStatin System. Using TruSeq Nano DNA LT Sample Prep Kit, genomic DNA was fragment and insert DNA of 350 bp was selected and connected adaptor sequences. Sixty nanograms of each DNA sample were performed on the HiSeq platform. Sequences showing low fluorescence purity were removed.

The FASTQ format sequence data set was uploaded to MG-RAST server version 3.5. For QC, after dereplication was performed using the DRISEE method, low quality ($25 < QV$) sequences were removed with Dynamic Trim. The encoded gene region of protein/rRNA was predicted using reads that passed QC according to the "FragGeneScan" algorithm. The predicted proteins were clustered (similarity $\geq 90\%$) by BLAST analysis using UCLUST. Sequence assignment was performed in MG-RAST server under conditions excluding the following: expected value $\leq 1 \times 10^{-5}$, minimum identity $\leq 60\%$, base pair ≤ 15, amino acid minimum alignment. Taxonomic annotation was performed using the NCBI database, and the functional annotation was performed using the SEED database (Overbeek et al., 2014). Post-assignment metagenomic sequence data was analyzed using MG-RAST tools and STAMP v2.0.9 software (Parks et al., 2014). To test if the abundance of each functional feature of the high and low growth sea urchin differed, Fisher's exact test with Newcombe-Wilson confidence interval calculation method and Storey's FDR for multiple test correction method was used with STAMP software. $p < 0.05$ was considered statistically significant. To visualize metagenomic results, profile bar plots and extended error bar plots were generated at Subsystem Levels 1 and 3. To plot data, results were filtered by q-value (< 0.05) and effect size (> 0.1 or > 0.2) (Yadav et al., 2015). To investigate the taxonomic affiliation of the significantly different functional features between the high and low growth sea urchin, we used the MG-RAST workbench tool implementing KEGG Orthology and GenBank database to annotate with functional features.

RESULTS

Total Sequence Reads, Quality Trimming and Amplicon Sequence Variant Designation

Meta16S Sequence

In Exp. I, a total of 239,928 raw reads from 17 samples [*M. nudus* ($n = 6$), *S. intermedius* ($n = 8$) and rearing seawater ($n = 3$)] were produced (**Supplementary Table 1**). After QC, eukaryotic-derived reads were removed from these subjects to obtain 153,084 reads (131,198 reads and 21,886 reads from sea urchin and seawater samples, respectively). The total number of ASVs obtained from 17 samples was 1,250.

From eight wild sea urchin samples, we obtained a total of 276,858 raw reads (*M. nudus* $n = 4$, *S. intermedius* $n = 4$). After trimmed and removed eukaryotic reads, 96,332 qualified reads from the sea urchin samples (31,857 and 64,475 reads from *M. nudus* and *S. intermedius*) were produced. A total of 147,224, and 309 ASVs from *M. nudus*, *S. intermedius*, and wild animals have been observed (**Supplementary Table 2**).

In Exp. II, a total of 1,223,407 raw reads were obtained from a total of 36 samples [*M. nudus* samples ($n = 32$) and rearing seawater ($n = 4$)]. After QC, reads derived from eukaryotic microorganisms were removed, and 880,046 reads (775,774 reads and 104,272 reads, respectively, from sea urchin and seawater samples) were obtained. The total number of ASVs obtained from 36 samples were 1,613 (**Supplementary Table 2**).

Shotgun Metagenome Sequence

From the high growth individuals reared, 4,435,332 and 2,268,127 reads were obtained at the 4th and 6th weeks, respectively. After quality filtering, 3,848,669 reads (4th week) and 2,188,052 (6th week) were used for MG-RAST annotation, and a total of 3,329,288 and 1,707,418 reads were annotated from the high growth individuals reared for each sample. From the low growth individuals reared, 3,346,079 and 3,192,106 reads were obtained at the 4th and 6th weeks, respectively. After Quality filtering, the remaining 3,254,461 reads (4th week) and 3,117,838 (6th week) were used for MG-RAST annotation. A total of 2,560,781 and 2,306,340 were annotated from the low growth individuals at the 4th and 6th weeks, respectively (**Supplementary Table 3**).

Overall Structure of Gut Microbiome of Sea Urchins *Mesocentrotus nudus* and *Strongylocentrotus intermedius* in Japan

Compared to previously reported data for American green sea urchin (*Lytechinus variegatus*) (Hakim et al., 2015, 2016) and purple sea urchin (*Strongylocentrotus purpuratus*) (Hakim et al., 2019) gut microbiome, we did not find any apparent differences in average dominance of sea urchin microbiome in Japan from those of American species green and purple sea urchins at phylum-level, which consisted of more than 80% *Proteobacteria* and *Bacteroidetes* (**Figure 1**). However, relative abundances of *Proteobacteria* and *Bacteroidetes* fluctuated (more than 15% standard deviation) in relation to each other depend on rearing conditions those of *Proteobacteria* decreased in *M. nudus* under circulated water aquarium, and those of *Bacteroidetes* showed the opposite results (**Figure 1A** and **Supplementary Figure 2**).

Key members of each sea urchin microbiome could be more clearly defined below class level at the family level (**Figures 1B–D**, **2** and **Supplementary Figures 3**, **4**). Families *Psychromonadaceae* and *Flavobacteriaceae* dominated 38–71% on sea urchins in Japan under all rearing conditions. Meanwhile, these two families dominated between 60 and 67% in wild sea urchins, whereas in seawater around 15–31%. The species of *S. purpuratus* and *L. variegatus* were dominated by 41% and less than 5.1% of *Psychromonadaceae* and *Flavobacteriaceae*, respectively. Only *Psychromonadaceae* was present in wild *S. purpuratus*. The relative abundances of families *Campylobacteraceae* and *Vibrionaceae* were affected by rearing conditions. *Campylobacteraceae* abundances increased in laboratory aquarium conditions in two species of sea urchins in Japan and *L. variegatus*. *Vibrionaceae* abundances increased in *M. nudus* in the circulated water aquarium and *L. variegatus*

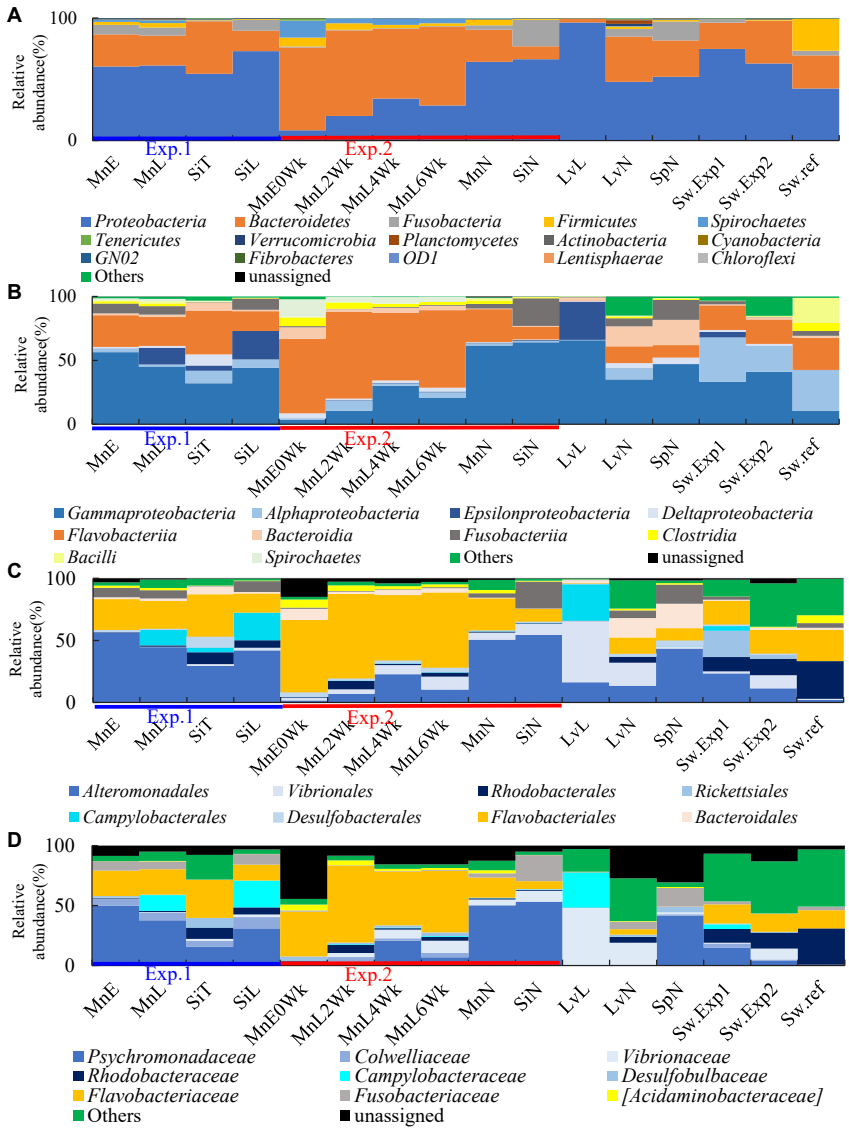

FIGURE 1 | Average microbial community structure of sea urchin gut microbiome. **(A)** Phylum **(B)** Class. **(C)** Order. **(D)** Family. Mn, *M. nudus*; Si, *S. intermedius*; Lv, *L. variegatus*; Sp, *S. purpuratus*; E, the Esan Seedling Center; T, the Toi Seedling Center; N, Natural; L, Laboratory; 0Wk, Zero week; 2Wk, two week; 4Wk, four week; 6Wk, six week; Sw.Exp1, Seawater Experiment 1; Sw.Exp2, Seawater Exp. 2; Sw.ref, Seawater reference.

in the laboratory aquarium. Abundance of *Rhodobacteraceae* (around 5–10%) was rather high in *S. intermedius* both in wild and laboratory reared individuals. *Fusobacteriaceae* was found in small quantities and was detected 2– 20% in all sea urchin species and under all rearing conditions (**Figure 1D**).

The gut microbiome of *S. intermedius* fed microalgae on the farm resembled those of *M. nudus* fed kelp thallus both in the farm and laboratory (**Figures 1**, **3**). In detail, dominant microbial taxa (>5%) of the gut microbiome of *S. intermedius* in the farm, laboratory, and in wild conditions consisted of *Psychromonadaceae* (16, 31, and 53%, respectively), *Flavobacteriaceae* (32, 13, and 7%), *Rhodobacteraceae* (10, 6, and 1%), and *Colwelliaceae* (5, 9, and 0.2%). *Fusobacteriaceae*, *Campylobacteraceae,* and *Vibrionaceae* fluctuated more in the *S. intermedius* gut microbiome. Similarly, those of the gut microbiome of *M. nudus* mainly consisted of *Psychromonadaceae* (38–50%), *Flavobacteriaceae* (17–21%), and *Fusobacteriaceae* (4–8%). As mentioned above, *Psychromonadaceae/Flavobacteriaceae/Vibrionaceae* ratio dynamically fluctuated in *M. nudus* in a recirculating-water system; 1:41:0.4 at the start of rearing were 1:7.3:1.4 at the end of 6th week rearing.

Factors Affecting Sea Urchin Gut Microbiome

Two sea urchins of different species were transplanted to a laboratory aquarium from farms to assess what factors, e.g.,

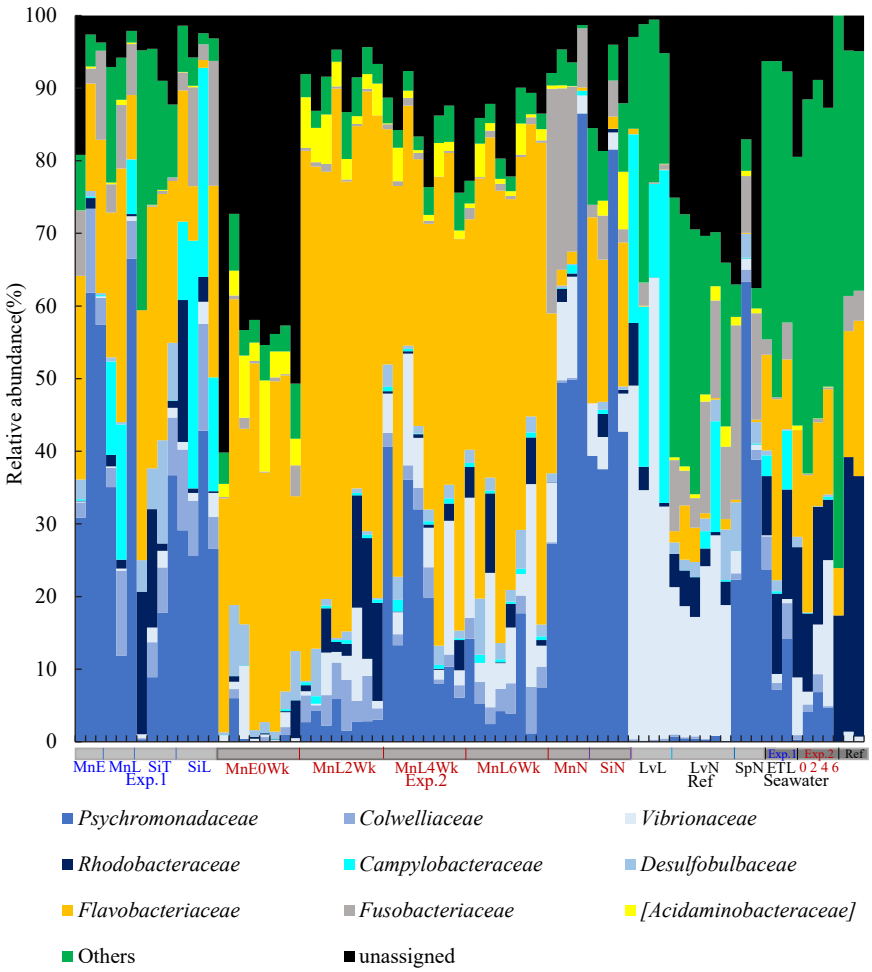

FIGURE 2 | Family-level individual microbial community structure of sea urchin gut microbiome. Mn, *M. nudus*; Si, *S. intermedius*; Lv, *L. variegatus*; Sp, *S. purpuratus*; E, the Esan Seedling Center; T, the Toi Seedling Center; N, Natural; L, Laboratory; 0Wk, Zero week; 2Wk, two week; 4Wk, four week; 6Wk, six week; Sw.Exp1, Seawater Experiment 1; Sw.Exp2, Seawater Exp. 2; Sw.ref, Seawater reference.

diets, rearing environments, and host species affect the shaping of the gut microbiomes of sea urchin in Exp. 1. PCoA plot based on unweighted UniFrac revealed a grouping of both gut microbiomes of *M. nudus* in farm and laboratory after 2 week feeding trials. Three of four individual gut microbiomes in the laboratory reared *S. intermedius* were shifted to the group of *M. nudus*, and the other one was likely to be closer to those of *M. nudus* (**Figure 3**).

Amplicon Sequence Variants Correlated to Hosts' Body Weight and Shell Length

A total of seven ASVs were found in the gut microbiota of sea urchins reared in a circulating aquarium in Exp. 2, showing a positive correlation with host test diameter and body weight (**Figure 4** and **Table 1**). The five ASVs identified correlated with the body weight of sea urchin ($r > 0.6$) with statistical significance ($p < 0.05$) (**Figures 4A,B,D**, and **Table 1**). Three of the five ASVs (BW1, BW2, and BW4) with a host weight gain and correlation coefficient of 0.6 or higher and a significant correlation coefficient ($p < 0.05$) were closest to *Saccharicrinis fermentans* sequence with 91.2–91.5% similarities (**Table 1**). The other two ASVs (BW3 and BW5) had the sequences closet to *Kiritimatiellaeota* bacterium S-5,007 (89.7% similarity) and *Saccharicrinis carchari* (88.2% similarity), respectively. Moreover, two ASVs correlated with test diameter (DM1, ASV had positive and DM2, ASV negative correlation) ($r > 0.6$, $r < -0.6$) with statistical significance ($p < 0.05$). One ASV (DM1) showed a positive correlation had the sequence closest to *S. fermentans* sequences (91.5% similarity) (**Table 1**). One ASV (DM2) showed a negative correlation with the sequences closest to *Flaviramulus ichthrvoenteri* sequence (88.6% similarity).

Functional Analysis of Sea Urchin Gut Microbiome

Shotgun metagenome analysis of gene function subsystem level 1 (**Supplementary Figure 5**) and subsystem level 3 (**Figure 5**) between each functional genes showed significantly different proportion at both 4th and 6th week. The comparison of

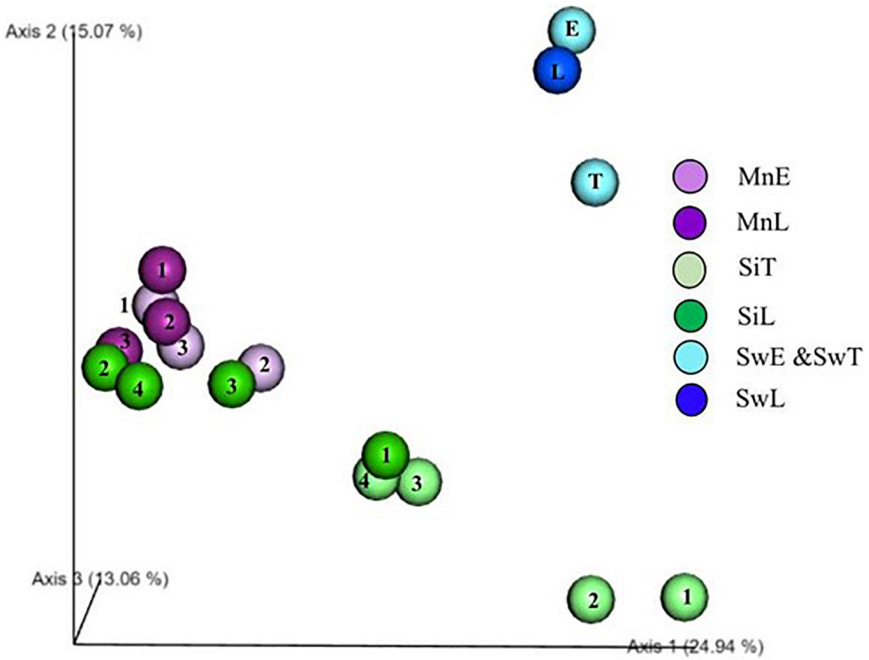

FIGURE 3 | PCoA plot of sea urchin microbiome. Unweighted Unifrac 3D PCoA plot. The numbers (1, 2, 3, 4) in symbol indicates individual number of sea urchin samples. Mn, *M. nudus*; Si, *S. intermedius*; E, the Esan Seedling Center; T, the Toi Seedling Center; L, Laboratory; Sw, Seawater.

functional genes between bacteria with higher and lower growth rates found abundance differences in more than 34 functional genes (**Supplementary Table 4**). The two highest genes occupied more than 15% on the relative proportion on functional genes level were a nitrite reductase [NAD(P)H] large subunit (EC 1.7.1.4) and periplasmic nitrate reductase precursor (EC 1.7.99.4), that affiliated to "nitrate and nitrite ammonification." We observed a rising trend in bacterial abundance between the 4th and 6th weeks (**Figure 5**), which correlates with the existence of potential genes involved in the growth of the sea urchin *M. nudus*. These potential genes were identified as belonging to the order *Vibrionales*.

DISCUSSION

Landmark findings on the reproductive physiology, development, and body structure of sea urchins are available (Ernst, 1997; Sodergren et al., 2006; Lawrence, 2013), however, knowledge on the structure and function of the gut microbiome, which is likely to influence host physiology and development, is extremely limited. N_2-fixation (Guerinot and Patriquin, 1981) and amino acid supply (Fong and Mann, 1980) reported in 1980s were the most recent representative findings on the functional aspects of the sea urchin microbiomes using classical feeding experiments. Gut microbial community studies of sea urchin have recently re-emerged using next-generation sequencing technology in contributing to accumulated knowledge; (1) the microbiome of purple sea urchin in European *Paracentrotus lividus* differs in each part of the gut tract (Meziti et al., 2007), (2) the gut microbiota of the American species of green sea urchin *L. variegatus* may complement host metabolism (Hakim et al., 2016), (3) the gut microbiome of the European species of purple sea urchin *P. lividus* inhibits the growth of microbes introduced from the environment and may play an important role in gut microbiota homeostasis (Laport et al., 2018), (4) the diversity and function of the gut microbiome of the American species of purple sea urchin may be reduced due to the increase in seawater temperature associated with global warming (Brothers et al., 2018), (5) geographical factors may have a more significant influence than diet on the formation of the symbiotic microbiome of larvae of the humpback sea urchin (Carrier et al., 2019), and 6) the possibility that sea urchin in the family *Shizadteridae* continue to have a symbiotic relationship with common gut bacteria even before species divergence (Ziegler et al., 2020). However, our understanding of the structure and function of the gut microbiota in sea urchin in Japan, such as *M. nudus* and *S. intermedius*, is behind other sea urchin species. It is necessary to expand our knowledge for further innovation of effective seed production technology for these sea urchin species in Japan. Even in marine invertebrates, fine-scale gut microbiome studies using individual microbiome approaches, which can monitor microbiome changes structurally and functionally without sacrificing individual animals, have revealed unexpected contributions of the gut microbiome to host growth and physiology of sea cucumber, which belong in the same phylum as sea urchin (Yamazaki et al., 2016). Therefore, for the first time we applied these individual microbiome approaches to expand our knowledge in finding new associations between the sea urchin host and its gut microbiomes.

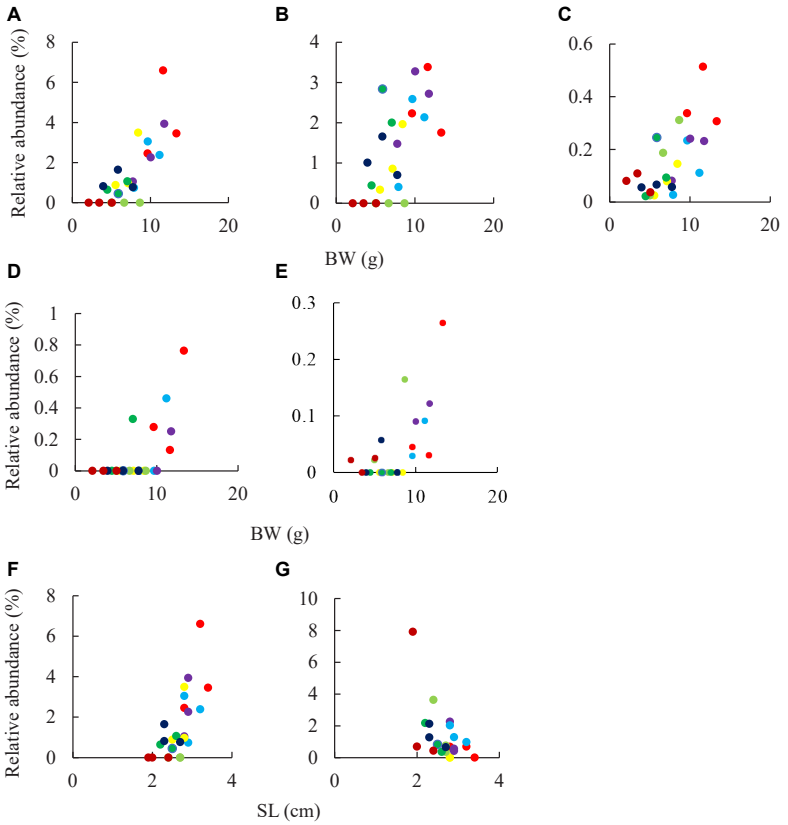

FIGURE 4 | Correlation between ASV abundance and host growth in Exp. 2. Same colors showed the data collected from same samples number at different time point. BW, hosts' bodyweight; SL, hosts' diameter. **(A)** BW1, **(B)** BW2, **(C)** BW3, **(D)** BW4, **(E)** BW5, **(F)** DM1, and **(G)** DM2, see **Table 1** for details. Sample numbers: 1, 2, 3, 4, 5, 6, 7, and 8.

TABLE 1 | ASVs correlated to growth of the sea urchin *M. nudus* (Exp. 2).

ASV ID	ID	Closest taxa	Identity (%) of the 16S rRNA gene sequences	Correlation	*p*-value
7ad7a993096d762eea0f11b6e9b12697	BW1	*Saccharicrinis fermentans*	91.5	0.768726	1.14E–05
45adbed4e7caeb4864617a35df730e45	BW2	*Saccharicrinis fermentans*	91.2	0.668635	0.000355
0acddd2c18bc6b015bf0f83dab2bb20b	BW3	*Kiritimatiellaeota* bacterium S-5,007	89.7	0.66822	0.000359
05b07909be6b43512e1d49e488c795df	BW4	*Saccharicrinis fermentans*	91.2	0.643274	0.000697
c7395fe383e772bb5df6a28ae6e900b1	BW5	*Saccharicrinis carchari*	88.2	0.641202	0.000734
7ad7a993096d762eea0f11b6e9b12697	DM1	*Saccharicrinis fermentans*	91.5	0.628922	0.000995
1292c35cfbc3711fd999120ffa6f9a69	DM2	*Flaviramulus ichthyoenteri*	88.6	–0.68511	0.000221

The increase of *Vibrionaceae* and *Campylobacteriaceae*, in more detail, genus *Vibrio* and *Arcobacter*, respectively, was observed in both *M. nudus* and *S. intermedius* after rearing in running water more than 2 weeks. Increases of these taxa have been reported in studies using American green sea urchin (Hakim et al., 2015, 2016). An increase of more than 20% in *Vibrionaceae* and *Campylobacteriaceae* observed in those reared sea urchin indicates that both bacterial families may be defined as a fluctuated community in the gut microbiome of sea urchin (Hakim et al., 2015, 2016).

By comparing our findings to those of other researchers (Hakim et al., 2015, 2016; Yao et al., 2019), it was determined that seawaters had a negligible effect on the gut microbiome of sea urchins. When two distinct species of sea urchins were transferred from the farm to the laboratory settings, comparable microbiome changes were found in the sea urchin fed with the kelp *S. japonicus* thalli. Our research discovered that diet has a significant effect on the gut microbiota of sea urchin species. It is reasonable to conclude that the rearing environment of sea urchin and host species have minimal impact on gut microbiomes. Our study established that diet significantly influences the gut microbiota of sea urchin species. The similar phenomenon was seen in a variety of species, including humans, indicating that gut

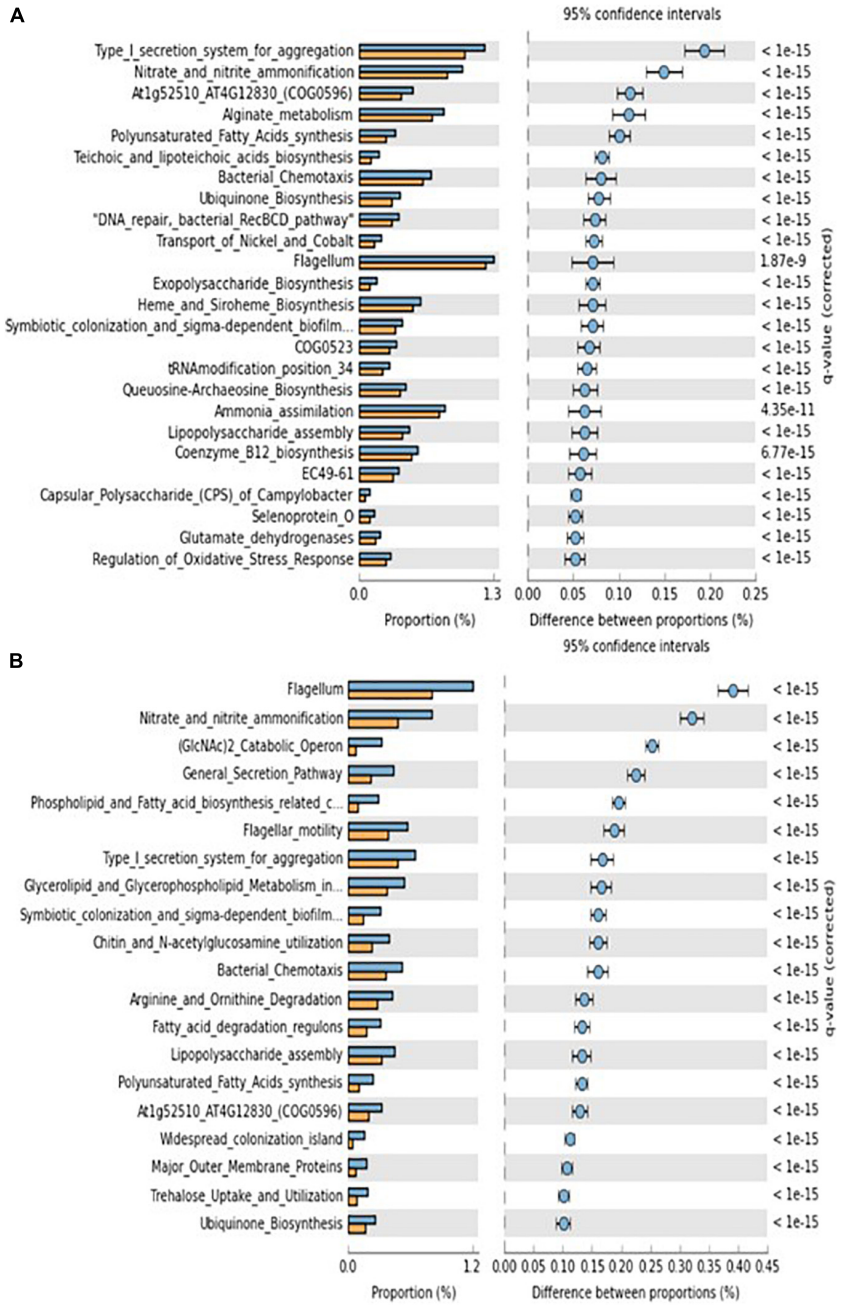

FIGURE 5 | Metagenome gene functions (subsystem level 3) significantly abundant at individuals showing higher lower growth rates. **(A)** 4 weeks and **(B)** 6 weeks. Blue and orange bars indicate higher and lower grown sea urchin individuals, respectively.

microbiota shaping mechanisms are evolutionarily conserved (e.g., Wilson et al., 2020).

Five ASVs showed strong positive correlations with body weight or test diameter in the sea urchin *M. nudus*. Among these ASVs, a bacterium similar to *S. fermentans* was affiliated. This bacterium has been reported to be capable of fermenting amygdalin, glucose, mannitol, and sucrose (Yang et al., 2014). Since the kelp, fed in these studies, contained relatively high amounts of mannitol, it may contribute to the growth of the host through fermentation of the diet ingredients. In addition, *S. fermentans* is also known to possess a N_2-fixing ability (Inoue et al., 2015). Guerinot and Patriquin (1981) reported the possibility that N_2-fixing bacteria exist in the digestive tract of sea urchins *S. droebachiensis* and play a role in supplying nitrogen sources to the host. Therefore, it is possible that *Saccharicrinis*- like bacteria also contribute to the growth of sea urchins *M. nudus* and *S. intermedius* through their N_2-fixing ability.

The number of functional genes involved in "nitrate and nitrite ammonification" was significantly higher in high-growth individuals at subsystem level 3 when sea urchin reared in a circulating aquarium. "Nitrate and nitrite ammonification" is also called dissimilatory nitrate reduction to ammonification (DNRA), a reaction in which nitrate is converted to ammonium under anaerobic conditions. The genes *nrfE*, *nrfF*, and *nrfG* are required to activate cytochrome c nitrite reductase, NrfA, in *Escherichia coli* (Eaves et al., 1998). One of the functions of NrfA is to produce ammonium in the periplasm, which is transported to the cytoplasm where it is converted to glutamine by an amino acid, for assimilation (Einsle, 2011). The utilization of ammonium produced by bacteria has been reported mainly in plants. In addition to this, recent studies on nitrogen dynamics in the digestive tract of aquatic insects have shown that there may be a pathway by which gut microorganisms take up nitrate-nitrogen from the host digestive tract and convert it to ammonium through DNRA for utilization by the host (Ayayee et al., 2019). Nitrate accumulation is commonly observed in a closed aquarium system, and the concentration reaches to 10 time higher than those determined in the ocean (e.g., Kim et al., 2017). Unfortunately, we did not determine the nitrate concentrations in this study, nitrate accumulation in the circulating aquarium might trigger the dynamics of DNRA by the gut microbiome of sea urchin. We might discover a veiled nitrogen metabolism through the gut microbiome of sea urchin, which could contribute host growths under those aquaculture conditions. Fong and Mann (1980) suggested the existence of gut microorganisms that supply amino acids to sea urchins. Although many studies have shown that N_2-fixing bacteria exist in the gut microbiota of sea urchin and that they may play a role in supplying nitrogen source to the host, few studies have addressed the possibility that other nitrogen cycling pathways may play a role in supplying nitrogen source to sea urchin host. The presence of DNRA-related respiratory cytochrome c nitrite reductase has been reported in several organisms, including *E. coli* and *Vibrio fischeri*, and it is likely that *Vibrionales*, which was found to be a candidate for the *nrfEFG* gene, also possesses it. *Vibrionales*, which were found as a candidate with the *nrfEFG* gene, are also likely to have the gene. In the future, it will be necessary to isolate gut microorganisms and clarify their nitrogen metabolisms that contribute to the nitrogen supply to the host, with a view to their application as probiotics in fisheries.

CONCLUSION

Overall, *Psychromonadaceae* and *Flavobacteriaceae* dominated in gut microbiomes of two species of sea urchins in Japan, *M. nudus* and *S. intermedius*. Diets rather than rearing environments and host species is the most potent factor structuring gut microbiomes of the sea urchins. *S. fermentans* was identified as ASV showing a positive correlation with host shell length and body weight in *M. nudus*, suggesting a link in the symbiotic association through nitrogen fixation. *Vibrionales* possessing genes responsible for nitrate and nitrite ammonification pathway also correlated to the growth of sea urchin species in Japan. Our study showed *M. nudus* and *S. intermedius* could be excellent candidates for studying marine invertebrates' structure and function relationships. Further studies in the utilization of gut microbiomes of sea urchin could allow us to develop sustainable technology of fisheries resources in a changing world.

DATA AVAILABILITY STATEMENT

The 16S rRNA and metagenome data sets generated in this study were deposited in DDBJ/GenBank/ENA database under BioProject accession number PRJDB12341.

AUTHOR CONTRIBUTIONS

MY, JY, SM, and YS did molecular biology experiments and data analysis. MY, JY, and YS collected samples. JY, SM, and TS conceived of the study and coordinated the experiments and data analysis. AH, MY, SM, and TS mainly wrote this manuscript. All authors read and approved the final manuscript.

FUNDING

The studies were supported by KAKEN 19K22262.

ACKNOWLEDGMENTS

We thank Toi Seedling Center and Esan Seedling Center for sample collection. We also thank to Ms. Kodama, Mr. Y. Nomura, and Dr. Y. Yamazaki, Hokkaido University, for technical assistant.

SUPPLEMENTARY MATERIAL

The Supplementary Material for this article can be found online at: https://www.frontiersin.org/articles/10.3389/fmars.2021.802754/full#supplementary-material

REFERENCES

Agatsuma, Y. (2013). "*Hemicentrotus pulcherrimus*, *Pseudocentrotus depressus*, and *Heliocidaris crassispina*," in *Sea Urchins: Biology and Ecology*, ed. J. M. Lawrence (San Diego, CA: Academic Press), 461–473. doi: 10.1016/b978-0-12-396491-5.00030-7

Ayayee, P., Bhattacharyya, S., Arnold, T., Werne, J., and Leff, L. (2019). *Experimental Investigation of Potential Biological Nitrogen Provisioning by Freshwater Insect Gut Microbiomes Using 15N Isotope Analysis*. Available online at: https://www.preprints.org/manuscript/201908.0034/v1 (accessed August 5, 2019).

Bokulich, N. A., Kaehler, B. D., Rideout, J. R., Dillon, M., Bolyen, E., Knight, R., et al. (2018). Optimizing taxonomic classification of marker-gene amplicon sequences with QIIME 2's q2-feature-classifier plugin. *Microbiome* 6:90. doi: 10.1186/s40168-018-0470-z

Bolyen, E., Rideout, J. R., Dillon, M. R., Bokulich, N. A., Abnet, C. C., Al-Ghalith, G. A., et al. (2019). Reproducible, interactive, scalable and extensible

microbiome data science using QIIME 2. *Nat. Biotechnol.* 37, 852–857. doi: 10.1038/s41587-019-0209-9

Brothers, C. J., Van Der Pol, W. J., Morrow, C. D., Hakim, J. A., Koo, H., and McClintock, J. B. (2018). Ocean warming alters predicted microbiome functionality in a common sea urchin. *Proc. R. Soc. B Biol. Sci.* 285:20180340. doi: 10.1098/rspb.2018.0340

Brown, K. E., King, C. K., and Harrison, P. L. (2020). Impacts of petroleum fuels on fertilization and development of the Antarctic sea urchin *Sterechinus neumayeri*. *Environ. Toxicol. Chem.* 39:2527–2539. doi: 10.1002/etc.4878

Callahan, B. J., McMurdie, P. J., Rosen, M. J., Han, A. W., Johnson, A. J. A., and Holmes, S. P. (2016). DADA2: high-resolution sample inference from Illumina amplicon data. *Nat. Methods* 13, 581–583. doi: 10.1038/nmeth.3869

Carrier, T. J., Dupont, S., and Reitzel, A. M. (2019). Geographic location and food availability offer differing levels of influence on the bacterial communities associated with larval sea urchins. *FEMS Microbiol. Ecol.* 95:fiz103. doi: 10.1093/femsec/fiz103

Cui, Z., Zhang, J., Sun, Z., Liu, B., Han, Y., Zhao, C., et al. (2022). Testis-specific expression pattern of dmrt1 and its putative regulatory region in the sea urchin (*Mesocentrotus nudus*). *Comp. Biochem. Physiol. B Biochem. Mol. Biol.* 257:110668. doi: 10.1016/j.cbpb.2021.110668

Ding, J., Zheng, D., Sun, J., Hu, F., Yu, Y., Zhao, C., et al. (2020). Effects of water temperature on survival, behaviors and growth of the sea urchin *Mesocentrotus nudus*: new insights into the stock enhancement. *Aquaculture* 519, 301–308. doi: 10.1016/j.aquaculture.2019.734873

Dworjanyn, S. A., and Byrne, M. (2018). Impacts of ocean acidification on sea urchin growth across the juvenile to mature adult life-stage transition is mitigated by warming. *Proc. R. Soc. B Biol. Sci.* 285:20172684. doi: 10.1098/rspb.2017.2684

Eaves, D. J., Grove, J., Staudenmann, W., James, P., Poole, R. K., White, S. A., et al. (1998). Involvement of products of the nrfEFG genes in the covalent attachment of haem c to a novel cysteine–lysine motif in the cytochrome c552 nitrite reductase from *Escherichia coli*. *Mol. Microbiol.* 28, 205–216. doi: 10.1046/j.1365-2958.1998.00792.x

Einsle, O. (2011). Structure and function of formate-dependent cytochrome c nitrite reductase, NrfA. *Methods Enzymol.* 496, 399–422. doi: 10.1016/B978-0-12-386489-5.00016-6

Ernst, S. G. (1997). A century of sea urchin development. *Am. Zool.* 37, 250–259. doi: 10.1093/icb/37.3.250

Faddetta, T., Ardizzone, F., Faillaci, F., Reina, C., Palazzotto, E., Strati, F., et al. (2020). Composition and geographic variation of the bacterial microbiota associated with the coelomic fluid of the sea urchin Paracentrotus lividus. *Sci. Rep.* 10:21443. doi: 10.1038/s41598-020-78534-5

Fan, Y., and Pedersen, O. (2021). Gut microbiota in human metabolic health and disease. *Nat. Rev. Microbiol.* 19, 55–71. doi: 10.1038/s41579-020-0433-9

Fong, W., Li, Q., and Yu, J. (2020). Gut microbiota modulation: a novel strategy for prevention and treatment of colorectal cancer. *Oncogene* 39, 4925–4943. doi: 10.1038/s41388-020-1341-1

Fong, W., and Mann, K. H. (1980). Role of gut flora in the transfer of amino acids through a marine food chain. *Can. J. Fish. Aquat. Sci.* 37:e100092. doi: 10.1139/f80-009

Formery, L., Orange, F., Formery, A., Yaguchi, S., Lowe, C. J., Schubert, M., et al. (2021). Neural anatomy of echinoid early juveniles and comparison of nervous system organization in echinoderms. *J. Comp. Neurol.* 529, 1135–1156. doi: 10.1002/cne.25012

García, E., Hernández, J. C., and Clemente, S. (2018). Robustness of larval development of intertidal sea urchin species to simulated ocean warming and acidification. *Mar. Environ. Res.* 139, 35–45. doi: 10.1016/j.marenvres.2018.04.011

Guerinot, M. L., and Patriquin, D. G. (1981). The association of N2-fixing bacteria with sea urchins. *Mar. Biol.* 62, 197–207. doi: 10.1007/BF00388183

Hakim, J. A., Koo, H., Dennis, L. N., Kumar, R., Ptacek, T., Morrow, C. D., et al. (2015). An abundance of *Epsilonproteobacteria* revealed in the gut microbiome of the laboratory cultured sea urchin, *Lytechinus variegatus*. *Front. Microbiol.* 6:1047. doi: 10.3389/fmicb.2015.01047

Hakim, J. A., Koo, H., Kumar, R., Lefkowitz, E. J., Morrow, C. D., Powell, M. L., et al. (2016). The gut microbiome of the sea urchin, *Lytechinus variegatus*, from its natural habitat demonstrates selective attributes of microbial taxa and predictive metabolic profiles. *FEMS Microbiol. Ecol.* 92:fiw146. doi: 10.1093/femsec/fiw146

Hakim, J. A., Schram, J. B., Galloway, A. W., Morrow, C. D., Crowley, M. R., Watts, S. A., et al. (2019). The purple sea urchin *Strongylocentrotus purpuratus* demonstrates a compartmentalization of gut bacterial microbiota, predictive functional attributes, and taxonomic co-occurrence. *Microorganisms* 7:35. doi: 10.3390/microorganisms7020035

Holm, S. (1979). A simple sequentially rejective multiple test procedure. *Scand. J. Stat.* 6, 65–70.

Houlihan, E. P., Espinel-Velasco, N., Cornwall, C. E., Pilditch, C. A., and Lamare, M. D. (2020). Diffusive boundary layers and ocean acidification: implications for sea urchin settlement and growth. *Front. Mar. Sci.* 7:972. doi: 10.3389/fmars.2020.577562

Inoue, J. I., Oshima, K., Suda, W., Sakamoto, M., Iino, T., Noda, S., et al. (2015). Distribution and evolution of nitrogen fixation genes in the phylum Bacteroidetes. *Microbes Environ.* 30, 44–50. doi: 10.1264/jsme2.ME14142

Kim, Y., Bonn, W. V., Aw, T. G., and Rose, J. B. (2017). Aquarium viromes: viromes of human-managed aquatic systems. *Front. Microbiol.* 8:1231. doi: 10.3389/fmicb.2017.01231

Kinjo, S., Kiyomoto, M., Yamamoto, T., Ikeo, K., and Yaguchi, S. (2018). HpBase: a genome database of a sea urchin, *Hemicentrotus pulcherrimus*. *Dev. Growth Differ.* 60, 174–182. doi: 10.1111/dgd.12429

Kudtarkar, P., and Cameron, R. A. (2017). Echinobase: an expanding resource for echinoderm genomic information. *Database* 2017:bax074. doi: 10.1093/database/bax074

Laport, M. S., Bauwens, M., Collard, M., and George, I. (2018). Phylogeny and antagonistic activities of culturable bacteria associated with the gut microbiota of the sea urchin (Paracentrotus lividus). *Curr. Microbiol.* 75, 359–367. doi: 10.1007/s00284-017-1389-5

Lawrence, J. M. (2013). *Sea Urchins: Biology and Ecology*. San Diego, CA: Academic Press.

Li, A., Espinoza, J., and Hamdoun, A. (2020). Inhibitory effects of neurotoxin β-N-methylamino-L-alanine on fertilization and early development of the sea urchin *Lytechinus pictus*. *Aquat. Toxicol.* 221:105425. doi: 10.1016/j.aquatox.2020.105425

Lozupone, C., Lladser, M. E., Knights, D., Stombaugh, J., and Knight, R. (2011). UniFrac: an effective distance metric for microbial community comparison. *ISME J.* 5, 169–172. doi: 10.1038/ismej.2010.133

Mann, K. H. (1977). Destruction of kelp-beds by sea-urchins: a cyclical phenomenon or irreversible degradation? *Helgoländer Meeresunters* 30, 455–467. doi: 10.1007/BF02207854

Martín-Durán, J. M., and Hejnol, A. (2021). A developmental perspective on the evolution of the nervous system. *Dev. Biol.* 475, 181–192. doi: 10.1016/j.ydbio.2019.10.003

Meziti, A., Kormas, K. A., Pancucci-Papadopoulou, M. A., and Thessalou-Legaki, M. (2007). Bacterial phylotypes associated with the digestive tract of the sea urchin *Paracentrotus lividus* and the ascidian *Microcosmus* sp. *Russ. J. Mar. Biol.* 33, 84–91. doi: 10.1134/S1063074007020022

Miller, P. M., Lamy, T., Page, H. M., and Miller, R. J. (2021). Sea urchin microbiomes vary with habitat and resource availability. *Limnol. Oceanogr. Lett.* 6, 119–126. doi: 10.1002/lol2.10189

Morais, L. H., Schreiber, H. L., and Mazmanian, S. K. (2021). The gut microbiota–brain axis in behaviour and brain disorders. *Nat. Rev. Microbiol.* 19, 241–255. doi: 10.1038/s41579-020-00460-0

Nobre, C. R., Santana, M. F. M., Maluf, A., Cortez, F. S., Cesar, A., Pereira, C. D. S., et al. (2015). Assessment of microplastic toxicity to embryonic development of the sea urchin *Lytechinus variegatus* (Echinodermata: Echinoidea). *Mar. Pollut. Bull.* 92, 99–104. doi: 10.1016/j.marpolbul.2014.12.050

Overbeek, R., Olson, R., Pusch, G. D., Olsen, G. J., Davis, J. J., Disz, T., et al. (2014). The SEED and the Rapid Annotation of microbial genomes using Subsystems Technology (RAST). *Nucleic Acids Res.* 42, D206–D214. doi: 10.1093/nar/gkt1226

Parks, D. H., Tyson, G. W., Hugenholtz, P., and Beiko, R. G. (2014). STAMP: statistical analysis of taxonomic and functional profiles. *Bioinformatics* 30, 3123–3124. doi: 10.1093/bioinformatics/btu494

Pikula, K., Zakharenko, A., Chaika, V., Em, I., Nikitina, A., Avtomonov, E., et al. (2020). Toxicity of carbon, silicon, and metal-based nanoparticles to sea

urchin *Strongylocentrotus intermedius*. *Nanomaterials* 10:1825. doi: 10.3390/nano10091825

Rendell-Bhatti, F., Paganos, P., Pouch, A., Mitchell, C., D'Aniello, S., Godley, B. J., et al. (2021). Developmental toxicity of plastic leachates on the sea urchin *Paracentrotus lividus*. *Environ. Pollut.* 269:115744. doi: 10.1016/j.envpol.2020.115744

Sakai, Y., Tajima, K. I., and Agatsuma, Y. (2003). "Mass production of seed of the Japanese edible sea urchins *Strongylocentrotus intermedius and Strongylocentrotus nudus*," in *Proceedings of the International Conference on Sea-Urchin Fisheries and Aquaculture*, eds. J. M. Lawrence and O. Guzmán (Lancaster, PA: DEStech Publication), 289–298.

Sharma, S., Awasthi, A., and Singh, S. (2019). Altered gut microbiota and intestinal permeability in Parkinson's disease: pathological highlight to management. *Neurosci. Lett.* 712:134516. doi: 10.1016/j.neulet.2019.134516

Sodergren, E., Weinstock, G. M., Davidson, E. H., Cameron, R. A., Gibbs, R. A., Angerer, R. C., et al. (2006). The genome of the sea urchin *Strongylocentrotus purpuratus*. *Science* 314, 941–952. doi: 10.1126/science.1133609

Stefánsson, G., Kristinsson, H., Ziemer, N., Hannon, C., and James, P. (2017). *Markets for sea urchins: A Review of Global Supply and Markets*. Reykjavik: Matís.

Takagi, S., Murata, Y., Inomata, E., Aoki, M. N., and Agatsuma, Y. (2019). Production of high quality gonads in the sea urchin *Mesocentrotus nudus* (A. Agassiz, 1864) from a barren by feeding on the kelp *Saccharina japonica* at the late sporophyte stage. *J. Appl. Phycol.* 31, 4037–4048. doi: 10.1007/s10811-019-01895-6

Tang, W., Meng, Z., Li, N., Liu, Y., Li, L., Chen, D., et al. (2021). Roles of gut microbiota in the regulation of hippocampal plasticity, inflammation, and hippocampus-dependent behaviors. *Front. Cell. Infect. Microbiol.* 10:876. doi: 10.3389/fcimb.2020.611014

Warner, J. F., Lord, J. W., Schreiter, S. A., Nesbit, K. T., Hamdoun, A., and Lyons, D. C. (2021). Chromosomal-level genome assembly of the painted sea urchin *Lytechinus pictus*: a genetically enabled model system for cell biology and embryonic development. *Genome Biol. Evol.* 13:evab061. doi: 10.1093/gbe/evab061

Wessel, G. M., Wada, Y., Yajima, M., and Kiyomoto, M. (2021). Bindin is essential for fertilization in the sea urchin. *Proc. Natl. Acad. Sci. U.S.A.* 118:e2109636118. doi: 10.1073/pnas.2109636118

Wilson, A. S., Koller, K. R., Ramaboli, M. C., Nesengani, L. T., Ocvirk, S., Chen, C., et al. (2020). Diet and the human gut microbiome: an international review. *Dig. Dis. Sci.* 65, 723–740.

Wilson, E. B. (1895). Archoplasm, centrosome and chromatin in the sea-urchin egg. *J. Morphol.* 11, 443–478.

Wood, N. J., Mattiello, T., Rowe, M. L., Ward, L., Perillo, M., Arnone, M. I., et al. (2018). Neuropeptidergic systems in pluteus larvae of the sea urchin *Strongylocentrotus purpuratus*: neurochemical complexity in a "simple" nervous system. *Front. Endocrinol.* 9:628. doi: 10.3389/fendo.2018.00628

Yadav, V., Varshney, P., Sultana, S., Yadav, J., and Saini, N. (2015). Moxifloxacin and ciprofloxacin induces S-phase arrest and augments apoptotic effects of cisplatin in human pancreatic cancer cells via ERK activation. *BMC Cancer* 15:581. doi: 10.1186/s12885-015-1560-y

Yamazaki, Y., Meirelles, P. M., Mino, S., Suda, W., Oshima, K., Hattori, M., et al. (2016). Individual Apostichopus japonicus fecal microbiome reveals a link with polyhydroxybutyrate producers in host growth gaps. *Sci. Rep.* 6:21631. doi: 10.1038/srep21631

Yang, S. H., Seo, H. S., Woo, J. H., Oh, H. M., Jang, H., Lee, J. H., et al. (2014). *Carboxylicivirga* gen. nov. in the family Marinilabiliaceae with two novel species, *Carboxylicivirga mesophila* sp. nov. and *Carboxylicivirga taeanensis* sp. nov., and reclassification of *Cytophaga fermentans* as *Saccharicrinis fermentans* gen. nov., comb. nov. *Int. J. Syst. Evol. Microbiol.* 64, 1351–1358. doi: 10.1099/ijs.0.053462-0

Yao, Q., Yu, K., Liang, J., Wang, Y., Hu, B., Huang, X., et al. (2019). The composition, diversity and predictive metabolic profiles of bacteria associated with the gut digesta of five sea urchins in Luhuitou fringing reef (northern South China Sea). *Front. Microbiol.* 10:1168. doi: 10.3389/fmicb.2019.01168

Youngblut, N. D., Reischer, G. H., Walters, W., Schuster, N., Walzer, C., Stalder, G., et al. (2019). Host diet and evolutionary history explain different aspects of gut microbiome diversity among vertebrate clades. *Nat. Commun.* 10:2200.

Zhao, C., Zhang, L., Shi, D., Ding, J., Yin, D., Sun, J., et al. (2018). Transgenerational effects of ocean warming on the sea urchin *Strongylocentrotus intermedius*. *Ecotoxicol. Environ. Saf.* 151, 212–219. doi: 10.1016/j.ecoenv.2018.01.014

Ziegler, A., Gilligan, A. M., Dillon, J. G., and Pernet, B. (2020). Schizasterid heart urchins host microorganisms in a digestive symbiosis of mesozoic origin. *Front. Microbiol.* 11:1697. doi: 10.3389/fmicb.2020.01697

Conflict of Interest: The authors declare that the research was conducted in the absence of any commercial or financial relationships that could be construed as a potential conflict of interest.

Publisher's Note: All claims expressed in this article are solely those of the authors and do not necessarily represent those of their affiliated organizations, or those of the publisher, the editors and the reviewers. Any product that may be evaluated in this article, or claim that may be made by its manufacturer, is not guaranteed or endorsed by the publisher.

frontiers in Marine Science

ORIGINAL RESEARCH
published: 31 January 2022
doi: 10.3389/fmars.2022.801344

Characterization of Microbiomes Associated With the Early Life Stages of Sea Cucumber *Apostichopus japonicus* Selenka

*Juanwen Yu[1], Yuichi Sakai[2], Sayaka Mino[1] and Tomoo Sawabe[1]**

[1] Laboratory of Microbiology, Faculty of Fisheries Sciences, Hokkaido University, Hakodate, Japan, [2] Hakodate Fisheries Research, Hokkaido Research Organization, Local Independent Administrative Agency, Hakodate, Japan

There is a lot of evidence indicating pioneer microbes in early life having various effects on later host biology. Because of the influential phylogenetic position of sea cucumber, which is a deep branching clade in Deuterostomia, the attention on the microbiome in sea cucumber has been increasing. Although microbes in sea cucumber have been reported in several studies, there is a lack of knowledge regarding the pioneer microbiota in the early life stages of sea cucumber. In this study, microbiota changes during the larval development of sea cucumber were assessed using a laboratory rearing system. Microbial community structure was likely to be related to the developmental stage and significant alterations were detected in the late auricularia stage. The relative abundances of *Oceanospirillales*, *Alteromonadales,* and *Rhodobacterales* significantly varied after gut formation. A total of 257 strains were isolated from larval developmental stages of sea cucumber and affiliated to 124 ASVs in the metagenomic analysis. This data demonstrates for the first-time dynamic changes of sea cucumber microbiota in the developmental stages in early life.

Keywords: pioneer microbiome, gut microbiome, holobiont, sea cucumber, *Apostichopus japonicus*

OPEN ACCESS

Edited by:
Fabiano Thompson, Federal University of Rio de Janeiro, Brazil

Reviewed by:
Francisco Vargas-Albores, Centro de Investigación en Alimentación y Desarrollo, Consejo Nacional de Ciencia y Tecnología (CONACYT), Mexico
Haruo Sugita, Nihon University, Japan

***Correspondence:**
Tomoo Sawabe
sawabe@fish.hokudai.ac.jp

Specialty section:
This article was submitted to Microbial Symbioses, a section of the journal Frontiers in Marine Science

Received: *25 October 2021*
Accepted: *10 January 2022*
Published: *31 January 2022*

Citation:
Yu J, Sakai Y, Mino S and Sawabe T (2022) Characterization of Microbiomes Associated With the Early Life Stages of Sea Cucumber Apostichopus japonicus Selenka. Front. Mar. Sci. 9:801344. doi: 10.3389/fmars.2022.801344

INTRODUCTION

Since the introduction of holobiont and hologenome concept, comprehensive studies on how holobiont assembly starts, in particular, which kinds of microorganisms first colonize when establishing the holobiont have been the subject of discussion. These first colonizers are called pioneer microbes, and have been widely studied in Deuterostomia animals with a view to investigating their composition and function in holobionts (Wopereis et al., 2014; Arrieta et al., 2015; Schokker et al., 2015; Gensollen et al., 2016). In humans, Therodor Escherich (1857–1911) was the pioneer in the progress of understanding human gut microflora, demonstrating the relationship between intestinal bacteria and physiology of digestion in infants (Escherich, 1886; Bettelheim, 1986; Shulman et al., 2007). Escherich's observations have been strengthened by the evidence that early life microbiota plays an important role in shaping the immune system (Gomez de Agüero et al., 2016; Korpela and de Vos, 2018), and in decreasing risks in developing allergic diseases (Koenig et al., 2011; Arrieta et al., 2014; Gensollen et al., 2016), with the development of modern sequencing technology and metagenomics today. A recent study in infant gut microbiome indicated there are dynamic changes in early life microbiome during the first year after birth,

and the newborns' gut microbiome gradually develops and resembles adult-like microbiomes with *Firmicutes* and *Bacteroidetes* as the most abundant taxa, followed by *Actinobacteria* and *Proteobacteria* (Bäckhed et al., 2015).

As many studies already indicate that pioneer microbiome in early life is crucial in Deuterostomia, an increasing number of studies focus on the influence of pioneer microbes on host biology which could then be used to benefit agriculture and aquaculture. Pioneer microbes' colonization in bird chicks showed an impact on the day of hatching through alteration of intestinal proteome which affects gastrointestinal tract immunity and cellular development (Wilson et al., 2019). The pioneer gut microbiota of tilapia larvae varied between individuals in different rearing environments (Giatsis et al., 2014). Although many previous studies have suggested the importance of early life microbiota in host biology, the structure and function of pioneer microbiota in marine Deuterostomia invertebrate has not been fully elucidated yet.

Sea cucumber (Echinodermata, Holothuroidea) is a marine invertebrate within Deuterostomia linage, and is a worldwide popular fishery and aquaculture resource, especially in Asian regions, due to its nutritive and medicinal value. In Asian region, sea cucumber has high commercial value and 200,000 tons a year in China and 6,500 tons a year in Japan are produced, which show that *Apostichopus japonicus* Selenka is one of the most consumed species (Ministry of Agriculture and Rural Affairs Fishery Administration, 2003-2012; MAFF, 2020). However, the fisheries of wild *A. japonicus* have declined worldwide and the animal has been placed on the red list of endangered species. Wild *A. japonicus* in China had already been reported as being overfished in the 1950s (Zhang and Liu, 1984; Hamel and Mercier, 2013). The huge demands for sea cucumber in recent decades has resulted in overfishing and over-exploitation in more than 70% of regions across the world (González-Wangüemert et al., 2018). Many studies have recommended regulation and management of sea cucumber fisheries and to develop restocking programs of overfished species in various regions including Brazil, Mexico, the Philippines, the Mediterranean, and Northeast Atlantic (González-Wangüemert et al., 2018; Jontila et al., 2018; Rogers et al., 2018; Gamboa-Álvarez et al., 2020). Due to the growing commercial demand for sea cucumber and decreasing wild stocks, aquaculture of sea cucumber has emerged and developed. *A. japonicus* is one of the most popular species in sea cucumber aquaculture, and artificial breeding was first attempted in 1937 and total output reached 170,830 tons in China, 2012 and 6,611 tons in Japan, 2019 (Inaba, 1937; Ministry of Agriculture and Rural Affairs Fishery Administration, 2003-2012).

In order to develop sea cucumber aquaculture, larval development of sea cucumber have been intensively studied (Chen and Chian, 1990; Sewell and McEuen, 2002; Ramofafia et al., 2003; Hu et al., 2010; Soliman et al., 2013). There are six major developmental stages in the early life of *A. japonicus* after the egg is fertilized; blastula, gastrula, auricularia, doliolaria, pentactula, and juvenile stages (Soliman et al., 2013; **Supplementary Figure 1**). Fundamental organs (buccal cavity, esophagus, intestine, cloaca, ciliary bands) appear in the auricularia stage and mature in the juvenile stage within 17 days on average after fertilization under optimal conditions. Primary tentacles and primary podium are used for attaching to habitat in the pentactula stage and then fully develop to tentacles and foot tube in the juvenile stage. Although some studies indicate food, culture conditions and bacterial control may relate to growth and survival rates of sea cucumber larvae, no certain links have been confirmed (Ramofafia et al., 2003; Hu et al., 2010).

Sea cucumber microbiome has been vigorously studied in recent decades in the aspects of diseases and host physiology. Rotting-edges syndrome caused by *Vibrio lentus* (Zhang et al., 2010) and stomach ulcer disease caused by *Vibrio splendidus* (Wang et al., 2006) occur in the auricularia to doliolaria stage. Off-plate syndrome is a serious disease caused by several bacteria that rapidly spreads and has a high mortality rate during the pentactula stage (Zhang et al., 2009). Probiotics have also been studied as potentially improving growth and stimulating the immune system in juvenile sea cucumbers (Ma et al., 2019). Intestinal microbial community composition altered by dietary supplementation benefits the growth of sea cucumber (Yang et al., 2015b). *Rhodobacterales* retaining PHB metabolism genes may play a key role in cultured sea cucumber growth (Yamazaki et al., 2016). Molecular ecological network analysis also indicates the stability of the intestinal community ecosystem is improved by probiotics and florfenicol has a positive impact on sea cucumber growth (Yang et al., 2017). All these studies suggest that microbiome in sea cucumber larvae development might be a crucial factor in developing seed production for sustainable aquaculture, however, there is a lack of knowledge of the structure and function of pioneer microbes of sea cucumber larvae and the dynamic changes during the larval development.

In this study, we set up a laboratory rearing system and performed Meta16S analysis in order to assess the changes to the microbiome during the larval development of sea cucumber and to detect the pioneer microbiota in the early developmental stages. Our results demonstrate that detection of pioneer microbiome in *A. japonicus* and stepwise changed microbiota that significantly related to organogenesis and larval development.

MATERIALS AND METHODS

Sample Collection and Rearing Conditions Under Laboratory Conditions

Fertilized eggs of the sea cucumber *A. japonicus* were prepared at 18.7°C at a farm in Hokkaido Aquaculture Promotion Corporation Kumaishi Branch, Japan (42.12574, 139.99966) on 11:00 am 5 August 2019. These eggs were transferred to the laboratory of Microbiology, Faculty of Fisheries Sciences, Hokkaido University whilst being kept at 18°C for 2 h, and then used immediately for experiments. Density of the fertilized eggs was set at 7,500 eggs/L in an 8 L volume aquarium after manual counting of these eggs in 0.1 mL seawater using a microscope (AxioImager Z2, Zeiss, Oberkochen, Germany) and reared at 18°C. The aquarium was prepared using a

sterilized 8 L glass bottle (Ishizuka glass Co. Ltd., Aichi, Japan) set in an incubator (MLR-352-PJ, PHC Corp., Tokyo, Japan). Each bottle was filled with 7.5 L natural filtrated seawater using a 50 μm mesh cartridge filter (SWP50P10, AS One, Osaka, Tokyo) used in the Kumaishi farm. Each 80 mL (7,500 eggs) of fertilized egg suspensions, corresponding to the final egg density of around 1 egg/mL, was added to each bottle, and rearing was started with aeration (SPP-25GA, Techno Takatsuki Co., Ltd., Osaka, Japan). Feeding started at 48 h after fertilization (on 7 August 2020), when early auricularia morphogenesis was observed in over 80% of individuals. A commercially available diatom, *Chaetoceros gracilis* (Hakodate Fisheries Research, Japan), was fed to the sea cucumber larvae daily.

Subsampling of Sea Cucumber Larvae and Microbes in Rearing Water

Sea cucumber larvae at five major developmental stages, gastrula, early and late auricularia, doliolaria, and pentactula after being confirmed by a microscopic observation (**Supplementary Figure 1**) were used for characterization of microbiomes and microbial isolations. Five liters of rearing seawater including sea cucumber larvae were filtered using a sterilized 40 μm nylon mesh (Falcon Cell Strainer, Durham, NC, United States), and washed once using 0.22 μm filter-sterilized seawater. Sterivex filter (SterivexTM-GV Sterile Vented Filter Unit 0.22 μm, EMD Millipore, Billerica, MA, United States) was used to prepare this sterilized seawater. The larvae on nylon filters were immediately frozen at −80°C until DNA extraction.

To prepare microbial fractions in rearing water, five liters of rearing water after passing through nylon mesh was filtered through a 0.22 μm Sterivex filter by positive pressure using filtered (0.22 μm) N_2 gas. These Sterivex filters were preserved at −80°C until DNA extraction.

Microbial DNA Extraction and 16S rRNA Gene Sequencing

Microbial DNA extraction from sea cucumber was performed using the NucleoSpin Soil Kit (MACHEREY-NAGEL, Düren, Germany), according to the manufacturer's protocol. Microbial DNA extraction from seawater was performed using the NucleoSpin Tissue kit (MACHEREY-NAGEL), according to the modified manufacturer's protocol. In brief, seawater samples were heated at 55°C for 1 h to add an active cell lysis process in TE buffer (10 mM Tris–HCl, 1 mM EDTA) containing 20% SDS and proteinase K (20 mg mL^{-1}) instead of buffer T1. In the third step Lyse Sample, 1 mL buffer B3 was used instead of 200 μL amount of the buffer.

The hypervariable V1-V2 region of the 16S rRNA gene was amplified by PCR with barcoded 27Fmod and 338R primers with Illumina adaptor sequences (Yamazaki et al., 2019). PCR amplicons were purified using AMPure XP magnetic purification beads (Beckman Coulter, Brea, CA, United States), and quantified using the Quant-iT PicoGreen dsDNA Assay Kit (Life Technologies Japan). Equal amount of each PCR amplicon was mixed and then sequenced using MiSeq Reagent Kit v3 (600-cycles) with the MiSeq Illumina platform. Based on sample specific barcodes, obtained reads were assigned to each sample.

Meta16S Analysis

The paired-end sequence data with quality scores (i.e., Fastq files) was analyzed using Quantitative Insights Into Microbial Ecology 2 (QIIME 2, version 2018.11) (Bolyen et al., 2019). Quality controls (e.g., trimming primers and denoising sequences, removing chimeric sequences) and merging paired-end sequences were performed using DADA2 (Callahan et al., 2016). Reads with 100% similarity constituted an amplicon sequence variance (ASV). Unlike the method to cluster sequences into operational taxonomic units (OTUs) with fixed threshold (usually 97%), this quality control method using DADA2 allows us to detect even a single nucleotide difference. ASVs were assigned to taxonomy using the Naive Bayes classifier and Greengenes database. Using subsampled reads, unweighted UniFrac distances as beta-diversity were calculated and visualized in prinicipal coordinate analysis (PCoA) plots (Lozupone et al., 2011). Significant differences of unweighted UniFrac distance were tested by permutational multivariate analysis of variance (PERMANOVA) (FDR-corrected $p < 0.05$). The phylogenic tree was generated by FastTree (Price et al., 2009). *Z*-score was calculated by genefilter package in R (Gentleman et al., 2021). R studio software (Version 1.2.5019) was used for heatmaps construction, *Z*-score calculation by genefilter package (Gentleman et al., 2021) and statistical significance of *t*-test to pick up the key ASVs.

Isolation and Identification of Microbes From Early Life Stages

Sea cucumber larvae at each life stage were also used for microbial isolations. Larvae were filtered with 40 μm nylon mesh (Falcon Cell Strainer, Durham, NC, United States), washed once with sterilized seawater, and then homogenized in 1 mL filter-sterilized natural seawater for 60 s manually. A 10-fold serial dilution of these homogenates was prepared using a filter-sterilized natural seawater, and then the dilutions were cultured on 1/5 strength ZoBell 2216E agar plate (0.1% polypeptone, 0.02% yeast extract, 1.5% agar, 75% natural seawater collected at Kumaishi farm) at 18°C. After calculating viable bacterial counts, ca. 30 bacterial colonies per plate were purified using the same agar plate.

The16S rRNA gene sequences of each isolate was amplified by colony PCR using GoTaq Green Mater Mix (Promega, Madison, WI, United States), 27F primer (20 pmol), 1492R primer (20 pmol) with the following thermal profile; initial denaturation at 96°C for 3 min, followed by 30 cycles of denaturation at 95°C for 1 min, annealing at 50°C for 1 min and extension at 72°C for 2 min, and final extension at 72°C for 7 min. PCR products of ∼1500 bp were visualized by electrophoresis with 1% agarose gels. PCR products were purified using a Wizard SV Gel and PCR clean-up system (Promega). PCR amplicons were directly sequenced by Hokkaido System Science (Sapporo,

Japan). Sequences were assembled using ChromasPro (Version 2.1.8, Technelysium Pty. Ltd., Australia). Almost complete sequences of 16S rRNA gene of 257 isolates were obtained in this study. In order to determine the phylogenetic position of isolates, the sequences were aligned using Clustal X (Version 2.1) (Larkin et al., 2007) with the top five most similar sequences indicated by megaBLAST and sequences of type strains retrieved from RDP release 11 as reference sequences (Cole et al., 2014). The phylogenetic tree was reconstructed using Maximum-Likelihood algorism with MEGA X (Version 10.1.7) after performing the best model selection, and was further edited by an online tool Interactive Tree of Life (Letunic and Bork, 2019).

Comparison of Sequences Obtained From Isolates and Meta16S Sequences

Integration of Meta16S sequences and 16S rRNA gene sequences of isolates were performed using QIIME2. Identification and taxonomic analysis of representative were also performed during the comparison. Dominate ASVs were identified and isolated and after combination with identification of isolated strains sequenced by 16S rRNA sequencing, taxonomic analysis reach to both gene and species level.

RESULTS

Microbial Community Structure Dynamics During Sea Cucumber Developmental Stages

A total of 974,753 Meta16S sequence reads were obtained from sea cucumber and seawater samples collected from fertilized eggs (FE), gastrula (GL), early auricularia (EA), late auricularia (LA), pentactula (PT), and juveniles (JN) (**Supplementary Table 1**). Reads passed quality control and removed eukaryotic reads (e.g., mitochondria and chloroplast) were used for microbial diversity analyses and taxonomic assignments; 106,713 and 134,940 qualified reads were generated from sea cucumber samples and seawater samples, respectively (**Supplementary Table 1**).

Unweighted UniFrac distance analysis revealed the dynamic changes of microbiotas associated with host development. The 2D PCoA plot based on unweighted UniFrac analysis obtained sea cucumber larvae and rearing seawater samples at each developmental stage indicates that (1) microbiotas between seawater and sea cucumber were not grouped, (2) microbiota between FE, GL, and EA juveniles were grouped but FE, GL, and EA seawater microbiotas were not, and (3) microbiota between PT and JN sea cucumber larvae were grouped and LA, PT, and JN seawater microbiota were grouped (**Figure 1**). Microbial community of sea cucumber samples according to the PCoA plot reveals a large variation between early and late auricularia stages, the time point before and after gut developed. The UniFrac distance matrix also showed similar tendency in microbiota grouping between sea cucumber and seawater (**Figures 2B,C**). A decreased alpha diversity based on Shannon index and increased beta diversity was observed after gut development (**Figures 2A,D**), indicating a less complex but more dissimilar microbial community after the digestive system had developed.

Characterization of Microbial Community Structure at Early Life Stages of *Apostichopus japonicus*

A total of 1,440 ASVs were obtained and further affiliated to 75 bacterial orders using a similarity threshold of 99% sequence identity; 144, 219, 157, 120, 327, and 254 ASVs, and 29, 30, 19, 28, 39, and 35 bacterial orders, were affiliated in FE, GL, EA, LA, PT, and JN stage, respectively (**Supplementary Table 2**). *Oceanospirillales* and *Alteromonadales* were the most abundant in FE, GL, and EA stages with relative abundance ranging from 24.1 to 29.9% and 32.6 to 46.2%, respectively (**Figure 3** and **Supplementary Table 2**). However, abundances of *Oceanospirillales* dramatically decreased to 3.2% in the LA stage and gradually increased in the PT (9.8%) and JN (49.1%) stages. Such a fluctuation in abundance was also observed in *Alteromonadales*, 32.5–46.2% in the FE to EA stages, but those decreased after EA (14.8, 10.6, and 6.3% in LA, PT, and JN stage, respectively) (**Figure 3** and **Supplementary Table 2**). *Vibrionales*, *Pseudomonadales,* and *Rhodobacterales* were the third most abundant taxa in FE, GL, and EA stages before gut organogenesis. *Vibrionales* was detected in FE (7.2%), GL (13.6%), and EA (12.1%) stages than LA (4.7%), PT (1.0%), and JN (0.3%). Likewise, *Pseudomonadales* was at FE (7.7%), but relative lower amounts in GL (4.6%), EA (2.4%), LA (5.0%), PT (1.0%), and JN (0.3%). In contrast, *Rhodobacterales* was observed in LA (26.0%), PT (37.0%), and JN (22.8%) with higher fractions than in the early three stages in FE (4.9%), GL (7.0%), and EA (9.8%). Relative abundance of *Flavobacteriales* was much lower in early stages of FE (3.6%), GL (2.1%), and EA (1.5%) but increased in LA (25.5%), PT (14.2%), and JN (3.4%).

On the other hand, the microbial community in seawater is significantly different from those associated with sea cucumber hosts (**Figure 2B**). A total of 232, 84, 139, 277, 163, and 69 features were detected in fertilized egg rearing seawater (FESW), gastrula seawater (GLSW), early auricularia seawater (EASW), late auricularia seawater (LASW), pentactula seawater (PTSW), and juvenile seawater (JNSW), respectively (**Figures 3**, **4**). *Alteromonadales* and *Oceanospirillales*, which were dominant at early three stages of sea cucumber samples, were rarely detected at FESW (1.3%, 1.7%), but significantly increased to become the second and third most abundant at GLSW (20.3%, 7.1%), followed by rising to the first and second most abundant at EASW (50.1%, 19.0%). Similar to sea cucumber samples, the abundance of *Oceanospirillales* also dropped in LASW (5.3%) but increased in PTSW (46.2%) and appeared to be present in JNSW (87.7%). The abundance of *Alteromonadales* in LASW (21.3%) decreased below a detectable limit (0.1%) in JNSW. *Vibrionales* and *Pseudomonadales* were also abundant in GLSW (5.0%, 4.3%) and EASW (3.7%, 10.7%), but relatively low in later stage PTSW (0.2%, 0.7%) and undetectable in JNSW. *Rhodobacterales* increased in later stages LASW and PTSW but limited at FE, GL and EA stage, during the host development progress. Different from the host bacterial community, *Flavobacteriales* was rarely

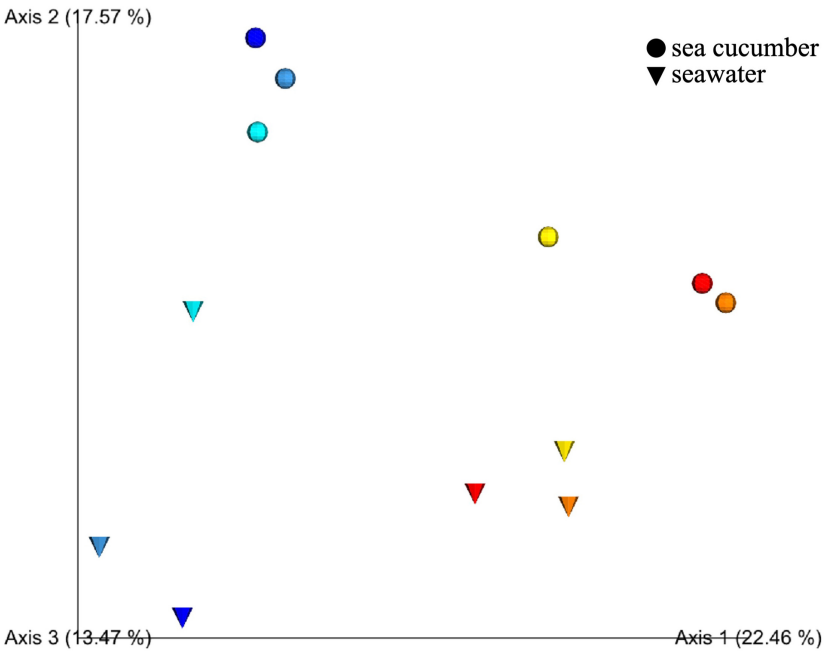

FIGURE 1 | Prinicipal coordinate analysis (PCoA) plot based on unweighted UniFrac distances obtained by comparison of microbiotas at each developmental stage of sea cucumber larva. Blue, fertilized egg; light blue, gastrula; cyan, early auricularia; yellow, late auricularia group; orange, pentactula group; red, juvenile. Circle and cone indicated microbiota from sea cucumber and rearing seawater, respectively.

detected in seawater samples, ranging from 0.3 to 8.5%. SAR11 clade, belonging to class *Alphaproteobacteria*, was observed in all samples of seawater, in particular, rich in FE and GL seawaters with 78.2 and 48.0% frequency, but low relative abundance in sea cucumbers (0.3% in GL) (**Figure 3** and **Supplementary Table 2**).

A further family level taxonomic distribution and heatmap based on relative abundance of top 50 abundant bacterial group revealed that (1) bacterial groups such as *Alteromonadaceae* (*Alteromonadales*), *Alcanivoracaceae* (*Oceanospirillales*), *Pseudoalteromonadaceae* (*Alteromonadales*), *Oleiphilaceae* (*Oceanospirillales*) first appeared and were abundant at FE stage, (2) *Rhodobacteriaceae* (*Rhodobacterales*), *Flavobacteriaceae* (*Flavobacteriales*), and *Marinobacteraceae* (*Alteromonadales*) increased from LA stage, and (3) *Colwelliaceae* (*Alteromonadales*) and *Halieaceae* (*Cellvibrionales*) increased at PT stage (**Figures 4**, **5**). Moreover, JN represents a unique microbiota compared to other life stages; *Nitrincolaceae* (*Oceanospirilales*), the population showed low levels in other life stages (0–7.3%), was significantly dominant in PT with 47.8% relative abundance. *Rhodobacteriaceae* (*Rhodobacterales*) was still the second most abundant family in JN, which appeared to be the most abundant family from the LA stage (22.8–37.0%) (**Figures 4**, **5**).

Dynamics profiling based on ASVs containing more than 500 reads revealed that 14 key ASVs significantly changed at different developmental stages in sea cucumber larvae (**Figures 6**, **7** and **Supplementary Figure 2**); these were assigned into 5 bacterial families, 4, 2, 4, 2, and 2 ASVs were assigned to *Nitrincolaceae* (*Oceanospirillales*), *Alcanivoracaceae* (*Oceanospirillales*), *Rhodobacteriaceae* (*Rhodobacterales*), *Flavobacteriaceae* (*Flavobacteriales*), and *Alteromonadaceae* (*Alteromonadales*). The ASVs assigned to *Nitrincolaceae* and *Rhodobacteraceae* showed different variation trends with corresponding seawater, but the relative abundance of them changed at specific developmental stages in sea cucumber larvae (**Figure 8**). In addition, 2 ASVs of ASV0013 and ASV0051 belonging to *Alteromonadaceae* and *Cellvibrionaceae*, respectively, were defined as core microbiome that present in sea cucumber 's microbiome during whole developmental process, which also detected in rearing seawater (**Supplementary Figure 3**).

Isolation of Key Bacterial Strains During the Larval Development of *Apostichopus japonicus*

A total of 257 strains were isolated from sea cucumber specimens and assigned to 45 species belonging to 32 genera, in which 89.1% of isolates were assigned to known species and 100% of isolates were assigned to known genera (**Figures 8**, **9** and **Supplementary Table 4**). A total of 42, 34, 22, 53, 37, 57, and 13 isolates were isolated from FE, GL, EA, LA, PT, JN, and fertilized egg rearing seawater (NSW), respectively, being counted up 10^2 to 10^4 CFU/g sample (**Supplementary Table 4**). A total of 20 of 42 isolates collected from FE specimen were identified as *Pseudoalteromonas* belonging to *Alteromonadales*, followed by *Alteromonas* (n = 7), *Vibrio* (n = 4), *Idiomarina* (n = 4), *Pseudomonas* (n = 3), *Marinobacter* (n = 2), *Paraglaciecola* (n = 1), and *Shewanella* (n = 1). *Marinobacter* (n = 14) also belonged to *Alteromonadales* was the most abundant genera in isolates collected from GL specimen, followed by *Pseudoalteromonas* (n = 9), *Alteromonas*

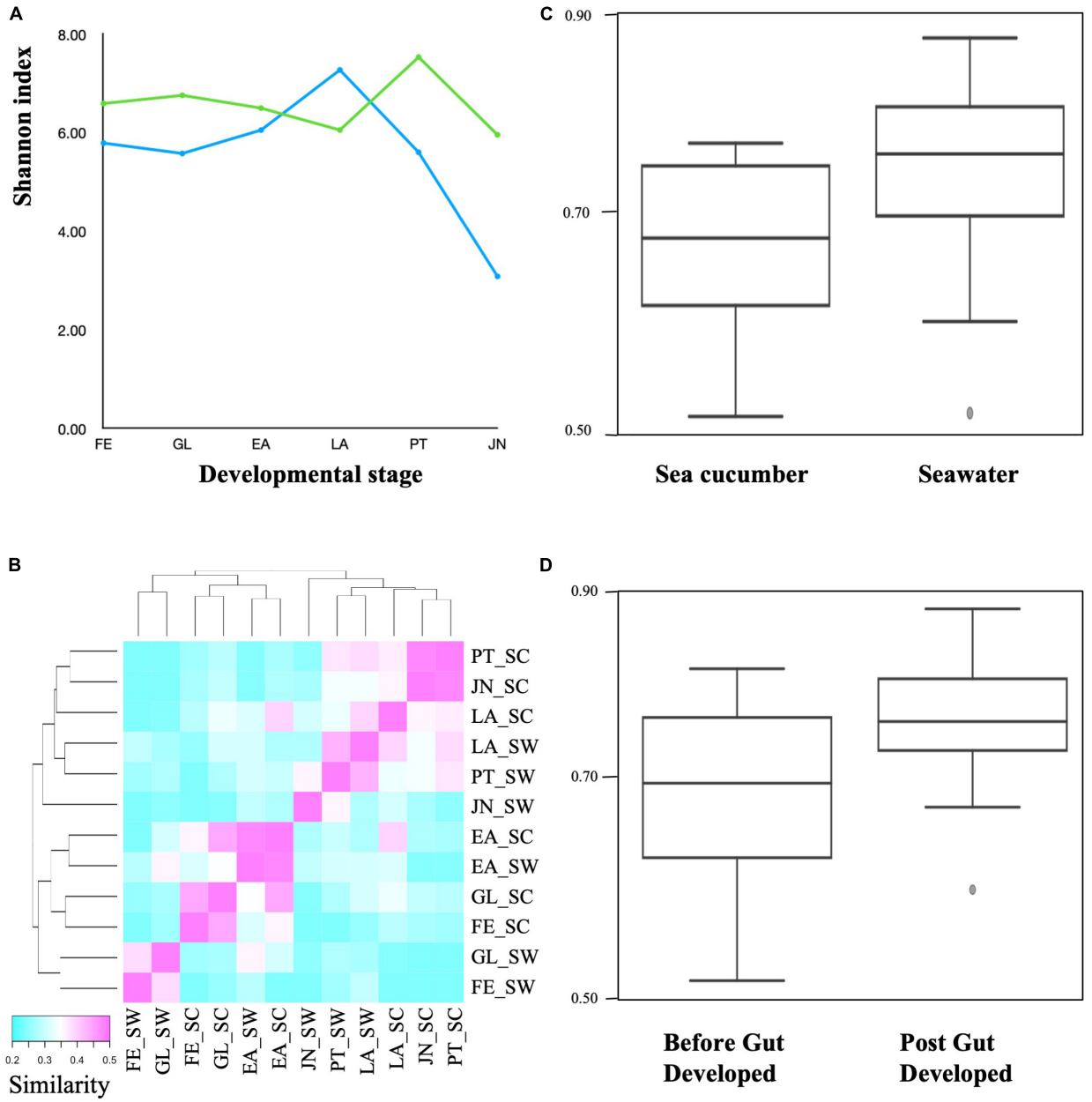

FIGURE 2 | Alpha and beta diversity among sea cucumber and seawater samples. **(A)** Shannon index. Green, sea cucumber samples; blue, seawater samples. **(B)** Heatmap based on unweighted UniFrac distance ($p < 0.05$, $q < 0.05$). Scale represent similarity within samples. FESC, Fertilized egg; GLSC, Gastrula; EASC, Early auricularia; LASC, Late auricularia; PTSC, Pentactula; JNSC, Juvenile; FESW, Fertilized egg rearing seawater; GLSW, Gastrula rearing seawater; EASW, Early auricularia rearing seawater; LASW, Late auricularia rearing seawater; PTSW, Pentactula rearing seawater; JNSW, Juvenile rearing seawater. **(C)** Unweighted Unifrac distance plot between sea cucumber and seawater ($p < 0.05$, $q < 0.05$). **(D)** Unweighted Unifrac distance plot between samples before and post-gut developed ($p < 0.05$, $q < 0.05$).

(n = 4), *Vibrio* (n = 4), *Neptunicella* (n = 1), *Sulfitobacter* (n = 1), and *Bacterioplanes* (n = 1). The most abundant genera in EA isolates were *Alteromonas* (n = 11) and *Pseudoalteromonas* (n = 4), both of them belonging to *Alteromonadales*, subsequently *Marinebacter* (n = 2), *Vibrio* (n = 2), and *Pseudomonas* (n = 1) were also obtained in EA. In LA isolates, 43 of 53 isolates were assigned to *Pseudoalteromonas*, which is the significant dominant genera compared to other genus *Marinobacter* (n = 4), *Alteromonas* (n = 3), and *Pseudomonas* (n = 2).

The composition of isolates showed a variation between LA and PT stages, which *Pseudoalteromonas*, *Marinobacter,* and *Alteromonas* belonging to the order *Alteromonadales* were the most abundant genera in FE to LA but absent in PT (**Figure 9**). In addition, taxonomic diversity of isolates was richer in later

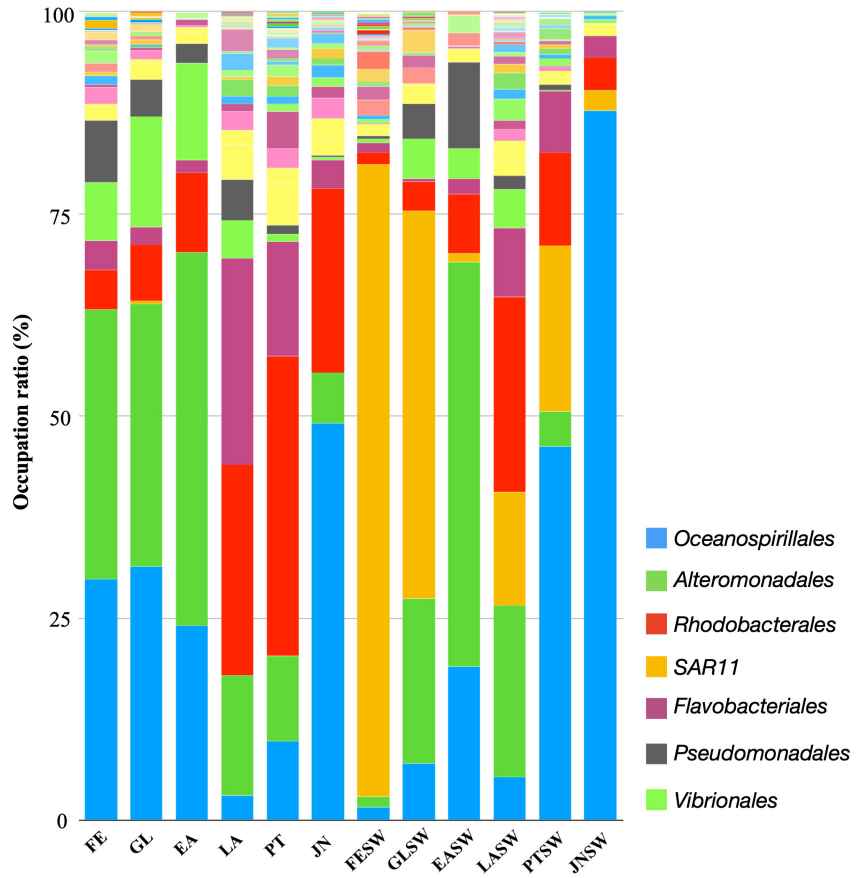

FIGURE 3 | Order-level taxonomic distribution among sea cucumber and seawater samples. Bars represent the relative percentage of each bacterial orders. FE, Fertilized egg; GL, Gastrula; EA, Early auricularia; LA, Late auricularia; PT, Pentactula; JN, Juvenile; FESW, Fertilized egg rearing seawater; GLSW, Gastrula rearing seawater; EASW, Early auricularia rearing seawater; LASW, Late auricularia rearing seawater; PTSW, Pentactula rearing seawater; JNSW, Juvenile rearing seawater.

stages such as PT and JN compared to earlier life stages. Likewise, *Thalassobius* (n = 9) and *Shimia* (n = 8) belonging to the order *Rhodobacterales* were the most abundant genera in PT, followed by *Pseudomonas* (n = 3), *Arenibacter* (n = 3), *Phaeobacter* (n = 3), *Muricauda* (n = 2), *Amphritea* (n = 2), and other 6 isolates assigned to 6 different genera. On the other hand, *Rhodobacterales* and *Alteromonadales* showed a higher possibility to be isolated in JN samples; a total of 20 of 57 isolates in JN were assigned to *Marinobacter* belonging to *Alteromonadales*; 7, 5, and 4 isolates were assigned to *Phaeobacter*, *Shimia,* and *Thalassobius* belonging to *Rhodobacterales*, respectively. The other isolates in JN were assigned to genera *Muricauda* (n = 3), *Alteromonas* (n = 3), *Neptunicella* (n = 3), *Aliiroseovarius* (n = 3), *Arenibacter* (n = 2), *Tropicibacter* (n = 2), *Pseudoalteromonas* (n = 2), *Pseudophaeobacter* (n = 1), *Williamsia* (n = 1), and *Spongiispira* (n = 1). Isolates from NSW were relatively unique compared to the sea cucumber samples. Genera *Sphingomonas*, *Sulfitobacter*, *Labrenzia*, *Rhodococcus*, *Kangiella,* and *Henticiella* were only isolated from NSW samples, which demonstrates a different microbial community structure.

Comparison of isolates with ASVs in Meta16S revealed a total of 124 ASVs were assigned to those sequences of isolates with 100% identity, including 51 dominant ASVs (>0.1% abundance) (**Supplementary Table 3**). In addition, 6 out of 14 key ASVs found in the Meta16S sequences were successfully isolated. ASV0013 and ASV0016 belonging to *Alteromonadaceae,* the relative abundance of these two key ASVs were 0.0090 and 0.0082, respectively. They showed a significant increase at the EA stage with the relative abundance of 0.046 and 0.037, assigning to 10 isolated strains from GL, EA, LA, and JN samples and identified as genus *Alteromonas*. One of them ASV0016 was absent at FE and then slightly increased in the gastrula stage. ASV0019, ASV0022, ASV0026, and ASV0030 belonging to *Rhodobacteriaceae,* the relative abundance of them were 0.0072, 0.0070, 0.0063, and 0.0060, respectively. They showed a significant increase at the PT stage with relative abundance of 0.033–0.040%, assigning to 13 isolated strains collected from JN and PT, which appeared from the early auricularia stage (**Supplementary Table 3**). Interestingly, these five key ASVs were not detected in the fertilized egg rearing seawater. In addition, although 75.8% sequences in Meta16S analysis were unassigned to known species or genera, the taxonomic level of 81 ASVs were improved to species or genus level after taxonomic analysis with isolated strains, in which one unassigned

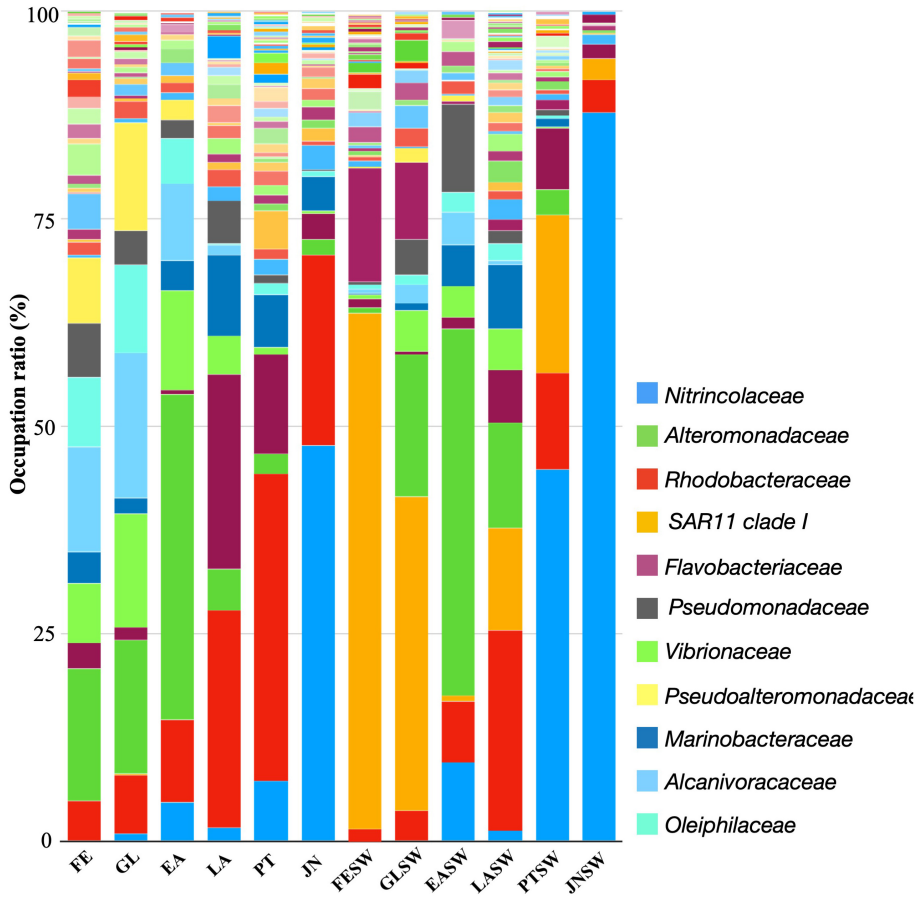

FIGURE 4 | Family-level taxonomic distribution among sea cucumber and seawater samples. Bars represent the relative percentage of each bacterial orders. FE, Fertilized Egg; GL, Gastrula; EA, Early Auricularia; LA, Late Auricularia; PT, Pentactula; JN, Juvenile; FESW, Kuma-shi seawater; GLSW, Gastrula rearing seawater; EASW, Early Auricularia rearing seawater; LASW, Late Auricularia rearing seawater; PTSW, Pentactula rearing seawater; JNSW, Juvenile rearing seawater.

ASV1407 was affiliated to strains NSW5 identified as *Kangiella geojedonens* and 10 uncultured ASVs were assigned to known species (**Supplementary Table 3**).

DISCUSSION

Microbiotas of sea cucumber *A. japonicus* has been intensively studied over recent decades aiming to discover beneficial bacteria that could contribute to sea cucumber aquaculture, disease control, and bioremediation (Chi et al., 2014; Yang et al., 2015b; Zhao et al., 2016; Chen et al., 2018; Ma et al., 2019). After the recent findings of potential physiological roles in gut microbiomes of the sea cucumber *A. japonicus* (Yamazaki et al., 2016), dynamics of the microbiome, in particular *How sea cucumbers shape their microbiomes?* has been a central question (Yamazaki et al., 2020). Among a series of studies on the sea cucumber microbiome, first colonizers on the animal guts called *Pioneer Microbes* are worth studying in sea cucumbers as they potentially contribute to improving aquaculture technology and accumulate biological knowledge on gut microbiome evolution compared to those in humans (Wopereis et al., 2014). Using a laboratory rearing system, we succeeded in conducting Meta16S sequencing to characterize microbiotas of fertilized eggs at major developmental stages up to juvenile and key bacteria were successfully isolated. To our knowledge, this is the first study to investigate the dynamics of microbiota during the larval development of sea cucumber and the possible relationship between early life microbiota and host biology in marine invertebrates.

New Insights Into the Dynamics of Microbiota Changes During Larval Development of Sea Cucumber

The pioneer microbiome in early life has been assessed mainly on human infant gut microbiome, and environmental factors, diets, developmental stage and genetics affecting microbiota shaping have been investigated (Nayak, 2010; Sullam et al., 2012; Mercier et al., 2015). *Bifidobacterium* and *Lactobacillus*, which are lactic acid utilizers, were prevalent in later infant microbiome (4–12 months) during breast feeding but decreased in adult-like microbiota when solid

FIGURE 5 | Dynamics of signature families at each stage. Scale represents relative abundance after *Z*-score calculation. FE, Fertilized egg; GL, Gastrula; EA, Early auricularia; LA, Late auricularia; PT, Pentactula; JN, Juvenile; FESW, Fertilized egg rearing seawater; GLSW, Gastrula rearing seawater; EASW, Early auricularia rearing seawater; LASW, Late auricularia rearing seawater; PTSW, Pentactula rearing seawater; JNSW, Juvenile rearing seawater.

food was introduced (Bäckhed et al., 2015; Hill et al., 2017). Similar to human infants, sea cucumber larvae's gut microbiota altered after feeding, which is probably linked to the changing of gut environment and its functional shifts. Many studies have also worked on pioneer microbiome using fish eggs and larvae to improve intensive aquaculture of larvae rearing (Vadstein et al., 2018), relationships to hatchability, and contribution to the formation of adult fish microbiota

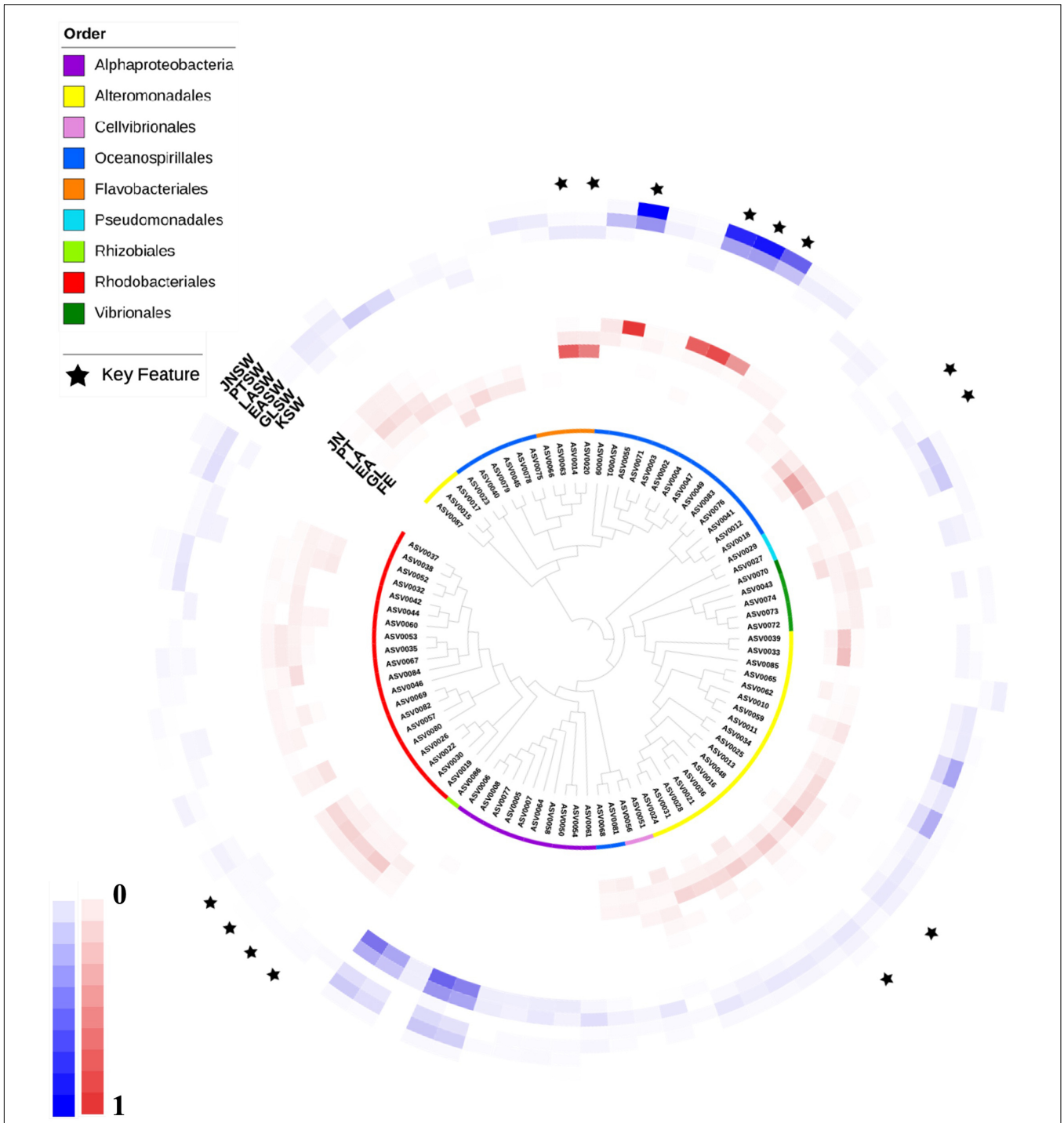

FIGURE 6 | A phylogenetic tree based on features having >500 reads with relative abundance. Inner circles represent taxonomic analysis at order lever. Red colored heatmap represent relative abundance of features in sea cucumber samples. Blue colored heatmap showed relative abundance of features in seawater samples. Key features were labeled with black stars. FE, Fertilized egg; GL, Gastrula; EA, Early auricularia; LA, Late auricularia; PT, Pentactula; JN, Juvenile; FESW, Fertilized egg rearing seawater; GLSW, Gastrula rearing seawater; EASW, Early auricularia rearing seawater; LASW, Late auricularia rearing seawater; PTSW, Pentactula rearing seawater; JNSW, Juvenile rearing seawater.

(Hansen and Olafsen, 1989, 1999; Califano et al., 2017). Whole-body microbiota of aquatic animals using fertilized eggs and post-hatch larvae of sea bream suggest that microbiotas of rearing water and diet affect the shaping of early life microbiota (Nikouli et al., 2019). The Meta16S analyses of sea cucumber during early developmental stages reveals several new findings

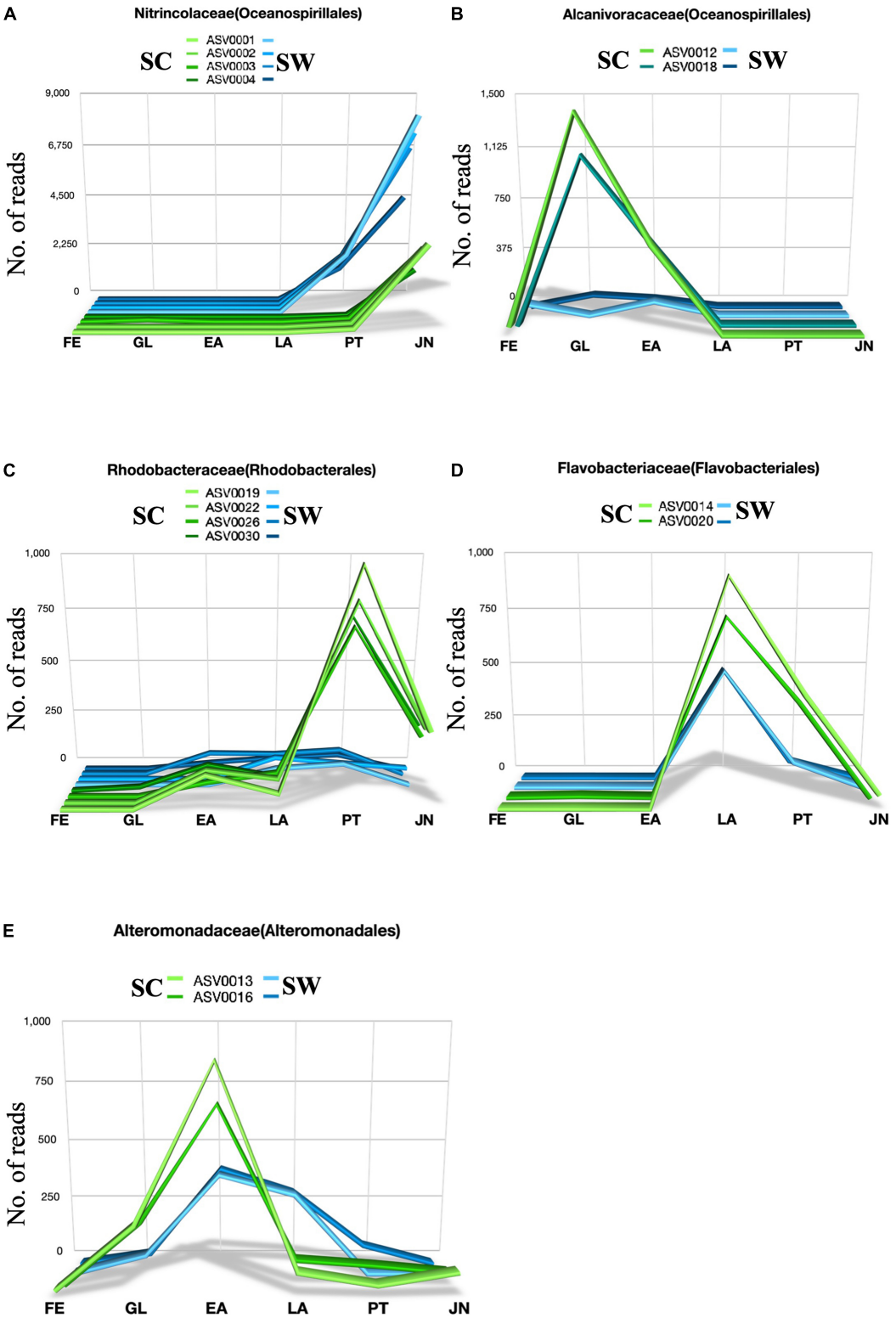

FIGURE 7 | Dynamics of relative abundance of key ASVs based on heatmap. 14 key ASVs were shown in panels **(A–E)**, respectively. X axis is developmental stage, and Y axis is number of reads. FE, Fertilized egg group; GL, Gastrula group; EA, Early auricularia group; LA, Late auricularia group; PT, Pentactula group; JN, Juvenile group.

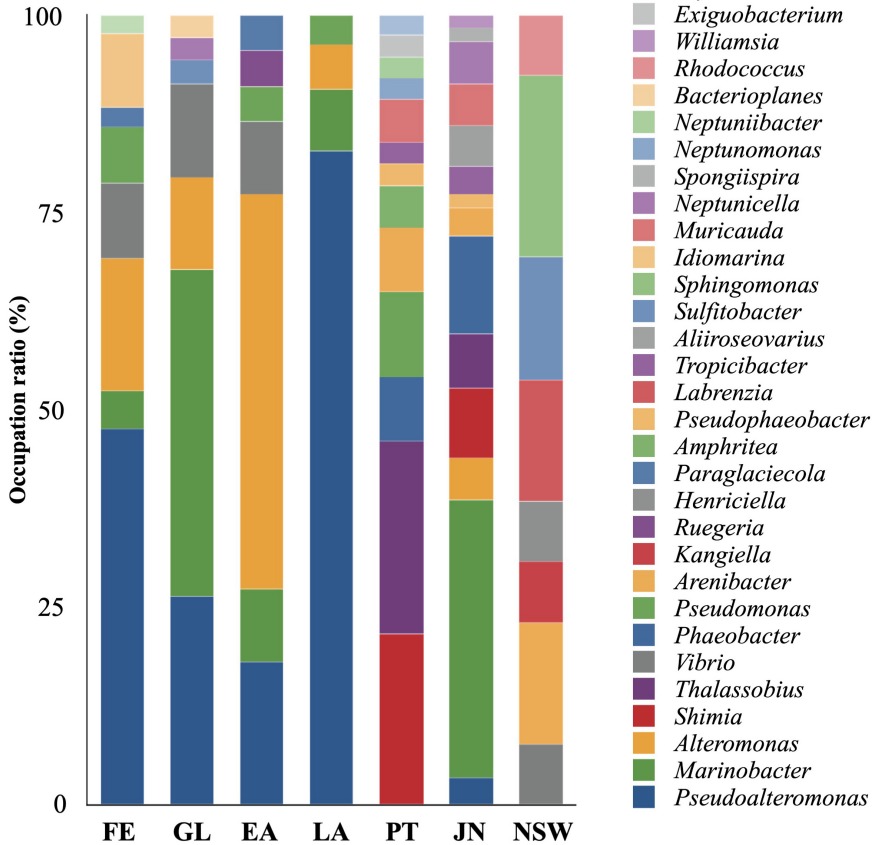

FIGURE 8 | Genus-level taxonomic distribution of isolates from sea cucumber and seawater. Bars represent proportion of isolates. FE, Fertilized egg; GL, Gastrula; EA, Early auricularia; LA, Late auricularia; PT, Pentactula; JN, Juvenile; NSW, Kumaishi nature seawater.

on microbiotas changes related to host development and organogenesis; (1) significant changes of microbiotas in the late auricularia stage, (2) possible first colonizers in gut assigned to *Rhodobacterales* and *Flavobacterales* appeared from auricularia stage, (3) significantly different microbiota in juveniles, and (4) significantly different microbiotas between host associated and environmental water.

Such microbiotas changes are likely to be related to organogenesis of the digestive system. Blastopore is formed in blastula and observed until the early auricularia stage. As the primitive gut-like structure in gastrula disappears, the buccal cavity, esophagus, intestine, cloaca and ciliary bands related to digestion, feeding and locomotion can be observed from the early auricularia stage and are well developed in the late auriculaira. Stomach, axohydrocoel and hyaline sphere are also clearly observed in the late auriculaira. After the pentacutula stage, sea cucumbers start a benthic lifestyle with more organogenesis of tentacles and ossicales formation, which are necessary for feeding and habitat settlement in adult individuals. Early life microbiome could be dynamically changed during the organogenesis, which allow microbes to colonize first on the tissue of host sea cucumber as they shape to a matured form.

Oceanospirillales, *Rhodobacteriales*, *Alteromonadales*, and *Flavobacterales* colonize sea cucumber's microbiota at different developmental stages and show significant changes during larval development. Many researchers have analyzed microbial communities and the impact of these individual bacteria on the host microbiome in sea cucumbers (Yang et al., 2015a; Yamazaki et al., 2016; Zhao et al., 2016; Kim et al., 2017; Li et al., 2018; Pagán-Jiménez et al., 2019; Ren et al., 2019; Yamazaki et al., 2019), but pioneer colonizers in fertilized eggs and larvae of sea cucumber have hardly been reported at all. *Rhodobacterales*, *Flavobacterales,* and *Alteromonadales* were also abundant in adult sea cucumber *A. japonicus* without similar microbial diversity (Yamazaki et al., 2016). Of particular interest in this study, *Rhodobacterales* was detected as the dominant bacterial order and key bacteria in microbiota in early life, which colonize in the early auricularia stage and significantly increase in the pentactula stage (**Figures 3**, **4**). *Rhodobacterales* is known as one of the primary surface colonizers and key players of biogeochemical cycling in marine environments, consisting of more than 350 species (Dang et al., 2008; Simon et al., 2017). Complicated taxonomic subgroups and worldwide distribution of *Rhodobacterales* helped increase research into the understanding the community

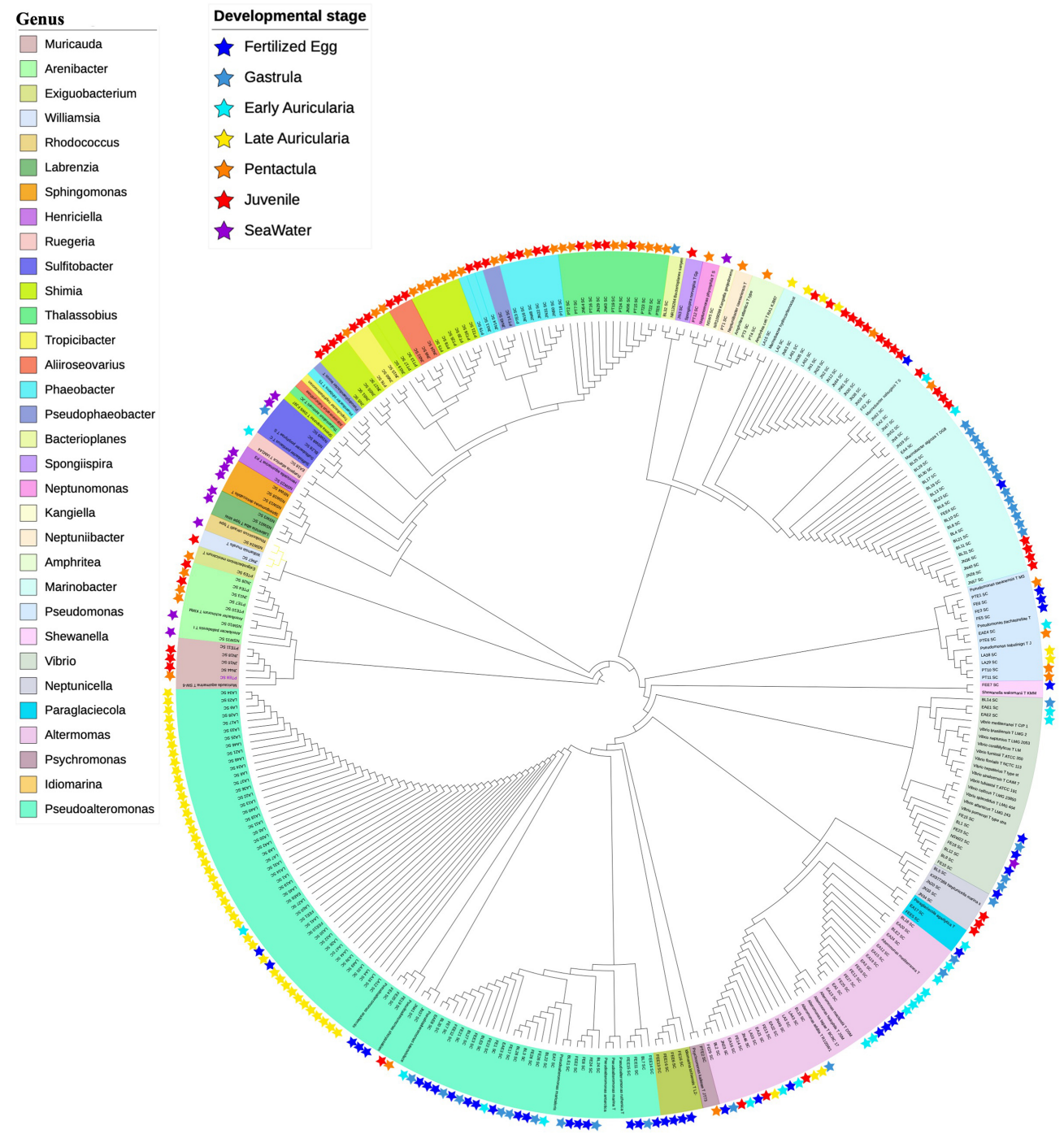

FIGURE 9 | Maximum-Likelihood phylogenetic tree based on partial 16S rRNA gene sequences of isolates. Isolates were shown with stars in specific color. Different genera were labeled with different color. 257 isolates were assigned to 32 genera and 45 species.

structures and molecular roles in *Rhodobacterales* (Fu et al., 2013; Rasmussen et al., 2018; Tavares et al., 2018). There are studies indicating *Rhodobacterales* could produce tropodithietic acid (TDA) against the pathogen *Vibrio* (Grotkjaer et al., 2016; Dittmann et al., 2020). In sea cucumber, Yamazaki et al. (2016) compared microbiota between larger and smaller individuals, in which *Rhodobacterales* was more abundant in larger sea cucumber, and it contains polyhydroxybutyrate (PHB) metabolism genes which could promote host growth (Yamazaki et al., 2016). Dietary β-glucan supplementation and dietary astragalus polysaccharide (APS) in sea cucumber *A. japonicus* have a positive impact on immune responses and enriched

relative abundance of *Rhodobacterales* in microbiota through the NF-κB signaling pathway (Yang et al., 2015b; Song et al., 2019). Currently, 51 isolates are assigned to *Rhodobacterales* and 13 of the 51 isolates are assigned to key ASVs detected in Meta16S analysis. The success of *Rhodobacterales* isolation opens up a way for us to perform bioassay, meta-transcriptomic analysis, molecular studies on host-microbiome association in the future.

Culture environments and supplied diets are always considered as major factors resulting in alteration of microbiota, many studies reveal the relationship of microbiotas between animal gut and environments. In some studies, microbiota of eggs shows highest similarity of 77% to that of rearing water (Nikouli et al., 2019). However, a study on sea bream discusses the potential effects of rearing water and diet on microbiota of different days post-hatch larvae, and they indicated that both rearing water and diet differ from host microbiota but somehow contribute to microbial community (Nikouli et al., 2019). According to Hansen and Olafsen (1989), there is a variation between microbiota in sea cucumber and rearing sea water. The microbiota of fertilized egg and gastrula in sea cucumber were significantly different from rearing water in our results. Only 6.3 and 15.5% ASVs in fertilized egg and gastrula were shared with rearing seawater and five key ASVs significantly changed along with developmental stages were not detected in early life rearing seawater. Nonetheless, with the development of sea cucumber larvae, the sharing ASVs increase to 42.5% at late auricularia stage but decreased to 8.3% at juvenile stage, indicating the majority of larvae microbiome were not affected by rearing seawater.

Factors Influencing Pioneer Colonizers of Sea Cucumber Gut Microbiome

Pioneer microbial colonization is related to birth process, gestational age, digestive system development and genetic factors (Benson et al., 2010; Karlsson et al., 2011; Gomez de Agüero et al., 2016; Borghi et al., 2019). In particular, genetic background of newborn individual influence gut microbial colonization, corresponding to functional development of digestive systems, were emerged in cod and chicken (Bakke et al., 2015; Schokker et al., 2015). Our results also show five key ASVs belonging to *Rhodobacterales* and *Flavobacteriales* are recognized as first colonizers in gut of sea cucumber's microbiota at different life stages. These bacteria were not detected in rearing seawater at corresponding life stages and before the feeding process. Based on these findings, it is assumed that the process of organ formation along with larval developments impacts first colonizers in gut as an influential factor. Interestingly, another variation of early life microbiota was also observed in juvenile individuals, which possess important organ tentacles. Therefore, we assume that organogenesis occurring in sea cucumber larvae is one of the likely factors resulting in the alteration of microbiota, but more insights into the role of individual pioneer colonizer are necessary for deeper understanding.

The auricularia stage is the longest period that primary organs of the digestive system are formed during larval development of sea cucumber, and is sustained for 8–12 days as reported in another study (Soliman et al., 2013). We also observed that the larvae in the auricularia stage have been continuously detected for more than 17 days, to a maximum 19 days after fertilization. We started feeding after the early auricularia stage, and buccal cavity, mouth, esophagus, stomach, intestine, and cloaca, these digestive organs in sea cucumber were clearly observed in late auricularia individuals. The late auricularia microbiota was different from the those of individuals before and after feeding, which indicates that organogenesis accompanied with feeding are major factors impacting on early life gut microbiota. As there are many studies on sea cucumber that indicate the supplied diet could regulate intestinal microbiota and immunity (Yang et al., 2015b; Chen et al., 2018; Song et al., 2019), dietary microalgae could be considered as one of the major factors causing alteration of microbiota observed in the auricularia stage, in fact microbiotas of seawater after diet microalgae spikes were different of those before the spikes. However, even in microbiotas changes of seawater between before and after diets spikes, we still observed differences between host-associated and environmental microbiotas, which means there is still a presence of host factors selecting colonizers and shaping microbiotas.

Culturing Pioneer Microbes

The combination of culture-independent and culture-dependent methods can improve the accuracy of taxonomic assignment in metagenomics. Also, the acquisition of reference genome sequences of isolates provides the possibility of meta-transcriptomes to understand the functions of host-associated bacteria. In this study, we were able to isolate 13 strains belonging to *Rhodobacterales* and they were also assigned 4 key ASVs detected by Meta16S analysis, emphasizing the importance of culture dependent method. *Rhodobacterales* has been reported as possible bacteria for promoting *A. japonicus* growth (Yamazaki et al., 2016). Our study opens the way to investigating the effects of individual bacteria on host physiology and emphasizes the importance of the culture dependent method.

In this study, we analyzed dynamic changes of microbiome for the first time alongside sea cucumber developmental stages and investigated potential factors impacting on the alteration of the microbiome during host development. Our results indicate early life microbiota in sea cucumber significant changes at the auricularia stage and is distinct from environmental seawater. We also isolated crucial bacteria candidates including pioneer microbes on fertilized egg and first colonizers in gut such as *Rhodobacterales* and *Alteromonadales* showing significant difference among larval developmental stages. Further study of individual host-associated bacteria could contribute to a deeper understanding of the interaction between bacteria and host biology.

DATA AVAILABILITY STATEMENT

The datasets presented in this study can be found in online repositories. The names of the repository/repositories and

accession number(s) can be found below: https://www.ddbj.nig.ac.jp/, DRR319863–DRR319874.

AUTHOR CONTRIBUTIONS

TS and JY designed the study. JY, TS, and YS performed experiments. JY and SM obtained and analyzed data. JY drafted the manuscript. All authors contributed to the article and approved the submitted version.

SUPPLEMENTARY MATERIAL

The Supplementary Material for this article can be found online at: https://www.frontiersin.org/articles/10.3389/fmars.2022.801344/full#supplementary-material

REFERENCES

Arrieta, M. C., Stiemsma, L. T., Amenyogbe, N., Brown, E. M., and Finlay, B. (2014). The intestinal microbiome in early life: health and disease. *Front. Immunol* 5:427. doi: 10.3389/fimmu.2014.00427

Arrieta, M. C., Stiemsma, L. T., Dimitriu, P. A., Thorson, L., Russell, S., Yurist-Doutsch, S., et al. (2015). Early infancy microbial and metabolic alterations affect risk of childhood asthma. *Sci. Transl. Med .7*:307ra152. doi: 10.1126/scitranslmed.aab2271

Bäckhed, F., Roswall, J., Peng, Y., Feng, Q., Jia, H., Kovatcheva-Datchary, P., et al. (2015). Dynamics and stabilization of the human gut microbiome during the first year of life. *Cell Host Microbe* 17, 690–703. doi: 10.1016/j.chom.2015.04.004

Bakke, I., Coward, E., Andersen, T., and Vadstein, O. (2015). Selection in the host structures the microbiota associated with developing cod larvae (*Gadus morhua*). *Environ. Microbiol.* 17, 3914–3924. doi: 10.1111/1462-2920.12888

Benson, A. K., Kelly, S. A., Legge, R., Ma, F., Low, S. J., Kim, J., et al. (2010). Individuality in gut microbiota composition is a complex polygenic trait shaped by multiple environmental and host genetic factors. *PNAS* 107, 18933–18938. doi: 10.1073/pnas.1007028107

Bettelheim, K. A. (1986). Commemoration of the publication 100 years ago of the papers by Dr. Th. Escherich in which are described for the first time the organisms that bear his name. *Zbl. Bakt. Hyg. A.* 261, 255–265. doi: 10.1016/s0176-6724(86)80043-8

Bolyen, E., Rideout, J. R., Dillon, M. R., Bokulich, N. A., Abnet, C. C., Al-Ghalith, G. A., et al. (2019). Reproducible, interactive, scalable and extensible microbiome data science using QIIME 2. *Nat. Biotechnol.* 37, 852–857. doi: 10.1038/s41587-019-0209-9

Borghi, E., Massa, V., Severgnini, M., Fazio, G., Avagliano, L., Menegola, E., et al. (2019). Antenatal microbial colonization of mammalian gut. *Reprod. Sci.* 26, 1045–1053. doi: 10.1177/1933719118804411

Califano, G., Castanho, S., Soares, F., Ribeiro, L., Cox, C. J., Mata, L., et al. (2017). Molecular taxonomic profiling of bacterial Communities in a gilthead seabream (*Sparus aurata*) hatchery. *Front. Microbiol.* 8:204. doi: 10.3389/fmicb.2017.00204

Callahan, B. J., McMurdie, P. J., Rosen, M. J., Han, A. W., Johnson, A. J. A., and Holmes, S. P. (2016). DADA2: high-resolution sample inference from Illumina amplicon data. *Nat. Methods* 13, 581–583. doi: 10.1038/nmeth.3869

Chen, C. P., and Chian, C. S. (1990). Larval development of the sea cucumber. *Actinopyga echinites* (*Echinodermata*: *Holothuroidea*). Bull. *Inst. Zool. Acad. Sin.* 29, 127–133.

Chen, J., Ren, Y., Li, Y., and Xia, B. (2018). Regulation of growth, intestinal microbiota, non-specific immune response and disease resistance of sea cucumber *Apostichopus japonicus* (Selenka) in biofloc systems. *Fish Shellfish Immunol.* 77, 175–186. doi: 10.1016/j.fsi.2018.03.053

Chi, C., Liu, J., Fei, S., Zhang, C., Chang, Y., Liu, X., et al. (2014). Effect of intestinal autochthonous probiotics isolated from the gut of sea cucumber (*Apostichopus japonicus*) on immune response and growth of *A. japonicus*. *Fish Shellfish Immunol.* 38, 367–373. doi: 10.1016/j.fsi.2014.04.001

Cole, J. R., Wang, Q., Fish, J. A., Chai, B., McGarrell, D. M., Sun, Y., et al. (2014). Ribosomal database project: data and tools for high throughput rRNA analysis. *Nucleic Acids Res.* 42, D633–D642. doi: 10.1093/nar/gkt1244

Dang, H., Li, T., Chen, M., and Huang, G. (2008). Cross-ocean distribution of Rhodobacterales bacteria as primary surface colonizers in temperate coastal marine waters. *Appl. Environ. Microbiol.* 74, 52–60. doi: 10.1128/aem.01400-07

Dittmann, K. K., Rasmussen, B. B., Melchiorsen, J., Sonnenschein, E. C., Gram, L., and Bentzon-Tilia, M. (2020). Changes in the microbiome of mariculture feed organisms after treatment with a potentially probiotic strain of *Phaeobacter inhibens*. *Appl. Environ. Microbiol.* AEM.499–AEM.520. doi: 10.1128/aem.00499-20

Escherich, T. (1886). *Die Darmbakterien des Säuglings und ihre Beziehungen Zur Physiologie der Verdauung*. Stuttgart: Ferndinand Enke.

Fu, Y., Keats, K. F., Rivkin, R. B., and Lang, A. S. (2013). Water mass and depth determine the distribution and diversity of Rhodobacterales in an Arctic marine system. *FEMS Microbiol. Ecol.* 84, 564–576. doi: 10.1111/1574-6941.12085

Gamboa-Álvarez, M. Á, López-Rocha, J. A., Poot-López, G. R., Aguilar-Perera, A., and Villegas-Hernández, H. (2020). Rise and decline of the sea cucumber fishery in Campeche Bank, Mexico. *Ocean Coast. Manag.* 184:105011. doi: 10.1016/j.ocecoaman.2019.105011

Gensollen, T., Iyer, S. S., Kasper, D. L., and Blumberg, R. S. (2016). How colonization by microbiota in early life shapes the immune system. *Science* 352, 539–544. doi: 10.1126/science.aad9378

Gentleman, R., Carey, V., and Huber, W. (2021). *genefilter: Genefilter: Methods for Filtering Genes from High-Throughput Experiments." R Package Version 1.74.1.*

Giatsis, C., Sipkema, D., Smidt, H., Verreth, J., and Verdegem, M. (2014). The colonization dynamics of the gut microbiota in tilapia larvae. *PLoS One* 9:e103641. doi: 10.1371/journal.pone.0103641

Gomez de Agüero, M., Ganal-Vonarburg, S. C., Fuhrer, T., Rupp, S., Uchimura, Y., Li, H., et al. (2016). The maternal microbiota drives early postnatal innate immune development. *Science* 351, 1296–1302. doi: 10.1126/science.aad2571

González-Wangüemert, M., Domínguez-Godino, J. A., and Cánovas, F. (2018). The fast development of sea cucumber fisheries in the Mediterranean and NE Atlantic waters: from a new marine resource to its over-exploitation. *Ocean Coast. Manag.* 151, 165–177. doi: 10.1016/j.ocecoaman.2017.10.002

Grotkjaer, T., Bentzon-Tilia, M., D'Alvise, P., Dourala, N., Nielsen, K. F., and Gram, L. (2016). Isolation of TDA-producing *Phaeobacter* strains from sea bass larval rearing units and their probiotic effect against pathogenic *Vibrio* spp. in Artemia cultures. *Syst. Appl. Microbiol.* 39, 180–188. doi: 10.1016/j.syapm.2016.01.005

Hamel, J. F., and Mercier, A. (2013). *Apostichopus japonicus. The IUCN Red List of Threatened Species 2013: e.T180424A1629389*. Gland: IUCN. doi: 10.2305/IUCN.UK.2013-1.RLTS.T180424A1629389.en

Hansen, G. H., and Olafsen, J. A. (1989). Bacterial colonization of cod (*Gadus morhua* L.) and halibut (*Hippoglossus hippoglossus*) eggs in marine aquaculture. *Appl. Environ. Microbiol.* 55, 1435–1446. doi: 10.1128/aem.55.6.1435-1446.1989

Hansen, G. H., and Olafsen, J. A. (1999). Bacterial interactions in early life stages of marine cold-water fish. *Microb. Ecol.* 38, 1–26. doi: 10.1007/s002489900158

Hill, C. J., Lynch, D. B., Murphy, K., Ulaszewska, M., Jeffery, I. B., O'Shea, C. A., et al. (2017). Evolution of gut microbiota composition from birth to 24 weeks in the infant met Cohort. *Microbiome* 5:4. doi: 10.1186/s40168-016-0213-y

Hu, C., Xu, Y., Wen, J., Zhang, L., Fan, S., and Su, T. (2010). Larval development and juvenile growth of the sea cucumber *Stichopus* sp. (Curry fish). *Aquaculture* 300, 73–79. doi: 10.1016/j.aquaculture.2009.09.033

Inaba, D. (1937). Artificial rearing of sea cucumbers. *Suisen Kenkyushi* 35, 241–246.

Jontila, J. B. S., Monteclaro, H. M., Quinitio, G. F., Santander-de Leon, S. M., and Altamirano, J. P. (2018). Status of sea cucumber fishery and populations across sites with different levels of management in Palawan, Philippines. *Ocean Coast. Manag.* 165, 225–234. doi: 10.1016/j.ocecoaman.2018.08.025

Karlsson, C. L. J., Molin, G., Cilio, C. M., and Ahrné, S. (2011). The pioneer gut microbiota in human neonates vaginally born at term—a pilot study. *Pediatr. Res.* 70, 282–286. doi: 10.1203/PDR.0b013e318225f765

Kim, T. Y., Lee, J. J., Kim, B. S., and Choi, S. H. (2017). Whole-body microbiota of sea cucumber (*Apostichopus japonicus*) from south Korea for improved seafood management. *J Microbiol. Biotechnol.* 27, 1753–1762. doi: 10.4014/jmb.1707.07067

Koenig, J. E., Spor, A., Scalfone, N., Fricker, A. D., Stombaugh, J., Knight, R., et al. (2011). Succession of microbial consortia in the developing infant gut microbiome. *PNAS* 108(Suppl. 1), 4578–4585. doi: 10.1073/pnas.1000081107

Korpela, K., and de Vos, W. M. (2018). Early life colonization of the human gut: microbes matter everywhere. *Curr. Opin. Microbiol.* 44, 70–78. doi: 10.1016/j.mib.2018.06.003

Larkin, M. A., Blackshields, G., Brown, N. P., Chenna, R., McGettigan, P. A., McWilliam, H., et al. (2007). Clustal W and Clustal X version 2.0. *Bioinformatics* 23, 2947–2948. doi: 10.1093/bioinformatics/btm404

Letunic, I., and Bork, P. (2019).). Interactive Tree Of Life (iTOL) v4: recent updates and new developments. *Nucleic Acids Res.* 47, W256–W259. doi: 10.1093/nar/gkz239

Li, C., Ren, Y., Jiang, S., Zhou, S., Zhao, J., Wang, R., et al. (2018). Effects of dietary supplementation of four strains of lactic acid bacteria on growth, immune-related response and genes expression of the juvenile sea cucumber *Apostichopus japonicus* Selenka. *Fish Shellfish Immunol.* 74, 69–75. doi: 10.1016/j.fsi.2017.12.037

Lozupone, C., Lladser, M. E., Knights, D., Stombaugh, J., and Knight, R. (2011). UniFrac: an effective distance metric for microbial community comparison. *ISME J.* 5, 169–172. doi: 10.1038/ismej.2010.133

Ma, Y., Li, L., Li, M., Chen, W., Bao, P., Yu, Z., et al. (2019). Effects of dietary probiotic yeast on growth parameters in juvenile sea cucumber, *Apostichopus japonicus*. *Aquaculture* 499, 203–211. doi: 10.1016/j.aquaculture.2018.09.043

MAFF (2020). *Japan statistics of Agriculture, Forestry and fisheries [Online]*. Available online at: https://www.maff.go.jp/j/tokei/kouhyou/kaimen_gyosei/index.html [Accessed October 22, 2021].

Mercier, A., Yang, H., and Hamel, J. F. (2015). *The Sea Cucumber Apostichopus japonicus : History, Biology and Aquaculture*. Cambridge, MA: Academic Press.

Ministry of Agriculture and Rural Affairs Fishery Administration (2003-2012). *China Fishery Statistical Yearbook*. Beijing. CN: China Agriculture Press.

Nayak, S. K. (2010). Role of gastrointestinal microbiota in fish. *Aquac. Res.* 41, 1553–1573. doi: 10.1111/j.1365-2109.2010.02546.x

Nikouli, E., Meziti, A., Antonopoulou, E., Mente, E., and Kormas, K. A. (2019). Host-associated bacterial succession during the rarly embryonic stages and first feeding in farmed gilthead sea bream (*Sparus aurata*). *Genes* 10:483. doi: 10.3390/genes10070483

Pagán-Jiménez, M., Ruiz-Calderón, J. F., Dominguez-Bello, M. G., and García-Arrarás, J. E. (2019). Characterization of the intestinal microbiota of the sea cucumber *Holothuria glaberrima*. *PLoS One* 14:e0208011. doi: 10.1371/journal.pone.0208011

Price, M. N., Dehal, P. S., and Arkin, A. P. (2009). FastTree: computing large minimum evolution trees with profiles instead of a distance matrix. *Mol. Biol. Evol.* 26, 1641–1650. doi: 10.1093/molbev/msp077

Ramofafia, C., Byrne, M., and Battaglene, S. (2003). Development of three commercial sea cucumber *Holothuria scabra*. *H. fuscogilva* and *Actinopyga mauritiana*: larval structure and growth. *Mar. Freshw. Res.* 54, 657–667. doi: 10.1071/MF02145

Rasmussen, B. B., Erner, K. E., Bentzon-Tilia, M., and Gram, L. (2018). Effect of TDA-producing *Phaeobacter inhibens* on the fish pathogen *Vibrio anguillarum* in non-axenic algae and copepod systems. *Microb. Biotechnol.* 11, 1070–1079. doi: 10.1111/1751-7915.13275

Ren, H., Li, Z., Xu, Y., Wang, L., and Li, X. (2019). Protective effectiveness of feeding phage cocktails in controlling *Vibrio parahaemolyticus* infection of sea cucumber *Apostichopus japonicus*. *Aquaculture* 503, 322–329. doi: 10.1016/j.aquaculture.2019.01.006

Rogers, A., Hamel, J. F., Baker, S. M., and Mercier, A. (2018). The 2009–2016 Belize sea cucumber fishery: resource use patterns, management strategies and socioeconomic impacts. *Reg. Stud. Mar. Sci.* 22, 9–20. doi: 10.1016/j.rsma.2018.05.003

Schokker, D., Veninga, G., Vastenhouw, S. A., Bossers, A., de Bree, F. M., Kaal-Lansbergen, L. M. T. E., et al. (2015). Early life microbial colonization of the gut and intestinal development differ between genetically divergent broiler lines. *BMC Genomics* 16:418. doi: 10.1186/s12864-015-1646-6

Sewell, M. A., and McEuen, F. S. (2002). "Phylum *Echinodermata*: *Holothuroidea*," in *Atlas of Marine Invertebrate Larvae*, ed. C. M. Young (San diego, CA: Academic Press), 513–530.

Shulman, S. T., Friedmann, H. C., and Sims, R. H. (2007). Theodor Escherich: the first pediatric infectious diseases physician? *Clin. Infect. Dis.* 45, 1025–1029. doi: 10.1086/521946

Simon, M., Scheuner, C., Meier-Kolthoff, J. P., Brinkhoff, T., Wagner-Döbler, I., Ulbrich, M., et al. (2017). Phylogenomics of Rhodobacteraceae reveals evolutionary adaptation to marine and non-marine habitats. *ISME J.* 11, 1483–1499. doi: 10.1038/ismej.2016.198

Soliman, T., Yamazaki, Y., Niiyama, H., and Tsunoda, K. (2013). Spontaneous captive breeding and larval development in the green and red variants of the Japanese sea cucumber *Apostichopus japonicus* (Selenka 1867). *Aquac. Res.* 44, 738–746. doi: 10.1111/j.1365-2109.2011.03078.x

Song, X., Feng, Z., Zhang, Y., and Zhu, W. (2019). Regulation of dietary astragalus polysaccharide (APS) supplementation on the non-specific immune response and intestinal microbiota of sea cucumber *Apostichopus japonicus*. *Fish Shellfish Immunol.* 94, 517–524. doi: 10.1016/j.fsi.2019.09.049

Sullam, K. E., Essinger, S. D., Lozupone, C. A., O'Connor, M. P., Rosen, G. L., Knight, R., et al. (2012). Environmental and ecological factors that shape the gut bacterial communities of fish: a meta-analysis. *Mol. Ecol.* 21, 3363–3378. doi: 10.1111/j.1365-294X.2012.05552.x

Tavares, N. K., VanDrisse, C. M., and Escalante-Semerena, J. C. (2018). Rhodobacterales use a unique L-threonine kinase for the assembly of the nucleotide loop of coenzyme B(12). *Mol. Microbiol.* 110, 239–261. doi: 10.1111/mmi.14100

Vadstein, O., Attramadal, K. J. K., Bakke, I., Forberg, T., Olsen, Y., Verdegem, M., et al. (2018). Managing the microbial community of marine fish larvae: a holistic perspective for larviculture. *Front. Microbiol.* 9:1820. doi: 10.3389/fmicb.2018.01820

Wang, Y., Sun, S., and Rong, X. (2006). Stomach ulcer disease in auricularia of sea cucumber (*Apostichopus japonicus*) and its etiological identification. *Fish. Sci. China* 13, 908–916.

Wilson, K. M., Rodrigues, D. R., Briggs, W. N., Duff, A. F., Chasser, K. M., and Bielke, L. R. (2019). Evaluation of the impact of in ovo administered bacteria on microbiome of chicks through 10 days of age. *Poult. Sci. J.* 98, 5949–5960. doi: 10.3382/ps/pez388

Wopereis, H., Oozeer, R., Knipping, K., Belzer, C., and Knol, J. (2014). The first thousand days – intestinal microbiology of early life: establishing a symbiosis. *Pediatr. Allergy Immunol.* 25, 428–438. doi: 10.1111/pai.12232

Yamazaki, Y., Meirelles, P. M., Mino, S., Suda, W., Oshima, K., Hattori, M., et al. (2016). Individual *Apostichopus japonicus* fecal microbiome reveals a link with polyhydroxybutyrate producers in host growth gaps. *Sci. Rep.* 6:21631. doi: 10.1038/srep21631

Yamazaki, Y., Sakai, Y., Mino, S., Suda, W., Hattori, M., Meirelles, P. M., et al. (2019). Repeated selective enrichment process of sediment microbiota occurred in sea cucumber guts. *Environ. Microbiol. Rep.* 11, 797–807. doi: 10.1111/1758-2229.12791

Yamazaki, Y., Sakai, Y., Yu, J., Mino, S., and Sawabe, T. (2020). Tracking the dynamics of individual gut microbiome of sea cucumber *Apostichopus japonicus* during gut regeneration. *Peer J.* 8:e10260. doi: 10.7717/peerj.10260.

Yang, G., Peng, M., Tian, X., and Dong, S. (2017). Molecular ecological network analysis reveals the effects of probiotics and florfenicol on intestinal microbiota homeostasis: an example of sea cucumber. *Sci. Rep.* 7:4778. doi: 10.1038/s41598-017-05312-1

Yang, G., Xu, Z., Tian, X., Dong, S., and Peng, M. (2015b). Intestinal microbiota and immune related genes in sea cucumber (*Apostichopus japonicus*) response to dietary β-glucan supplementation. *Biochem. Biophys. Res. Commun.* 458, 98–103. doi: 10.1016/j.bbrc.2015.01.074

Yang, G., Tian, X., Dong, S., Peng, M., and Wang, D. (2015a). Effects of dietary *Bacillus cereus* G19, *B. cereus* BC-01, and *Paracoccus marcusii* DB11 supplementation on the growth, immune response, and expression of immune-related genes in coelomocytes and intestine of the sea cucumber (*Apostichopus japonicus* Selenka). *Fish Shellfish Immunol.* 45, 800–807. doi: 10.1016/j.fsi.2015.05.032

Zhang, C. Y., Chen, G., Xu, Z., Yan, P. S., and Wang, Y. G. (2010). Etiology of rotting edges syndrome in cultured larval *Apostichopus japonicus* at auricularia stage and analysis of reservoir of pathogens. *Acta. Microbiol. Sin.* 50, 687–693.

Zhang, C., Chen, G., Xu, Z., Yan, P., Wang, G., and Wang, Y. (2009). Etiology of off-plate syndrome in cultured larval *Apostichopus japonicus* at attachment

stage and analysis of reservoir of pathogens. *Wei Sheng Wu Xue Bao* 49, 631–637.

Zhang, Y., and Liu, Y. (1984). The review of research progress and exploration of resources proliferation of *Stichopus japonicus*. *Mar. Fish.* 2, 57–60.

Zhao, Y., Yuan, L., Wan, J., Sun, Z., Wang, Y., and Sun, H. (2016). Effects of potential probiotic *Bacillus cereus* EN25 on growth, immunity and disease resistance of juvenile sea cucumber *Apostichopus japonicus*. *Fish Shellfish Immunol.* 49, 237–242. doi: 10.1016/j.fsi.2015.12.035

Conflict of Interest: The authors declare that the research was conducted in the absence of any commercial or financial relationships that could be construed as a potential conflict of interest.

Publisher's Note: All claims expressed in this article are solely those of the authors and do not necessarily represent those of their affiliated organizations, or those of the publisher, the editors and the reviewers. Any product that may be evaluated in this article, or claim that may be made by its manufacturer, is not guaranteed or endorsed by the publisher.

frontiers in Marine Science

ORIGINAL RESEARCH
published: 23 March 2022
doi: 10.3389/fmars.2022.844983

Genomic Analyses of Halioticoli Clade Species in *Vibrionaceae* Reveal Genome Expansion With More Carbohydrate Metabolism Genes During Symbiotic to Planktonic Lifestyle Transition

Chunqi Jiang, Sayaka Mino and Tomoo Sawabe *

Laboratory of Microbiology, Faculty of Fisheries Sciences, Hokkaido University, Hakodate, Japan

OPEN ACCESS

Edited by:
Fabiano Thompson, Federal University of Rio de Janeiro, Brazil

Reviewed by:
Xiao-Hua Zhang, Ocean University of China, China
Diogo Antonio Tschoeke, Federal University of Rio de Janeiro, Brazil

***Correspondence:**
Tomoo Sawabe
sawabe@fish.hokudai.ac.jp

Specialty section:
This article was submitted to Microbial Symbioses, a section of the journal Frontiers in Marine Science

Received: *29 December 2021*
Accepted: *07 March 2022*
Published: *23 March 2022*

Citation:
Jiang C, Mino S and Sawabe T (2022) Genomic Analyses of Halioticoli Clade Species in Vibrionaceae Reveal Genome Expansion With More Carbohydrate Metabolism Genes During Symbiotic to Planktonic Lifestyle Transition. Front. Mar. Sci. 9:844983. doi: 10.3389/fmars.2022.844983

Vibrionaceae is one of the most diverse bacterial families and is currently classified into over 50 clades, some members of which play an important role in the symbiotic relationships with humans and animals. Halioticoli clade, which currently consists of 10 species: 8 species associated with the gut of abalone (symbiotic), 1 species (*V. breoganii*) from bivalves, and 1 species (*V. ishigakensis*) from subtropical seawater (planktonic). To accelerate studies in the evolution, ecogenomics, and biotechnology of Halioticoli clade species, the genomic backbones and pangenome analyses based on complete genome sequences are needed. Genome sizes of Halioticoli clade species ranged from 3.5 Mb to 4.8 Mb, with *V. ishigakensis* the biggest. The evolutionary relationships using multilocus sequence analysis based on eight housekeeping genes and 125 single-copy core genes revealed a division of five sub-clades in this clade; 1) *V. breoganii*, *V. comitans*, *V. inusitatus* and *V. superstes*, 2) *V. ezurae*, *V. neonatus*, and *V. halioticoli*, 3) *V. rarus*, 4) *V. gallicus*, and 5) *V. ishigakensis*. The pan-genomic analysis combined with function and metabolism estimations showed that the planktonic group (sub-clade 5) contained the greatest number of specific genes, and more genes responsible for carbohydrate metabolisms, especially the genes encoding D-galactonate degradation. These results demonstrated that the genome expanded by acquiring more abilities for utilizing various carbohydrates during the evolution from symbiotic to a planktonic lifestyle. Moreover, according to Carbohydrate-Active enZYmes (CAZy) profiling, genes encoding alginate degrading enzymes (*aly*), classified into PL6, PL7, PL15, and PL17 were common in the ten genomes, but sub-clade 1 had the most. Meanwhile, sub-clade 1and 5 also possessed abundant genes related to macroalgae substrates degradation (GHs), which are also responsible for the genome expansion of sub-clade 1 and 5.

Keywords: vibrionaceae, marine invertebrate, symbiosis, planktonic, halioticoli clade, complete genome

INTRODUCTION

Currently, over 190 species consisting of 9 genera have been accurately described in the family *Vibrionaceae* (Parte et al., 2020), which is one of the most diverse bacterial families, play an important role in geochemistry, pathogenicity, ecology, and systematics (Thompson et al., 2004; Gomez-Gil et al., 2014; Lee and Raghunath, 2018). Vibrios were further classified into 51 clades by multilocus sequence analysis (MLSA) in the most recent description of "Vibrio clade 3.0" (Jiang et al., 2022). Members of these clades have continued to be of great interest because of their symbiotic relationships with humans and animals, which can be referred to as parasitism, mutualism or commensalism (Moya et al., 2008). Representatively, *Vibrio cholerae*, the causative agent of the potent diarrheal disease cholera, is one of the most notorious human pathogens (Orata et al., 2015). The pathogenicity of members in the Cholerae clade has also been discovered although they were first described as non-pathogenic environmental strains (Kirchberger et al., 2014; Guardiola-Avila et al., 2021). On the other hand, the mutualism symbiosis between Hawaiian bobtail squid *Euprymna scolopes* and the bioluminescent bacteria *Vibrio fischeri* has been studied for decades because this model is uniquely suited to the investigation of symbiosis from both host and bacterial perspectives, putting the *Vibrio*-squid symbiosis at the forefront of host-microbe interactions (Nyholm and McFall-Ngai, 2004; Septer, 2019). Moreover, the recent rapid expansion in bacterial genome data has provided insights into the adaptive, diversifying and reductive evolutionary processes that occur in host-microbe interactions (Toft and Andersson, 2010). It has been reported about the general feature of genome-size reduction and AT content increase in endosymbiont genomes than free-living relatives, and the degree of them was related to the age of association (Wernegreen, 2002; Moya et al., 2008).

V. halioticoli was originally isolated from the gut of abalone *Haliotis discus hannai* as a non-motile alginolytic vibrio in 1998 (Sawabe et al., 1998). The dominance in the gut of Japanese abalone and the acetic acid production by *V. halioticoli via* fermentation of alginate, which is major components of ingested kelps, suggested a mutual relationship between *V. halioticoli* and abalones (Tanaka et al., 2002; Sawabe, 2006). The Halioticoli clade was first proposed in 2007 (Sawabe et al., 2007b), and most of the species have been discovered associated with abalone, particular in the guts (**Table 1**). Currently, ten species, *V. breoganii*, *V. comitans*, *V. ezurae*, *V. gallicus*, *V. halioticoli*, *V. inusitatus*, *V. ishigakensis*, *V. neonatus*, *V. rarus*, and *V. superstes*, have been described. Halioticoli clade species were discovered not only in Japanese abalone but also major abalone species outside Japan; *V. neonatus* (*H. discus discus*), *V. ezurae* (*H. diversicolor diversicolor*), *V. comitans* (*H. gigantea*), *V. rarus* (*H. madaka*) and *V. inusitatus* (*H. rufescens*) were isolated from the gut of Japanese abalone (Sawabe et al., 2004a; Sawabe et al., 2007a). *V. superstes* was isolated from the gut of Australian abalone *H. laevigata* and *H. rubra* (Hayashi et al., 2003), and *V. gallicus* was isolated from the gut of the French abalone *H. tuberculate* (Sawabe et al., 2004b). In 2009, the first non-abalone associated Halioticoli clade species, *V. breoganii*, was discovered from Spanish clams *Ruditapes philippinarum* and *Ruditapes decussatus* (Beaz Hidalgo et al., 2009). Nevertheless, draft genomes of *V. halioticoli*, *V. superstes*, were reported in 2014, but not much genome characterization has been completed yet. Recently, a genome of a reference strain of *V. breoganii* was completed, and the genome was rich in genes responsible for degrading macroalgal carbohydrates, which is likely to be characterized as a vegetarian vibrio compared to *V. halioticoli* genome (Corzett et al., 2018).

More interestingly, a first planktonic Halioticoli clade species, *V. ishigakensis*, was isolated from seawater taken in the Okinawa coral reef area, Japan (Gao et al., 2016). Rather different phenotypes (**Table S1**) of the non-motile Halioticoli species could be a key reference species to elucidate evolutionary processes from symbiotic to planktonic or vice versa in the Halioticoli clade species. However, the lack of genome sequences limits our knowledge of this clade. Here, we present the complete genome sequences of type strains of all current Halioticoli clade species and performed the first genomic analyses for this clade to evaluate their ecogenomics, evolutionary history, and possible biotechnology applications.

MATERIALS AND METHODS

Genome Sequencing, Assembly, and Annotation

DNA extraction was performed using Wizard genomic DNA purification kit (Promega, USA) following the manufacturer's instructions. The Nanopore sequencing library was prepared using the Rapid Barcoding Kit (SQK-RBK004) and sequenced

TABLE 1 | Isolation information of Halioticoli clade species.

Halioticoli species	Year	Sample	Host	Country	16S rRNA accession
V. breoganii	2009	–	*Ruditapes philippinarum* and *R. decussatus*	Spain	EF599161
V. comitans	2007	Gut	*Haliotis discus discus, H. gigantea* and *H. madaka*	Japan	DQ922915
V. ezurae	2004	Gut	*H. diversicolor aquatilis* and *H. diversicolor diversicolor*	Japan	AY426980
V. gallicus	2004	Gut	*H. tuberculata*	France	AJ440009
V. halioticoli	1998	Gut	*H. discus hannai*	Japan	AB000390
V. inusitatus	2007	Gut	*H. rufescens*	USA	DQ922920
V. ishigakensis	2016	–	Seawater of Okinawa in coral reef areas	Japan	KP790249
V. neonatus	2004	Gut	*H. discus discus*	Japan	AY426979
V. rarus	2007	Gut	*H. rufescens*	USA	DQ914239
V. superstes	2003	Gut	*H. laevigata* and *H. rubra*	Australia	AY155585

using MinION device (Oxford Nanopore Technologies, Oxford, UK). Raw reads were basecalled using Guppy 1.1. The Illumina DNA library was prepared using Nextera XT DNA Library Preparation Kit (Illumina) and sequenced with the Illumina MiSeq platform. Then, the complete genome sequences of Halioticoli clade type strains were assembled by means of the hybrid assembly approach using both Nanopore and Illumina reads by Unicycler 0.4.7 (Tanaka et al., 2018; Jiang et al., 2022). Finally, the genome sequences were annotated using DDBJ Fast Annotation and Submission Tool (DFAST) (Tanizawa et al., 2018) and deposited in the DDBJ/GenBank/ENA under BioProject PRJDB11924 with accession numbers as **Table 2**.

Multilocus Sequence Analysis (MLSA)

MLSA was performed according to the previous description (Sawabe et al., 2013). Briefly, the entire nucleotide sequences of the eight housekeeping genes (*ftsZ*, *gapA*, *gyrB*, *mreB*, *pyrH*, *recA*, *rpoA*, and *topA*) were obtained after genome annotation. The sequences were aligned using MUSCLE (Edgar, 2004). Split decomposition analysis using the concatenated sequence was performed using SplitsTree 4.14.8 with a neighbor net drawing and a Jukes-Cantor correction. Phylogenetic analysis using the same concatenated sequence was constructed using Maximum Likelihood (ML), Neighbor-Joining (NJ), and Minimum-Evolution (ME) methods with 500 bootstraps by MEGA-X v10.1.8 (Kumar et al., 2018).

General Genomic Comparisons

Genomic comparisons were performed based on chromosomes. The ten genomes from the Halioticoli clade were compared with the genome of *V. ishigakensis* JCM 19231^T by BLASTn and visualized using BRIG v.0.95 (Alikhan et al., 2011). Synteny between the same genomes was analyzed using the Artemis Comparison Tool (ACT) v.18.1.0 (Carver et al., 2005).

Core/Accessory/Specific Gene Identification in Pan-Genome Analysis

Pan-genome analysis was performed using Halioticoli clade genomes by the Anvi'o program ver. 7 (Eren et al., 2015). Firstly, each genome sequence file was converted to an anvi'o contigs database (anvi-gen-contigs-database) using Prodigal (Hyatt et al., 2010), these contigs databases were decorated with hits from HMM models (anvi-run-hmms). An anvi'o genome storage was generated (anvi-gen-genomes-storage) using prepared contigs databases, and then, the pan-genome was analyzed (anvi-pan-genome) using NCBI's blastp for amino acid sequence similarity search and the MCL algorithm (Van Dongen and Abreu-Goodger, 2012) for cluster identification in amino acid sequence similarity search results. In addition, Average Nucleotide Identity (ANI) values were calculated using the PyANI with ANIb method (anvi-compute-genome-similarity) (Pritchard et al., 2016). Finally, it was visualized and decorated (anvi-display-pan). Core genes were filtered (anvi-get-sequences-for-gene-clusters) and extracted in fasta files (anvi-get-sequences-for-gene-clusters) for further analysis.

Function/Metabolism Estimation and Enrichment Analysis

Gene annotation was performed using Clusters of Orthologous Groups 2020 (COG20) (Galperin et al., 2021) for function estimation (anvi-run-ncbi-cogs), and Kyoto Encyclopedia of Genes and Genomes (KEGG) (Aramaki et al., 2020) for metabolism estimation (anvi-estimate-metabolism) (Muto et al., 2013). In addition, the enrichment scores of function/

TABLE 2 | General genomic characteristics of Halioticoli clade species.

Sub clade	Halioticoli clade species	Size (bp)			Total size (bp)	GC Content (%)	Number					Accession number
		Chr1	Chr2	Plasmid			CDSs	tRNA	5S rRNA	16S rRNA	23S rRNA	
1	*V. breoganii* CAIM 1829^T	2,855,070	1,381,607	–	4,236,677	45.1	3,726	103	10	9	9	AP024864-AP024865
1	*V. comitans* LMG 23416^T	3,011,658	1,500,259	5,386	4,517,303	44.1	3,963	102	10	9	9	AP024866-AP024868
1	*V. inusitatus* LMG 23434^T	2,861,464	1,547,609	5,386	4,414,459	43.0	3,852	102	10	9	9	AP024878-AP024880
1	*V. superstes* JCM 21480^T	3,070,129	1,667,808	–	4,737,937	44.6	4,148	102	10	9	9	AP024909-AP024910
2	*V. ezurae* JCM 21522^T	2,753,547	1,009,479	–	3,763,026	43.4	3,251	105	10	9	9	AP024869-AP024870
2	*V. halioticoli* IAM 14596^T	2,785,698	1,098,310	244,363	4,128,371	42.9	3,586	105	9	8	8	AP024875-AP024877
2	*V. neonatus* JCM 21521^T	2,746,110	1,094,535	–	3,840,645	43.2	3,317	103	10	9	9	AP024885-AP024886
3	*V. rarus* LMG 23674^T	2,846,978	1,007,363	22,852	3,877,193	43.0	3,386	107	11	10	10	AP024900-AP024902
4	*V. gallicus* LMG 21878^T	2,528,163	989,994	–	3,518,157	43.8	3,101	95	10	9	9	AP024871-AP024872
5	*V. ishigakensis* JCM 19231^T	2,969,692	1,816,305	–	4,785,997	46.2	4,318	97	9	8	8	AP024881-AP024882

metabolism in different groups were identified using an R script developed by Amy Willis (anvi-compute-functional-enrichment) (Shaiber et al., 2020).

CAZy Annotation and Genomic Islands (GEIs) Prediction

Carbohydrate-Active enZYmes (CAZy) were annotated using the dbCAN2 meta server (HMMdb v9) with HMMER, DIAMOND, and eCAMI tools (Zhang et al., 2018), and domains supported by more than two tools were used in this study. Genomic islands (GEIs) predictions were calculated by IslandViewer4 with IslandPick, IslandPath-DIMOB, and SIGI-HMM methods (Bertelli et al., 2017) using the GenBank files after DFAST annotation, predictions supported by at least one method were used in this study. Results were visualized using ggplot2.

RESULTS

General Genomic Characteristics of the Halioticoli Clade Species

Genomes of all species consisted of two chromosomes and four of them (*V. comitans* LMG 23416^T, *V. halioticoli* IAM 14596^T, *V. inusitatus* LMG 23434^T, and *V. rarus* LMG 23674^T) had one plasmid (**Table 2**). The genome sizes of Chromosome 1 (Chr. 1) ranged from 2,528,163 to 3,070,129 bp, and those of Chromosome 2 (Chr. 2) ranged from 989,994 to 1,816,305 bp. These genomes showed 42.9-46.2% GC content, identified 3,101-4,318 CDS, 25-31 rRNA, and 95-107 tRNA. *V. ishigakensis* JCM 19231^T had the biggest genome with the highest GC content, the largest numbers of CDS, rRNA, and tRNA. In contrast, *V. gallicus* LMG 21878^T had the smallest genome with the lowest GC content and the smallest numbers of CDS and tRNA. Compared to the genome size and GC content among 189 other *Vibrionaceae* species, Halioticoli clade species showed a relatively narrow GC content range but variable genome size (**Figure 1**).

Evolutionary Relationships of the Halioticoli Clade

To explore the evolutionary history of Halioticoli clade species, the MLSA network and phylogenetic tree using concatenated eight house-keeping genes with *V. cholerae* ATCC 14035^T and *E. coli* K-12 MG1655 as outgroups were constructed (**Figures 2**, **S1**). Both methods indicated five evolutionary directions in the Halioticoli clade: sub-clade 1) *V. breoganii*, *V. comitans*, *V. inusitatus*, and *V. superstes*, sub-clade 2) *V. ezurae*, *V. neonatus*, and *V. halioticoli*, sub-clade 3) *V. rarus*, sub-clade 4) *V. gallicus*, and sub-clade 5) *V. ishigakensis*. In which, sub-clade 1 to 4 consist of symbiotic species, and sub-clade 5 consists of the only one planktonic species. In addition, genome size and GC content relationship also showed the clustering of sub-clades and the differentiation between symbiotic and planktonic species (**Figure 1**), suggesting that genome expansions may occur during evolution.

Comparative Genomics of the Halioticoli Clade

Analyses of homologous gene conservation and gene order across two or more genomes of different species play a vital role in comparative genomics since they can provide further

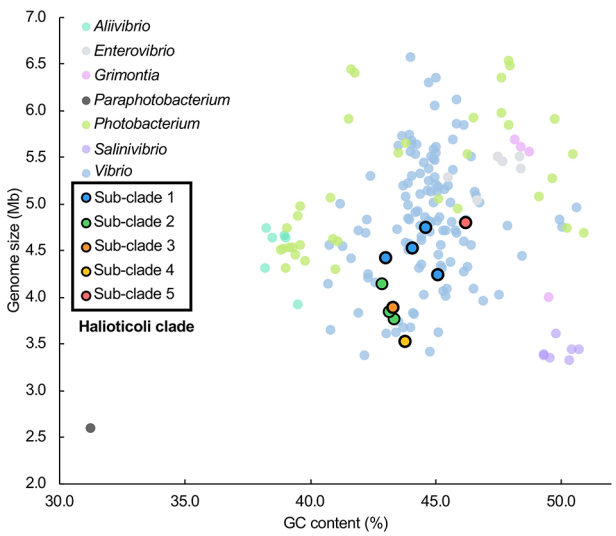

FIGURE 1 | Genome size and GC content relationship for Halioticoli clade species in 189 *Vibrionaceae* species (7 genera). Data were obtained from Jiang et al. (2022). Compared to the genome size and GC content among 189 other *Vibrionaceae* species, Halioticoli clade species showed a relatively narrow GC content range but variable genome size. In addition, the clustering of sub-clades and the differentiation between different sub-clades species suggest that genome expansions may occur during evolution.

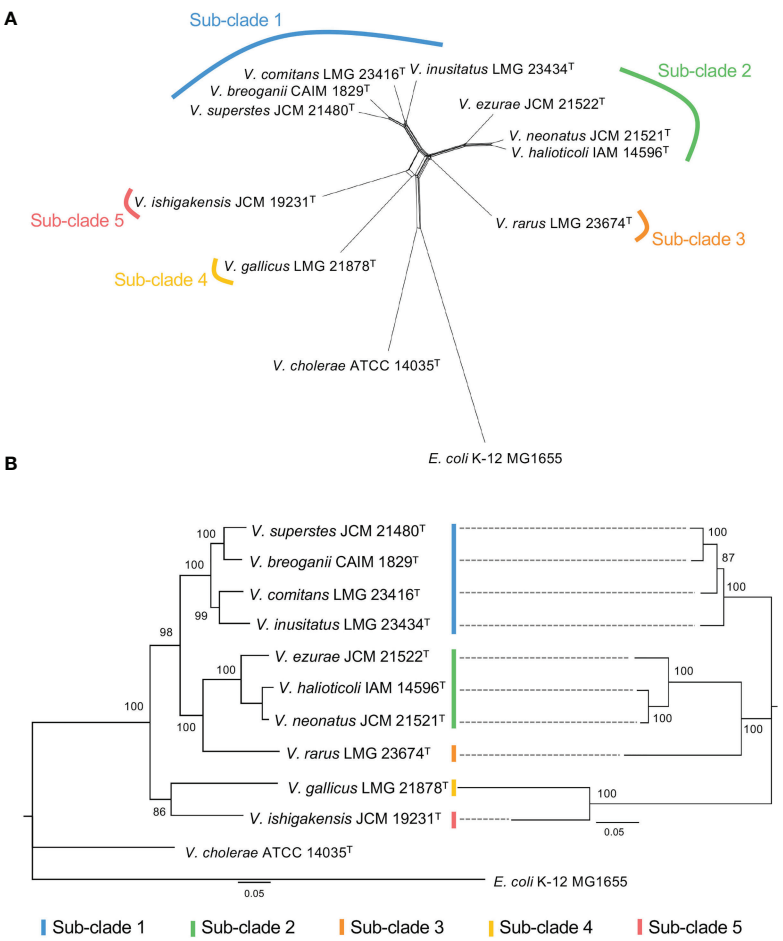

FIGURE 2 | **(A)** Split network of Halioticoli clade based on concatenated sequences of eight protein coding genes (*ftsZ*, *gapA*, *gyrB*, *mreB*, *pyrH*, *recA*, *rpoA*, and *topA*). **(B)** Phylogenetic analysis of Halioticoli clade based on 8 eight protein coding genes (Left) and 125 single copy core genes (Right) using Maximum Likelihood (ML) method and General Time Reversible model with 500 bootstraps. Bootstrap values are shown at the branch points. All branches were both recovered in Neighbor-Joining (NJ) and Minimum-Evolution (ME) trees.

insights into evolutionary processes that contribute to diversity, chromosomal dynamics, and interspecies rearrangement rates (Bhutkar et al., 2006; Lee et al., 2018; de la Haba et al., 2019). The nucleotide identity comparison using BLASTn of both chromosomes (Chr. 1 and Chr. 2) for Halioticoli clade species was performed using *V. ishigakensis* JCM 19231^T as the reference genome (**Figure 3A**). The analysis revealed a higher nucleotide similarity in Chr. 1 but a lower similarity in Chr. 2, which indicates the genomes of Chr. 1 were highly conserved but those of Chr. 2 was relatively varied. Intra-sub-clade and inter-sub-clade genome rearrangement mappings of both chromosomes demonstrated that 1) similar gene arrangements amongst genomes of intra-subclade species in sub-clades 1 and 2, and 2) less similar of those arrangements among those of inter-subclade species (**Figures 3B**, **S2**).

Relatively more GEIs and transposase/integrase were predicted in sub-clades 2 and 3, which were likely to be shared common ancestry (**Figures 2**, **S1**, **S3**). The lowest number of GEIs and transposase/integrase were found in *V. gallicus* (sub-clade 4) and *V. comitans* (sub-clade 1), respectively. Interestingly, *V. ishigakensis* showed opposite results that much higher GEIs numbers but much lower transposase/integrase numbers.

Pangenomic Analysis of the Halioticoli Clade

Pan-genomics is capable of investigating the relationships between a given group of genomes by means of characterizing the core and accessory genes, providing a unique insight in the phylogeny and taxonomy analysis (Eren et al., 2015; Delmont and Eren, 2018). The ten genomes of Halioticoli clade species were used for pan-genome analysis using Anvi'o v7. In the Halioticoli clade pan-genome (**Figure 4**), a total of 8,062 gene clusters (GCs) with 36,612 genes were defined, in which 2,130 GCs with 22,123 genes (60%) were recognized in the core-genome (1,973 GCs with 19,730 genes were recognized as the

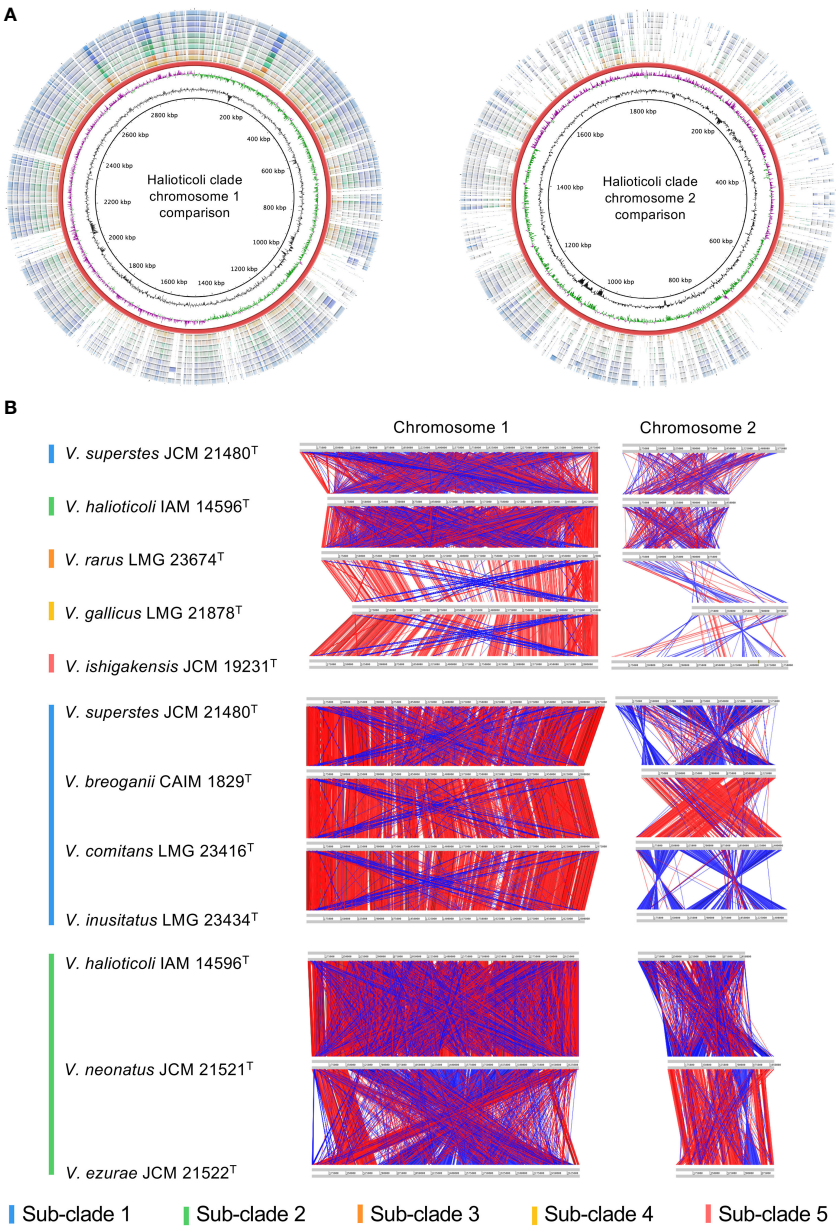

FIGURE 3 | Genomic comparison in Halioticoli clade. **(A)** Circular map designed to compare the nucleotide identity of all genomes against *V. ishigakensis* JCM 19231^T. The genomes were compared by BLASTn, and the percent identity between them was determined by the intensity of color in each ring. The rings from inner to outer are presented as follows: the GC content and CG skew of *V. ishigakensis* JCM 19231^T, the genomes of *V. ishigakensis* JCM 19231^T, *V. gallicus* LMG 21878^T, *V. rarus* LMG 23674^T, *V. halioticoli* IAM 14596^T, *V. neonatus* JCM 21521^T, *V. ezurae* JCM 21522^T, *V. inusitatus* LMG 23434^T, *V. comitans* LMG 23416^T, *V. breoganii* CAIM 1829^T, and *V. superstes* JCM 21480^T, respectively. **(B)** Genomic synteny plots were analyzed using Artemis Comparison Tool. Gray lines indicate each genome size. Red bars indicate the conserved genomic regions, and blue bars indicate genomic inversions. A bigger and clearer plot is available in **Figure S1**.

single-copy core-genome), and 2,456 GCs with 10,881 genes (30%) were recognized in the accessory-genome. The remaining genes were recognized as species-specific genes as in **Figure 4**, among which, *V. ishigakensis* (sub-clade 5) possessed the most specific genes (922), 2-5 times more than other species. In addition, gene cluster analysis also showed that sub-clade 5 gained the highest number of GCs (4134), followed by sub-clade 1 (3,732 in average), sub-clade 2 (3,250 in average), sub-clade 3 (3193), and sub-clade 4 (2987). These results showed positive relationships with genome size.

Due to the difficulty to use a large number of single-copy genes (SCGs), a set of 125 better-SCGs was filtered using a custom setting (–min-geometric-homogeneity-index 1, –max-functional-homogeneity-index 0.9). The concatenated amino

acid sequence of the 125 better-SCGs was used for constructing a more accurate phylogenetic tree, and the result showed that the topology was congruent with the one constructed by eight housekeeping genes (**Figures 2B**, **4**), the five sub-clades could be identified as well. Moreover, the five sub-clades could also be illustrated by clustering in the ANI matrix, and sub-clade species showed at least 85.5% intra ANI similarity.

Function Estimation and Metabolism Reconstruction of the Halioticoli Clade

The Clusters of Orthologous Genes (COGs) database has been a popular tool for functional and comparative genomics of bacteria and archaea in recent decades with the newest update of COG20 (Galperin et al., 2021). COG20 function estimation for each genome of Halioticoli clade species showed that the same function structure was shared among the species, as well as in the core-genome (**Figure S4A**). However, the result in the species-specific genomes was diverse in some aspects (**Figure 5A**). Despite the poorly characterized and unknown functions, the planktonic species, *V. ishigakensis*-specific genome had the most diverse and abundant gene sets in each function category. Among them, *V. ishigakensis* showed more abundant in the metabolism functions, in particular in the "Carbohydrate transport and metabolism" function. In addition, the functions of "Transcription", "Signal transduction mechanisms", and "Cell wall membrane envelope biogenesis" were also abundant. It is likely that these functions were an adaptation for survival in planktonic environments. The symbiotic species-specific genomes showed poorer ability in metabolizing, with the *V. superstes*-specific one being the most powerful. To further investigate the metabolism functions in the Halioticoli clade, metabolism pathway modules were reconstructed using the KEGG database. As in the function structure, the Halioticoli clade species shared the common metabolism structure in complete genomes (**Figure S4B**), but different structures in species-specific genomes (**Figure 5B**). A wide range of genes responsible for diverse metabolism pathways was only detected in the *V. ishigakensis*-specific genome, in particular carbohydrate metabolism genes were highly detected. On the other hand, other species-specific genomes, demonstrated their advantages, such as a remarkable detection for "cofactor and vitamin metabolism" in the *V. rarus*-specific genome. In addition, the enrichment analyses of metabolism pathway modules indicated that the *V. ishigakensis* shared almost all enriched modules with other species with the exception of D-galactonate degradation (M00552), which is exclusively and most enriched in itself (**Figure 6**).

Furthermore, the COG20 and KEGG annotations were also performed for gene clusters (GCs) of each Halioticoli clade species. Same COG20 functions were shared among the clade but with different abundance. *V. ishigakensis*, which has the biggest genome size, gained the highest number of GCs with a wide range of COG functions, in particular GCs classified into "Transcription (K)", "Cell wall/membrane/envelope biogenesis (M)", and "Carbohydrate transport and metabolism (G)". In more detail, numbers of GCs were 1.2, 1.6, 1.7, and 1.7 folds in K, 1.1, 1.3, 1.3, and 1.4 folds in M, and 1.4, 1.9, 2.3, and 1.9 folds in G, compared with those numbers of sub-clades 1, 2, 3 and 4, respectively. On the contrary, the lowest number of GCs were observed in *V. gallicus*, numbers of GCs classified to "Cell cycle control, cell division, chromosome partitioning (D)", "Posttranslational modification, protein turnover, chaperones (O)", and "Defense mechanisms (V)" were reduced (**Figure 7A**). KEGG annotation of GCs which were lost or gained showed "Polyamine biosynthesis" (E6, in **Figures 7B**, **S5**) were gained in sub-clades 1, 3, and 5 but lost in sub-clades 2 and 4, and GCs encoded trans-2,3-dihydro-3-hydroxyanthranilate isomerase [EC:5.3.3.17] in "Biosynthesis of other bacterial compounds (I5)" were gained in sub-clades 1 and 5 but lost in other sub-clades. In more details, glycine/D-amino acid oxidase (deaminating) (*dadA*) (PDB:3AWI) and acyl-CoA reductase or other NAD-dependent aldehyde dehydrogenase (*adhE*) (PDB:1A4S), both of which can use putrescine to produce GABA (M00136), were gained in the sub-clades 1 and 3; and genes (*rfbB*, *rfbC*, *rfbD*, and *rmlA1*) involved in the biosynthesis of the dTDP-L-rhamnose (M00793) were lost in the sub-clade4 (**Figure S6**).

More Abundant CAZy Were Predicted in the Planktonic Species

Carbohydrate-Active enZYmes (CAZy) were predicted for each genome to describe the catalytic modules (enzymes) encoded in these genomes. Generally, each genome of the Halioticoli clade species contained 4 main enzymes classes: Carbohydrate Esterases (CEs), Glycoside Hydrolases (GHs), GlycosylTransferases (GTs), and Polysaccharide Lyases (PLs); and one associated module: Carbohydrate-Binding Modules (CBMs); only some of them contained few Auxiliary Activities (AAs) class enzymes (**Figure 8E**). Among them, Sub-clade 5 (*V. ishigakensis*) had the most CAZy (120), followed by sub-clade 1 (95-109), as a result of the abundance of GHs in these sub-clades (**Figure 8A**). Meanwhile, kinds of polysaccharide lyases (PL6, PL7, PL15, and P17) involved in alginate degradation were found enriched in the Halioticoli clade species, while *V. ishigakensis* had fewer numbers (15) than most symbiotic species (19-21) (**Figure 8C**). Compared to the planktonic sub-clade, symbiotic sub-clades showed higher ability on alginate degradation but with different advantages, which is a higher capacity of intracellular degradation (PL15 and PL17) in sub-clade 1, but a higher capacity of extracellular degradation (PL6 and PL7) in sub-clade 2 and 3.These finds indicate that *V. ishigakensis* obtained a powerful ability for degrading diverse glycosidic bonds but became weaker in degrading polysaccharides during the evolution from the gut environment to the planktonic environment.

DISCUSSION

Ten species in the Halioticoli clade, including the first described species of *V. halioticoli* (Sawabe et al., 1998) and the most recently described one of *V. ishigakensis* (Gao et al., 2016), have been found to date, making the clade robust in the family *Vibrionaceae* (Jiang et al., 2022). However, the evolutionary

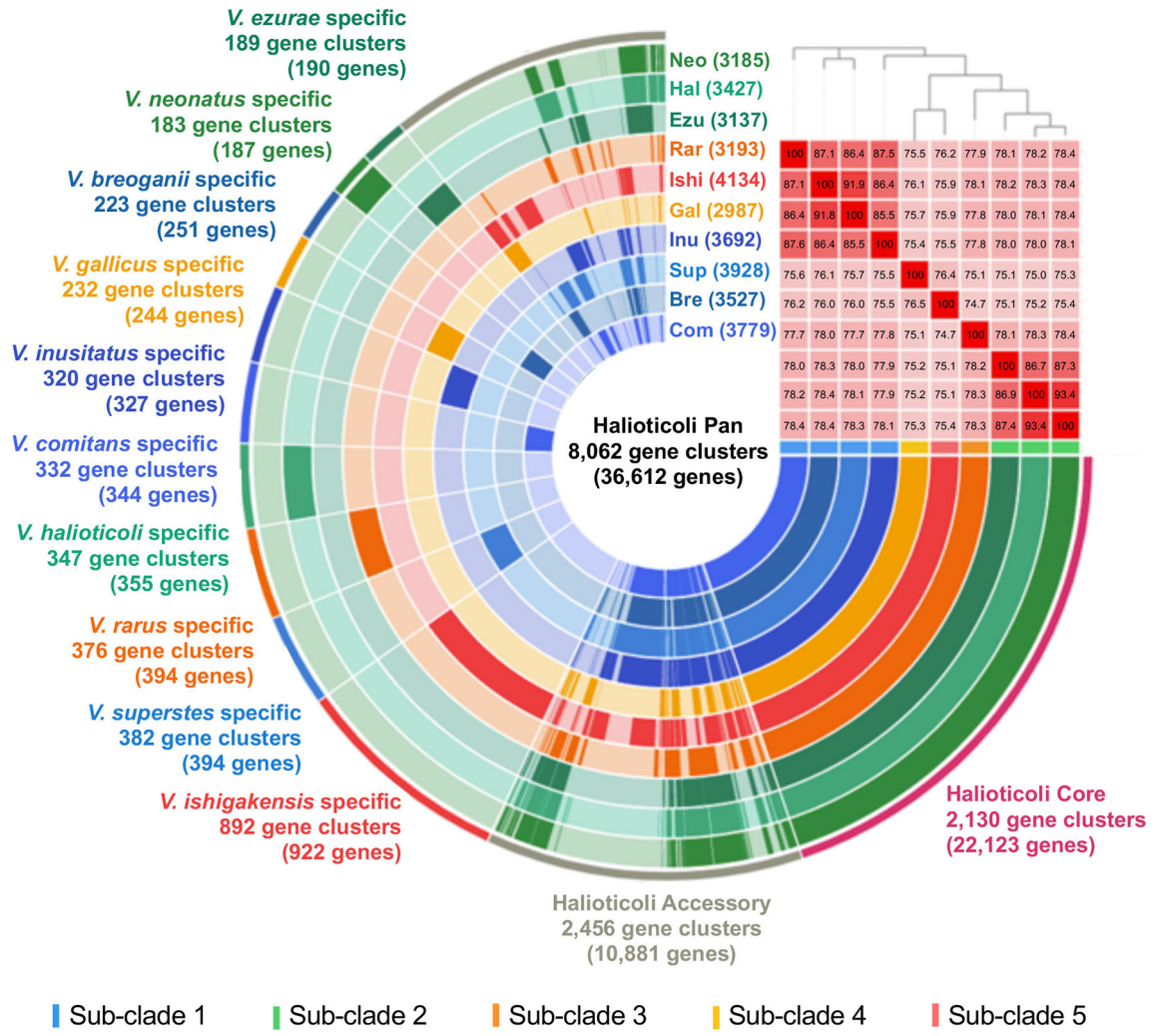

FIGURE 4 | The pan-genome analysis of the Halioticoli clade species. Circle bars represent the occurrence of gene clusters in each genome. Gene cluster represents a group of homologues identified based on the amino acid sequence similarity. Heatmap in the upper right corner represents ANI calculation between these genomes (the barrier for species identification is 95%), and the above phylogenetic tree was constructed using amino acid sequences of 125 better single-copy genes by embedded FastTree tool. Abbreviations for the Halioticoli clade species are represented as Bre, *V. breoganii* CAIM 1829^T; Com, *V. comitans* LMG 23416^T; Ezu, *V. ezurae* JCM 21522^T; Gal, *V. gallicus* LMG 21878^T; Hal, *V. halioticoli* IAM 14596^T; Inu, *V. inusitatus* LMG 23434^T; Ish, *V. ishigakensis* JCM 19231^T; Neo, *V. neonatus* JCM 21521^T; Rar, *V. rarus* LMG 23674^T; and Sup, *V. superstes* JCM 21480^T. Numbers in parentheses after abbreviations represent the total numbers of gene clusters in each species.

history of them remains unknown due to the lack of complete genome sequence comparisons. We succeeded in getting all complete genomes, and it showed that all of them were composed of two chromosomes while part of them with one additional plasmid, in which, the planktonic species, *V. ishigakensis* had the biggest genome size and highest GC content (**Table 2**). On the basis of the genome sequences, phylogenetic analyses using three methods all clearly showed the five evolutionary directions (**Figures 2**, **S1**). *V. gallicus* were deeply branched, followed to *V. ishigakensis* in this clade.

Comparative genomic analyses have been widely employed to explore the diversity, evolution, and chromosomal dynamics between given genomes, such as *Methylophilaceae* (Jimenez-Infante et al., 2016), *Salinivibrio* (de la Haba et al., 2019), and *Erysipelothrix* (Grazziotin et al., 2021). Here, we utilized the complete genomes of Halioticoli clade species to construct a circular map of nucleotide identity comparison and a linear synteny comparison for both chromosomes (Chr. 1 and Chr. 2). As with previous studies (Okada et al., 2005; Kirkup et al., 2010), the results showed that the structure of Chr. 1 was more stable and conserved than Chr. 2 during the evolution (more gaps could be found), and it was more evident in the intra-subclades species than inter-subclades species (**Figure 3**). This may be explained by the mutations, rearrangements or horizontal gene transfer (HGT) of genomes, in which, HGT is an important mechanism for the evolution of microbial genomes, enabling the bacteria to

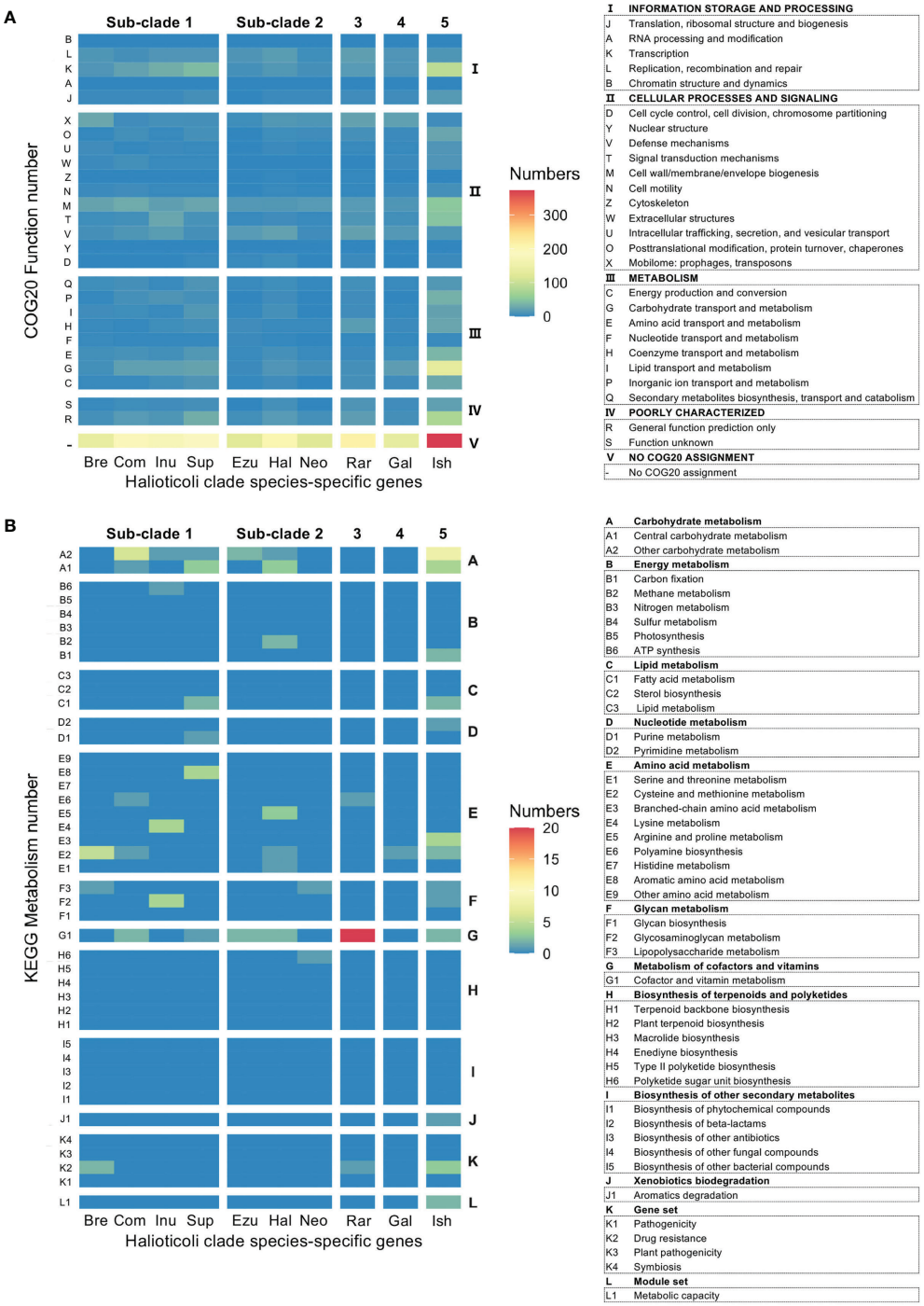

FIGURE 5 | Heatmap representation based on the number of hits in specific genes for each Halioticoli clade species, **(A)** COG20 function prediction, and **(B)** KEGG metabolism prediction. The left and right axis ticks represent different subcategories and categories, respectively. Abbreviations for the Halioticoli clade species are represented as **Figure 4**.

adapt to the environment (Dobrindt et al., 2004). A significant part of the HGT has been facilitated by genomic islands (GEIs), which plays an important role in promoting the adaptive evolution of commensal, symbiotic and environmental bacteria (Dobrindt et al., 2004; Juhas et al., 2009). Results showed that *V. gallicus* contained the least number of GEIs. The numbers of GEIs predicted on Chr. 2 were higher than those on Chr. 1 in most species while the opposite occurred in the sub-clade

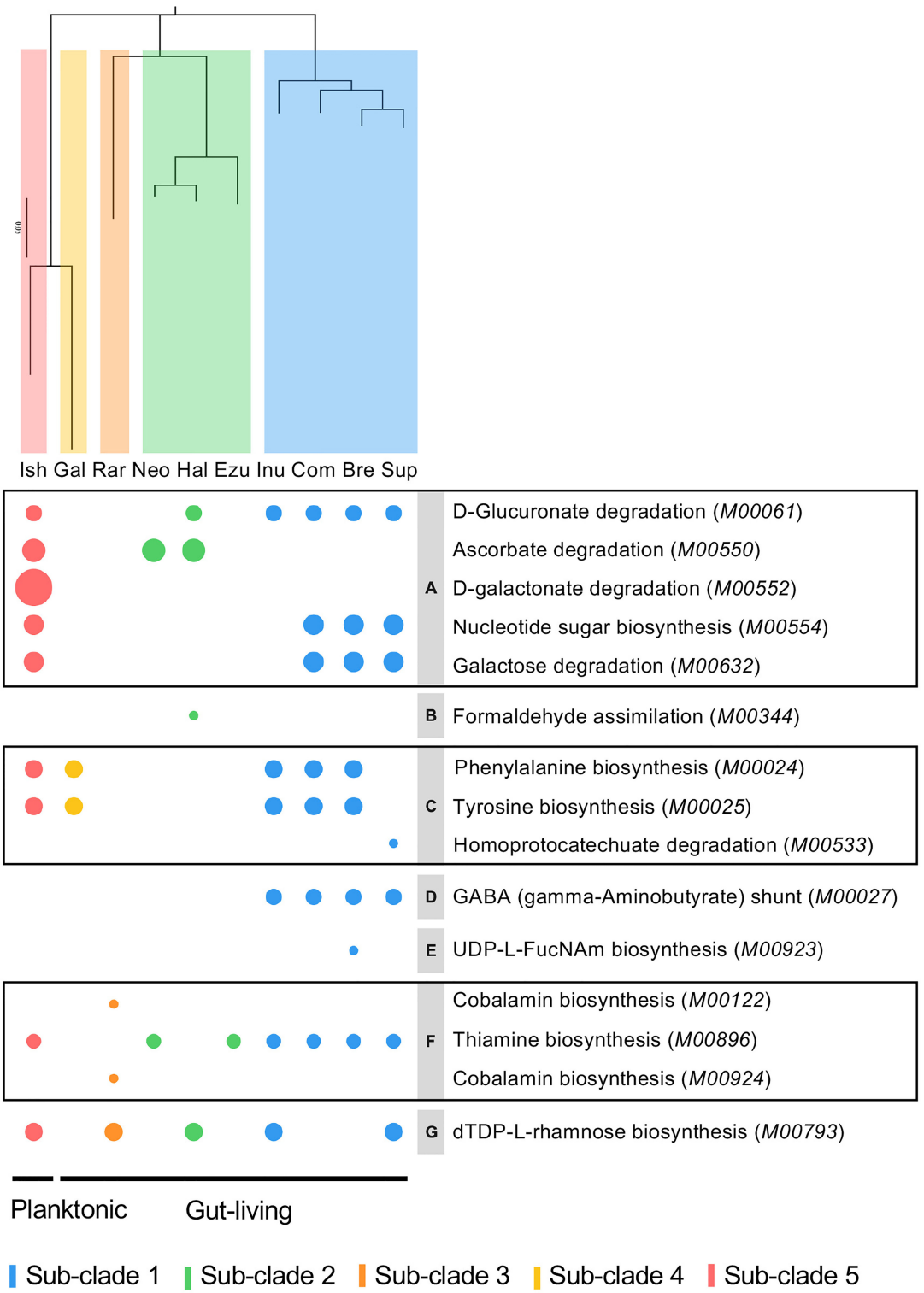

FIGURE 6 | Bubble plot based on enrichment of KEGG pathway modules in Halioticoli clade. Bubble size represents the enrichment score, colour represents different groups. Phylogenetic tree was constructed accordingly to **Figure 2B**. The italic contents of parentheses represent the module accession numbers in the KEGG database. Gray parts indicate the secondary category of the KEGG module as follows, **(A)** Other carbohydrate metabolism, **(B)** Methane metabolism, **(C)** Aromatic amino acid metabolism, **(D)** Other amino acid metabolism, **(E)** Lipopolysaccharide metabolism, **(F)** Cofactor and vitamin metabolism, **(G)** Polyketide sugar unit biosynthesis. Related genes were listed in **Table S2**.

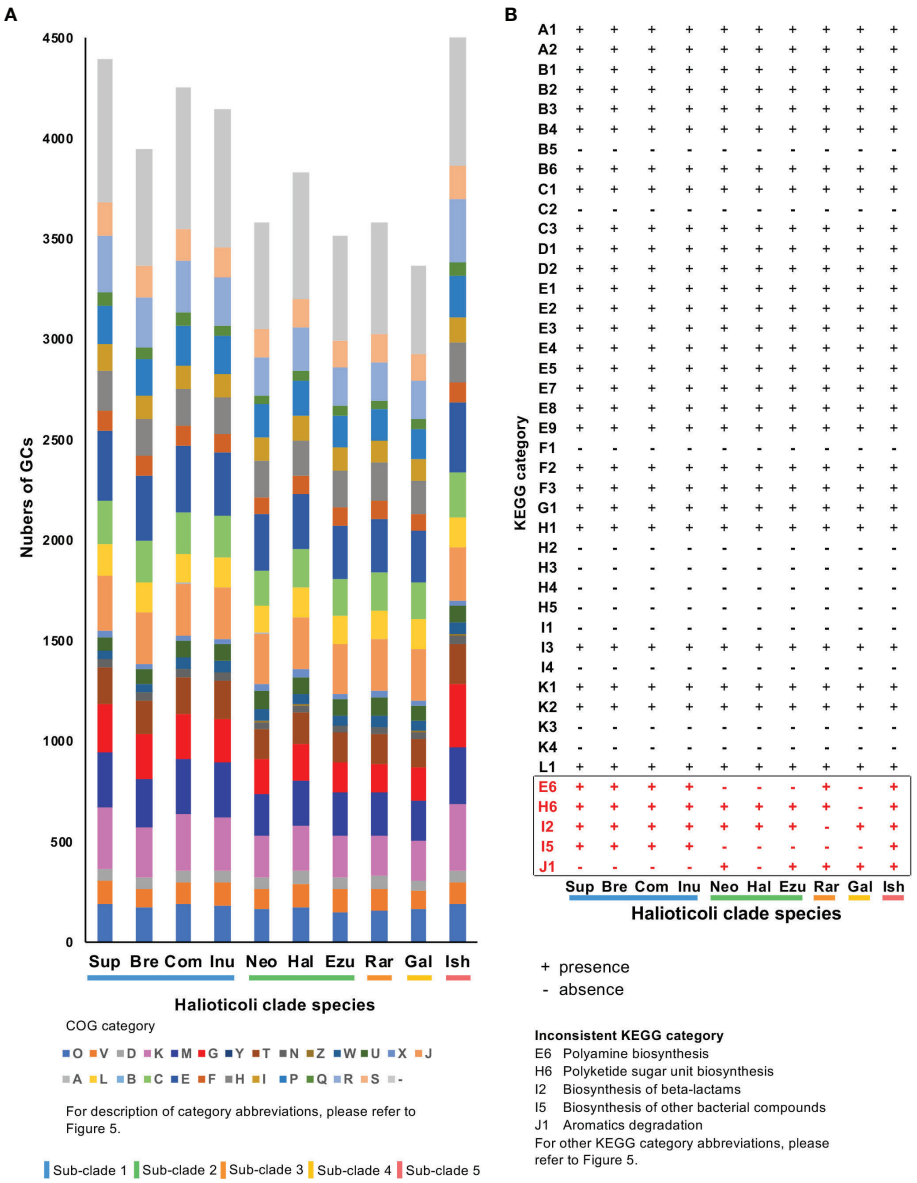

FIGURE 7 | COG and KEGG annotation of gene clusters (GCs) for each Halioticoli clade species. **(A)** Numbers of GCs for each COG functional category. **(B)** Presence and absence of each KEGG category. Numbers of GCs for each KEGG category please refer to **Figure S5**. Abbreviations for COG and KEGG categories are represented as **Figure 5**. The Abbreviations for the Halioticoli clade species are represented as **Figure 4**.

2 species (**Figure S3A**). Besides, although the HGT of GEIs was predicted from accessory genes, some genes/proteins could be found shared in the same sub-clade species, such as pectin degradation protein KdgF (*kdgF*) in sub-clade 1 and DNA methyltransferase (*hsdM*) in sub-clade 2. We also searched transposase and integrase as presence of HGT events, transposase related genes were significantly abundant (**Figure S3B**). In which, except of the one integrase/recombinase *xerC* and *xerD* were found shared on the Chr. 1 of core-genomes, the other transposase and integrase related genes were distributed among the accessory and specific genomes.

In this study, we also estimated the COG function and reconstructed the metabolism pathway for each species genome, core/accessory genomes, and species-specific genomes. The function and metabolism structures were shared in the whole genome of each halioticoli clade species and their core-genome (**Figure S4**), but diverged in the accessory-genome and species-specific genomes (**Figure 5**). According to the reconstruction of metabolism pathways using KEGG database, most of the genes were involved in the carbohydrate and amino acid metabolisms. Moreover, there was a significant detection in the cofactor and vitamin metabolism by *V. rarus*-specific

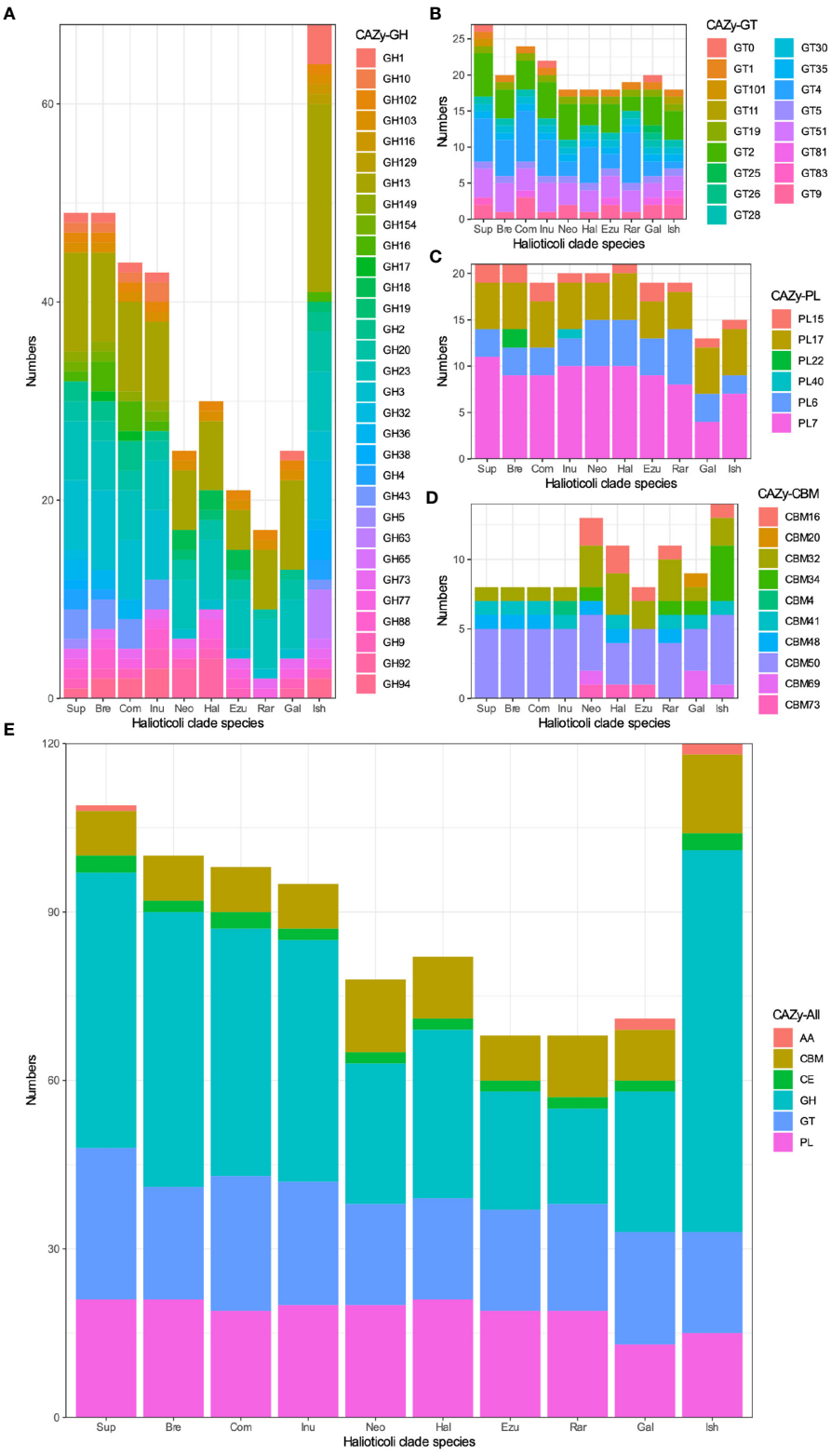

FIGURE 8 | The numbers of Carbohydrate-active enzyme (CAZy) predicted in each Halioticoli clade species, annotated by dbCAN2 meta server. **(A)** Glycoside Hydrolases (GH), **(B)** GlycosylTransferases (GT), **(C)** Polysaccharide Lyases (PL), **(D)** Carbohydrate-Binding Modules (CBM), and **(E)** The total CAZy numbers. Abbreviations for the Halioticoli clade species are represented as **Figure 4**.

genomes, due to the related genes of cobalamin/B12 biosynthesis. Furthermore, the enrichment scores of metabolism pathway modules between different groups showed that almost all enriched pathway modules in the planktonic group (sub-clade 5, *V. ishigakensis*) were shared with other groups, except the D-galactonate degradation (M00552) was enriched exclusively in itself and was the most enriched module (**Figure 6**). This module has been reported involved in the catabolism of carrageenan, which is one of main components of red algal cell walls (Gobet et al., 2018; Schultz-Johansen et al., 2018). For the symbiotic group, most enriched modules were detected in the sub-clade 1, and subclade-specific enriched modules could be found as well, for example, GABA (γ-aminobutyrate) shunt (M00027) in sub-clade 1 and cobalamin biosynthesis (M00122 and M00924) in sub-clade 3 (*V. rarus*). The γ-aminobutyrate (GABA) shunt is a metabolic pathway that bypasses two steps of the tricarboxylic-acid (TCA) cycle to produce succinate, as an alternative route in plants and mammals, while it has not been extensively studied in bacteria but is thought to play a role in glutamate metabolism, anaplerosis, and antioxidant defense (Bouche et al., 2003; Feehily et al., 2013). In addition, GABA has also been found abundant in many algae species (Belghit et al., 2017), the enrichment of related modules could be caused by algae associations in the gut of algae-eating animals.

Prediction of Carbohydrate-Active enZYmes (CAZy) showed a subclade-based grouping as well. *V. ishigakensis* contained the most CAZy, which was due to the abundance of GHs (**Figure 8**). The significant presence (19) of GH13, which is a main α-amylase family (van der Maarel et al., 2002; Janeček and Zámocká, 2020), was likely responsible for the diversity and abundance of carbohydrate metabolisms detected above for *V. ishigakensis*. Sub-clade 1 and 5 species are likely capable of utilizing a variety of β-glucans, which are an important group of glucose-based polysaccharides composed of β-glycosidic bonds found primarily in algal cell walls (Corzett et al., 2018), due to the possesses of enzymes identified in GH3 and GH16. We also found other enzymes involved in algal carbohydrates (Mann et al., 2013) exclusively in these two sub-clades, including GH 36 and GH43, which is related to breaking down carrageenans/carbohydrates and cell wall-degrading, respectively (Tang et al., 2017). Furthermore, genes encoding alginate degrading enzymes (*aly*), classified into PL6, PL7, PL15, and PL17 were commonly found in the genomes of Halioticoli clade species, but the number in *V. ishigakensis* was relatively smaller. A similar signature of GH and PL CAZy has been described in *V. breoganii*, indicating the evolution of specialization for macroalgal substrates (Corzett et al., 2018). As a result of the above results, it appears that all species of sub-clade 1 have evolved to specialize in macroalgae, which could function as alternative sources for bioenergy production using macroalgae. In addition, chitin utilization is a conservative function in the family *Vibrionaceae* except for *V. breoganii* (Hunt et al., 2008; Corzett et al., 2018), but it has not been mentioned in other Halioticoli clade species. In our study, same as *V. breoganii*, members of sub-clade 1, sub-clade 3, and sub-clade 4 lacked any domain of GH18, GH19, GH116, and GH129, or motif of CBM5, CBM14, and CBM73, which are implicated in chitin utilization (**Figure S7**). However, two chitinase (ChiA, GH18 family), one chitodextrinase (GH19) and one motif (CBM73) were found distributed among the members of sub-clade 2. These results indicate that species of sub-clade 2 were likely to be able to utilize chitin while that of sub-clade 1, sub-clade 3, and sub-clade 4 were not.

CONCLUSION

In this study, the first pan-genomic analysis of the Halioticoli clade was completed thanks to the complete genomes of the type strains of this clade. The results obtained regarding the phylogenetic analysis and pan-genome analysis, as well as function and metabolism estimation, will help us to elucidate the evolutionary processes of these species from symbiotic to planktonic lifestyle. It appears that genome expansion encoding more carbohydrate metabolism occurred during symbiotic as a gut-living to free-living environments, planktonic species acquired more abilities to utilize a variety of carbohydrates for surviving in the environment while symbiotic species were evolved to specialize in macroalgae utilization. These generic backbones could contribute to developing bioenergy potential using macroalgae as biocatalysts.

DATA AVAILABILITY STATEMENT

The datasets presented in this study can be found in online repositories. The names of the repository/repositories and accession number(s) can be found below: DDBJ [accession: PRJDB11924].

AUTHOR CONTRIBUTIONS

CJ conceived, designed and performed the experiments, analyzed the data, visualized the data, and drafted and reviewed the manuscript. SM analyzed the data and reviewed the manuscript. TS conceived and designed the experiments and reviewed the manuscript. All authors contributed to the article and approved the submitted version.

FUNDING

This study was partly supported by MEXT KAKEN 19H03041.

SUPPLEMENTARY MATERIAL

The Supplementary Material for this article can be found online at: https://www.frontiersin.org/articles/10.3389/fmars.2022.844983/full#supplementary-material

Supplementary Figure 1 | The concatenated split network based on nucleotide sequences of eight housekeeping genes retrieved from 191 *Vibrionaceae* species. The *ftsZ*, *gapA*, *gyrB*, *mreB*, *pyrH*, *recA*, *rpoA*, and *topA* gene sequences were concatenated and the tree was reconstructed using the SplitsTree4 ver. 4.14.8. Sequence data was obtained from Jiang et al., 2022.

Supplementary Figure 2 | Genomic synteny plots were analyzed using Artemis Comparison Tool. Gray lines indicate each genome size. Red bars indicate the conserved genomic regions, and blue bars indicate genomic inversions.

Supplementary Figure 3 | (A) The numbers of Genomic island (GEI) predicted of both chromosomes in each Halioticoli clade species, annotated by IslandViewer 4. **(B)** The numbers of transposase and integrase related genes predicted in each Halioticoli clade species. Abbreviations for the Halioticoli clade species are represented as Bre, *V. breoganii* CAIM 1829^T; Com, *V. comitans* LMG 23416^T; Ezu, *V. ezurae* JCM 21522^T; Gal, *V. gallicus* LMG 21878^T; Hal, *V. halioticoli* IAM 14596^T; Inu, *V. inusitatus* LMG 23434^T; Ish, *V. ishigakensis* JCM 19231^T; Neo, *V. neonatus* JCM 21521^T; Rar, *V. rarus* LMG 23674^T; and Sup, *V. superstes* JCM 21480^T.

Supplementary Figure 4 | Distribution of **(A)** COG20 function and **(B)** KEGG metabolism predication across the accessory-genome, core-genome, and each complete genome of Halioticoli clade species. Abbreviations for the Halioticoli clade species are represented as Bre, *V. breoganii* CAIM 1829^T; Com, *V. comitans* LMG 23416^T; Ezu, *V. ezurae* JCM 21522^T; Gal, *V. gallicus* LMG 21878^T; Hal, *V. halioticoli* IAM 14596^T; Inu, *V. inusitatus* LMG 23434^T; Ish, *V. ishigakensis* JCM 19231^T; Neo, *V. neonatus* JCM 21521^T; Rar, *V. rarus* LMG 23674^T; and Sup, *V. superstes* JCM 21480^T.

Supplementary Figure 5 | Numbers of gene clusters (GCs) for each KEGG category. The Abbreviations for the Halioticoli clade species are represented as Bre, *V. breoganii* CAIM 1829^T; Com, *V. comitans* LMG 23416^T; Ezu, *V. ezurae* JCM 21522^T; Gal, *V. gallicus* LMG 21878^T; Hal, *V. halioticoli* IAM 14596^T; Inu, *V. inusitatus* LMG 23434^T; Ish, *V. ishigakensis* JCM 19231^T; Neo, *V. neonatus* JCM 21521^T; Rar, *V. rarus* LMG 23674^T; and Sup, *V. superstes* JCM 21480^T.

Supplementary Figure 6 | Gene loci mapping of Halioticoli clade. **(A)** Circular map of CDS comparison between all genomes against *V. ishigakensis* JCM 19231^T, performed by CGView Server (cgview.ca). **(B)** Gene loci of gained or lost gene clusters.

Supplementary Figure 7 | Prediction of chitin utilization related genes in each Halioticoli clade species. Abbreviations for the Halioticoli clade species are represented as Bre, *V. breoganii* CAIM 1829^T; Com, *V. comitans* LMG 23416^T; Ezu, *V. ezurae* JCM 21522^T; Gal, *V. gallicus* LMG 21878^T; Hal, *V. halioticoli* IAM 14596^T; Inu, *V. inusitatus* LMG 23434^T; Ish, *V. ishigakensis* JCM 19231^T; Neo, *V. neonatus* JCM 21521^T; Rar, *V. rarus* LMG 23674^T; and Sup, *V. superstes* JCM 21480^T. Members of sub-clade 1, sub-clade 3, and sub-clade 4 lacked any domain of GH18, GH19, GH116, and GH129, or motif of CBM5, CBM14, and CBM73, which are implicated in chitin utilization.

REFERENCES

Alikhan, N. F., Petty, N. K., Ben Zakour, N. L., and Beatson, S. A. (2011). BLAST Ring Image Generator (BRIG): Simple Prokaryote Genome Comparisons. *BMC Genomics* 12, 402. doi: 10.1186/1471-2164-12-402

Aramaki, T., Blanc-Mathieu, R., Endo, H., Ohkubo, K., Kanehisa, M., Goto, S., et al. (2020). KofamKOALA: KEGG Ortholog Assignment Based on Profile HMM and Adaptive Score Threshold. *Bioinformatics* 36, 2251–2252. doi: 10.1093/bioinformatics/btz859

Beaz Hidalgo, R., Cleenwerck, I., Balboa, S., Prado, S., De Vos, P., and Romalde, J. L. (2009). *Vibrio Breoganii* Sp. Nov., a Non-Motile, Alginolytic, Marine Bacterium Within the *Vibrio Halioticoli* Clade. *Int. J. Syst. Evol. Microbiol.* 59, 1589–1594. doi: 10.1099/ijs.0.003434-0

Belghit, I., Rasinger, J. D., Heesch, S., Biancarosa, I., Liland, N., Torstensen, B., et al. (2017). In-Depth Metabolic Profiling of Marine Macroalgae Confirms Strong Biochemical Differences Between Brown, Red and Green Algae. *Algal. Res.* 26, 240–249. doi: 10.1016/j.algal.2017.08.001

Bertelli, C., Laird, M. R., Williams, K. P., Lau, B. Y., Hoad, G., Winsor, G. L., et al. (2017). IslandViewer 4: Expanded Prediction of Genomic Islands for Larger-Scale Datasets. *Nucleic Acids Res.* 45, W30–W35. doi: 10.1093/nar/gkx343

Bhutkar, A., Russo, S., Smith, T. F., and Gelbart, W. M. (2006). Techniques for Multi-Genome Synteny Analysis to Overcome Assembly Limitations. *Genome Inform.* 17, 152–161. doi: 10.11234/gi1990.17.2_152

Bouche, N., Fait, A., Bouchez, D., Moller, S. G., and Fromm, H. (2003). Mitochondrial Succinic-Semialdehyde Dehydrogenase of the γ-Aminobutyrate Shunt is Required to Restrict Levels of Reactive Oxygen Intermediates in Plants. *Proc. Natl. Acad. Sci.* 100, 6843–6848. doi: 10.1073/pnas.1037532100

Carver, T. J., Rutherford, K. M., Berriman, M., Rajandream, M. A., Barrell, B. G., and Parkhill, J. (2005). ACT: The Artemis Comparison Tool. *Bioinformatics* 21, 3422–3423. doi: 10.1093/bioinformatics/bti553

Corzett, C. H., Elsherbini, J., Chien, D. M., Hehemann, J. H., Henschel, A., Preheim, S. P., et al. (2018). Evolution of a Vegetarian Vibrio: Metabolic Specialization of *Vibrio Breoganii* to Macroalgal Substrates. *J. Bacteriol.* 200, e00020–18. doi: 10.1128/JB.00020-18

De la Haba, R. R., López-Hermoso, C., Sánchez-Porro, C., Konstantinidis, K. T., and Ventosa, A. (2019). Comparative Genomics and Phylogenomic Analysis of the Genus *Salinivibrio*. *Front. Microbiol.* 10. doi: 10.3389/fmicb.2019.02104

Delmont, T. O., and Eren, A. M. (2018). Linking Pangenomes and Metagenomes: The *Prochlorococcus* Metapangenome. *PeerJ* 6, e4320. doi: 10.7717/peerj.4320

Dobrindt, U., Hochhut, B., Hentschel, U., and Hacker, J. (2004). Genomic Islands in Pathogenic and Environmental Microorganisms. *Nat. Rev. Microbiol.* 2, 414–424. doi: 10.1038/nrmicro884

Edgar, R. C. (2004). MUSCLE: Multiple Sequence Alignment With High Accuracy and High Throughput. *Nucleic Acids Res.* 32, 1792–1797. doi: 10.1093/nar/gkh340

Eren, A. M., Esen, Ö.C., Quince, C., Vineis, J. H., Morrison, H. G., Sogin, M. L., et al. (2015). Anvi'o: An Advanced Analysis and Visualization Platform for 'Omics Data. *PeerJ* 3, e1319. doi: 10.7717/peerj.1319

Feehily, C., O'Byrne, C. P., and Karatzas, K. A. G. (2013). Functional γ-Aminobutyrate Shunt in *Listeria Monocytogenes*: Role in Acid Tolerance and Succinate Biosynthesis. *Appl. Environ. Microbiol.* 79, 74–80. doi: 10.1128/AEM.02184-12

Galperin, M. Y., Wolf, Y. I., Makarova, K. S., Vera Alvarez, R., Landsman, D., and Koonin, E. V. (2021). COG Database Update: Focus on Microbial Diversity, Model Organisms, and Widespread Pathogens. *Nucleic Acids Res.* 49, D274–D281. doi: 10.1093/nar/gkaa1018

Gao, F., Al-saari, N., Rohul Amin, A. K. M., Sato, K., Mino, S., Suda, W., et al. (2016). *Vibrio Ishigakensis* Sp. Nov., in Halioticoli Clade Isolated From Seawater in Okinawa Coral Reef Area, Japan. *Syst. Appl. Microbiol.* 39, 330–335. doi: 10.1016/j.syapm.2016.04.002

Gobet, A., Barbeyron, T., Matard-Mann, M., Magdelenat, G., Vallenet, D., Duchaud, E., et al. (2018). Evolutionary Evidence of Algal Polysaccharide Degradation Acquisition by *Pseudoalteromonas Carrageenovora* 9^T to Adapt to Macroalgal Niches. *Front. Microbiol.* 9. doi: 10.3389/fmicb.2018.02740

Gomez-Gil, B., Thompson, C. C., Matsumura, Y., Sawabe, T., Iida, T., Christen, R., et al. (2014). "The Famlily Vibrionaceae," in *The Prokaryotes* (Berlin, Heidelberg: Springer Berlin Heidelberg), 659–747. doi: 10.1007/978-3-642-38922-1_225

Grazziotin, A. L., Vidal, N. M., Hoepers, P. G., Reis, T. F. M., Mesa, D., Caron, L. F., et al. (2021). Comparative Genomics of a Novel Clade Shed Light on the Evolution of the Genus *Erysipelothrix* and Characterise an Emerging Species. *Sci. Rep.* 11, 3383. doi: 10.1038/s41598-021-82959-x

Guardiola-Avila, I., Sánchez-Busó, L., Acedo-Félix, E., Gomez-Gil, B., Zúñiga-Cabrera, M., González-Candelas, F., et al. (2021). Core and Accessory Genome Analysis of *Vibrio Mimicus*. *Microorganisms* 9, 191. doi: 10.3390/microorganisms9010191

Hayashi, K., Sawabe, T., Thompson, F. L., Swings, J., Gudkovs, N., Christen, R., et al. (2003). *Vibrio Superstes* Sp. Nov., Isolated From the Gut of Australian Abalones *Haliotis Laevigata* and *Haliotis Rubra*. *Int. J. Syst. Evol. Microbiol.* 53, 1813–1817. doi: 10.1099/ijs.0.02625-0

Hunt, D. E., Gevers, D., Vahora, N. M., and Polz, M. F. (2008). Conservation of the Chitin Utilization Pathway in the *Vibrionaceae*. *Appl. Environ. Microbiol.* 74, 44–51. doi: 10.1128/AEM.01412-07

Hyatt, D., Chen, G. L., LoCascio, P. F., Land, M. L., Larimer, F. W., and Hauser, L. J. (2010). Prodigal: Prokaryotic Gene Recognition and Translation Initiation Site Identification. *BMC Bioinf.* 11, 119. doi: 10.1186/1471-2105-11-119

Janeček, Š., and Zámocká, B. (2020). A New GH13 Subfamily Represented by the α-Amylase From the Halophilic Archaeon *Haloarcula Hispanica*. *Extremophiles* 24, 207–217. doi: 10.1007/s00792-019-01147-y

Jiang, C., Tanaka, M., Nishikawa, S., Mino, S., Romalde, J. L., Thompson, F. L., et al. (2022). Vibrio Clade 3.0: New *Vibrionaceae* Evolutionary Units Using Genome-Based Approach. *Curr. Microbiol.* 79, 1–15. doi: 10.1007/s00284-021-02725-0

Jimenez-Infante, F., Ngugi, D. K., Vinu, M., Alam, I., Kamau, A. A., Blom, J., et al. (2016). Comprehensive Genomic Analyses of the OM43 Clade, Including a Novel Species From the Red Sea, Indicate Ecotype Differentiation Among Marine Methylotrophs. *Appl. Environ. Microbiol.* 82, 1215–1226. doi: 10.1128/AEM.02852-15

Juhas, M., van der Meer, J. R., Gaillard, M., Harding, R. M., Hood, D. W., and Crook, D. W. (2009). Genomic Islands: Tools of Bacterial Horizontal Gene Transfer and Evolution. *FEMS Microbiol. Rev.* 33, 376–393. doi: 10.1111/j.1574-6976.2008.00136.x

Kirchberger, P. C., Turnsek, M., Hunt, D. E., Haley, B. J., Colwell, R. R., Polz, M. F., et al. (2014). *Vibrio Metoecus* Sp. Nov., a Close Relative of *Vibrio Cholerae* Isolated From Coastal Brackish Ponds and Clinical Specimens. *Int. J. Syst. Evol. Microbiol.* 64, 3208–3214. doi: 10.1099/ijs.0.060145-0

Kirkup, B. C., Chang, L., Chang, S., Gevers, D., and Polz, M. F. (2010). *Vibrio Chromosomes* Share Common History. *BMC Microbiol.* 10, 137. doi: 10.1186/1471-2180-10-137

Kumar, S., Stecher, G., Li, M., Knyaz, C., and Tamura, K. (2018). MEGA X: Molecular Evolutionary Genetics Analysis Across Computing Platforms. *Mol. Biol. Evol.* 35, 1547–1549. doi: 10.1093/molbev/msy096

Lee, J., Lee, D., Sim, M., Kwon, D., Kim, J., Ko, Y., et al. (2018). Mysyntenyportal: An Application Package to Construct Websites for Synteny Block Analysis. *BMC Bioinf.* 19, 216. doi: 10.1186/s12859-018-2219-x

Lee, L. H., and Raghunath, P. (2018). Editorial: *Vibrionaceae* Diversity, Multidrug Resistance and Management. *Front. Microbiol.* 9. doi: 10.3389/fmicb.2018.00563

Mann, A. J., Hahnke, R. L., Huang, S., Werner, J., Xing, P., Barbeyron, T., et al. (2013). The Genome of the Alga-Associated Marine Flavobacterium *Formosa Agariphila* KMM 3901^T Reveals a Broad Potential for Degradation of Algal Polysaccharides. *Appl. Environ. Microbiol.* 79, 6813–6822. doi: 10.1128/AEM.01937-13

Moya, A., Peretó, J., Gil, R., and Latorre, A. (2008). Learning How to Live Together: Genomic Insights Into Prokaryote–Animal Symbioses. *Nat. Rev. Genet.* 9, 218–229. doi: 10.1038/nrg2319

Muto, A., Kotera, M., Tokimatsu, T., Nakagawa, Z., Goto, S., and Kanehisa, M. (2013). Modular Architecture of Metabolic Pathways Revealed by Conserved Sequences of Reactions. *J. Chem. Inf. Model.* 53, 613–622. doi: 10.1021/ci3005379

Nyholm, S. V., and McFall-Ngai, M. J. (2004). The Winnowing: Establishing the Squid - Vibrios Symbiosis. *Nat. Rev. Microbiol.* 2, 632–642. doi: 10.1038/nrmicro957

Okada, K., Iida, T., Kita-Tsukamoto, K., and Honda, T. (2005). Vibrios Commonly Possess Two Chromosomes. *J. Bacteriol.* 187, 752–757. doi: 10.1128/JB.187.2.752-757.2005

Orata, F. D., Kirchberger, P. C., Méheust, R., Barlow, E. J., Tarr, C. L., and Boucher, Y. (2015). The Dynamics of Genetic Interactions Between *Vibrio Metoecus* and *Vibrio Cholerae*, Two Close Relatives Co-Occurring in the Environment. *Genome Biol. Evol.* 7, 2941–2954. doi: 10.1093/gbe/evv193

Parte, A. C., Sardà Carbasse, J., Meier-Kolthoff, J. P., Reimer, L. C., and Göker, M. (2020). List of Prokaryotic Names With Standing in Nomenclature (LPSN) Moves to the DSMZ. *Int. J. Syst. Evol. Microbiol.* 70, 5607–5612. doi: 10.1099/ijsem.0.004332

Pritchard, L., Glover, R. H., Humphris, S., Elphinstone, J. G., and Toth, I. K. (2016). Genomics and Taxonomy in Diagnostics for Food Security: Soft-Rotting Enterobacterial Plant Pathogens. *Anal. Methods* 8, 12–24. doi: 10.1039/C5AY02550H

Sawabe, T. (2006). "The Mutual Partnership Between Vibrio Halioticoli and Abalones", in *The Biology of Vibrios*. Eds. F. L. Thompson, B. Austin and J. Swings. (Washington, D.C: ASM Press), 219–230. Available at: http://hdl.handle.net/2115/48579.

Sawabe, T., Fujimura, Y., Niwa, K., and Aono, H. (2007a). *Vibrio Comitans* Sp. Nov., *Vibrio Rarus* Sp. Nov. And *Vibrio Inusitatus* Sp. Nov., From the Gut of the Abalones *Haliotis Discus Discus*, *H. Gigantea*, *H. Madaka* and *H. Rufescens*. *Int. J. Syst. Evol. Microbiol.* 57, 916–922. doi: 10.1099/ijs.0.64789-0

Sawabe, T., Hayashi, K., Moriwaki, J., Fukui, Y., Thompson, F. L., Swings, J., et al. (2004a). *Vibrio Neonatus* Sp. Nov. And Vibrio Ezurae Sp. Nov. Isolated From the Gut of Japanese Abalones. *Syst. Appl. Microbiol.* 27, 527–534. doi: 10.1078/0723202041748154

Sawabe, T., Hayashi, K., Moriwaki, J., Thompson, F. L., Swings, J., Potin, P., et al. (2004b). *Vibrio Gallicus* Sp. Nov., Isolated From the Gut of the French Abalone *Haliotis Tuberculata*. *Int. J. Syst. Evol. Microbiol.* 54, 843–846. doi: 10.1099/ijs.0.02804-0

Sawabe, T., Kita-Tsukamoto, K., and Thompson, F. L. (2007b). Inferring the Evolutionary History of Vibrios by Means of Multilocus Sequence Analysis. *J. Bacteriol.* 189, 7932–7936. doi: 10.1128/JB.00693-07

Sawabe, T., Ogura, Y., Matsumura, Y., Feng, G., Amin, A. R., Mino, S., et al. (2013). Updating the Vibrio Clades Defined by Multilocus Sequence Phylogeny: Proposal of Eight New Clades, and the Description of Vibrio Tritonius Sp. Nov. *Front. Microbiol.* 4. doi: 10.3389/fmicb.2013.00414

Sawabe, T., Sugimura, I., Ohtsuka, M., Nakano, K., Tajima, K., Ezura, Y., et al. (1998). *Vibrio Halioticoli* Sp. Nov., a Non-Motile Alginolytic Marine Bacterium Isolated From the Gut of the Abalone *Haliotis Discus Hannai*. *Int. J. Syst. Bacteriol.* 48, 573–580. doi: 10.1099/00207713-48-2-573

Schultz-Johansen, M., Bech, P. K., Hennessy, R. C., Glaring, M. A., Barbeyron, T., Czjzek, M., et al. (2018). A Novel Enzyme Portfolio for Red Algal Polysaccharide Degradation in the Marine Bacterium *Paraglaciecola Hydrolytica* S66^T Encoded in a Sizeable Polysaccharide Utilization Locus. *Front. Microbiol.* 9. doi: 10.3389/fmicb.2018.00839

Septer, A. N. (2019). The Vibrio-Squid Symbiosis as a Model for Studying Interbacterial Competition. *mSystems* 4, e00180–19. doi: 10.1128/mSystems.00108-19

Shaiber, A., Willis, A. D., Delmont, T. O., Roux, S., Chen, L. X., Schmid, A. C., et al. (2020). Functional and Genetic Markers of Niche Partitioning Among Enigmatic Members of the Human Oral Microbiome. *Genome Biol.* 21, 292. doi: 10.1186/s13059-020-02195-w

Tanaka, M., Mino, S., Ogura, Y., Hayashi, T., and Sawabe, T. (2018). Availability of Nanopore Sequences in the Genome Taxonomy for *Vibrionaceae* Systematics: Rumoiensis Clade Species as a Test Case. *PeerJ* 6, e5018. doi: 10.7717/peerj.5018

Tanaka, R., Sawabe, T., Yoshimizu, M., and Ezura, Y. (2002). Distribution of *Vibrio Halioticoli* Around an Abalone-Farming Center in Japan. *Microbes Environ.* 17, 6–9. doi: 10.1264/jsme2.2002.6

Tang, K., Lin, Y., Han, Y., and Jiao, N. (2017). Characterization of Potential Polysaccharide Utilization Systems in the Marine Bacteroidetes *Gramella Flava* JLT2011 Using a Multi-Omics Approach. *Front. Microbiol.* 8. doi: 10.3389/fmicb.2017.00220

Tanizawa, Y., Fujisawa, T., and Nakamura, Y. (2018). DFAST: A Flexible Prokaryotic Genome Annotation Pipeline for Faster Genome Publication. *Bioinformatics* 34, 1037–1039. doi: 10.1093/bioinformatics/btx713

Thompson, F. L., Iida, T., and Swings, J. (2004). Biodiversity of Vibrios. *Microbiol. Mol. Biol. Rev.* 68, 403–431. doi: 10.1128/MMBR.68.3.403-431.2004

Toft, C., and Andersson, S. G. E. (2010). Evolutionary Microbial Genomics: Insights Into Bacterial Host Adaptation. *Nat. Rev. Genet.* 11, 465–475. doi: 10.1038/nrg2798

van der Maarel, M. J. E., van der Veen, B., Uitdehaag, J. C., Leemhuis, H., and Dijkhuizen, L. (2002). Properties and Applications of Starch-Converting Enzymes of the α-Amylase Family. *J. Biotechnol.* 94, 137–155. doi: 10.1016/S0168-1656(01)00407-2

Van Dongen, S., and Abreu-Goodger, C. (2012), 281–295. doi: 10.1007/978-1-61779-361-5_15

Wernegreen, J. J. (2002). Genome Evolution in Bacterial Endosymbionts of Insects. *Nat. Rev. Genet.* 3, 850–861. doi: 10.1038/nrg931

Zhang, H., Yohe, T., Huang, L., Entwistle, S., Wu, P., Yang, Z., et al. (2018). Dbcan2: A Meta Server for Automated Carbohydrate-Active Enzyme Annotation. *Nucleic Acids Res.* 46, W95–W101. doi: 10.1093/nar/gky418

Conflict of Interest: The authors declare that the research was conducted in the absence of any commercial or financial relationships that could be construed as a potential conflict of interest.

Publisher's Note: All claims expressed in this article are solely those of the authors and do not necessarily represent those of their affiliated organizations, or those of the publisher, the editors and the reviewers. Any product that may be evaluated in

this article, or claim that may be made by its manufacturer, is not guaranteed or endorsed by the publisher.

frontiers in Marine Science

ORIGINAL RESEARCH
published: 28 March 2022
doi: 10.3389/fmars.2022.840384

Temperature Affects Antagonism Among Coral-Associated Bacteria

Anjie Guo[1,2], *Jie Li*[1,3]*, *Lin Wang*[1,3], *Huimin Ju*[1,2], *Qiqi Li*[1,2], *Lijuan Ren*[4] *and Si Zhang*[1,3]

[1] CAS Key Laboratory of Tropical Marine Bio-Resources and Ecology, South China Sea Institute of Oceanology, Chinese Academy of Sciences, Guangzhou, China, [2] University of Chinese Academy of Sciences, Beijing, China, [3] Innovation Academy of South China Sea Ecology and Environmental Engineering, Chinese Academy of Sciences, Guangzhou, China, [4] Department of Ecology and Institute of Hydrobiology, Jinan University, Guangzhou, China

Reef-building corals are invertebrate animals that associate with diverse microorganisms, including Symbiodiniaceae, bacteria, fungi, and archaea. This symbiotic consortium, called the holobiont, is a dynamic system and rapidly responds to environmental temperatures. At present, the effects of temperature on bacteria-bacteria interactions in the coral-associated bacterial community are not clear. Antagonism is considered one of the potential structuring forces in coral microbial communities. Here, we examined the antagonistic interactions among 32 coral-associated bacteria and the physiological and biochemical characteristics of these isolates at different temperatures. The results showed that the antagonism breadth (i.e. the total number of antagonistic interactions) increased but antagonism intensity (i.e. the size of the inhibition zone) decreased at 32°C. The antagonistic interaction network was nested and sender-determined both at 25°C and 32°C, suggesting that the competition networks of coral-associated bacteria were more influenced by the antagonist strains than sensitive strains. Furthermore, we found that the elevated temperature increased the complexity of the antagonistic network. By evaluating the correlations between antagonism and the phylogenetic and phenotypic distances, we demonstrated that the antagonism probability correlated with the phylogenetic distance rather than phenotypic distance. Moreover, the antagonist strains have a wider metabolic niche space, i.e., grew on more carbon sources, than the antagonized strains at 25°C, while there was no difference at 32°C, suggesting the trade-off between antagonism and resource exploitation shifted in the antagonistic interactions under the higher temperature. These findings will be helpful for understanding the bacterial interactions in coral holobionts and the assembly of bacterial community in altered environments, especially under heat stress.

Keywords: antagonistic interactions, coral-associated bacteria, phenotypic pattern, community assembly, competition-relatedness hypothesis

OPEN ACCESS

Edited by:
Anderson B. Mayfield, Atlantic Oceanographic and Meteorological Laboratory (NOAA), United States

Reviewed by:
Jean Lim, University of Miami, United States
Stephanie M. Rosales, Oregon State University, United States

***Correspondence:**
Jie Li
lijietaren@scsio.ac.cn

Specialty section:
This article was submitted to Microbial Symbioses, a section of the journal Frontiers in Marine Science

Received: *21 December 2021*
Accepted: *08 March 2022*
Published: *28 March 2022*

Citation:
Guo A, Li J, Wang L, Ju H, Li Q, Ren L and Zhang S (2022) Temperature Affects Antagonism Among Coral-Associated Bacteria. Front. Mar. Sci. 9:840384. doi: 10.3389/fmars.2022.840384

INTRODUCTION

Reef-building corals associate with dinoflagellates within *Symbiodiniaceae* and other groups of microorganisms, such as fungi, bacteria, archaea, and viruses, that inhabit the coral tissue, mucus, gastro-vascular cavity, and skeleton (Rohwer et al., 2002; van Oppen and Blackall, 2019). The coral-associated microbiome is highly dynamic, the structure and composition of which can rapidly change with environmental conditions, such as temperature, pH, and eutrophication (Meron et al., 2012; Jessen et al., 2013; Pootakham et al., 2018). Previous studies have shown that coral-associated bacteria play an essential role in coral health, including translocating fixed nitrogen (Olson et al., 2009), preventing infection with pathogens (Nissimov et al., 2009; Rypien et al., 2010), and inducing coral larval settlement and metamorphosis (Negri et al., 2001; Tebben et al., 2011). Coral-associated bacteria could act as a defense barrier against pathogenic microbes to facilitate homeostasis and contribute to the survival of the coral holobiont (Glasl et al., 2016) through antibiotics production, living space occupation, and nutrients competition (Rohwer and Kelley, 2004).

Global coral reef ecosystems are threatened by climate change (e.g., increasing seawater temperatures, ocean acidification, and more frequent tropical storms) and direct anthropogenic pressure (e.g., pollution, over-exploitation, and eutrophication). According to records, the scale, frequency and intensity of coral bleaching events are increased caused by anthropogenic global warming, which leads to coral morbidity and mortality and has substantially decimated coral reefs (Hughes et al., 2017; Hughes et al., 2018; Sully et al., 2019). Notably, heat stress changes the community structures of coral-associated bacteria (Ainsworth and Hoegh-Guldberg, 2009; Littman et al., 2010; Littman et al., 2011; Lee et al., 2015; Tout et al., 2015; Ziegler et al., 2017; Grottoli et al., 2018; Li et al., 2021), and the abundances of potential pathogens subsequently increase (Littman et al., 2010; Littman et al., 2011; Tout et al., 2015). In addition, coral-associated bacterial communities may contribute to the thermal resilience of the coral host (Littman et al., 2010; Ziegler et al., 2017; Grottoli et al., 2018; Epstein et al., 2019; Li et al., 2021), suggesting that adaptation through changes in bacterial communities may constitute different possible mechanisms for counteracting adverse environmental effects (Ziegler et al., 2017). However, the mechanism of coral-associated bacterial assembly has not been well elucidated (Zhang et al., 2021). Antagonism among bacteria has been considered one of the potential structuring forces in microbial communities (Vetsigian et al., 2011; Perez-Gutierrez et al., 2013; Garcia-Bayona and Comstock, 2018), while it has rarely been investigated in coral holobionts, especially through experimental tests based on pure cultures (Long et al., 2005; Rypien et al., 2010). Additionally, the correlation between antagonism and phenotypical properties of coral-associated bacteria has not been studied.

The competition-relatedness hypothesis proposed by Darwin over 150 years ago (Darwin, 1859) is that phylogenetically closely related species are more likely to compete strongly than distantly associated species due to their functional similarity. This hypothesis has been proven (e.g., in oak, trees, and bacteria) (Cavender-Bares et al., 2004; Kunstler et al., 2016; Russel et al., 2017) or denied (e.g., in vascular plants and green algae) (Cahill et al., 2008; Venail et al., 2014; Alexandrou et al., 2015) according to researches on various subjects. Case and Gilpin (1974) hypothesized a trade-off between interference competition (i.e., antagonism) and resource exploitation efficiency. Russel et al. (2017) further speculated that antagonists were generalists, and there is a trade-off between specializing in exploiting few resources efficiently or growing on many resources and antagonizing the specialists. To test whether the antagonistic interactions occurred among the coral-associated bacteria satisfy these hypotheses, we investigated the antagonisms among 30 bacteria isolated from the tissue of coral *Pocillopora damicornis* and two pathogenic vibrions and the physiological and biochemical characteristics of these isolates at different temperatures. On the basis of these results, we analyzed the correlations between antagonism and phenotypic and phylogenetic characteristics, the trade-off between antagonism and resource exploitation, and the effects of temperature on the antagonistic interaction network. This study will help understand the bacterial interactions in coral holobionts and the assembly of bacterial community under altered environments.

MATERIALS AND METHODS

Antagonistic Interaction Assays

Bacterial strains used in this study (**Table S1**) were mainly isolated from the tissue of the healthy coral *P. damicornis*, with strains *Vibrio mediterranei* DSM 13774 and *Vibrio coralliilyticus* DSM 19607 isolated from the bleached corals *Oculina patagonica* (Kushmaro et al., 1996) and *P. damicornis* (Ben-Haim and Rosenberg, 2002), respectively. Strains DSM 13774 and DSM 19607 were provided by DSMZ (German Collection of Microorganisms and Cell Cultures). Antagonistic interactions were tested on marine agar 2216 (MA; BD; Becton, Dickinson and Company) using Burkholder diffusion assays (Burkholder et al., 1966). Each isolate was streaked from the -80°C glycerol stock on MA, and a single colony was then transferred to 6 ml of marine broth 2216 (MB; Becton, Dickinson and Co.) and shaken at 25°C for 24 h. The OD_{600} was measured for each isolate before starting the assay using spectrophotometer (TU-1810, Persee General Instrument co., LTD, Beijing). Ten milliliters of top lawn bacteria (1 ml of bacterial culture added to 100 ml MA with 0.6% [w/v] agar, gently mixed) was poured on a sterile MA (with 1.5% agar) petri dish plate. The lawn was allowed to cool, and then 10 µl of each producer isolate was spotted onto the agar in petri dish plates (12 cm×12 cm). Control producer spots consisted of 10 µl of marine broth. Plates were incubated at 25°C and 32°C for 48 h, respectively, and then imaged. Antagonism was considered to occur when the semidiameter of the zone of inhibition was at least 0.4 mm greater than the semidiameter of the colony formed by the potential producer. This size of inhibition was chosen because it represents a spatial scale relevant to bacterial interactions (Long and Azam, 2001). The semidiameters of the inhibition halo and colony were measured by digital imaging

software (ImageJ, NIH), and the decimal places were set to 3 in Set Measurements of ImageJ software. We tested the antagonistic interactions of 32 isolates in pairs, and the experiment was 32×32 (1024) times. Each experiment was carried out in 3 replicates. There are fourteen antagonistic interactions with ambiguous results that were re-verified with 3 replicates.

Assessment of Phenotypic Fingerprint

The phenotypic fingerprint of each isolate, including 71 carbon source utilization assays and 23 chemical sensitivity assays (the detailed assays were presented in **Table S2**), was tested by using BIOLOG GEN III MicroPlate (Biolog Inc.). Isolates were cultured for three days on MA at 25°C, a single fresh colony was then picked and dispersed in the modified inoculating fluid A (Biolog Inc.) with increasing salinity to 30‰ for maintaining the osmotic pressure as the salinity of culture medium MA was approximately 30 ‰, and the turbidity of the suspension was 92-95%T. The cell suspension was inoculated into the GENIII MicroPlate (100 µl per well) and incubated at 25°C and 32°C respectively. Color reactions in the microplate wells were determined using the Biolog Microbial Identification System, MicroStation Reader (Biolog Inc., ELx808BLG, USA) with absorbance measured at 590 nm every 24 h for a total duration of 7 days. The "borderline" value was scored as positive if the value of absorbance was higher than that of the negative control.

Phylogenetical and Statistical Analyses

For each interaction pair of coral-associated bacteria, one antagonistic pair was defined by the inhibition value in three statuses: x=1 if isolate A inhibited B, y=1 if B inhibited A or if both x and y were 1, which means reciprocal inhibition. If both x and y were zero, which means no inhibition occurred. A phylogenetic tree was constructed based on 16S rRNA gene sequences using the neighbor-joining method with MEGA X (Kumar et al., 2018), and the best DNA model Tamura-Nei was used. Topologies of the phylogenetic trees were evaluated using the bootstrap method with 1000 resamplings. Pairwise phylogenetic distances were calculated using the Tamura-Nei model with MEGA X (Kumar et al., 2018). Phenotypic dissimilarity was quantified by calculating the Jaccard distance according to the results of the GEN III MicroPlate tests. Correlations between antagonism and the phylogenetic and phenotypic distances were evaluated with logistic regression (*glm*, binomial family). To infer whether the correlation between antagonism and the phenotypic distances was confounded by the correlation between the phylogenetic and phenotypic distances, linear regression for phenotypic distance with phylogenetic distance was performed. The residuals (the variation was not explained by phylogenetic distance) were then used as independent variables in the logistic regressions (Russel et al., 2017). These analyses were performed using R version 4.0.1 (R Core Team, 2020).

Network Analysis

The interaction frequency was calculated as the number of antagonistic interactions observed divided by the number of total possible antagonistic interactions determined by the number of strains tested (Vetsigian et al., 2011). Sender-receiver asymmetry, which represents whether the network is more determined by the sender or receiver strains on average, was evaluated by comparing the variance of the sender and receiver degrees (Vetsigian et al., 2011; Perez-Gutierrez et al., 2013). The sender degree of one isolate means the number of isolates it inhibits, and the receiver degree represents the number of isolates that inhibit the isolate (Perez-Gutierrez et al., 2013). The network diameter, the longest path connecting any two strains (Newman, 2003), was calculated using the network analyzer tool implemented in Cytoscape v3.8.0 (Shannon et al., 2003). Nestedness, a property of the interaction network, was calculated as defined by Bascompte and colleagues (Bascompte et al., 2003) using the algorithm implemented in BINMATNEST (binary matrix nestedness temperature calculator) (Rodriguez-Girones and Santamaria, 2006). Antagonistic interaction networks among coral-associated bacteria were visualized with yFiles, a hierarchical layout option of Cytoscape v3.8.0 (Shannon et al., 2003). The "nodes" represent strains in the networks, and the "edges" depict directed antagonistic interactions. The connectivity of a network is the total number of interactions (Landi et al., 2018), represented by the total number of edges in this study. The width of the "edges" was multiple enlarged based on the intensity value (i.e., the size of the inhibition zone) among the antagonism interactions. The size of the "nodes" was enlarged according to the total number of sender and receiver degrees.

RESULTS

Alterations in Physiological and Biochemical Characteristics at Different Temperatures

Comparing the phenotypic fingerprints of each isolate at 25°C and 32°C, we found that the physiological and biochemical characteristics of most strains varied at different temperatures except *Marimonas* sp. SCSIO 12655 and *Halioglobus* sp. SCSIO 12614 (**Figure 1**). *Microbacterium* sp. SCSIO 12466 showed the highest number of variations with 20 tested characteristics due to increased temperature (**Figure 1** and **Table S1**). In contrast, *Erythrobacter* sp. SCSIO 12564 showed only one varied characteristic (i.e. resistance to minocycline), and the tested phenotypical characteristics of strains *Halioglobus* sp. SCSIO 12614 and *Marimonas* sp. SCSIO 12655 were not affected by the increasing temperature (**Figure 1** and **Table S1**). According to the total number of positive tests, more kinds of sugar and amino acids could be utilized at the higher temperature (**Figure S1**). α-D-glucose and L-glutamic acid were commonly utilized at low temperature (**Figure S1**), while α-D-glucose, L-alanine and L-glutamic acid were commonly utilized at high temperature (**Figure S1**). In addition, the resistance of five antibiotics (Troleandomycin, Rifamycin SV, Minocycline, Lincomycin, Vancomycin) had no change under the evaluated temperature (**Figure S1**).

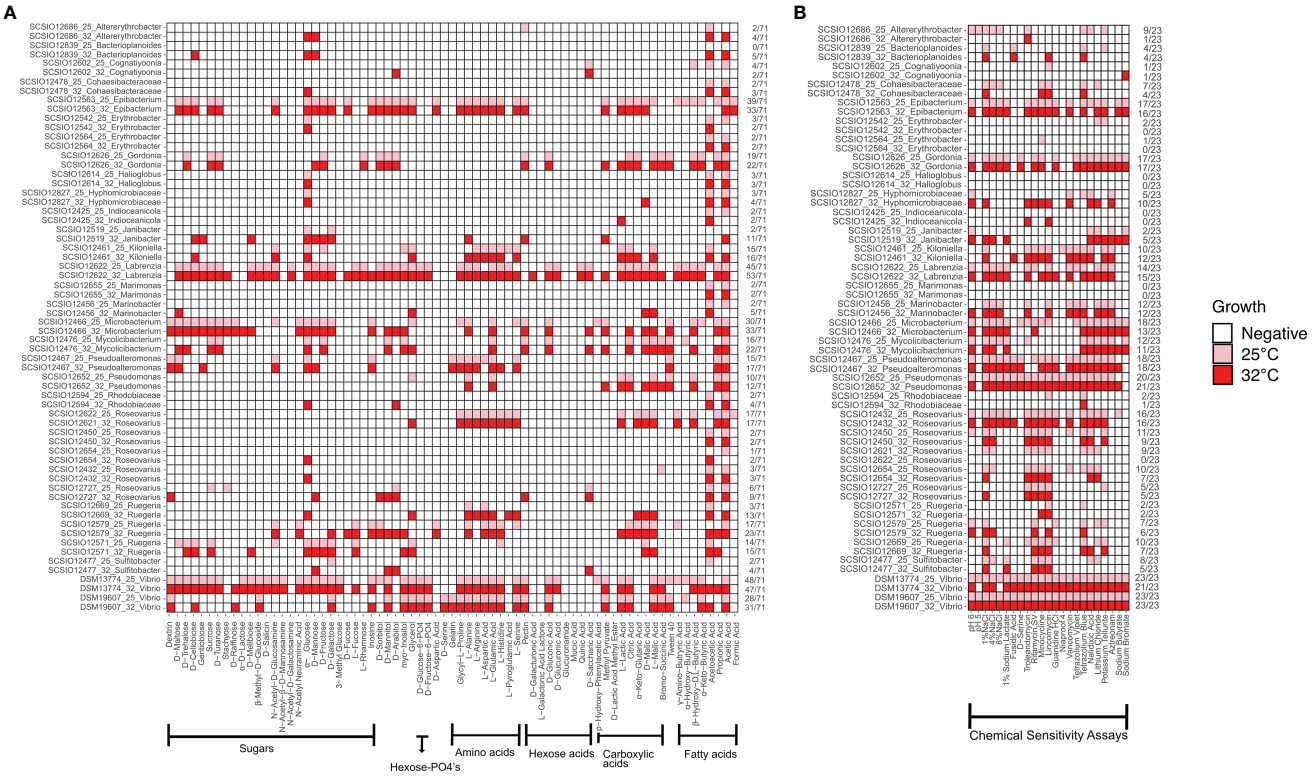

FIGURE 1 | Phenotypic fingerprints of the coral-associated isolates at 25°C and 32°C. The pink (red) square of the heat map indicates that the phenotypic test is positive at 25°C (32°C). The white square of the heat map indicates that the phenotypic test is negative at 25°C and 32°C. Seventy-one carbon sources **(A)** plus 23 chemical sensitivity assays **(B)** were listed on the top of the heatmap. Isolates listed on the left side were ordered by taxa name. The categories of physiological and biochemical characteristics are shown at the bottom. The number of positive tests and the sum for each row were presented on the right side of the heatmap.

Variation of Antagonistic Interactions at Different Temperatures

Twenty out of the 32 isolates inhibited at least one isolate (**Table 1** and **Figure 2**). Ten of the twelve strains belonging to *Rhodobacteraceae* showed antagonistic activities (**Table 1**). Among them, strain SCSIO 12563 presented the strongest antagonistic activity that inhibited 19 (25°C) or 18 (32°C) strains belonging to various taxonomic groups (**Table 1** and **Figure 2**). Seven isolates (*Epibacterium* sp. SCSIO 12563, *Bacterioplanoides* sp. SCSIO 12839, *Ruegeria* sp. SCSIO 12669, *Roseovarius* sp. SCSIO 12450, *Roseovarius* sp. SCSIO 12626, *Mycolicibacterium* sp. SCSIO 12476, *Gordonia* sp. SCSIO 12652) were not inhibited by any isolates at either 25°C or 32°C (**Figure 2**). In addition, strain *Microbacterium* sp. SCSIO 12466 showed autoinhibition (**Figure 2**).

V. mediterranei DSM 13774 was inhibited by strain *Epibacterium* sp. SCSIO 12563 at both 25°C and 32°C (**Tables 1**, **S3** and **Figure 2**). The growth of *V. coralliilyticus* DSM 19607 was inhibited by strain *Marimonas* sp. SCSIO 12655 at 25°C (**Tables 1**, **S4** and **Figure 2**). *V. mediterranei* DSM 13774 did not inhibit any isolate growth, while *V. coralliilyticus* DSM 19607 inhibited *Marinobacter* sp. SCSIO 12456 at both 25°C and 32°C (**Tables 1**, **S5** and **Figure 2**).

The total number of antagonistic interactions at 32°C was approximately 20% higher than that at 25°C (**Figure S2**). Twenty-one antagonistic interactions occurred only at higher temperature (32°C), while 8 occurred only at 25°C (**Figure 2** and **Table S4**). At the level of order or class, the mean number of inhibited isolates increased at higher temperature for producers belonging to *Rhodobacterales*, *Sphingomonadales*, *Rhizobiales*, and *Actinobacteria* (**Figure S3**). At the level of strain, *Ruegeria* sp. SCSIO 12571, *Cognatiyoonia* sp. SCSIO 12602, *Roseovarius* sp. SCSIO 12654, *Marimonas* sp. SCSIO 12655, *Altererythrobacter* sp. SCSIO 12686, and *Janibacter* sp. SCSIO 12652 was able to inhibit more isolates with increasing temperature (**Figure 2**). These results indicated that more antagonistic interactions occurred at the higher temperature. Additionally, among the antagonistic interactions that occurred at both 25 and 32°C (**Tables S3** and **S5**), most of them (62.2%) showed compromised inhibition activities at 32°C, while three strains (*Epibacterium* sp. SCSIO 12563, *Marimonas* sp. SCSIO 12655, and *Microbacterium* sp. SCSIO 12466) showed significantly increased inhibition activities (**Table S5**).

Effects of Elevated Temperature on Antagonistic Interactions Network

We further compared the structures of the antagonistic interaction networks at different temperatures (**Figure 3**), and found that the number of nodes increased by 1, and the number of edges increased by 28% at higher temperature (**Figure 3** and **Table S6**). Additionally,

TABLE 1 | Inhibitory activity of coral-associated bacteria.

Class	Family	Isolate	The number of bacteria inhibited at 25°C/32°C				
			ALF	ACT	GAM	VM	VC
ALF	*Cohaesibacteraceae*	SCSIO 12478					
	Erythrobacteraceae	SCSIO 12686	0/1	1/1	1/0		
		SCSIO 12542	1/1				
		SCSIO 12564	1/1				
	Hyphomicrobiaceae	SCSIO 12827					
	Kiloniellaceae	SCSIO 12461					
	Rhodobacteraceae	SCSIO 12669		1/0			
		SCSIO 12563	15/15	1/1	2/1	1/1	
		SCSIO 12579	1/1				
		SCSIO 12571	2/5	2/2	1/1		
		SCSIO 12477					
		SCSIO 12602	1/3	0/1	1/1		
		SCSIO 12655	0/3	1/2	1/0		1/0
		SCSIO 12450	2/2				
		SCSIO 12654	2/2	0/2	1/0		
		SCSIO 12432	2/2				
		SCSIO 12727					
		SCSIO 12621	0/1				
	Rhodobiaceae	SCSIO 12594	0/1	0/1			
	Rhodospirillaceae	SCSIO 12425	1/0				
	Stappia_f	SCSIO 12622					
ACT	*Intrasporangiaceae*	SCSIO 12519					
	Microbacteriaceae	SCSIO 12466		1/1			
	Mycobacteriaceae	SCSIO 12476					
	Nocardiaceae	SCSIO 12626		0/1			
GAM	*Halieaceae*	SCSIO 12614					
	Marinobacter_f	SCSIO 12456					
	Oceanospirillaceae	SCSIO 12839					
	Pseudoalteromonadaceae	SCSIO 12467	1/0				
	Pseudomonadaceae	SCSIO 12652	1/1	0/1			
	Vibrionaceae	DSM 13774					
	Vibrionaceae	DSM 19607			1/1		

ALF, Alphaproteobacteria; ACT, Actinobacteria_c; GAM, Gammaproteobacteria' VM, Vibrio mediterranei; VC, Vibrio coralliilyticus.

the interaction frequency increased at 32°C (25°C, 0.04 and 32°C, 0.06) (**Table 2**). The value of sender-receiver asymmetry was negative at 25°C (-0.22) and 32°C (-0.15), indicating that the interaction matrix was sender-determined and temperature independent (**Table 2**). The values of nestedness, a vital descriptor of ecological network architecture (Landi et al., 2018), showed that the antagonistic network was significantly nested at both temperatures (**Table 2**; $P < 0.00001$ both at 25°C and 32°C). To test the relation between sender degree and receiver degree at different temperatures, we depicted their antagonistic interaction using a heatmap (**Figure S4**). The nested heatmap results showed that the antagonists were highly resistant, while the inhibited strains were unlikely to antagonize other strains (**Figure S4**).

The Correlation Between Antagonism Probability and Phylogenetic and Phenotypic Distance

Among the 496 antagonistic test pairs (pairs of tested strains), we found that the antagonistic probability increased with decreasing 16S rRNA gene phylogenetic distance (**Figures 4A, B**). Furthermore, the correlation between antagonistic probability and phylogenetic distance was stronger at higher temperature (25°C, $P = 0.028$, pseudo-$R^2 = 0.021$; 32°C, $P = 0.020$, pseudo-$R^2 = 0.021$; logistic regression used throughout unless otherwise noted) (**Figures 4A, B**).

To further assess whether the correlation between antagonism and phylogeny was driven by the metabolic niche space of individual isolates, the correlation between antagonism probability and phenotypic distance (calculated on the basis of the dissimilarity of the phenotypic fingerprints) was evaluated. There was no correlation between antagonism and phenotypic distances (25°C, $P = 0.885$; 32°C, $P = 0.891$) (**Figures 4C, D**). As the phylogenetic distance correlated with the phenotypic distance at both 25°C and 32°C (25°C, $P < 0.01$; 32°C, $P < 0.05$) (**Figure S5**), we also analyzed the correlation between antagonism probability and phenotypic distance by using the residuals from the linear regression for phenotypic distance with the phylogenetic distances. The results showed that antagonism did not correlate with phenotypic distances at either 25°C or 32°C (25°C, $P = 0.510$; 32°C, $P = 0.908$) (**Figure S6**).

The Trade-Off Between Antagonism and Resource Exploitation at Different Temperatures

In order to investigate the trade-off between antagonism and resource exploitation, we tested whether the antagonist had a

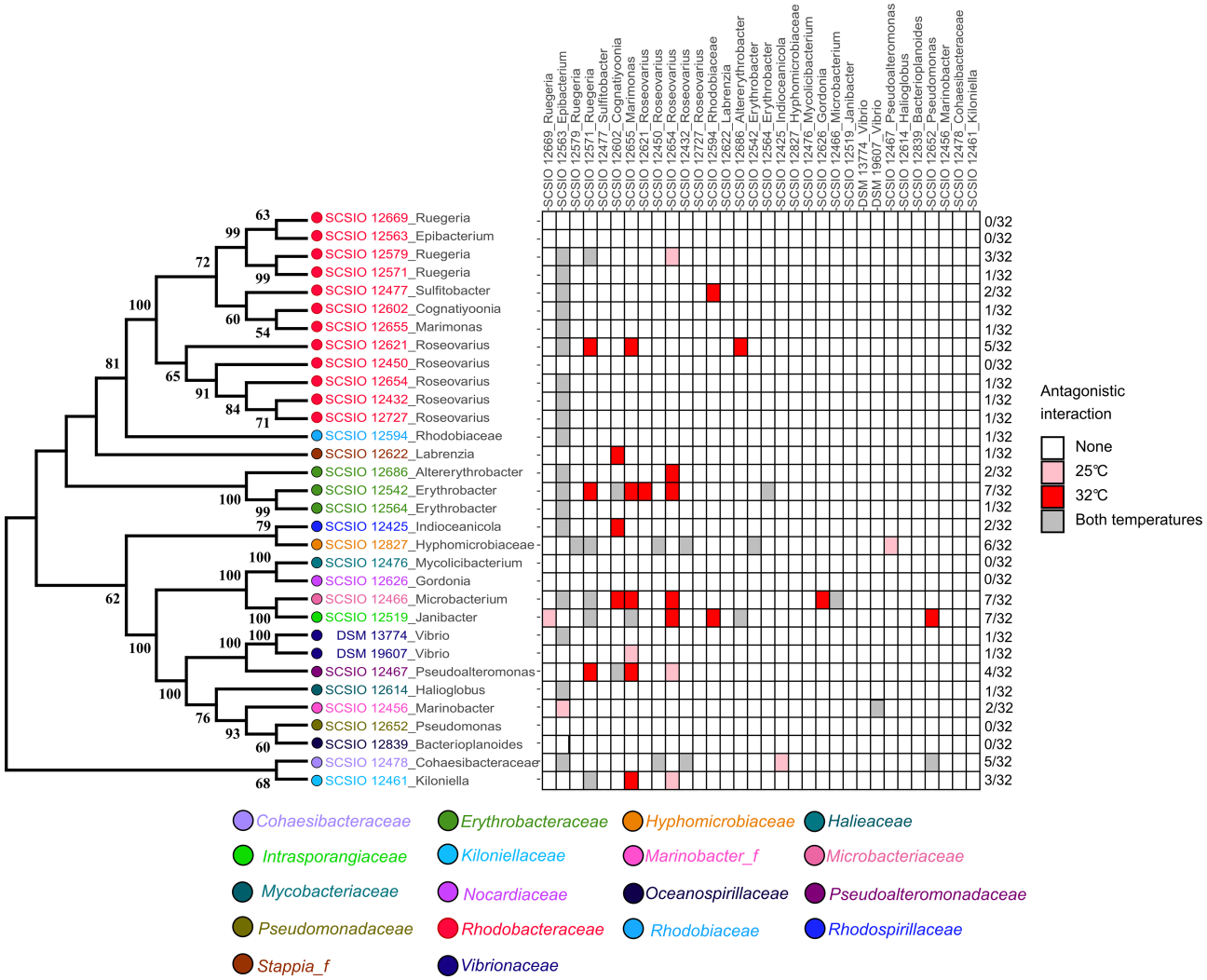

FIGURE 2 | Heat map of the antagonistic interactions among the coral-associated bacteria integrated with a phylogenetic tree. Isolates listed on the top of the heatmap are producers, and those listed on the left side are inhibited. Colors of the strains numbers represent the taxonomic information at the family level. The number of antagonistic interactions and the sum for each row were presented on the right side of the heatmap. Pink and red blocks indicate antagonism at 25°C and 32°C, respectively. The gray block represents antagonism at both temperatures.

wider metabolic niche space (growth on the 71 carbon sources of the Biolog GENIII MicroPlate) for each antagonistic interaction, and compared it to the non-antagonistic interactions. We found that the antagonists tended to have a wider metabolic niche space, i.e., grew on more carbon sources than the antagonized strains at 25°C (Fisher's exact test, odds ratio = 2.064, $P = 0.028$), but not at 32°C (odds ratio = 0.825, $P = 0.498$) (**Figure 5**).

DISCUSSION

It is generally recognized that bacterial communities associated with corals alter under heat stress (Ziegler et al., 2017; Grottoli et al., 2018; Li et al., 2021), while the biotic interactions and their role in community assembly have not been elucidated. Here, through investigating the antagonism among coral-associated bacteria under different temperatures, we uncovered the alterations of antagonistic interactions due to the increased temperature and the correlation with genetic relationships and metabolic capabilities and hypothesized an association between bacterial antagonism interactions and community assembly in the coral holobiont.

Temperature Affects Antagonistic Interactions of Coral-Associated Bacteria

The results obtained in this study and reported previously indicated that antagonism was a common phenomenon in the coral-associated bacterial community, and temperature distinctly altered the breadth and intensity of antagonistic interactions (Rypien et al., 2010; Aguirre-von-Wobeser et al., 2014; Tang

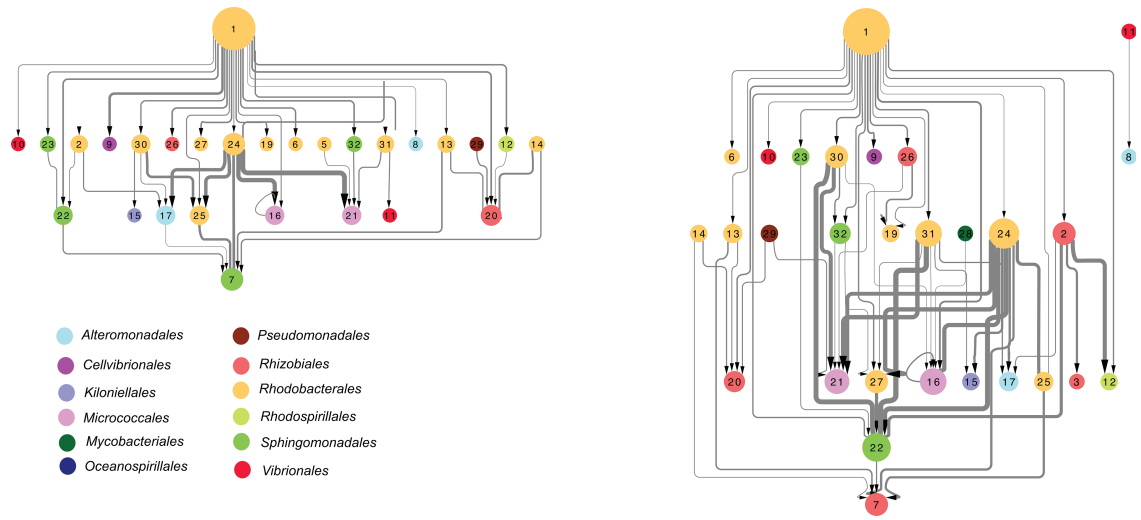

FIGURE 3 | The antagonistic interaction network included antagonistic pairs and intensity at 25°C **(A)** and 32°C **(B)**. The "edges" depict directed inhibitory interactions, and the "nodes" represent strains. The size of the "edges" shows the intensity of the interactions. The size of the "nodes" represents the total number of degrees, including sender degrees and receiver degrees. The code of each isolate was included in **Table S1**. Colors of the nodes represent the taxonomic information of isolates at the order level.

et al., 2019). The intensity of most antagonistic interactions decreased at higher temperature, which is consistent with previous results (Rypien et al., 2010). In contrast to the findings of Rypien et al. (2010), more antagonistic interactions occurred at higher temperature in this study, suggesting that the breadth of antagonism increased with increasing temperature. Previous studies showed that 6% or 12% of tested isolates were able to inhibit *V. mediterranei* (Nissimov et al., 2009; Rypien et al., 2010), and 3% or 10% were able to inhibit *V. coralliilyticus* (Rypien et al., 2010; Miura et al., 2019; Tang et al., 2019). Results of this study showed that strain *Epibacterium* sp. SCSIO 12563 inhibited the growth of *V. mediterranei* DSM 13774, and *Marimonas* sp. SCSIO 12655 inhibited *V. coralliilyticus* DSM 19607. Those two isolates (SCSIO 12563 and SCSIO 12655) were affiliated to different species in comparison to the antagonists observed in the previous studies (Nissimov et al., 2009; Rypien et al., 2010; Miura et al., 2019; Tang et al., 2019). These results suggest that these two opportunistic vibrion might face a challenging growth environment due to antagonistic interactions in the coral holobiont. Moreover, the growth of *V. coralliilyticus* DSM 19607 was only inhibited by strain *Marimonas* sp. SCSIO 12655 at 25°C, while the inhibition was removed at 32°C. The removal of inhibition might contribute to the enrichment of vibrion at higher temperature (Bourne et al., 2008; Frydenborg et al., 2014; Tout et al., 2015; Rajeev et al., 2021) and allow compromising the health of coral host (Gavish et al., 2021).

The antagonistic networks of coral-associated bacteria were sender-determined both at 25 and 32°C, which means that the structures of the networks were more influenced by antagonists than sensitive strains. Furthermore, our results showed that the antagonistic interaction network was significantly nested, with nestedness scores of 0.984 (25°C) and 0.969 (32°C). The highly nested and sender-determined network suggests that the antagonistic interaction network of the coral-associated bacteria community is more determined by antagonists. The nested antagonistic interaction networks were also respectively observed among *Gammaproteobacteria* in the oligotrophic water environment (Aguirre-von-Wobeser et al., 2014) and *Carnobacterium maltaromaticum* strains isolated from

TABLE 2 | Antagonism network parameters under different temperatures.

Parameter	Observed Value	
	25°C	32°C
The interaction frequency	0.04	0.06
Sender-receiver asymmetry	-0.22	-0.15
The network diameter	5.0	4.0
Nestedness	0.984	0.969

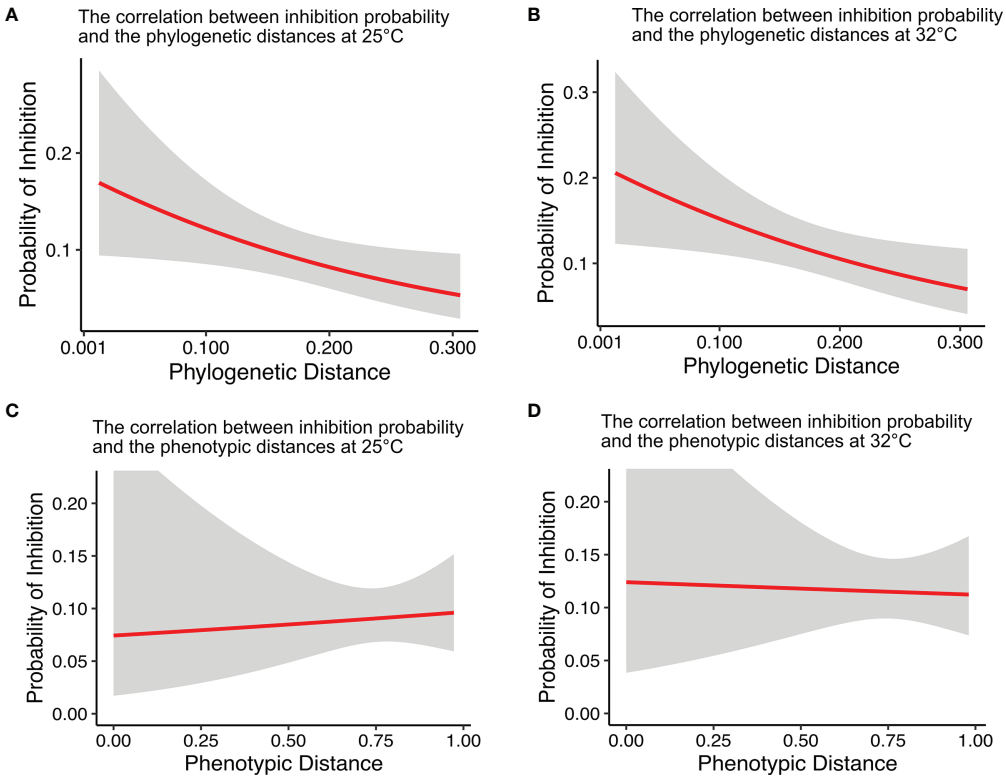

FIGURE 4 | The correlation between inhibition probability and the phylogenetic **(A, B)** and phenotypic distances **(C, D)** at 25°C **(A, C)** and 32°C **(B, D)**. The probability of inhibition increased with decreasing phylogenetic distance. The red line is a logistic regression, and the gray shaded area denotes the 95% confidence interval (**A**, 25°C, $P = 0.0284$, pseudo-$R^2 = 0.021$; **B**, 32°C, $P = 0.020$; pseudo-$R^2 = 0.021$; **C**, 25°C, $P = 0.891$; **D**, 32°C, $P = 0.775$, n = 496).

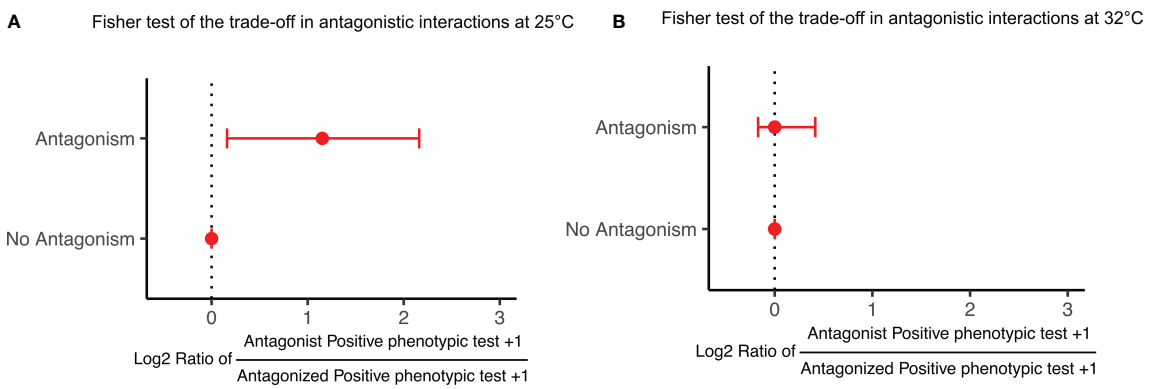

FIGURE 5 | Fisher test of the trade-off in antagonistic interactions at 25°C **(A)** and 32°C **(B)**. The log2 ratios between the number of carbon source utilized by the antagonists compared with the antagonized are larger than 0 when antagonism was observed ($P = 0.052$, n = 44), but not different from 0 for the non-antagonistic interactions ($P = 0.999$, n = 948) at 25°C **(A)**; however, no differences from 0 for all interactions at 32°C **(B)** (antagonism: $P = 0.881$, n = 57; no antagonism: $P = 0.981$, n = 935). One autoinhibition pair was removed. P values are one-tailed tests of whether medians are larger than 0 estimated from 1,000 bootstrap realizations. Points are medians, and error bars are 90% bootstrapped confidence limits of the medians (equivalent to a 5% one-tailed test of the median).

diverse habitats (e.g., dairy products, diseased fish, and meat products) (Ramia et al., 2020). These results suggested that the nested network is a common feature among bacteria antagonism interactions.

Coral-associated bacterial communities are known to alter in response to increasing seawater temperature (Tout et al., 2015; McDevitt-Irwin et al., 2017; Grottoli et al., 2018; Pootakham et al., 2018; Li et al., 2021). In this study, the antagonistic

interaction network was found to be more hierarchical and complex at 32°C than 25°C (**Figure 3**). The study of Welsh et al. (2016) showed that heat stress decreased the complexity (network edges) of the coral mucus associated bacterial network, and the number of mutual exclusion was decreased in the network at the higher temperature (29-30°C). We should mentioned that the strains used in this study were isolated from coral tissue, while Welsh et al. (2016) investigated the network of bacteria associated with corals mucus. The microbial communities in different compartments of coral holobiont might show distinct networks. Even so, the inconsistent results obtained in this and previous studies highlight the necessity of interpretation of the interactions among coral-associated bacteria on the basis of both wet lab and dry lab results. The interactions among culturable strains could be experimentally investigated, while these results may not be enough for comprehensively understanding the interactions in the whole coral-associated bacterial community. On the other side, although the co-occurrence network constructed based on the relative abundances acquired through culture-independent analyses provides information for the whole bacterial community, it needs more cautions in interpreting the interactions presented in the co-occurrence network (Blanchet et al., 2020).

Competition (including antagonism) is considered one of the factors in community assembly (Perez-Gutierrez et al., 2013; Rocha et al., 2015; Zapien-Campos et al., 2015; Garcia-Bayona and Comstock, 2018). We hypothesize accordingly that the alteration of antagonistic interactions due to increased temperature is one of the processes that governs the assembly of coral-associated bacterial community, and encourage verifying it in combination with studies on natural communities.

Antagonism Correlates With Phylogenetic Rather Than Phenotypic Distance

Our results showed that closely related bacteria have a higher probability of antagonism than more distantly related bacteria, consistent with previous reports (Russel et al., 2017; Gonzalo et al., 2020). Moreover, we found that the correlation between antagonism and phylogenetic distance was stronger at higher temperature (32°C), implying that phylogenetically similar bacteria are likely to compete more fiercely under heat stress in coral holobionts. In contrast to the results of Russel et al. (2017), antagonism did not significantly correlate with phenotypic distances among coral-associated bacteria in this study, while this was similar to the finding in isolates of *Pseudomonas aeruginosa* from household drains (Mojesky and Remold, 2020). In the previous studies of both Russel et al. (2017) and Mojesky and Remold (2020), the utilization of 31 carbon sources were tested. These results suggest differential associations between antagonism and physiological and biochemical properties occur in distinct habitats, and phylogenetic similarity might predict the inhibition among bacteria associated with corals. Considering that the limitation in the range of phenotypic characteristics that could be screened using BIOLOG GEN III MicroPlate, expanding the tested index is necessary in the future.

Temperature Affects the Trade-Off Strategy

We investigated whether the antagonizing strains are generalists growing on many resources, and found that antagonists were indeed generalists at 25°C (**Figure 5A**), growing on ~20-130% more carbon sources than the inhibited strains. This result supports the hypothesis, i.e., the antagonist is also generalist, proposed by Russel et al. (2017). Meanwhile, the findings obtained at 32°C did not support this hypothesis, as the numbers of carbon sources utilized by antagonizing and antagonized strains were similar (**Figure 5B**). Additionally, more antagonistic interactions occurred due to the increased temperature (**Figure S2** and **Table S4**). These results suggest that temperature significantly affects the trade-off between antagonism and resource exploitation in the antagonistic interactions of coral-associated bacteria. We further speculated that the shift of trade-off is an adaptation to nutrient reduction in bleached coral under thermal stress (Morris et al., 2019; Rädecker et al., 2021).

CONCLUSION

In this study, we investigated phenotypic fingerprints and antagonistic interactions of 32 coral-associated bacteria at different temperatures. We found that most of the tested strains showed alterations in the phenotypic fingerprints. Additionally, the elevated temperature increased the breadth of antagonism but decreased antagonism intensity among coral-associated bacteria. The complexity of the antagonistic network increased at the higher temperature. Our results showed that antagonism between coral-associated bacteria correlates with their genetic relationship rather than metabolic similarity. Moreover, increased temperature shifted the trade-off between antagonism and resource exploitation in the antagonistic interactions of coral-associated bacteria. The results of this study will be helpful in understanding of coral-associated bacterial interactions, and imply that the antagonistic interactions are involved in the assembly of coral-associated bacterial community.

DATA AVAILABILITY STATEMENT

The datasets presented in this study can be found in online repositories. The names of the repository/repositories and accession number(s) can be found in the article/**Supplementary Material**.

AUTHOR CONTRIBUTIONS

AG, JL, HJ, and QL performed the analyses. JL and SZ conceived this study. AG, JL, LW, LR, and SZ drafted the

manuscript, and all authors commented on the manuscript and made suggestions.

FUNDING

The work was supported by the National Natural Science Foundation of China (42122045 and 41890853), K. C. Wong Education Foundation (GJTD-2020-12), Key Science and Technology Project of Hainan Province (ZDKJ202018), and Institution of South China Sea Ecology and Environmental Engineering, Chinese Academy of Sciences (ISEE2021ZD03).

ACKNOWLEDGMENTS

We thank Yiyang Zou and Yicong Zheng for their assistance in the experiment.

SUPPLEMENTARY MATERIAL

The Supplementary Material for this article can be found online at: https://www.frontiersin.org/articles/10.3389/fmars.2022.840384/full#supplementary-material

REFERENCES

Aguirre-von-Wobeser, E., Soberon-Chavez, G., Eguiarte, L. E., Ponce-Soto, G. Y., Vazquez-Rosas-Landa, M., and Souza, V. (2014). Two-Role Model of an Interaction Network of Free-Living Gamma-Proteobacteria From an Oligotrophic Environment. *Environ. Microbiol.* 16 (5), 1366–1377. doi: 10.1111/1462-2920.12305

Ainsworth, T. D., and Hoegh-Guldberg, O. (2009). Bacterial Communities Closely Associated With Coral Tissues Vary Under Experimental and Natural Reef Conditions and Thermal Stress. *Aquat. Biol.* 4 (3), 289–296. doi: 10.3354/ab00102

Alexandrou, M. A., Cardinale, B. J., Hall, J. D., Delwiche, C. F., Fritschie, K., Narwani, A., et al. (2015). Evolutionary Relatedness Does Not Predict Competition and Co-Occurrence in Natural or Experimental Communities of Green Algae. *Proc. R. Soc B-Biol. Sci.* 282, 20141745. doi: 10.1098/rspb.2014.1745

Bascompte, J., Jordano, P., Melian, C. J., and Olesen, J. M. (2003). The Nested Assembly of Plant-Animal Mutualistic Networks. *Proc. Natl. Acad. Sci. U. S. A.* 100 (16), 9383–9387. doi: 10.1073/pnas.1633576100

Ben-Haim, Y., and Rosenberg, E. (2002). A Novel Vibrio Sp Pathogen of the Coral Pocillopora Damicornis. *Mar. Biol.* 141 (1), 47–55. doi: 10.1007/s00227-002-0797-6

Blanchet, F. G., Cazelles, K., and Gravel, D. (2020). Co-Occurrence Is Not Evidence of Ecological Interactions. *Ecol. Lett.* 23 (7), 1050–1063. doi: 10.1111/ele.13525

Bourne, D., Iida, Y., Uthicke, S., and Smith-Keune, C. (2008). Changes in Coral-Associated Microbial Communities During a Bleaching Event. *ISME J.* 2 (4), 350–363. doi: 10.1038/ismej.2007.112

Burkholder, P. R., Pfister, R. M., and Leitz, F. H. (1966). Production of a Pyrrole Antibiotic by a Marine Bacterium. *Appl. Microbiol.* 14 (4), 649–653. doi: 10.1128/aem.14.4.649-653.1966

Cahill, J. F. Jr., Kembel, S. W., Lamb, E. G., and Keddy, P. A. (2008). Does Phylogenetic Relatedness Influence the Strength of Competition Among Vascular Plants? *Perspect. Plant Ecol.* 10 (1), 41–50. doi: 10.1016/j.ppees.2007.10.001

Case, T. J., and Gilpin, M. E. (1974). Interference Competition and Niche Theory. *Proc. Natl. Acad. Sci. U. S. A.* 71 (8), 3073–3077. doi: 10.1073/pnas.71.8.3073

Cavender-Bares, J., Ackerly, D. D., Baum, D. A., and Bazzaz, F. A. (2004). Phylogenetic Overdispersion in Floridian Oak Communities. *Am. Nat.* 163, 823–843, 6. doi: 10.1086/386375

Darwin, C. (1859). *On the Origin of Species by Means of Natural Selection* (London: John Murray).

Epstein, H. E., Torda, G., and van Oppen, M. J. H. (2019). Relative Stability of the Pocillopora Acuta Microbiome Throughout a Thermal Stress Event. *Coral Reefs.* 38, 373–386. doi: 10.1007/s00338-019-01783-y

Frydenborg, B. R., Krediet, C. J., Teplitski, M., and Ritchie, K. B. (2014). Temperature-Dependent Inhibition of Opportunistic Vibrio Pathogens by Native Coral Commensal Bacteria. *Microb. Ecol.* 67, 392–401. doi: 10.1007/s00248-013-0334-9

Garcia-Bayona, L., and Comstock, L. E. (2018). Bacterial Antagonism in Host-Associated Microbial Communities. *Science* 361, aat2456. doi: 10.1126/science.aat2456

Gavish, A. R., Shapiro, O. H., Kramarsky-Winter, E., and Vardi, A. (2021). Microscale Tracking of Coral-Vibrio Interactions. *ISME Commun.* 1, 1–18. doi: 10.1038/s43705-021-00016-0

Glasl, B., Herndl, G. J., and Frade, P. R. (2016). The Microbiome of Coral Surface Mucus has a Key Role in Mediating Holobiont Health and Survival Upon Disturbance. *ISME J.* 10 (9), 2280–2292. doi: 10.1038/ismej.2016.9

Gonzalo, M., Deveau, A., and Aigle, B. (2020). Inhibitions Dominate But Stimulations and Growth Rescues Are Not Rare Among Bacterial Isolates From Grains of Forest Soil. *Microb. Ecol.* 80 (4), 872–884. doi: 10.1007/s00248-020-01579-6

Grottoli, A. G., Martins, P. D., Wilkins, M. J., Johnston, M. D., Warner, M. E., Cai, W.-J., et al. (2018). Coral Physiology and Microbiome Dynamics Under Combined Warming and Ocean Acidification. *PloS One* 13, 0191156. doi: 10.1371/journal.pone.0191156

Hughes, T. P., Anderson, K. D., Connolly, S. R., Heron, S. F., Kerry, J. T., Lough, J. M., et al. (2018). Spatial and Temporal Patterns of Mass Bleaching of Corals in the Anthropocene. *Science* 359 (6371), 80–83. doi: 10.1126/science.aan8048

Hughes, T. P., Kerry, J. T., Alvarez-Noriega, M., Alvarez-Romero, J. G., Anderson, K. D., Baird, A. H., et al. (2017). Global Warming and Recurrent Mass Bleaching of Corals. *Nature* 543, 373–377. doi: 10.1038/nature21707

Jessen, C., Lizcano, J. F. V., Bayer, T., Roder, C., Aranda, M., Wild, C., et al. (2013). *In-Situ* Effects of Eutrophication and Overfishing on Physiology and Bacterial Diversity of the Red Sea Coral Acropora Hemprichii. *PloS One* 8, e60291. doi: 10.1371/journal.pone.0062091

Kumar, S., Stecher, G., Li, M., Knyaz, C., and Tamura, K. (2018). MEGA X: Molecular Evolutionary Genetics Analysis Across Computing Platforms. *Mol. Biol. Evol.* 35 (6), 1547–1549. doi: 10.1093/molbev/msy096

Kunstler, G., Falster, D., Coomes, D. A., Hui, F., Kooyman, R. M., Laughlin, D. C., et al. (2016). Plant Functional Traits Have Globally Consistent Effects on Competition. *Nature* 529, 204–207. doi: 10.1038/nature16476

Kushmaro, A., Loya, Y., Fine, M., and Rosenberg, E. (1996). Bacterial Infection and Coral Bleaching. *Nature* 380, 396–396. doi: 10.1038/380396a0

Landi, P., Minoarivelo, H. O., Brannstrom, A., Hui, C., and Dieckmann, U. (2018). Complexity and Stability of Ecological Networks: A Review of the Theory. *Popul. Ecol.* 60 (4), 319–345. doi: 10.1007/s10144-018-0628-3

Lee, S. T. M., Davy, S. K., Tang, S.-L., Fan, T.-Y., and Kench, P. S. (2015). Successive Shifts in the Microbial Community of the Surface Mucus Layer and Tissues of the Coral Acropora Muricata Under Thermal Stress. *FEMS Microbiol. Ecol.* 91, fiv142. doi: 10.1093/femsec/fiv142

Li, J., Long, L. J., Zou, Y. Y., and Zhang, S. (2021). Microbial Community and Transcriptional Responses to Increased Temperatures in Coral Pocillopora Damicornis Holobiont. *Environ. Microbiol.* 23 (2), 826–843. doi: 10.1111/1462-2920.15168

Littman, R. A., Bourne, D. G., and Willis, B. L. (2010). Responses of Coral-Associated Bacterial Communities to Heat Stress Differ With Symbiodinium Type on the Same Coral Host. *Mol. Ecol.* 19 (9), 1978–1990. doi: 10.1111/j.1365-294X.2010.04620.x

Littman, R., Willis, B. L., and Bourne, D. G. (2011). Metagenomic Analysis of the Coral Holobiont During a Natural Bleaching Event on the Great Barrier Reef. *Environ. Microbiol. Rep.* 3 (6), 651–660. doi: 10.1111/j.1758-2229.2010.00234.x

Long, R. A., and Azam, F. (2001). Microscale Patchiness of Bacterioplankton Assemblage Richness in Seawater. *Aquat. Microb. Ecol.* 26 (2), 103–113. doi: 10.3354/ame026103

Long, R. A., Rowley, D. C., Zamora, E., Liu, J. Y., Bartlett, D. H., and Azam, F. (2005). Antagonistic Interactions Among Marine Bacteria Impede the Proliferation of Vibrio Cholerae. *Appl. Environ. Microbiol.* 71 (12), 8531–8536. doi: 10.1128/aem.71.12.8531-8536.2005

McDevitt-Irwin, J. M., Baum, J. K., Garren, M., and Vega Thurber, R. L. (2017). Responses of Coral-Associated Bacterial Communities to Local and Global Stressors. *Fron. Mar. Sci.* 4, 262. doi: 10.3389/fmars.2017.00262

Meron, D., Rodolfo-Metalpa, R., Cunning, R., Baker, A. C., Fine, M., and Banin, E. (2012). Changes in Coral Microbial Communities in Response to a Natural pH Gradient. *ISME J.* 6 (9), 1775–1785. doi: 10.1038/ismej.2012.19

Miura, N., Motone, K., Takagi, T., Aburaya, S., Watanabe, S., Aoki, W., et al. (2019). Ruegeria Sp. Strains Isolated From the Reef-Building Coral Galaxea Fascicularis Inhibit Growth of the Temperature-Dependent Pathogen Vibrio Coralliilyticus. *Mar. Biotechnol.* 21 (1), 1–8. doi: 10.1007/s10126-018-9853-1

Mojesky, A. A., and Remold, S. K. (2020). Spatial Structure Maintains Diversity of Pyocin Inhibition in Household Pseudomonas Aeruginosa. *Proc. R. Soc B-Biol. Sci.* 287, 20201706. doi: 10.1098/rspb.2020.1706

Morris, L. A., Voolstra, C. R., Quigley, K. M., Bourne, D. G., and Bay, L. K. (2019). Nutrient Availability and Metabolism Affect the Stability of Coral–Symbiodiniaceae Symbioses. *Trends Microbiol.* 27 (8), 678–689. doi: 10.1016/j.tim.2019.03.004

Negri, A. P., Webster, N. S., Hill, R. T., and Heyward, A. J. (2001). Metamorphosis of Broadcast Spawning Corals in Response to Bacteria Isolated From Crustose Algae. *Mar. Ecol. Prog. Ser.* 223, 121–131. doi: 10.3354/meps223121

Newman, M. E. J. (2003). The Structure and Function of Complex Networks. *SIAM Rev.* 45 (2), 167–256. doi: 10.1137/s003614450342480

Nissimov, J., Rosenberg, E., and Munn, C. B. (2009). Antimicrobial Properties of Resident Coral Mucus Bacteria of Oculina Patagonica. *FEMS Microbiol. Lett.* 292 (2), 210–215. doi: 10.1111/j.1574-6968.2009.01490.x

Olson, N. D., Ainsworth, T. D., Gates, R. D., and Takabayashi, M. (2009). Diazotrophic Bacteria Associated With Hawaiian Montipora Corals: Diversity and Abundance in Correlation With Symbiotic Dinoflagellates. *J. Exp. Mar. Biol. Ecol.* 371 (2), 140–146. doi: 10.1016/j.jembe.2009.01.012

Perez-Gutierrez, R. A., Lopez-Ramirez, V., Islas, A., Alcaraz, L. D., Hernandez-Gonzalez, I., Olivera, B. C., et al. (2013). Antagonism Influences Assembly of a Bacillus Guild in a Local Community and Is Depicted as a Food-Chain Network. *ISME J.* 7 (3), 487–497. doi: 10.1038/ismej.2012.119

Pootakham, W., Mhuantong, W., Putchim, L., Yoocha, T., Sonthirod, C., Kongkachana, W., et al. (2018). Dynamics of Coral-Associated Microbiomes During a Thermal Bleaching Event. *MicrobiologyOpen* 7 (5). doi: 10.1002/mbo3.604

Rädecker, N., Pogoreutz, C., Gegner, H. M., Cárdenas, A., Roth, F., Bougoure, J., et al. (2021). Heat Stress Destabilizes Symbiotic Nutrient Cycling in Corals. *Proc. Natl. Acad. Sci. U. S. A.* 118 (5), e2022653118. doi: 10.1073/pnas.2022653118

Rajeev, M., Sushmitha, T. J., Aravindraja, C., Toleti, S. R., and Pandian, S. K. (2021). Thermal Discharge-Induced Seawater Warming Alters Richness, Community Composition and Interactions of Bacterioplankton Assemblages in a Coastal Ecosystem. *Sci. Rep.* 11 (1), 17341. doi: 10.1038/s41598-021-96969-2

Ramia, N. E., Mangavel, C., Gaiani, C., Muller-Gueudin, A., Taha, S., Revol-Junelles, A.-M., et al. (2020). Nested Structure of Intraspecific Competition Network in Carnobacterium Maltaromaticum. *Sci. Rep.* 10 (11), 1–9. doi: 10.1038/s41598-020-63844-5

R Core Team (2020). *R: A Language and Environment for Statistical Computing* (Vienna, Austria: R Foundation for Statistical Computing).

Rocha, J., Pinto, M. P., Boubli, J. P., and Grelle, C. E. V. (2015). The Role of Competition in Structuring Primate Communities Under Different Productivity Regimes in the Amazon. *PloS One* 10 (12), e0145699–e0145699. doi: 10.1371/journal.pone.0145699

Rodriguez-Girones, M. A., and Santamaria, L. (2006). A New Algorithm to Calculate the Nestedness Temperature of Presence-Absence Matrices. *J. Biogeogr.* 33 (5), 924–935. doi: 10.1111/j.1365-2699.2006.01444.x

Rohwer, F., and Kelley, S. (2004). "Culture-Independent Analyses of Coral-Associated Microbes," in *Coral Health and Disease*. Eds. E. Rosenberg and Y. Loya (Berlin, Heidelberg: Springer).

Rohwer, F., Seguritan, V., Azam, F., and Knowlton, N. (2002). Diversity and Distribution of Coral-Associated Bacteria. *Mar. Ecol.: Prog. Ser.* 243, 1–10. doi: 10.3354/meps243001

Russel, J., Roder, H. L., Madsen, J. S., Burmolle, M., and Sorensen, S. J. (2017). Antagonism Correlates With Metabolic Similarity in Diverse Bacteria. *Proc. Natl. Acad. Sci. U. S. A.* 114 (40), 10684–10688. doi: 10.1073/pnas.1706016114

Rypien, K. L., Ward, J. R., and Azam, F. (2010). Antagonistic Interactions Among Coral-Associated Bacteria. *Environ. Microbiol.* 12 (1), 28–39. doi: 10.1111/j.1462-2920.2009.02027.x

Shannon, P., Markiel, A., Ozier, O., Baliga, N. S., Wang, J. T., Ramage, D., et al. (2003). Cytoscape: A Software Environment for Integrated Models of Biomolecular Interaction Networks. *Genome Res.* 13 (11), 2498–2504. doi: 10.1101/gr.1239303

Sully, S., Burkepile, D. E., Donovan, M. K., Hodgson, G., and van Woesik, R. (2019). A Global Analysis of Coral Bleaching Over the Past Two Decades. *Nat. Commun.* 10 (1), 1264. doi: 10.1038/s41467-019-09238-2

Tang, K., Zhan, W., Zhou, Y., Xu, T., Chen, X., Wang, W., et al. (2019). Antagonism Between Coral Pathogen Vibrio Coralliilyticus and Other Bacteria in the Gastric Cavity of Scleractinian Coral Galaxea Fascicularis. *Sci. China Earth Sci.* 63 (1), 157–166. doi: 10.1007/s11430-019-9388-3

Tebben, J., Tapiolas, D. M., Motti, C. A., Abrego, D., Negri, A. P., Blackall, L. L., et al. (2011). Induction of Larval Metamorphosis of the Coral Acropora Millepora by Tetrabromopyrrole Isolated From a Pseudoalteromonas Bacterium. *PloS One* 6 (4), e19082. doi: 10.1371/journal.pone.0019082

Tout, J., Siboni, N., Messer, L. F., Garren, M., Stocker, R., Webster, N. S., et al. (2015). Increased Seawater Temperature Increases the Abundance and Alters the Structure of Natural Vibrio Populations Associated With the Coral Pocillopora Damicomis. *Front. Microbiol.* 6. doi: 10.3389/fmicb.2015.00432

van Oppen, M. J. H., and Blackall, L. L. (2019). Coral Microbiome Dynamics, Functions and Design in a Changing World. *Nat. Rev. Microbiol.* 17 (9), 557–567. doi: 10.1038/s41579-019-0223-4

Venail, P. A., Narwani, A., Fritschie, K., Alexandrou, M. A., Oakley, T. H., and Cardinale, B. J. (2014). The Influence of Phylogenetic Relatedness on Species Interactions Among Freshwater Green Algae in a Mesocosm Experiment. *J. Ecol.* 102 (5), 1288–1299. doi: 10.1111/1365-2745.12271

Vetsigian, K., Jajoo, R., and Kishony, R. (2011). Structure and Evolution of Streptomyces Interaction Networks in Soil and In Silico. *PloS Biol.* 9 (10), e1001184. doi: 10.1371/journal.pbio.1001184

Welsh, R. M., Zaneveld, J. R., Rosales, S. M., Payet, J. P., Burkepile, D. E., and Thurber, R. V. (2016). Bacterial Predation in a Marine Host-Associated Microbiome. *ISME J.* 10 (6), 1540–1544. doi: 10.1038/ismej.2015.219

Zapien-Campos, R., Olmedo-Alvarez, G., and Santillan, M. (2015). Antagonistic Interactions are Sufficient to Explain Self-Assemblage of Bacterial Communities in a Homogeneous Environment: A Computational Modeling Approach. *Front. Microbiol.* 6. doi: 10.3389/fmicr.2015.00489

Zhang, J., Hu, A., Sun, Y., Yang, Q., Dong, J., Long, L., et al. (2021). Dispersal Limitation Expands the Diversity of Coral Microbiome Metacommunity in the South China Sea. *Front. Mar. Sci.* 8. doi: 10.3389/fmars.2021.658708

Ziegler, M., Seneca, F. O., Yum, L. K., Palumbi, S. R., and Voolstra, C. R. (2017). Bacterial Community Dynamics are Linked to Patterns of Coral Heat Tolerance. *Nat. Commun.* 8, 14213. doi: 10.1038/ncomms14213

Conflict of Interest: The authors declare that the research was conducted in the absence of any commercial or financial relationships that could be construed as a potential conflict of interest.

Publisher's Note: All claims expressed in this article are solely those of the authors and do not necessarily represent those of their affiliated organizations, or those of the publisher, the editors and the reviewers. Any product that may be evaluated in this article, or claim that may be made by its manufacturer, is not guaranteed or endorsed by the publisher.

frontiers | Frontiers in Marine Science

ORIGINAL RESEARCH
published: 11 May 2022
doi: 10.3389/fmars.2022.864872

Composition and Potential Functions of Bacterial Communities Associated With *Aurelia* Polyps

Yongxue Li[1,2], *Wenjin Hao*[3], *Saijun Peng*[1,2], *Tingting Sun*[1,2], *Jianmin Zhao*[1,4,5] *and Zhijun Dong*[1,4,5*]

[1] Muping Coastal Environment Research Station, Yantai Institute of Coastal Zone Research, Chinese Academy of Sciences, Yantai, China, [2] University of Chinese Academy of Sciences, Beijing, China, [3] School of Life Science, Nantong University, Nantong, China, [4] Key Laboratory of Coastal Environmental Processes and Ecological Remediation, Yantai Institute of Coastal Zone Research, Chinese Academy of Sciences, Yantai, China, [5] Center for Ocean Mega-Science, Chinese Academy of Sciences, Qingdao, China

Jellyfish and their associated microbes form an ecological unit called the holobiont. Changes in the composition of dominant microbial assemblages may influence the environmental resilience and function of the holobionts. Differentiating the microbial communities from diverse jellyfish is essential for characterizing the functional contributions of microorganisms but has not been fully explored. In this study, based on 16S rRNA gene sequencing, we investigated the composition of microbial communities associated with two *Aurelia* polyp species (*Aurelia coerulea* and *Aurelia solida*) obtained from seven locations, which were maintained under the same environmental conditions. Sequence analysis showed that the genera *Sphingomonas*, *Phyllobacterium*, and *Ralstonia* were the most abundant members of the *Aurelia*-associated microbial communities and dominated the core microbiome of the *Aurelia* polyps in this study. Functional prediction revealed that chemoheterotrophy and aerobic chemoheterotrophy, based on the FAPROTAX dataset, were the primary functions of the associated microbes of *Aurelia* polyps. In addition, the comparison of microbial communities from different *Aurelia* polyp populations revealed interspecific instead of intraspecific variation, indicating a correlation between the composition of the symbiotic microbiota and genetic background of *Aurelia* polyps.

Keywords: microbiome, *Aurelia*, host genotypes, high-throughput sequencing, jellyfish blooms

OPEN ACCESS

Edited by:
Jie Li,
Chinese Academy of Sciences, China

Reviewed by:
Tinkara Tinta,
National Institute of Biology, Slovenia
Zhi Zhou,
Hainan University, China

***Correspondence:**
Zhijun Dong
zjdong@yic.ac.cn

Specialty section:
This article was submitted to Microbial Symbioses, a section of the journal Frontiers in Marine Science

Received: *28 January 2022*
Accepted: *14 April 2022*
Published: *11 May 2022*

Citation:
Li Y, Hao W, Peng S, Sun T, Zhao J and Dong Z (2022) Composition and Potential Functions of Bacterial Communities Associated With Aurelia Polyps. Front. Mar. Sci. 9:864872. doi: 10.3389/fmars.2022.864872

INTRODUCTION

Interactions between organisms are factors determining the coexistence of species and maintenance of biodiversity. It is well established that animals act as hosts for multilineage consortia of microbial communities (i.e., bacteria, archaea, eukaryotes, and viruses) (McFall-Ngai et al., 2013), and microbial assemblages are an important factor in the regulation of host biology. Host-associated microbial communities exert nonnegligible forces on physiological metabolism regulation, immune function, and complex host behaviors (Rook et al., 2017). For instance, the gut microbial

communities of humans and insects assist in inhibiting the invasion and colonization of pathogenic bacteria and provide essential amino acids and vitamins for the physiological metabolism of hosts (Esser et al., 2019). The intestinal microbial communities of several insects significantly improve the environmental adaptability of hosts (Zhang and Leadbetter, 2012). Therefore, understanding the composition and structure of host-associated microbial communities is important in enabling insights into the functional contributions of microbes to hosts.

The colonization of a symbiotic consortium is influenced by many factors, such as the transmission of microbes from the external environment to hosts (Martinson et al., 2017), among-microbe interactions (Martinson et al., 2017), and ecological drift (Costello et al., 2012). Studies have found obvious dissimilarities between the microbiomes associated with aquatic animals (Stevens and Olson, 2015), amphibians (Walke et al., 2014), and terrestrial animals (Ren et al., 2017) from different regions. Additionally, the hosts act as ecological filters to selectively assemble specific species from the regional species pool based on their requirements and resources (Adair et al., 2020), causing the microbiomes of different species living in the same environment to be significantly different. Likewise, hosts of the same species often retain similarities in their microbial communities across various environmental conditions (Cheng et al., 2020). This retained microbiome, termed the "core microbiome", may play an important role in supporting the basic physio-chemical metabolism of hosts (Dietz et al., 2020).

As bacterial life had already existed for approximately three billion years when animals first evolved, microbe-animal interactions likely coevolved with the hosts over millions of years (Knoll, 2015). Based on their early appearance on the evolutionary scene, Cnidarians were likely among the first animals to establish associations with microorganisms (Bosch, 2013). The moon jellyfish *Aurelia* belongs to the phylum Cnidaria (class: Scyphozoa) and is the most common scyphozoan jellyfish in global coastal waters (Dong et al., 2018). The diphasic life cycle of *Aurelia* alternates between free-living pelagic medusa and sessile benthic polyp phases (Lucas, 2001). The composition and structure of microbial communities associated with the jellyfish *Aurelia* have been well investigated. Weiland-Braüuer et al. found that the composition of the microbiota associated with *Aurelia aurita* changed with the compartments of the adult medusae (mucus versus gastric cavity) and the life stages, particularly during the transition from the benthic to the pelagic stages (Weiland-Bräuer et al., 2015). Kramar et al. reported that the composition of *Aurelia solida*-associated microbial communities changed in relation to the period of the bloom (Kramar et al., 2019). Moreover, the presence of potentially pathogenic bacteria (i.e., *Vibrio* and Mycoplasmataceae) in the *Aurelia*-associated microbiome regarded *Aurelia* as a vector of pathogens (Tinta et al., 2019; Peng et al., 2021).

In the present study, we focused on the polyps of two moon jellyfish species, *Aurelia coerulea* and *A. solida*, which were incubated in the same environmental conditions with the same food source for 6 months to explore the relationship between polyps and symbiotic microbes. *Aurelia* polyp is a suitable model organism for the interaction between microbes and animals because of its simple body construction (basic immune and nervous systems), easy culture in the laboratory, high regeneration output, and short asexual reproduction cycle (Chiaverano and Graham, 2017). Based on the genetic and evolutionary relationships of the species, we hypothesized that the microbial community structure and functional characteristics of the species would vary under the same environmental conditions. In addition, the potential ecological functions of bacterial communities associated with *Aurelia* polyps were also discussed in the present study.

MATERIALS AND METHODS

Animal Collection and Culture

The polyps of *A. coerulea* and *A. solida* were originally obtained from the laboratory of Agustin Schiariti (Instituto Nacional de Investigación y Desarrollo Pesquero). *A. coerulea* were collected from the USA, China, Japan, Spain, and France and abbreviated as AC_{USA}, AC_{CHI}, AC_{JAP}, AC_{SPA} and AC_{FRA}, respectively. *A. solida* were collected from Israel and Slovenia and abbreviated as AS_{ISR} and AS_{SLO}, respectively, as detailed in **Table 1**. The polyps of the different *Aurelia* populations were kept separately in tanks. All polyps were cultured at 15°C in ambient fresh seawater with a salinity of 30 practical salinity units and kept on a day:night lighting rhythm of 12:12 h for 6 months of incubation time. Freshly hatched *Artemia salnia* were fed to the *Aurelia* polyps as their sole food source once every two days during the incubation period. Homogenization of cultivation conditions was performed to ensure stability and monovariability (i.e., host genotypes) of the symbiotic microbial communities of polyps from different *Aurelia* species and populations. The polyps were incubated in sterile seawater (0.22-μm filtered) baths for 1 day to clear the digestive system before DNA extraction. Species were identified based on 16S mtRNA pairwise sequence alignment technology.

TABLE 1 | The native locations of *Aurelia* polyps.

Sample	Location	Country	Species
AC_{FRA}	Roscoff	France	*Aurelia coerulea*
AC_{JAP}	Shirahama	Japan	*Aurelia coerulea*
AC_{CHI}	Fenghuang Lake	China	*Aurelia coerulea*
AC_{USA}	Monterery Bay Aquarium	USA	*Aurelia coerulea*
AC_{SPA}	Catalunya	Spain	*Aurelia coerulea*
AS_{ISR}	Red sea	Israel	*Aurelia solida*
AS_{SLO}	Koper port	Slovenia	*Aurelia solida*

DNA Extraction and 16S rRNA Gene Amplification Sequencing

Bacterial DNA of *Aurelia* polyps from 7 populations was isolated using a Wizard genomic DNA purification kit (Promega, Madison, WI, USA) according to the manufacturer's protocols. Each *Aurelia* population encompassed 5 replicates (10 polyps each) to yield read libraries sufficient for analysis. PCR amplification of the V4 hypervariable region of the 16S rRNA gene was performed with the primers 515F (5'-GTGCCAGCMG CCGCGGTAA-3') and 806R (5'-GGACTACHVGGGTWTCTA AT-3') (Hugerth et al., 2014). All PCRs were carried out in 30 μL reactions with 15 μL of Phusion® High-Fidelity PCR Master Mix (New England Biolabs, USA), 0.2 μM forward and reverse primers, and approximately 10 ng of template DNA. Thermal cycling consisted of initial denaturation at 98°C for 1 min, followed by 30 cycles of denaturation at 98°C for 10 s, annealing at 50°C for 30 s and elongation at 72°C for 30 s, with a final elongation at 72°C for 5 min. PCR products were detected by electrophoresis in a 2% (w/v) agarose gel. PCR amplicons of each sample with bright bands were mixed in equal-density ratios and purified with a GeneJET™ Gel Extraction Kit (Thermo Scientific, USA). Sequencing libraries were generated using an Ion Plus Fragment Library Kit 48 Rxns (Thermo Scientific) following the manufacturer's recommendations. Then, the library concentration was assessed with a Qubit@ 2.0 Fluorometer (Thermo Scientific). The amplicon libraries were sequenced on the Ion S5™ XL platform at Novogene Bioinformatics Technology Co., Ltd. (Beijing, China).

Sequence Assembly, Quality Control, and Taxonomic Assignment

Single-end reads were assigned to samples based on their unique barcode and truncated by cutting off the barcode and primer sequence. Quality filtering of the raw reads was performed under specific filtering conditions to obtain high-quality clean reads according to the Cutadapt (v1.9.1, http://cutadapt.readthedocs.io/en/stable/) quality control process (Kechin et al., 2017). The reads were compared with the reference database (Silva 132 database, https://www.arb-silva.de/) (Quast et al., 2013) using the UCHIME algorithm (UCHIME algorithm, http://www.drive5.com/usearch/manual/uchime_algo.html) (Edgar et al., 2011) to detect chimera sequences and then the chimera sequences were removed to obtain clean reads (Haas et al., 2011). The singleton and non-target sequences were removed from the analysis.

Sequence analyses were performed using UPARSE software (UPARSE v7.0.100 http://drive5.com/uparse/) (Edgar, 2013). First, sequences with ≥ 97% similarity were assigned to the same operational taxonomic unit (OTU), and a representative sequence for each OTU was screened for further annotation. Then, the Silva 132 database (https://www.arb-silva.de/) (Quast et al., 2013) was used to annotate each representative sequence with taxonomic information based on the Mothur algorithm, and a representative sequence for each OTU was assigned to a taxonomic level using the RDP classifier (Edgar, 2013). Furthermore, multiple sequence alignments were conducted using MUSCLE software (version 3.8.31, http://www.drive5.com/muscle/) (Edgar, 2004) to study the phylogenetic relationships among different OTUs and the divergence in the dominant species among different samples (groups).

Definition of Rare, Conditionally Rare, Abundant, and Core Taxa

Microbial communities normally consist of a few abundant and many rare species (Easson et al., 2020). In this study, the thresholds for rare, conditionally rare, and abundant taxa were defined based on relative sequence abundance cutoffs, with reference to recent publications (Liu et al., 2017). "Rare taxa" were defined as OTUs with a relative sequence abundance < 0.01% in all samples. "Conditionally rare taxa" were defined as OTUs that were rare (relative sequence abundance < 0.01%) in some but not all samples and were never abundant (relative sequence abundance ≥ 1%). "Abundant taxa" were defined as the OTUs that did not fall in either the rare or conditionally rare categories. "Core taxa" was defined as the OTUs present in all *Aurelia* polyps in this study.

Statistical Analysis and Visualization

The OTU abundance data were normalized corresponding to the sample with the fewest sequences for further analysis of alpha diversity and beta diversity. The Shannon and CHAO1 diversity indices were calculated based on the normalized OTU matrix with QIIME (version 1.7.0) and visualized with the ggplot2 package of R software (version 2.15.3). Nonparametric Kruskal–Wallis tests, nonparametric Mann–Whitney U tests, and t tests were performed to identify significant differences in functional and relative bacterial abundance between different samples. The beta diversity of samples was calculated based on Bray–Curtis dissimilarity at the OTU level and used to perform principal coordinate analysis (PCoA), which was visualized with the ggplot2 and vegan packages of R software (version 2.15.3). In addition, Wilcoxon match-pair tests and permutational analysis of molecular variance (PERMANOVA) were constructed to test for significant differences in microbial alpha and beta diversity between *Aurelia* polyp species using the vegan package of R software (version 2.15.3). Furthermore, the relative sequence abundance of samples at diverse classification levels was visualized by the ggplot2 and reshape2 packages of R software (version 2.15.3). The relative sequence abundance of functional bacterial communities was calculated based on the FAPROTAX database and visualized by the pheatmap package of R software (version 2.15.3).

RESULTS

Bacterial Community Profiling

After filtering the raw data, a total of 2,456,681 clean reads from 35 *Aurelia* polyp samples were obtained, with an average sequence length of 372 bp. A total of 1,213 OTUs were present in the *Aurelia* polyp samples, clustered into 36 phyla, 49 classes, 107 orders, 190 families, and 400 genera.

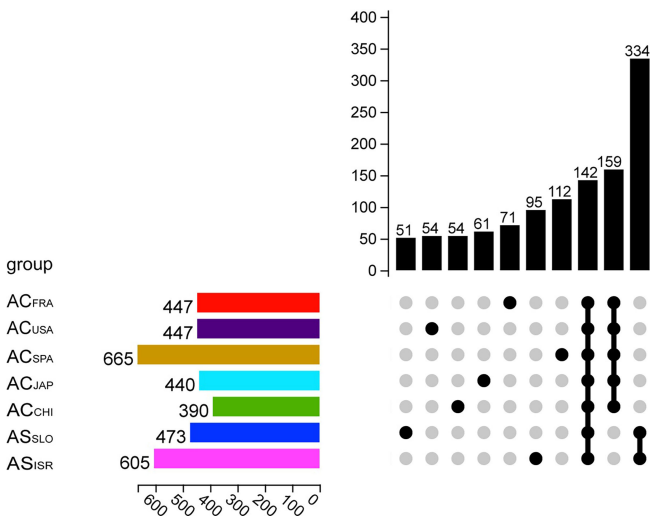

FIGURE 1 | Upset plot showing OTU information of different *Aurelia* polyp groups. The horizontal column on the left represents the average number of OTUs in the microbiome of each group (n = 5). Each single point in the matrix below indicates that the vertical column above it showd the number of OTUs unique to the corresponding *Aurelia* polyp group, while the points on the matrix grouped by a line indicate that the vertical column shows the number of OTUs common to those groups.

Variation in Microbial Composition

A total of 159 OTUs were present in all *A. coerulea* polyp groups, accounting for 82.06% (AC_{SPA})–98.58% (AC_{CHI}) of the total relative sequence abundance (**Figure 1**). In the *A. coerulea polyps*, 36 bacterial phyla, 48 classes, 98 orders, 179 families, and 366 genera were detected. The microbiomes of *A. solida* polyps contained 25 phyla, 40 classes, 84 orders, 145 families, and 257 genera. A total of 334 OTUs were shared between both groups of *A. solida* polyps and accounted for 96.64% and 98.97% of the total relative sequence abundance in AS_{ISR} and AS_{SLO}, respectively (**Figure 1**). Each *Aurelia* polyp group contained unique OTUs, which all had low relative sequence abundance (< 1%, **Figure 1**).

At the phylum and class levels, bacterial communities associated with both *Aurelia* polyp species were dominated by Proteobacteria (mainly classes Alphaproteobacteria and Gammaproteobacteria), Firmicutes (mainly class Clostridia), Bacteroidetes, Acidobacteira and Actinobacteria, together comprising 97.01% (AC_{SPA}) – 99.71% (AC_{JAP}) of the total richness (**Figure 2**). The relative abundances of the other 31 phyla in each *Aurelia* polyp population were <1%, together comprising 0.29% (AC_{JAP}) – 2.99% (AC_{SPA}) of the total richness (**Figure 2**). At the family and genus levels, the polyp microbiomes were dominated by Sphingomonadaceae (mainly the genera *Sphingomonas* and *Sphingobacterium*), Rhizobiaceae (mainly the genus *Phyllobacterium*) and Burkholderiaceae (mainly the genus *Ralstonia*), comprising 53.2% (AC_{SPA})–95.5% (AC_{CHI}) of the total bacterial abundance associated with *A. coerulea* and *A. solida* (**Figure 2**).

At the family level, unidentified Clostridiales (Mann–Whitney U test, $p = 0.039$) were significantly more abundant in *A. solida* than in *A. coerulea*, while Sphingomonadaceae (t test, $p = 0.038$) and Rhizobiaceae (t test, $p = 0.024$) were more abundant in *A. coerulea*. At the genus level, the *A. coerulea* polyps had significantly higher relative sequence abundance of the genera *Sphingomonas* (t test, $p = 0.043$) and *Phyllobacterium* (t test, $p = 0.023$) than *A. solida* polyps.

Variation in Microbial Diversity

To further reveal the inter- and intraspecific differences in the microbiomes of *Aurelia* polyps, the microbes of the two *Aurelia* polyp species were compared based on microbial alpha diversity and beta diversity, as detailed in **Figure 3**.

Regarding interspecific differences in microbial alpha diversity, *A. coerulea* polyps had a lower average Shannon index (2.998) than *A. solida* polyps (3.119), as well as a lower average CHAO1 index (219 and 237 in *A. coerulea* and *A. solida* polyps, respectively, **Figure 3**). However, no significant difference between the *A. coerulea* and *A. solida* groups was detected in either the Shannon indices or CHAO1 indices (Wilcoxon match-pairs test, $p = 0.5566$, **Figure 3**). Regarding intraspecific differences, AC_{CHI} had the highest average Shannon indices of the *A. coerulea* groups (3.367), followed by AC_{SPA}, AC_{FRA}, AC_{USA}, and AC_{JAP} had the lowest (2.635). The highest average CHAO1 index of the *A. coerulea* polyps was found in AC_{SPA} (285), followed by AC_{USA}, AC_{FRA} and AC_{JAP}, and the lowest was found in AC_{CHI} (186). Within the *A. solida* groups, AS_{ISR} had a higher average CHAO1 index (263) than AS_{SLO} (212) but had a lower mean Shannon index (2.449 in AS_{ISR} and 2.831 in AS_{SLO}). Nonetheless, no significant difference was found between the Shannon and CHAO1 indices of polyps in the *A. coerulea* and *A. solida* groups (Wilcoxon match-pairs test, $p > 0.05$, **Figure 3**).

In terms of the interspecific comparison, PCoA based on Bray–Curtis distance demonstrated a significant difference in microbial beta diversity between the microbiomes of the *A. coerulea* and *A. solida* polyps (PERMANOVA test, $p = 0.016$, **Figure 3**).

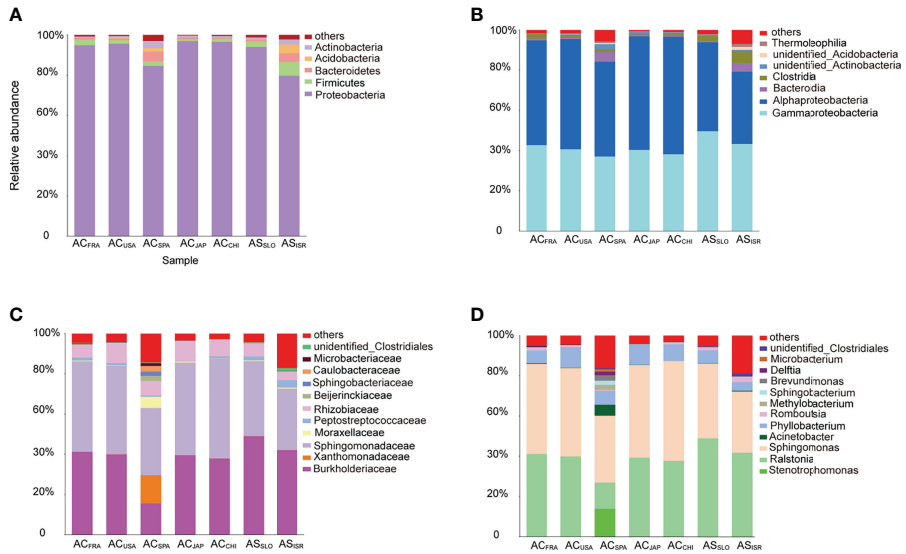

FIGURE 2 | Stacked bar plots of bacterial taxa with relative sequence abundance higher than 1% at the **(A)** phylum level, **(B)** class level, **(C)** family level, and **(D)** genus level in the *Aurelia*-associated bacterial communities. The less abundant taxa are grouped under "others".

Furthermore, significant differences were identified between the abundant and core microbial taxa associated with *A. coerulea* polyps and *A. solida* polyps (PERMANOVA test, $p = 0.044$ and $p = 0.03$, respectively), but there was no significant difference between the rare microbial taxa associated with the two species (PERMANOVA test, $p = 0.403$, **Table 2**). Similarity percentage analysis (Simper) illustrated that the genera *Stenotrophomonas*, *Ralstonia*, and *Sphingobacterium* were the main contributors to the difference in

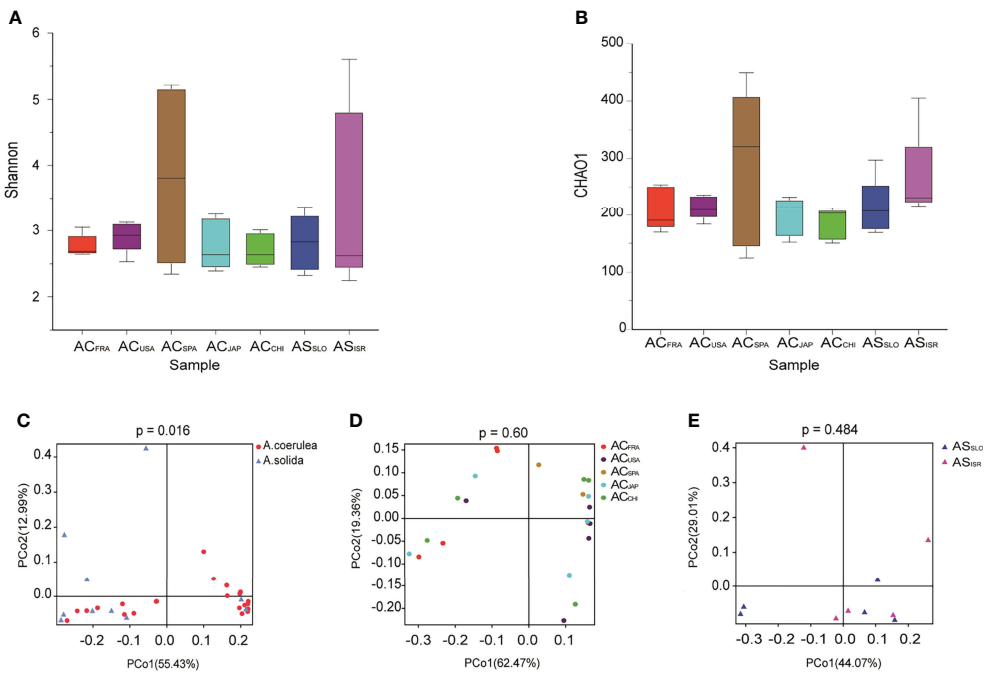

FIGURE 3 | Variation in microbial diversity of different polyp groups. Alpha diversity and richness are represented by Shannon indices **(A)** and CHAO1 **(B)** of *Aurelia* polyp microbiomes. PCoA (Principal coordinates analysis) visualization of bacterial beta - diversity of **(C)** all samples grouped by different types without outline, **(D)** *A. coerulea* polyps samples grouped by location without Outliers, and **(E)** *A. solida* polyp samples grouped by location. PERMANOVA tests were used to analyze significant differences between microbial diversity in different groups.

TABLE 2 | PERMANOVA tests of bacterial community structure of *Aurelia* polyps based on Bray–Curtis dissimilarities of OTU abundance.

Comparison group	Taxa types	OTU numbers	df	F	Pr (>F)
A. coerilea vs *A. solida*	core	20	34	2.698	0.030*
	rare	627	34	1.051	0.403
	conditionally rare	0	NA	NA	NA
	abundant	586	34	2.287	0.044*
A. coerulea	core	20	24	1.618	0.074
	rare	250	24	1.019	0.420
	conditionally rare	772	24	1.172	0.148
	abundant	38	24	1.426	0.087
A. solida	core	20	9	0.947	0.384
	rare	193	9	0.964	0.530
	conditionally rare	519	9	0.779	0.884
	abundant	32	9	0.850	0.438

"NA" represented not available. The values of $p < 0.05$ were marked with "".*

the microbial community between the two species, which contributed 26.8%, 26.1%, and 10.6% to the difference value, respectively (**Figure 4**). In terms of the intraspecific comparison, PCoA showed no significant intraspecific variation among the groups of *A. coerulea* polyps (PERMANOVA test, $p = 0.60$, **Figure 3**) or *A. solida* polyps (PERMANOVA test, $p = 0.484$, **Figure 3**). Furthermore, no significant difference was detected in the rare, conditionally rare, abundant taxa, or core taxa of the intraspecific groups (PERMANOVA test, $p > 0.05$, **Table 2**).

Core Bacterial Microbiome

In total, 20 OTUs were found in all *Aurelia* polyp samples. These 20 OTUs were defined as the "core microbiome" of *Aurelia* polyps, accounting for 57.19% (AC_{SPA})–96.86% (AC_{CHI}) of the total microbial richness (**Figure 5**). The genera *Sphingomonas*, *Ralstonia*, and *Phyllobacterium* were prominent in the core microbiome of the *Aurelia* polyps, accounting for 79.76% (AS_{ISR})–92.64% (AS_{SLO}) and 57.19% (AC_{SPA})–96.13% (AC_{CHI}) of the total core microbial richness in *A. coerulea* polyps and *A. solida* polyps, respectively (**Figure 5**). Notably, 6 OTU members of the core microbiome had significantly different abundances between *A. coerulea* and *A. solida* polyps: OTU_2 (Mann–Whitney U test, $p = 0.034$), OTU_1043 (Mann–Whitney U test, $p = 0.026$), and OTU_1244 (Mann–Whitney U test, $p = 0.037$) all belonging to the genus *Ralstonia*, were significantly more abundant in *A. solida* polyps than in *A. coerulea* polyps. However, OTU_3 (genus *Phyllobacterium*, t test, $p = 0.026$), OTU_1100 (genus *Sphingomonas*, t test, $p = 0.026$), and OTU_1287 (genus *Sphingomonas*, Mann–Whitney U test, $p = 0.011$) were significantly more abundant in *A. coerulea* polyps than in *A. solida* polyps.

Predicted Functions of *Aurelia*-Associated Microbiomes

Ecological functional annotation of polyp-associated microbial communities was conducted based on the FAPROTAX database. A total of 1,247 functional assignments for 8, 326 OTUs were

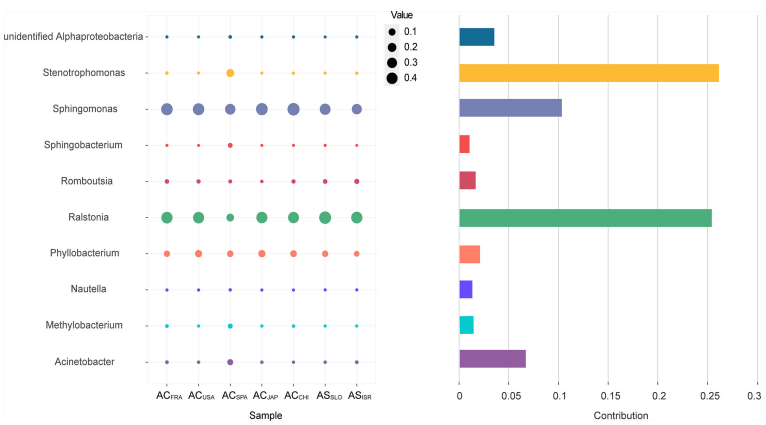

FIGURE 4 | The top 10 genera contributing to the interspecific difference in the microbial community. The vertical axis represents the species. The horizontal axis represents the samples. The bubble size represents the relative sequence abundance of the species. Contribution represents the contribution of the genus in the difference between the *A. coerulea* and *A. solida*.

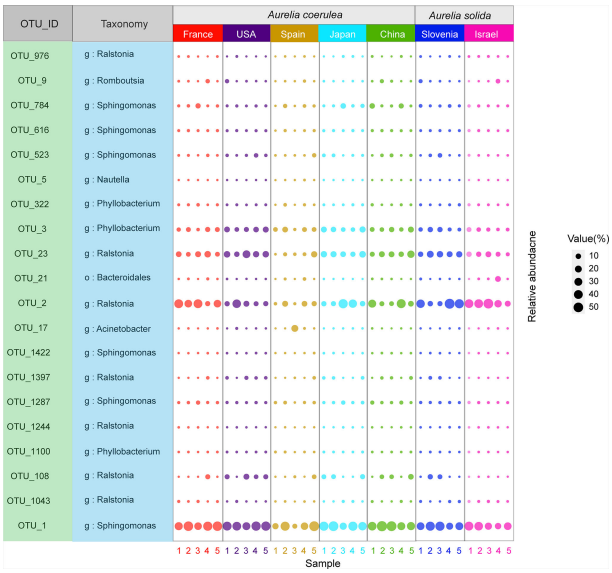

FIGURE 5 | Bubble plot of the core microbiome of *Aurelia* polyps, with bubble size indicating the relative sequence abundance of bacterial taxa.

obtained. OTUs without any functional annotation were excluded from the analysis. Functional group abundances in each sample were calculated as the cumulative relative sequence abundance of OTUs assigned to each functional group after normalizing by the cumulative abundances of OTUs associated with at least one function. Generally, chemoheterotrophy (42.7~70.0% of total OTUs) and anaerobic chemoheterotrophy (36.8~65.5% of total OTUs) were the primary functions in both *A. coerulea* and *A. solida* polyps, followed by functions related to the N cycle, such as nitrate reduction, nitrogen respiration, and denitrification (**Figure 6**). Furthermore, microbial communities associated with *A. coerulea* polyps had significantly higher abundances of

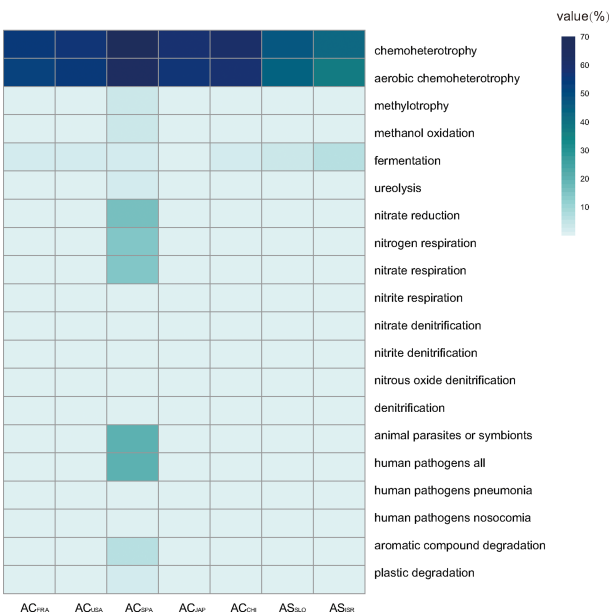

FIGURE 6 | Heatmap matrix on the top 20 functional groups with the highest cumulative OTU relative sequence abundance in *Aurelia* polyp samples based on analysis of FAPROTAX.

chemoheterotrophic bacterial taxa than those associated with *A. solida* polyps (Mann–Whitney U test, $p = 0.004$).

DISCUSSION

Composition of Bacterial Communities Associated With *Aurelia* Polyps

Bacterial communities associated with hosts are shaped by host selection and environmental conditions (Gould et al., 2018). Previous researchers have highlighted environmental factors shaping the structure of microbial communities in hosts such as coral (Zhang et al., 2014; Osman et al., 2020), sponge (Zhang et al., 2014; Easson et al., 2020), and sea anemone (Mortzfeld et al., 2016; Morelan et al., 2019). In this study, despite long-term cultivation in the same environment and feed, we found interspecific variation in beta diversity among *Aurelia* polyps and intraspecific similarity among *Aurelia* polyps. Therefore, our results suggest that the genotype of *Aurelia* polyps is an important factor in the structure of the symbiotic bacterial communities. Weiland-Bräuer et al. concluded that there were large differences in the microbial compositions of *Aurelia* polyps between North Sea/Roscoff and Baltic Sea subpopulations, similar to the present study (Weiland-Bräuer et al., 2015).

Animal hosts are known to be able to modulate their associated microbiome in terms of genotype regulation, such as *via* genetic expression or innate immune response activation (Borges, 2017). For example, in research using hydras as model animals, the variation in antimicrobial peptide genes in different species led to variation in the microbiomes among those species (Bosch, 2013). As part of the evolutionarily ancient marine phylum Cnidaria, *Aurelia* jellyfish may influence the structure of their microbiomes by producing various proteins or antimicrobial peptides *via* gene expression, which interferes with bacterial quorum sensing (selecting microbes from the environment or promoting the colonization and enrichment of targeted microbes) and inhibits bacterial colonization (Weiland-Bräuer et al., 2019). In addition, vertical transmission of bacterial communities from parents to offspring could be another reason for the differences between the bacterial communities of *A. coerulea* and *A. solida* polyps.

The Core Microbiota of *Aurelia* Polyps

Hosts can conditionally shape the structure of microbial communities by interacting to maintain an overall stable state, especially cnidarians (Ainsworth et al., 2015). In the present study, the families Sphingomonadaceae (i.e., genera *Sphingomonas*), Rhizobiaceae (i.e., genera *Phyllobacterium*), and Burkholderiaceae (i.e., genera *Ralstonia*) were detected in all *Aurelia* polyp samples with high relative sequence abundances. Similarly, Weiland-Bräuer et al. proposed that the relative sequence abundance of Sphingomonadaceae was high in *Aurelia* collected in Roscoff, the North Sea, and the Baltic Sea throughout the life stages and decreased with the transition of *Aurelia* polyps to strobila to ephyra to juvenile medusae (Weiland-Bräuer et al., 2015). Peng et al. also detected a high abundance of Sphingomonadaceae and Burkholderiaceae in the associated bacterial community of wild *Aurelia* medusae (Peng et al., 2021). Several studies have suggested that cnidarian-associated bacterial communities are potentially involved in functional interactions and play a positive role in host-environment adaptation (Ziegler et al., 2017; Podell et al., 2020; Roach et al., 2020; Tong et al., 2020). Hence, the family Sphingomonadaceae may be a member of the core microbial communities associated with *Aurelia* populations worldwide. Further studies on the function of Sphingomonadaceae would help to gain insight into the impact of microorganisms on hosts.

Bacteria are functional components of most marine multicellular organisms, especially cnidarians (Morelan et al., 2019). Previous studies have agreed that the core microbiome was closely related to the health, growth, environmental adaptability, and production of the hosts (Bosch, 2013; Ainsworth et al., 2015; Brown et al., 2017; Weigel and Erwin, 2017; Weiland-Bräuer et al., 2020). In our study, a total of 20 core OTUs were identified in the bacterial communities of the scyphozoan body parts, predominantly the genera *Sphingomonas*, *Ralstonia*, and *Phyllobacterium*. The genus *Sphingomonas* (family Sphingomonadaceae), a dibenzofuran- and dibenzodioxin-degrading bacterium with potentially interesting properties for bioaugmentation of contaminated sites (Roggo et al., 2013), was the most abundant taxon in the microbiomes of all *Aurelia* polyps. Furthermore, Feng et al. (2017) identified that certain *Sphingomonas* spp. were potentially able to degrade chlorpyrifos, indicating that *Sphingomonas* could enhance the survival rate of *Aurelia* polyps in contaminated environments. The genus *Phyllobacterium*, which can produce exopolysaccharide (Li et al., 2017), was also dominant in *Aurelia* polyps. The exopolysaccharide could form protective barriers between cells and the environment, regulate cell growth and senescence, and affect cell division and differentiation (Flores-Felix et al., 2018), suggesting that the genus *Phyllobacterium* may be closely related to the transformation process between *Aurelia* life stages and host-environment adaptation.

Potential Functions of Bacterial Communities Associated With *Aurelia* Polyps

Functional prediction is the first step in determining how microbiome biochemical processes affect the ecological functions of hosts (Ross et al., 2018). FAPROTAX is a promising tool for predicting ecologically relevant functions of bacterial and archaeal taxa derived from 16S rRNA amplicon sequencing (Louca et al., 2016). In this study, according to the FAPROTAX database, aerobic chemoheterotrophy in relation to C cycling was the primary function of *Aurelia* polyp-associated bacteria associated with numerous bacteria, such as Sphingomonadaceae and Microbacteriaceae. This demonstrated that *Aurelia* polyps were the main foundation of essential nutrients to support the microbial growth of the associated bacterial communities. Ross et al. (2018) reported that *Aurelia* medusae are potential bacterial vectors and may harm aquaculture activities, as their microbiomes harbor potential fish pathogens. Similarly, in this study, some potential animal pathogens (i.e., Coxiellaceae) or parasites (i.e.,

Bdellovibrionaceae and Haliangiaceae) were present in both *A. coerulea* and *A. solida* polyps. Moreover, nitrification and denitrification, two functions related to the N cycle that have been reported to be involved in waste removal in host coral (Beman et al., 2007), were potential functions that were abundant in both *Aurelia* polyp species. Hence, these bacteria may have similar N cycle-related functions in *Aurelia* polyps, assisting with the adaptation of polyps to nitrate stress in the ambient environment.

Unique Microbes Associated With *Aurelia* Polyps

Each intraspecific group had unique bacterial taxa, which accounted for less than 1% of the relative sequence abundance. These unique bacteria are often overlooked because of their low abundance but may be critical to the functional maintenance of hosts (Shade et al., 2014). For example, *Actinobacteria* sp. and *Ralstonia* sp., located in zooxanthellae and coral intestinal epithelial cells, have low abundance and perform a vital role in the metabolism of the coral *Acropora granulosa* (Ainsworth et al., 2015). Unlike the relative stability of the core microbiome in *Aurelia* polyps (**Figure 1**; **Table 2**), the unique microbes were less controlled and more sensitive to environmental variation. We speculated that unique microbes were preserved by the hosts from the native environment and potentially contributed to the environmental resilience of *Aurelia* polyps. Further study on unique microbes could comprehensively elucidate the mechanism of host selection for microbes in the environment.

CONCLUSION

In this study, we investigated the bacterial communities associated with two moon jellyfish species (*A. coerulea* and *A. solida*) obtained from seven locations and incubated under the same environmental conditions. We found that the genera *Sphingomonas*, *Phyllobacterium*, and *Ralstonia* dominated the core microbial communities of the *Aurelia* polyps. These *Aurelia*-associated microbes may potentially play an important role in host's fitness and host's environmental adaptation by promoting nutrient uptake. Furthermore, the comparison of microbial communities from different *Aurelia* polyp populations revealed interspecific variation, indicating a correlation between the composition of the associated bacterial community and genetic background of *Aurelia* polyps.

DATA AVAILABILITY STATEMENT

The datasets presented in this study can be found in online repositories. The names of the repository/repositories and accession number(s) can be found below: https://www.ncbi.nlm.nih.gov/bioproject/ PRJNA799918.

AUTHOR CONTRIBUTIONS

YL: Data analysis, writing - original draft, writing - review & editing. WH: writing - review & editing. SP: Data analysis. TS: Sample process. JZ: Conceptualization, funding acquisition. ZD: Conceptualization, investigation, data analysis, funding acquisition, writing - review & editing. All authors contributed to the article and approved the submitted version.

FUNDING

This research was supported by grants from the NSFC-Shandong Joint Fund (No. U2106208), National Natural Science Foundation of China (No. 41876138), the National Key Research and Development Program of China (2018YFC1406501), and the Strategic Priority Research Program of the Chinese Academy of Sciences (No. XDA23050301).

ACKNOWLEDGEMENTS

We wish to thank Marine Biology Station Piran, National Institute of Biology, for making the collection possible, and to Dr. Agustin Schiariti from the Instituto Nacional de Investigación y Desarrollo Pesquero for keeping the cultures and providing us with *Aurelia* polyps.

REFERENCES

Adair, K. L., Bost, A., Bueno, E., Kaunisto, S., Kortet, R., Peters-Schulze, G., et al. (2020). Host Determinants of Among-Species Variation in Microbiome Composition in Drosophilid Flies. *Isme J.* 14, 217–229. doi: 10.1038/s41396-019-0532-7

Ainsworth, T. D., Krause, L., Bridge, T., Torda, G., Raina, J. B., Zakrzewski, M., et al. (2015). The Coral Core Microbiome Identifies Rare Bacterial Taxa as Ubiquitous Endosymbionts. *Isme J.* 9, 2261–2274. doi: 10.1038/ismej.2015.39

Beman, J. M., Roberts, K. J., Wegley, L., Rohwer, F., and Francis, C. A. (2007). Distribution and Diversity of Archaeal Ammonia Monooxygenase Genes Associated With Corals. *Appl. Environ. Microb.* 73, 5642–5647. doi: 10.1128/Aem.00461-07

Borges, R. M. (2017). Co-Niche Construction Between Hosts and Symbionts: Ideas and Evidence. *J. Genet.* 96, 483–489. doi: 10.1007/s12041-017-0792-9

Bosch, T. C. G. (2013). Cnidarian-Microbe Interactions and the Origin of Innate Immunity in Metazoans. *Annu. Rev. Microbiol.* 67, 499–518. doi: 10.1146/annurev-micro-092412-155626

Brown, T., Otero, C., Grajales, A., Rodriguez, E., and Rodriguez-Lanetty, M. (2017). Worldwide Exploration of the Microbiome Harbored by the Cnidarian Model, *Exaiptasia Pallida* (Agassiz in Verrill 1864) Indicates a Lack of Bacterial Association Specificity at a Lower Taxonomic Rank. *PeerJ* 5, e3235. doi: 10.7717/peerj.3235

Cheng, Z. Q., Lei, S. N., Li, Y., Huang, W., Ma, R. Q., Xiong, J., et al. (2020). Revealing the Variation and Stability of Bacterial Communities in Tomato Rhizosphere Microbiota. *Microorganisms* 8, 170. doi: 10.3390/microorganisms8020170

Chiaverano, L. M., and Graham, W. M. (2017). Morphological Plasticity in *Aurelia* Polyps, With Subsequent Effects on Asexual Fecundity and Morphology of Young Medusae. *Mar. Ecol. Prog. Ser.* 582, 79–92. doi: 10.3354/meps12314

Costello, E. K., Stagaman, K., Dethlefsen, L., Bohannan, B. J. M., and Relman, D. A. (2012). The Application of Ecological Theory Toward an Understanding of the Human Microbiome. *Science* 336, 1255–1262. doi: 10.1126/science.1224203

Dietz, M. W., Salles, J. F., Hsu, B. Y., Groothuis, T. G. G., van der Velde, M., Verkuil, Y. I., et al. (2020). Prenatal Transfer of Gut Bacteria in Rock Pigeon. *Microorganisms* 8, 61. doi: 10.3390/microorganisms8010061

Dong, Z. J., Wang, L., Sun, T. T., Liu, Q. Q., and Sun, Y. F. (2018). Artificial Reefs for Sea Cucumber Aquaculture Confirmed as Settlement Substrates of the Moon Jellyfish *Aurelia Coerulea*. *Hydrobiologia* 818, 223–234. doi: 10.1007/s10750-018-3615-y

Easson, C. G., Chaves-Fonnegra, A., Thacker, R. W., and Lopez, J. V. (2020). Host Population Genetics and Biogeography Structure the Microbiome of the Sponge *Cliona Delitrix*. *Ecol. Evol.* 10, 2007–2020. doi: 10.1002/ece3.6033

Edgar, R. C. (2004). MUSCLE: Multiple Sequence Alignment With High Accuracy and High Throughput. *Nucleic Acids Res.* 32, 1792–1797. doi: 10.1093/nar/gkh340

Edgar, R. C. (2013). UPARSE: Highly Accurate OTU Sequences From Microbial Amplicon Reads. *Nat. Methods* 10, 996. doi: 10.1038/Nmeth.2604

Edgar, R. C., Haas, B. J., Clemente, J. C., Quince, C., and Knight, R. (2011). UCHIME Improves Sensitivity and Speed of Chimera Detection. *Bioinformatics* 27, 2194–2200. doi: 10.1093/bioinformatics/btr381

Esser, D., Lange, J., Marinos, G., Sieber, M., Best, L., Prasse, D., et al. (2019). Functions of the Microbiota for the Physiology of Animal Metaorganisms. *J. Innate Immun.* 11, 393–404. doi: 10.1159/000495115

Feng, F. Y., Ge, J., Li, Y. S., Cheng, J. J., Zhong, J. F., and Yu, X. Y. (2017). Isolation, Colonization, and Chlorpyrifos Degradation Mediation of the Endophytic Bacterium *Sphingomonas* Strain HJY in Chinese Chives (Allium Tuberosum). *J. Agr. Food. Chem.* 65, 1131–1138. doi: 10.1021/acs.jafc.6b05283

Flores-Felix, J. D., Velazquez, E., Garcia-Fraile, P., Gonzalez-Andres, F., Silva, L. R., and Rivas, R. (2018). *Rhizobium* and *Phyllobacterium* Bacterial Inoculants Increase Bioactive Compounds and Quality of Strawberries Cultivated in Field Conditions. *Food Res. Int.* 111, 416–422. doi: 10.1016/j.foodres.2018.05.059

Gould, A. L., Zhang, V. V., Lamberti, L., Jones, E. W., Obadia, B., Korasidis, N., et al. (2018). Microbiome Interactions Shape Host Fitness. *P. Natl. Acad. Sci. U. S. A.* 115, E11951–E11960. doi: 10.1073/pnas.1809349115

Haas, B. J., Gevers, D., Earl, A. M., Feldgarden, M., Ward, D. V., Giannoukos, G., et al. (2011). Chimeric 16s rRNA Sequence Formation and Detection in Sanger and 454-Pyrosequenced PCR Amplicons. *Genome Res.* 21, 494–504. doi: 10.1101/gr.112730.110

Hugerth, L. W., Wefer, H. A., Lundin, S., Jakobsson, H. E., Lindberg, M., Rodin, S., et al. (2014). DegePrime, a Program for Degenerate Primer Design for Broad-Taxonomic-Range PCR in Microbial Ecology Studies. *Appl. Environ. Microb.* 80, 5116–5123. doi: 10.1128/Aem.01403-14

Kechin, A., Boyarskikh, U., Kel, A., and Filipenko, M. (2017). CutPrimers: A New Tool for Accurate Cutting of Primers From Reads of Targeted Next Generation Sequencing. *J. Comput. Biol.* 24, 1138–1143. doi: 10.1089/cmb.2017.0096

Knoll, A. H. (2015). *Life on a Young Planet: The First Three Billion Years of Evolution on Earth* (Princeton, NJ: Princeton University Press). doi: 10.1515/9781400866045

Kramar, M. K., Tinta, T., Lucic, D., Malej, A., and Turk, V. (2019). Bacteria Associated With Moon Jellyfish During Bloom and Post-Bloom Periods in the Gulf of Trieste (Northern Adriatic). *PloS One* 14, e0198056. doi: 10.1371/journal.pone.0198056

Liu, M., Yu, Z., Yu, X. Q., Xue, Y. Y., Huang, B. Q., and Yang, J. (2017). Invasion by Cordgrass Increases Microbial Diversity and Alters Community Composition in a Mangrove Nature Reserve. *Front. Microbiol.* 8, 2503. doi: 10.3389/fmicb.2017.02503

Li, Y. P., Zhang, G. L., Du, C. Y., Mou, H. J., Cui, J. F., Guan, H. S., et al. (2017). Characterization of High Yield Exopolysaccharide Produced by *Phyllobacterium* Sp 921F Exhibiting Moisture Preserving Properties. *Int. J. Biol. Macromol.* 101, 562–568. doi: 10.1016/j.ijbiomac.2017.03.089

Louca, S., Parfrey, L. W., and Doebeli, M. (2016). Decoupling Function and Taxonomy in the Global Ocean Microbiome. *Science* 353, 1272–1277. doi: 10.1126/science.aaf4507

Lucas, C. H. (2001). Reproduction and Life History Strategies of the Common Jellyfish, *Aurelia Aurita*, in Relation to Its Ambient Environment. *Hydrobiologia* 451, 229–246. doi: 10.1023/A:1011836326717

Martinson, V. G., Douglas, A. E., and Jaenike, J. (2017). Community Structure of the Gut Microbiota in Sympatric Species of Wild Drosophila. *Ecol. Lett.* 20, 629–639. doi: 10.1111/ele.12761

McFall-Ngai, M., Hadfield, M. G., Bosch, T. C. G., Carey, H. V., Domazet-Loso, T., Douglas, A. E., et al. (2013). Animals in a Bacterial World, a New Imperative for the Life Sciences. *P. Natl. Acad. Sci. U. S. A.* 110, 3229–3236. doi: 10.1073/pnas.1218525110

Morelan, I. A., Gaulke, C. A., Sharpton, T. J., Thurber, R. V., and Denver, D. R. (2019). Microbiome Variation in an Intertidal Sea Anemone Across Latitudes and Symbiotic States. *Front. Mar. Sci.* 6, 7. doi: 10.3389/fmars.2019.00007

Mortzfeld, B. M., Urbanski, S., Reitzel, A. M., Kunzel, S., Technau, U., and Fraune, S. (2016). Response of Bacterial Colonization in *Nematostella Vectensis* to Development, Environment and Biogeography. *Environ. Microbiol.* 18, 1764–1781. doi: 10.1111/1462-2920.12926

Osman, E. O., Suggett, D. J., Voolstra, C. R., Pettay, D. T., Clark, D. R., Pogoreutz, C., et al. (2020). Coral Microbiome Composition Along the Northern Red Sea Suggests High Plasticity of Bacterial and Specificity of Endosymbiotic Dinoflagellate Communities. *Microbiome* 8, 8. doi: 10.1186/s40168-019-0776-5

Peng, S. J., Hao, W. J., Li, Y. X., Wang, L., Sun, T. T., Zhao, J. M., et al. (2021). Bacterial Communities Associated With Four Blooming Scyphozoan Jellyfish: Potential Species-Specific Consequences for Marine Organisms and Humans Health. *Front. Microbiol.* 12. doi: 10.3389/fmicb.2021.647089

Podell, S., Blanton, J. M., Oliver, A., Schorn, M. A., Agarwal, V., Biggs, J. S., et al. (2020). A Genomic View of Trophic and Metabolic Diversity in Clade-Specific *Lamellodysidea* Sponge Microbiomes. *Microbiome* 8, 97. doi: 10.1186/s40168-020-00877-y

Quast, C., Pruesse, E., Yilmaz, P., Gerken, J., Schweer, T., Yarza, P., et al. (2013). The SILVA Ribosomal RNA Gene Database Project: Improved Data Processing and Web-Based Tools. *Nucleic Acids Res.* 41, D590–D596. doi: 10.1093/nar/gks1219

Ren, T. T., Boutin, S., Humphries, M. M., Dantzer, B., Gorrell, J. C., Coltman, D. W., et al. (2017). Seasonal, Spatial, and Maternal Effects on Gut Microbiome in Wild Red Squirrels. *Microbiome* 5, 163. doi: 10.1186/s40168-017-0382-3

Roach, T. N. F., Little, M., Arts, M. G. I., Huckeba, J., Haas, A. F., and George, E. E. (2020). A Multiomic Analysis of *in Situ* Coral-Turf Algal Interactions. *P. Natl. Acad. Sci. U. S. A.* 117, 13588–13595. doi: 10.1073/pnas.1915455117

Roggo, C., Coronado, E., Moreno-Forero, S. K., Harshman, K., Weber, J., and van der Meer, J. R. (2013). Genome-Wide Transposon Insertion Scanning of Environmental Survival Functions in the Polycyclic Aromatic Hydrocarbon Degrading Bacterium *Sphingomonas Wittichii* RW1. *Environ. Microbiol.* 15, 2681–2695. doi: 10.1111/1462-2920.12125

Rook, G., Bakhed, F., Levin, B. R., Mcfall-Ngai, M. J., and Mclean, A. R. (2017). Evolution, Human-Microbe Interactions, and Life History Plasticity. *Lancet* 390, 521–530. doi: 10.1016/S0140-6736(17)30566-4

Ross, A. A., Muller, K. M., Weese, J. S., and Neufeld, J. D. (2018). Comprehensive Skin Microbiome Analysis Reveals the Uniqueness of Human Skin and Evidence for Phylosymbiosis Within the Class Mammalia. *P. Natl. Acad. Sci. U. S. A.* 115, E5786–E5795. doi: 10.1073/pnas.1801302115

Shade, A., Jones, S. E., Caporaso, J. G., Handelsman, J., Knight, R., Fierer, N., et al. (2014). Conditionally Rare Taxa Disproportionately Contribute to Temporal Changes in Microbial Diversity. *Mbio* 5, e01371-14. doi: 10.1128/mBio.01371-14

Stevens, J. L., and Olson, J. B. (2015). Bacterial Communities Associated With Lionfish in Their Native and Invaded Ranges. *Mar. Ecol. Prog. Ser.* 531, 253–262. doi: 10.3354/meps11323

Tinta, T., Kogovsek, T., Klun, K., Malej, A., Herndl, G. J., and Turk, V. (2019). Jellyfish-Associated Microbiome in the Marine Environment: Exploring its Biotechnological Potential. *Mar. Drugs* 17, 94. doi: 10.3390/md17020094

Tong, H. Y., Cai, L., Zhou, G. W., Zhang, W. P., Huang, H., and Qian, P. Y. (2020). Correlations Between Prokaryotic Microbes and Stress-Resistant Algae in Different Corals Subjected to Environmental Stress in Hong Kong. *Front. Microbiol.* 11, 686. doi: 10.3389/fmicb.2020.00686

Walke, J. B., Becker, M. H., Loftus, S. C., House, L. L., Cormier, G., Jensen, R. V., et al. (2014). Amphibian Skin may Select for Rare Environmental Microbes. *Isme J.* 8, 2207–2217. doi: 10.1038/ismej.2014.77

Weigel, B. L., and Erwin, P. M. (2017). Effects of Reciprocal Transplantation on the Microbiome and Putative Nitrogen Cycling Functions of the Intertidal Sponge, *Hymeniacidon Heliophila*. *Sci. Rep.-Uk* 7, 43247. doi: 10.1038/srep43247

Weiland-Bräuer, N., Fischer, M. A., Pinnow, N., and Schmitz, R. A. (2019). Potential Role of Host-Derived Quorum Quenching in Modulating Bacterial Colonization in the Moon Jellyfish *Aurelia Aurita*. *Sci. Rep.-Uk* 9, 34. doi: 10.1038/s41598-018-37321-z

Weiland-Bräuer, N., Neulinger, S. C., Pinnow, N., Kunzel, S., Baines, J. F., and Schmitz, R. A. (2015). Composition of Bacterial Communities Associated With *Aurelia Aurita* Changes With Compartment, Life Stage, and Population. *Appl. Environ. Microb.* 81, 6038–6052. doi: 10.1128/Aem.01601-15

Weiland-Bräuer, N., Pinnow, N., Langfeldt, D., Roik, A., Gullert, S., Chibani, C. M., et al. (2020). The Native Microbiome is Crucial for Offspring Generation and Fitness of *Aurelia Aurita*. *Mbio* 11, e02336-20. doi: 10.1128/mBio.02336-20

Zhang, X. N., and Leadbetter, J. R. (2012). Evidence for Cascades of Perturbation and Adaptation in the Metabolic Genes of Higher Termite Gut Symbionts. *Mbio* 3, e00223-12. doi: 10.1128/mBio.00223-12

Zhang, F., Vicente, J., and Hill, R. T. (2014). Temporal Changes in the Diazotrophic Bacterial Communities Associated With Caribbean Sponges *Ircinia Stroblina* and *Mycale Laxissima*. *Front. Microbiol.* 5, 561. doi: 10.3389/fmicb.2014.00561

Ziegler, M., Seneca, F. O., Yum, L. K., Palumbi, S. R., and Voolstra, C. R. (2017). Bacterial Community Dynamics are Linked to Patterns of Coral Heat Tolerance. *Nat. Commun.* 8, 14213. doi: 10.1038/ncomms14213

Conflict of Interest: The authors declare that the research was conducted in the absence of any commercial or financial relationships that could be construed as a potential conflict of interest.

Publisher's Note: All claims expressed in this article are solely those of the authors and do not necessarily represent those of their affiliated organizations, or those of the publisher, the editors and the reviewers. Any product that may be evaluated in this article, or claim that may be made by its manufacturer, is not guaranteed or endorsed by the publisher.

frontiers | Frontiers in Marine Science

ORIGINAL RESEARCH
published: 19 May 2022
doi: 10.3389/fmars.2022.867234

Plume Layer Influences the Amazon Reef Sponge Microbiome Primary Producers

*Otávio H. B. Pinto[1], Till L. V. Bornemann[2], Rafael S. Oliveira[1], Tayna D. Frederico[1], Betania F. Quirino[3], Alexander J. Probst[2,4], Mayanne A. M. de Freitas[5], Fabiano L. Thompson[5] and Ricardo H. Kruger[1]**

[1] Laboratory of Enzymology, Institute of Biological Sciences, Department of Cell Biology, University of Brasília, Brasília, Brazil, [2] Aquatic Microbial Ecology, Environmental Microbiology and Biotechnology, Department of Chemistry, University of Duisburg-Essen, Essen, Germany, [3] Genetics and Biotechnology Laboratory, Embrapa-Agroenergy, Brasília, Brazil, [4] Centre of Water and Environmental Research (ZWU), University of Duisburg-Essen, Essen, Germany, [5] Department of Genetics, Institute of Biology, Federal University of Rio de Janeiro, Rio de Janeiro, Brazil

OPEN ACCESS

Edited by:
Sébastien Duperron, Muséum National d'Histoire Naturelle, France

Reviewed by:
Cara Fiore, Appalachian State University, United States
Marie-Charlotte Cheutin, Université de Montpellier, CNRS, France

***Correspondence:**
Ricardo H. Kruger
kruger@unb.br

Specialty section:
This article was submitted to Microbial Symbioses, a section of the journal Frontiers in Marine Science

Received: *31 January 2022*
Accepted: *13 April 2022*
Published: *19 May 2022*

Citation:
Pinto OHB, Bornemann TLV, Oliveira RS, Frederico TD, Quirino BF, Probst AJ, de Freitas MAM, Thompson FL and Kruger RH (2022) Plume Layer Influences the Amazon Reef Sponge Microbiome Primary Producers. Front. Mar. Sci. 9:867234. doi: 10.3389/fmars.2022.867234

Symbiont relationships between corals and photosynthetic microorganisms sustain coral reef existence. However, the Great Amazon Reef System (GARS) stays under a plume layer that attenuates the entry of light, and instead of corals, sponges are the major reef epifauna, for which little is known about the function of the associated microbiome. Here, we used genome-resolved metagenomics to investigate how the sponge microbiome supports its host and overcomes the reduced light availability, recovering 205 MAGs from *Agelas* and *Geodia* sponges with completeness >70% and contamination <10%. Beta diversity estimates based on the 16S rRNA genes indicated the microbiomes of Amazon and Caribbean sponges to be distinct ($P<0.01$), with heterotrophic lifestyles being prevalent in Amazon sponge microbiomes ($P<0.05$). Nevertheless, genes indicating the carbon fixation pathways 3-Hydroxypropionate/4-Hydroxybutyrate cycle, 3-Hydroxypropionate bicycle, Reductive Tricarboxylic Acid Cycle, and Calvin-Benson-Bassham cycle could be recovered in low abundance. The presence of Cyanobacteria, represented by both 16S rRNA analyses and low-quality MAGs indicated light incidence on the reef. The metabolic profile shows that the GARS sponge microbiome had genes for sulfate reduction, sulfur oxidation, nitric oxide reduction, ammonia oxidation, nitrate reduction, nitrite ammonification, nitrite oxidation, and nitrite reduction, indicating that the microbiome might play a role in detoxification of the holobiont. We conclude, that neither the plume-limited photosynthesis of the sponge microbiome nor the primary producers sustain the organic carbon input for the sponges, which likely live off plume-associated organic carbon and their heterotrophic microbiota.

Keywords: Carbon fixation, Host-associated, Metagenome-assembled genomes (MAGs), Sponge microbiome, the Great Amazon Reef System (GARS)

INTRODUCTION

Coral reefs are one of the most diverse ecosystems on the planet (Connell, 1978). Scleractinian corals that secrete calcium carbonate layers through the epidermis of the lower half of the column and the pedal disc are principal reef-builders (Drake et al., 2020). Other organisms such as coralline algae and hexactinellid sponges can contribute to reef formation when they leave their silica and carbonate skeletons. Despite occupying about 0.2% of the seafloor, coral reefs are responsible for sheltering and feeding at least one quarter of marine life (Knowlton and Jackson, 2001).

The coral food source comes from zooxanthellae, microscopic algae that live inside of it in a symbiotic relationship, and supply 90% of the coral's nutritional needs. Corals prefer shallow, warm, and oligotrophic waters to fix carbon by oxygenic photosynthesis using Calvin-Benson-Bassham (CBB) cycle (Stanley Jr, 2006). Muddy waters of large tropical rivers often inhibit the formation of coral reefs as sediment covers them and consequently decrease the light availability for the zooxanthella, compromising its source of nutrients. Despite the fact that tropical rivers exhibit these features, some biogenic reefs can be found at the Amazon River mouth.

Recently, scientists recognized a new biogenic reef system of 56,000 km^2 in the Amazon River mouth close to offshore oil companies (i.e., BHP-Billiton, Queiroz Galvão, Ecopetrol, Total, BP, and Petrobras) - the Great Amazon Reef System (GARS) (Moura et al., 2016). A mud layer called "plume", formed by organic and inorganic suspended material that spreads across the Atlantic Ocean, influences the formation of this reef. Instead of corals, coralline algae built the GARS foundation with small patches, platforms, and walls covered by scleractinians, sponges, octocorals, and black corals. Sponges that are adapted to this environment are the major reef epifauna. A total of 61 sponge taxa were identified in this ecosystem, with the most commonly found being *Agelas* spp., *Aplysina* spp., *Callyspongia vaginalis*, *Clathria nicolea*, *Monanchora arbuscula*, *Oceanapia bartschi*, and *Geodia* spp. (Moura et al., 2016). Sponges are known to filter water by choanocytes cells whose flagellar movement creates a water flux into their pores to capture dissolved organic matter (DOM), digest it (i.e., phagocytosis), and release particulate organic matter (POM) to higher trophic levels *via* the sponge loop (de Goeij et al., 2013).

Sponges have co-evolved with microbes for over 800 million years (Turner, 2021). The sponges' microbiota can represent approximately 35% of the holobiont biomass (Webster and Thomas, 2016). More than 47 sponge-inhabiting phyla were described, some of which were found exclusively in these invertebrates (Reveillaud et al., 2014). Their microbiota provides the holobionts the capacity to fix carbon, metabolize nitrogen, sulfur, and phosphate (Pita et al., 2018). Moreover, sessile organisms such as sponges rely on chemical compounds produced by their microbiota to defend against predators, competitors, and invading organisms such as bacteria, viruses, and microeukaryotes. In many cases, compounds isolated from sponge's microbiota are used as drug precursors and bioactive molecules in the pharmaceutical industry - being the most promising source for new bioactive products in the marine environment (Blunt et al., 2017). However, linking a specific microorganism from the sponge microbiota to a specific metabolic function and taxonomic group is a challenge, since many microorganisms are hard to cultivate in the laboratory, due to unknown growth requirements (Lewis and Ettema, 2019). Culture-independent techniques such as genome-resolved metagenomics allow reconstruction of draft genomes from the environment, enabling metabolic inferences for microorganisms that are little known or do not have yet cultivated representatives (Tyson et al., 2004).

In this context, the GARS sponge microbiome study provides insights into sponge microbiota's role and provides information for ecological surveillance, and prospecting focused on biotechnological research. In this work, we used metagenome-assembled genomes (MAGs) to investigate the potential metabolic contribution of the sponges microbiome (Hügler and Sievert, 2011) to sustain this holobiont in a reduced-light environment.

MATERIALS AND METHODS

Sample Collection, DNA Extraction, and Sequencing

Sponges were collected at the Amazon River mouth on September 27, 2014, latitude 1°17'59.3"N and longitude 46° 46'43.9"W. The selected sponges were *Agelas dispar*, *Agelas clathrodes*, *Agelas clathrodes*, *Geodia cf. corticostylifera*, *Geodia neptuni*, and *Geodia* sp. The criterion used for sponge selection was the availability of least three individuals per genus. The collected material was placed in plastic-containers holding 20 L of seawater at approximately 24°C and transported to the laboratory. In the laboratory, sponges were transferred to a container with 250 mL of sterile seawater and left for 5 to 10 minutes to remove microorganisms from the water not associated with the sponges. The sponge tissue was then dried and dissected with a scalpel, carefully removing associated macroscopic organisms. Approximately 1 g of sponge tissue was frozen in liquid nitrogen and powdered. DNA was extracted from the powder obtained and purified using 4 M guanidine hydrochloride, 50 mM Tris-HCl pH 8.0, 0.05 M EDTA, 0.5% sodium N-lauroylsarcosine and 1% β-mercaptoethanol, followed by a phenol/chloroform step, precipitation by isopropanol, and resuspension in 50 μL of ultrapure water (Trindade-Silva et al., 2012).

Sponge-microbiome holobiont libraries were constructed for each individual sample using the TruSeq Nano DNA kit, and sequenced with Novaseq system (Illumina®) at 20 GB sequencing depth with 150 bp paired-end reads. Reads were trimmed using Sickle (https://github.com/najoshi/sickle; version 1.33) with default parameters; BBtools (https://sourceforge.net/projects/bbmap/; version 35) was to check and if present remove Illumina adaptors and phiX sequences. Each metagenome was assembled individually using MetaSpades

version 3.1.3 (Nurk et al., 2017), and scaffolds smaller than 1 kb were removed.

16S Ribosomal RNA Taxonomic Composition and Beta Diversity

Metaxa2 extracted the ribosomal 16S RNA (16S rRNA) sequences from reads of the sponge-microbiome holobiont metagenomes, and compared it to the SSU default database (Bengtsson-Palme et al., 2015). We compared our data with the 16S rRNA (i.e., amplicon) microbiome associated with the sponges *Agelas* (SRR7068155, SRR7068157, SRR7068159, SRR7068173, SRR7068176, and SRR7068181) and *Geodia* (SRS9041395, SRS9041405, SRS9041416, SRS9041427, SRS9041573, and SRS9041575) from the Caribbean region (Indraningrat et al., 2019) (**Supplementary Data Set S1**). The Amazon plume water samples (i.e., whole metagenome sequencing) were also used for comparison (NCBI Bio-Project number PRJNA796108) (Silva et al., 2017). Those sequences were classified using Metaxa2 as described above.

To infer the influences of the Amazon plume water on the sponge microbiome, 16S rRNA classification data were normalized to their respective sequencing depth (i.e., relative abundance) and root-square transformed using the Hellinger method in the "decostand" function with R (R Core Team, 2021) (https://www.r-project.org/; version 4.1.2) package vegan (Oksanen et al., 2013). Shannon index was calculated using function "diversity", and Bray-Curtis dissimilarities were calculated using the "vegdist" function and their first two Principal Coordinates were plotted (PCoA). To test for the presence of statistically significant differences between microbiomes associated with Amazon sponges, Caribbean sponges, and the Amazon Plume water, we used Permutational Multivariate Analysis of Variance (PERMANOVA) with the "adonis2" command in the vegan package using 10,000 permutations and $\alpha = 0.05$. Kruskal-Wallis tested significant differences between three or more groups (i.e., Shannon index, MW-score functions), Wilcoxon tested for two groups comparisons (i.e., taxa differences between GARS and Caribbean microbiome), p-value adjusted with Benjamini-Hochberg method. We construct a Venn diagram using the venn package in R software (https://github.com/dusadrian/venn).

Metagenome Assemblies, Binning, and Analyses

We used MaxBin2 v2.2.4 with 40 and 107 markers (Wu et al., 2016) to recover metagenome assembled-genomes (MAGs). MAGs were aggregated using DASTOOL v1.1.2 (Sieber et al., 2018) and manually curated based on GC content, coverage and taxonomy using uBin v0.9.14 (Bornemann et al., 2020). MAGs were dereplicated with dRep v.3.2.2 (Olm et al., 2017), quality was checked with CheckM v1.0.13 (Parks et al., 2015), and coverage was calculated using CoverM v0.6.1 (https://github.com/wwood/CoverM).

MAGs with completeness >70% and contamination <10% were considered high-quality and used for further analysis (Bornemann et al., 2022). METABOLIC v4.0 (METabolic And BiogeOchemistry anaLyses In miCrobes) (Zhou et al., 2022) annotated and profiled metabolic traits, and assigned taxonomy to the selected MAGs. MW-score (metabolic weight score) was used to measure autotrophic and heterotrophic metabolism, as well as nitrogen and sulfur cycle functions on high-quality MAGs. MW-score is calculated by summing up all the coverage values of genes belonging to the function, and subsequently normalizing it to overall gene coverage.

METABOLIC determines carbon fixation pathways completeness by checking for the presence/absence of KEGG Orthology (KO) using hidden Markov model (HMM) profiles on KEGG modules. For dicarboxylate/4-hydroxybutyrate (DC/4-HB) cycles, Wood-Ljungdahl (WL) pathway, and reductive tricarboxylic acid (rTCA) pathways, we used METABOLIC 75% default cutoff. For 3-Hydroxypropionate/4-hydroxybutyrate (3HP/4HB), 3-Hydroxypropionate bicycle (3HP), and CBB we used custom cutoffs. Hmmsearch (https://hmmer.org/; HMMER 3.1b2) comparison with genomes that participate in each carbon fixation pathway determined custom E-values cutoff. We searched for the missing genes using hmmsearch on Hmm profiles described above with a less restricted cutoff. We defined 36% pathway completeness and key-enzyme 4-hydroxybutyryl-CoA dehydratase/vinylacetyl-CoA-Delta-isomerase (K14534) for 3HP/4HB. This choice was based on the comparison of 3HP/4HB genes with some high-quality Thermoproteota MAGs (>95% completeness and no contamination) and *Nitrosopumilus maritimus* (GCF_000018465.1), which is well known to participate in this pathway. For 3HP, we used 58% pathway completeness. For CBB, we selected MAGs with 70% pathway completeness and searched for the key-enzyme Rubisco using hmmsearch with a less restrictive cutoff (E-value, 1.3E-117) to classify the Rubisco type.

High-quality MAGs were assigned to a taxonomic group using GTDB-Tk database version 202 (Parks et al., 2018) on METABOLIC workflow. GTDB-Tk concatenates a set of 120 bacterial and 122 archaeal ubiquitous single-copy markers to build the phylogeny (Parks et al., 2017). We removed taxonomically distant reference genomes to improve visualization. Protein alignments were performed using MAFFT v7.405 (Katoh, 2002) with default parameters. A phylogenetic tree was obtained using FastTree v2.1.11 (Price et al., 2010), and visualized with Geneious Prime 2022.0.1 (https://www.geneious.com). We rooted the tree using the following genomes: for Archaea phylogeny *Methanosarcina acetivorans* (RS_GCF_000007345.1) was used, while for bacteria phylogeny we used *Mycoplasma genitalium* (RS_GCF_000027325.1). Genomic data (draft genomes and metagenomic reads) used in this study are deposited at NCBI under Bio-Project number PRJNA795684.

RESULTS

The Plume Water Contributes to a Unique and High Diversity GARS Sponge Microbiome

A total of 1.26 billion fastq sponge microbiome reads were recovered. These belonged to *Agelas dispar* (16.27% of total), *Agelas clathrodes* (18.02% of total), *Agelas clathrodes* (17.06% of

total), *Geodia cf. corticostylifera* (14.84% of total), *Geodia neptuni* (13.81% of total), and *Geodia* sp. (20% of total).

Based on 16S rRNA composition analysis (**Figure 1**), the GARS microbiomes of *Agelas* and *Geodia* sponges showed little differences at phylum level, and a high abundance of unclassified bacteria (25.8 ± 2.90%). Relative abundance shows that Proteobacteria (30.3 ± 5.1%) was the most abundant taxon in all samples. The dominant classes in the Proteobacteriota superphylum were Gammaproteobacteria (14.38 ± 2.79%), Alphaproteobacteria (7.46 ± 2.39%) and Deltaproteobacteria (4.54 ± 0.84%). Betaproteobacteria was also detected, but in fewer proportion. The other most abundant phyla were Firmicutes (16.5 ± 4.3%), Actinobacteriota (8.8 ± 1.2%), Chloroflexota (4.7 ± 0.9%), Acidobacteriota (4.0 ± 1.3%), Thermoproteota (3.9 ± 1.7%), Nitrospirota (2.1 ± 0.5%), and Spirochaetota (1.7 ± 0.7%).

Shannon alpha diversity (**Figure 2A**) indicted higher diversity in the GARS sponge microbiome, followed by plume water and Caribbean sponge (Kruskal-Wallis test, chi-squared = 16.328, df = 2, $P < 0.001$). The GARS sponge microbiome showed to be the most The GARS sponge microbiome showed to be the most unique with 1476 taxa. The Amazon plume water influences the GARS sponge microbiome with 92 taxa uniquely shared. Sponge samples shared exclusively 488 taxa, and 186 were ubiquitous in all groups tested (**Figure 2B**).

Beta diversity analysis (**Figure 2C**) showed that the Amazon sponge microbiome composition differed from the Caribbean and plume water samples (PERMANOVA, df = 2, F = 8.6343, R^2 = 0.42884, $P < 0.001$). On the class level, there were 32 taxa (**Figure 2D**) statistically different that contributed to the differences between the GARS and Caribbean sponge microbiome (Wilcoxon test, $P < 0.05$). The Amazon sponge microbiome is more similar to that of the Caribbean sponges, which are unimpacted by the plume, than to the plume water samples. Amazon *Agelas* and *Geodia* microbiomes grouped, while the *Agelas dispar* microbiome was found to be the most different among the six. We detected subgroups between Caribbean samples relative to the *Agelas* from Curacao and *Geodia* from Cayman Island and Belize locations (i.e., marked in blue). The Curacao *Agelas* samples are the six bottom blue circles in the cluster, while the *Geodia* samples near Cayman Island and Belize are the six top blue rectangles (**Figure 2C**).

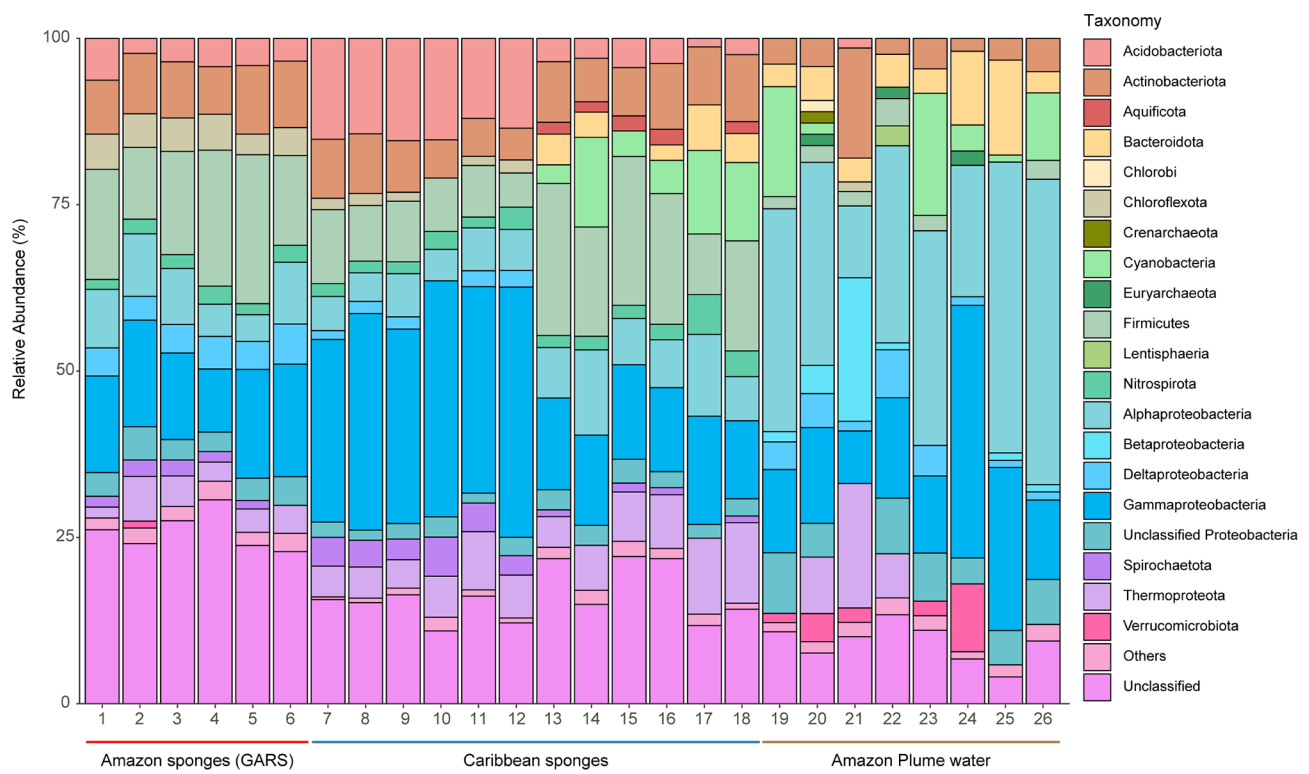

FIGURE 1 | Relative abundance of 16S ribosomal RNA (16S rRNA) sequences in different microbiomes from GARS sponges, Caribbean sponges, and Amazon plume water. Amazon sponges (GARS) are highlighted with a red bar below: 1, *Agelas dispar*; 2, *Agelas clathrodes* 1; 3 *Agelas clathrodes* 2; 4, *Geodia cf. corticostylifera*; 5, *Geodia neptuni*; 6, *Geodia* sp. Caribbean sponges are highlighted with a blue bar below. Carribean *Geodia* sp. samples: 7, SRS9041575; 8, SRS9041573; 9, SRS9041427; 10, SRS9041416; 11, SRS9041405; 12, SRS9041395. Carribean *Agelas sventres* samples: 13, SRR7068181; 14, SRR7068176; 15, SRR7068173; 16, SRR7068159; 17, SRR7068157; 18, SRR7068155. Amazon plume water samples are highlighted with a brown bar below: 19, St15; 20, St11; 21, St10; 22, St6; 23, St5; 24, St4; 25, St3; and 26, St1. Relative abundance of 16S rRNA sequences are colored according to phyla. "Others" are microbiome phyla that were below 1% relative abundance. We split Proteobacteria superphylum into classes.

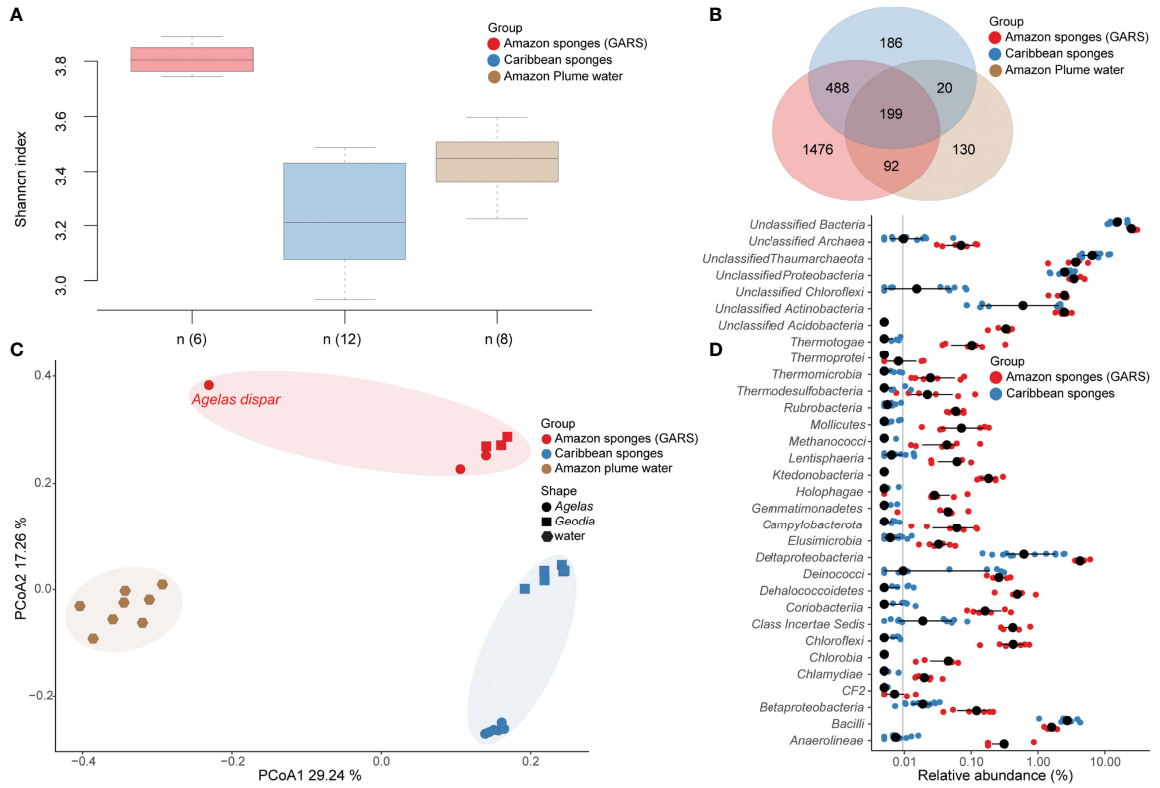

FIGURE 2 | Microbiome composition comparison between GARS sponges Caribbean sponges and Amazon plume water samples. **(A)** Shannon Alpha diversity variation in sponge's microbiome from the GARS (red) and the Caribbean (blue), as well as the Amazon plume water (brown) microbiome (Kruskal-Wallis test, chi-squared = 16.328, df = 2, $P < 0.001$). The (n) represents the number of samples in each box plot. Wilcoxon pairwise comparisons show that all groups tested were statistically different ($P < 0.05$). **(B)** Venn diagram of microbiome taxa that are unique or shared between sponges from the GARS (red) and the Caribbean (blue), as well as the Amazon plume water microbiome (brown). **(C)** Beta diversity of microbiomes associated with *Agelas* and *Geodia* sponges from the GARS (red) and the Caribbean (blue), as well as the Amazon plume water microbiome (brown) by principal coordinate analysis (PCoA) of Bray–Curtis dissimilarity ($R^2 = 0.43$ $P=0.0001$). Each point represents a microbiome sample, *Agelas* are represented by circles, *Geodia* by rectangles, and water samples by hexagons. **(D)** Microbiome class level relative abundance differences between GARS and Caribbean sponges. GARS sponge's microbiome is shown by red circles, while Caribbean sponges microbiome is shown by blue circles. Black circles are the median relative abundance for a specific taxa to the class level.

Metagenome-Assembled Genome Classification

A total of 1,054 metagenome-assembled genomes (MAGs) were recovered from the Amazon reef sponge microbiome. Of these, 205 MAGs had completeness greater than 70%, and contamination below 10% (**Supplementary Data Set S2**). Within these 205 high-quality MAGs, we recovered bacterial genomes belonging to: Proteobacteria (49), Chloroflexota (47), Acidobacteriota (18), Actinobacteriota (16), Desulfobacterota (14), Bdellovibrionota (10), Poribacteria (10), Latescibacterota (8), Gemmatimonadota (5), Spirochaetota (4), Nitrospinota (3), Nitrospirota (3), Verrucomicrobiota (3), Deinococcota (2), Bacteroidota (1), and SAR324 (1). For archaea, we recovered Thermoproteota (10), and Nanoarchaeota (1). Within the 1,054 genomes, two Cyanobacteria MAGs were identified, but were not included in our analysis because they did not meet the quality cut-off. 16S rRNAs genes of Firmicutes origin were one of the most abundant in the metagenome, but they lack representatives in high-quality MAGs.

GARS Sponge Microbiome Metabolism Analysis

As shown in **Figure 3**, autotrophic metabolism related genes represent a small portion of the community's genes. 3HB/4HP and 3HP were the most significant autotrophic pathways and scored higher than rTCA (Wilcoxon test, $P < 0.01$). CBB metabolism scored the lowest of all autotrophic networks studied. Genes related to WL and DC/4-HB profile were absent. Gene coverage and metabolic profiles revealed absence of photosynthetic capacity in the high-quality MAGs from the plume-adapted Amazon sponge microbial community. On the other hand, heterotrophic metabolism represented by fermentation, acetate oxidation, complex carbon degradation, and aromatics degradation functions were more abundant than autotrophic gene metabolism coverage in high-quality MAGs (Kruskal-Wallis test, $P < 0.05$).

Sulfate reduction was the most abundant function identified in the plume-adapted Amazon sponge microbial community, with sulfur oxidation and nitric oxide reduction functions also

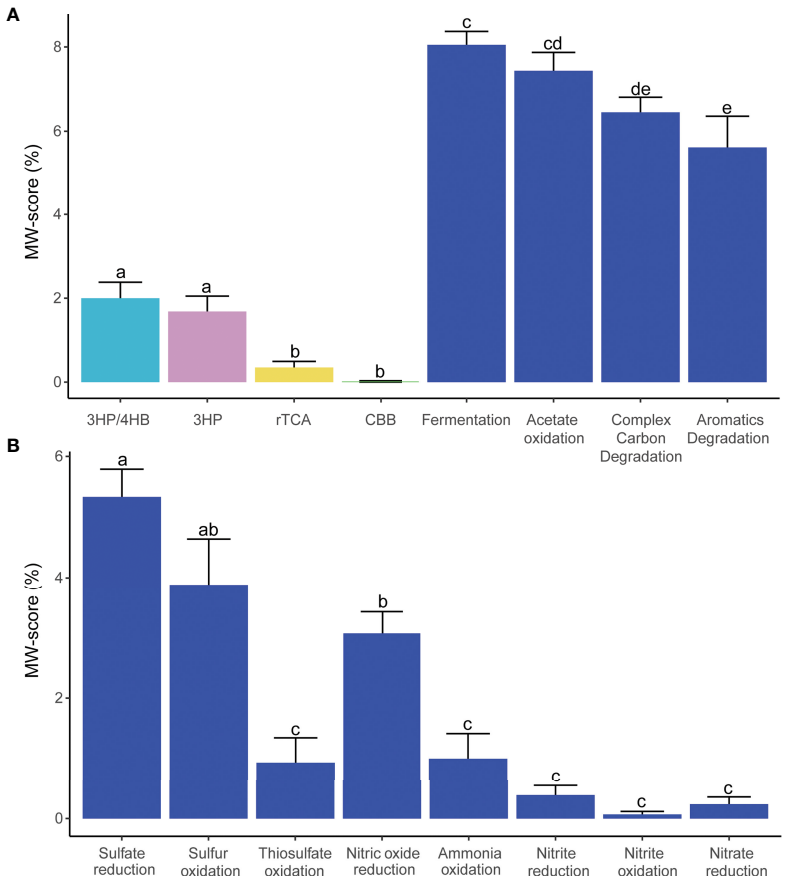

FIGURE 3 | Microbiome metabolism profile based on metabolic weight score (MW-score). **(A)** Comparison between autotrophic and heterotrophic metabolisms. Autotrophic: 3-Hydroxypropionate/4-hydroxybutyrate (3HP/4HB), 3-Hydroxypropionate bicycle (3HP), Reductive tricarboxylic acid (rTCA), and Calvin–Benson–Bassham cycle (CBB); Heterotrophic: Fermentation, Acetate oxidation, Complex carbon degradation, and Aromatics degradation. **(B)** Comparison between sulfur and nitrogen metabolism. Bars with different letters indicate statistical differences at $P < 0.05$; those with the same letters indicate no statistical difference.

being high. Sulfate reduction was a widespread function detected in 13 phyla with contribution from Chloroflexota (32), Gammaproteobacteria (14), Acidobacteriota (13), Thermoproteota (10), Poribacteria (9), Latescibacterota (6), Alphaproteobacteria (4), Gemmatimonadota (3), Verrucomicrobiota (3), Actinobacteriota (2), Deinococcota (2), Desulfobacterota (1), Nitrospinota (1), and Nitrospirota (1) MAGs. Sulfur oxidation was predicted in nine phyla, including Gammaproteobacteria (15), Alphaproteobacteria (14), Desulfobacterota (13), Thermoproteota (10), Actinobacteriota (9), Chloroflexota (8), Acidobacteriota (7), Bdellovibrionota (1), Latescibacterota (1), and Poribacteria (1) MAGs. We detected nine phyla predicted to participate in nitric oxide reduction function; associated with MAGs from Gammaproteobacteria (13), Desulfobacterota (10), Poribacteria (9), and Acidobacteriota (5), Alphaproteobacteria (3), Nitrospinota (3), Chloroflexota (2), Spirochaetota (2), Latescibacterota (1), and Nitrospirota (1) (**Supplementary Data Set S3**). We did not detect differences between reductive and oxidative metabolisms.

We detected the presence of other metabolic networks, although not as abundantly represented, such as thiosulfate oxidation, ammonia oxidation, nitrite reduction, nitrite oxidation, and nitrate reduction. Sulfide oxidation, sulfur reduction, sulfite reduction, nitrogen fixation, nitrous oxide reduction, and anammox functions were absent.

Metagenome-Assembled Genomes (MAGs) Autotrophic Metabolism Prediction

As shown in **Figure 4**, from 205 high-quality MAGs, 36 were predicted to participate in autotrophic metabolism pathways. We predicted the highest number of genomes with rTCA function belonging to Acidobacteriota (6), Actinobacteriota (4), Gammaproteobacteria (2), Chloroflexota (2), Latescibacterota (2), Bacteroidota (1), Verrucomicrobiota (1), and Spirochaetota (1). The key-enzymes succinate dehydrogenase/fumarate reductase, and 2-oxoglutarate/2-oxoacid ferredoxin oxidoreductase were detected for all selected MAGs, the exception was ATP-citrate lyase alpha-subunit, which was not identified. METABOLIC detected ATP-citrate lyase alpha-subunit gene in Nitrospirota and Desulfobacterota MAGs that had 3HP completeness between 66-41% and were not selected for analysis. METABOLIC did not detect ATP-citrate lyase alpha-subunit in selected high-quality MAGs, but they were

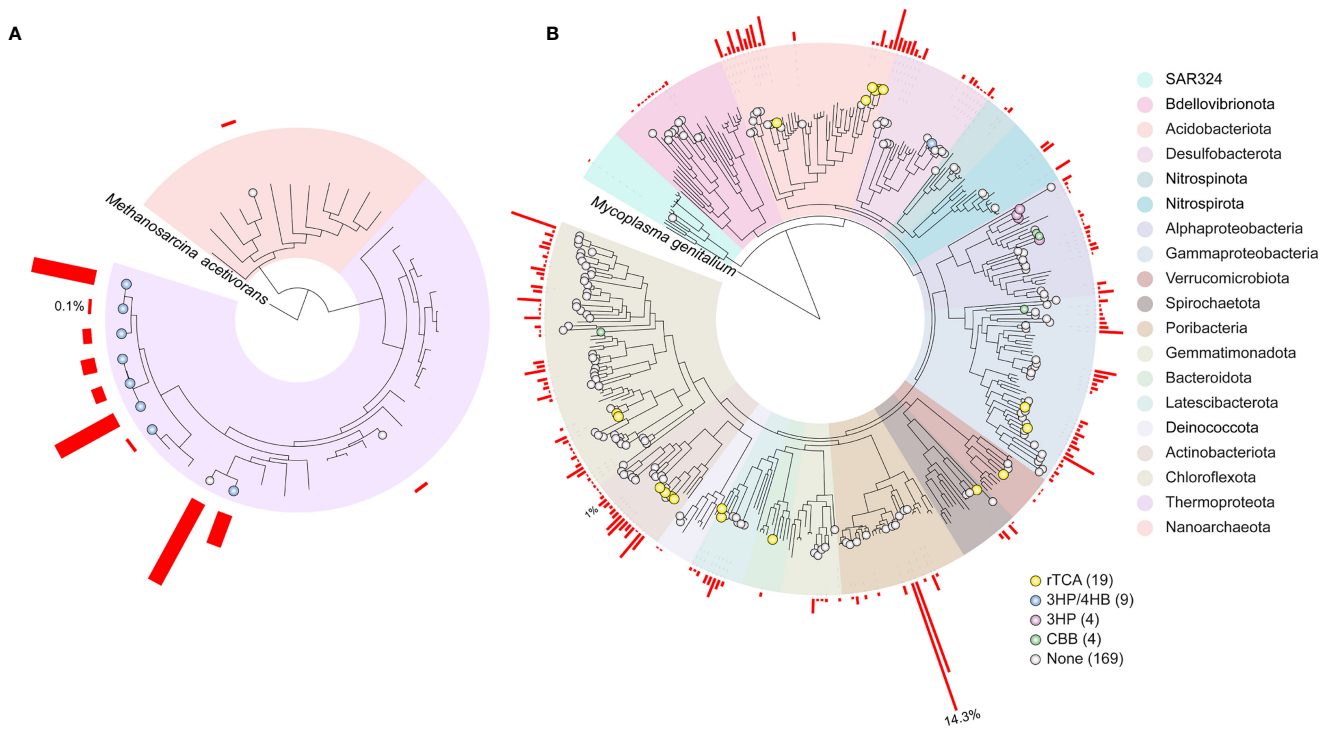

FIGURE 4 | Phylogeny of metagenome-assembled genome (MAGs) in GARS. **(A)** Archaea MAGs phylogeny, **(B)** Bacteria MAGs phylogeny. The bacterial and archaeal trees are rooted to *Methanosarcina acetivorans* (RS_GCF_000007345.1) and *Mycoplasma genitalium* (RS_GCF_000027325.1), respectively. MAGs related to carbon fixation pathways are shown with circles: Reductive tricarboxylic acid (rTCA), yellow; Calvin–Benson–Bassham cycle (CBB), green; 3-Hydroxypropionate/4-hydroxybutyrate (3HP/4HB), blue; 3-Hydroxypropionate bicycle (3HP), purple. MAGs that did not meet the chosen METABOLIC carbon fixation cut-off are marked in grey (none). The number of MAGs in each carbon fixation pathway is shown in parentheses. Phylogeny of the MAGs is shaded by phylum, Proteobacteria were split into classes. The red bars next to each MAG represents the its abundance coverage (%) in the GARS sponge microbiome.

detected with E-value between 2.00E-71 and 7.7E-68, using hmmsearch.

We selected eight Thermoproteota Nitrosopumilaceae, and one Desulfobacterota with possible involvement in the 3-hydroxypropionate/4-hydroxybutyrate (3-HP/4-HB) cycle. All selected genomes presented the key enzyme 4-hydroxybutyryl-CoA dehydratase/vinylacetyl-CoA-Delta-isomerase. These genomes showed 36% maximum completeness for the 3-HP/4-HB, but considering a less restrictive E-values cutoff, Thermoproteota genomes have all missing genes. Meanwhile, malonyl-CoA/succinyl-CoA reductase (NADPH) was absent for Desulfobacterota even in these less restrictive conditions.

The CBB cycle was identified in four MAGs. The Rubisco type I prediction was assigned to one Alphaproteobacteria Rhodobacterales and one Gammaproteobacteria Arenicellales. The Rubisco type IV prediction was assigned to one Dehalococcoidia within Chloroflexota and one Rhodobacterales.

We observed the highest completeness 3-Hydroxypropionate bicycle (3-HP) genes (58.3%) in four Rhodobacteraceae. These genomes lack the key enzymes: malonyl-CoA reductase/3-hydroxypropionate dehydrogenase (NADP+) and acrylyl-CoA reductase (NADPH)/3- hydroxypropionyl-CoA dehydratase/3-hydroxypropionyl-CoA synthetase. Considering a less restrictive gene cutoff, we detected all missing genes.

DISCUSSION

We found that the sponge's microbiome from the Great Amazon Reef System (GARS) is a unique community. The Amazon water turbidity-related microbiome influences the GARS sponge microbiome. However, data suggest more influences due to environmental features than to the shared microbiota. Significantly, and in contrast to other Reef systems, photosynthetic microorganisms (Cyanobacteria) were only present in low proportion in both 16S rRNA and MAG community analysis. GARS microbiome's high diversity suggests that the plume layer does not restrict or enrich the microbiota for a specific taxonomic group. Moreover, 32 taxa on the class level were statistically different between the sponge microbiomes from GARS and traditional Caribbean reefs, indicating muddy water contributes to an adapted microbiota. Microbiome comparisons between the Caribbean (i.e., Curacao, Cayman Island, and Belize) and the Amazon region using

sponges from the same genera, and two different genera, show that the findings are more general than they would be if we had made this comparison using a single genus and Caribbean location. Light in the GARS floor is faint but sufficient; a study shows the presence of photosynthetically available radiation (PAR) between 0.01 and 19.3 μE m^{-2} s^{-1} (Francini-Filho et al., 2018). Such ratio can support photosynthesis, and coralline algae reef-builders have been present in the GARS for at least 4487 years before today (Moura et al., 2016). Studies suggested high sedimentation as a principal stress factor in GARS, which results in total or partial GARS coverage in sediment (Moura et al., 2016; Omachi et al., 2019).

The data indicate a predominant heterotrophic lifestyle for the GARS sponge microbiota. The large amount of organic matter carried by the Amazon River may explain the sponge's success in this ecosystem (Medeiros et al., 2015; Moura et al., 2016). A study revealed that dissolved organic carbon in the GARS region varies from 102.3 to 165.69 μM, and particulate organic carbon from 4.1 to 6.21 μM (unpublished data). The sponges' microbiota also recycles and benefits from DOM (Azam et al., 1983) and contribute to more than half of the sponges' diet (Kazanidis et al., 2018; Rix et al., 2020; Bart et al., 2021). Estimates that one sponge kilogram can filter 50,000 L of water daily and remove more than 90% of microbes in the water (Hill and Hill, 2009). Studies have demonstrated that photosynthetic net reduction and heterotrophic capacity enhancement are adaptive responses to overcome extreme conditions in turbid reefs (Burt et al., 2020).

Autotrophic microorganisms have an auxiliary role in the GARS sponge microbiome. MW-score indicates Calvin–Benson–Bassham (CBB) as the least relevant carbon fixation pathway present in the plume-adapted Amazon sponge microbial community, in stark contrast to the open ocean, where Cyanobacteria and algae are the major organisms responsible for carbon fixation through the CBB pathway (Raven, 2009; Bowler et al., 2010). Our MAGs analysis predicted CBB to occur in Rhodobacterales and Arenicellales. Rubisco type IV detected in a Chloroflexota MAG are related to functions other than carbon fixation (Tabita et al., 2007a; Tabita et al., 2007b). The presence of CBB cycle genes, especially Rubisco, in Proteobacteria and Rhodobacterales, has already been described, including the sponge microbiome (Badger and Bek, 2008; Asplund-Samuelsson and Hudson, 2021).

Metabolic predictions indicated 3HP/4HB as the most relevant carbon fixation pathway in the GARS sponge's microbiome, significantly more abundant than CBB and rTCA (Wilcoxon test, $P < 0.05$). We predicted 3HP/4HB to occur in Thermoproteota and one Desulfobacterota MAG. The 3HP/4HB capability for the Desulfobacterota MAG remains uncertain as one of the two marker genes, the malonyl-CoA/succinyl-CoA reductase (NADPH) gene, could not be identified in this MAG. Additionally, the bacterial 4-hydroxybutyryl-CoA dehydratase is involved in the fermentation of aminobutyrate (Buckel and Golding, 2006). These findings were based on high-quality MAGs gene content and coverage observations - not expression data. Furthermore, it is important to note that genome-resolved metagenomics recovers just a fraction of the genomes present in the microbial community. The purpose of this study was to use *in silico* analyses to access the microbial functional capacity of samples for which there is no experimental information available.

Thaumarchaeota's (Thermoproteota) variation in the 3HP/4HB pathway is well-described and considered the most energy-efficient aerobic carbon fixation pathway (Walker et al., 2010; Pester et al., 2011; Konneke et al., 2014). Studies have demonstrated the presence of Thaumarchaeota in the Amazon plume water and the sponge microbiome (Engelberts et al., 2020; Pinto et al., 2020). Our data indicate that these microorganisms play multiple roles in the sponge-microbiome holobiont physiology; besides carbon fixation, we predicted ammonia oxidation, sulfur oxidation, and sulfate reduction functions. Ammonia is the sponge's main waste product, which is toxic at high levels. Ammonia oxidation can prevent its accumulation within sponge tissues. The same happens for sulfur oxidation, which prevents hydrogen sulfide levels to become high (Taylor et al., 2007).

Another predicted carbon fixation pathway was the 3-hydroxypropionate bicycle (3HP). This pathway was first described in *Chloroflexus aurantiacus*, a Chloroflexaceae member able to perform anoxygenic photosynthesis (Herter et al., 2001; Zarzycki et al., 2009). In our taxonomic analysis, we identified the presence of Chloroflexota MAGs related to Anaerolineae, Dehalococcoidia, and UBA223 families, not previously described as having this pathway. The MAGs predicted to encode this pathway in our GARS sponge microbiome were classified as Rhodobacteraceae. One study suggested *Dinoroseobacter shibae* a member of Rhodobacteraceae with mixotrophic metabolism, assimilating glucose by Entner-Doudoroff and fixing carbon by 3-hydroxypropionate bicycle (Tomasch et al., 2011). Alternative CO_2 fixation pathways may facilitate the assimilation of simple organic substances, conferring a competitive advantage over obligate autotrophs or heterotrophs (Hügler and Sievert, 2011). The genomic comparison of 3HP genes between our MAGs and *D. shibae* showed that they are similar.

The same uncertainty occurs for rTCA genes encoding MAGs, where hmmsearch detected the ATP-citrate lyase alpha-subunit only when a less restrictive cutoff was used. The rTCA pathway was predicted to be the most taxonomically wide-spread pathway in the GARS sponge microbiome within Acidobacteriota, Gammaproteobacteria, Latescibacterota, Bacteroidota, Chloroflexota, Actinobacteriota, Verrucomicrobiota, and Spirochaetota. An incomplete rTCA cycle was found in phylum Acidobacteriota (Fernandez et al., 2020), Bacteroidota *Salinibacter ruber* (Bagheri et al., 2019) and other phyla like Actinobacteriota and Chloroflexota (Vikram et al., 2016). Among our low-quality MAGs, we have recovered members of Aquificota, which like Chlorobiota and Campylobacterota are often described to participate in rTCA (Hügler and Sievert, 2011). Due to the oxygen sensibility of its enzymes, the rTCA pathway is usually found in anaerobes associated with deep-sea hydrothermal vents and dark oceans and in microorganisms found in microaerophilic conditions (Berg, 2011; Erb, 2011). These data corroborate with

dissolved oxygen (i.e., 3.25-3.81 mg. L-1) values reported in the GARS (unpublished data).

Prediction of the complex metabolic pathways was the main limitation of this study. Those pathways have many promiscuous genes, which makes it difficult to establish their involvement in any specific pathway. Furthermore, database profiles are incomplete. Sometimes genes that have already been shown to participate in a pathway have not yet been included in the database. An example is the 3HP/4HB pathway that lacks genes from Thaumarchaeta on the KEGG profile – making it difficult to identify non-classic pathways. Crenarchaeal Sulfolobales genes were used to construct the 3HP/4HB pathway profile found in the database used in this study. Additionally, the metabolic characterization of organisms based on their metabolic potential can not be used to predict their *in vivo* metabolism. Hence, further experimental validation is necessary, either culture independently through, e.g., Meta-Transcriptomics and -Proteomics, or through cultivation followed by the characterization of the culture.

In summary, our data indicate that although the plume induces a low light stress on the GARS sponge microbiome, it does not completely prevent Cyanobacteria occurrence. Specifically, we found a predominance of heterotrophic compared to autotrophic metabolism in the plume-adapted Amazon sponge microbial community. We propose that in GARS, sponges accumulate dissolved organic matter (DOM), which is assimilated by themselves as well as its heterotrophic microbiota. In addition, the sponges' microbiota might act in the detoxification of toxic compounds released by the sponge.

Other turbid reefs present similar conditions of restricted luminosity or sedimentation to those found by GARS sponges (Zweifler (Zvifler) et al., 2021). However, none of these environments receive such a large water flux. The Amazon River discharges 20% of global freshwater into the Atlantic Ocean (Richey et al., 1990; Dai and Trenberth, 2002). This huge water flux into the ocean drastically changes environmental parameters such as salinity, pH, luminosity, oxygenation, and sedimentation, thus creating the unique environment of GARS. This study shows a different biomass accumulation strategy for GARS sponge microbiome from that of traditional sponge microbiomes. The uniqueness of the GARS sponge microbiome is ripe for biotechnological exploration, as new genes and drug precursors may be discovered. In addition, from an ecological perspective, the GARS microbiome data may be useful for surveillance efforts of potential impacts of offshore oil and gas operations near this region.

DATA AVAILABILITY STATEMENT

The datasets presented in this study can be found in online repositories. The names of the repository/repositories and accession number(s) can be found below: https://www.ncbi.nlm.nih.gov/, PRJNA796108.

AUTHOR CONTRIBUTIONS

OP and RK designed the study. Data analyses were performed by OP, TB, AP, TF, and RO. Data collection was performed by FT and MF. The manuscript was drafted by OP and revised by all authors, BQ critically reviewed and substantially edited the manuscript. All authors have read and approved the manuscript.

FUNDING

This study was financially supported by the Conselho Nacional de Desenvolvimento Científico e Tecnológico (CNPq), Coordenação de Aperfeiçoamento de Pessoal de Nível Superior (CAPES), which also provided financial support for the first author (OP), Fundação de Amparo à Pesquisa do Estado do Rio de Janeiro (FAPERJ), and Fundação de Apoio à Pesquisa do Distrito Federal (FAP-DF). TB and AP were supported by the Ministry of Culture and Science of North Rhine-Westphalia (Nachwuchsgruppe "Dr. Alexander Probst").

ACKNOWLEDGMENTS

The authors thank Conselho Nacional de Desenvolvimento Científico e Tecnológico (CNPq), Fundação de Amparo à Pesquisa do Estado do Rio de Janeiro (FAPERJ), and Fundação de Apoio à Pesquisa do Distrito Federal (FAP-DF) for financial support. Pinto acknowledges fellowships from Coordenação de Aperfeiçoamento de Pessoal de Nível Superior (CAPES).

SUPPLEMENTARY MATERIAL

The Supplementary Material for this article can be found online at: https://www.frontiersin.org/articles/10.3389/fmars.2022.867234/full#supplementary-material

REFERENCES

Asplund-Samuelsson, J., and Hudson, E. P. (2021). Wide Range of Metabolic Adaptations to the Acquisition of the Calvin Cycle Revealed by Comparison of Microbial Genomes. *PloS Comput. Biol.* 17, e1008742. doi: 10.1371/journal.pcbi.1008742

Azam, F., Fenchel, T., Field, J., Gray, J., Meyer-Reil, L., and Thingstad, F. (1983). The Ecological Role of Water-Column Microbes in the Sea. *Mar. Ecol. Prog. Ser.* 10, 257–263. doi: 10.3354/meps010257

Badger, M. R., and Bek, E. J. (2008). Multiple Rubisco Forms in Proteobacteria: Their Functional Significance in Relation to CO2 Acquisition by the CBB Cycle. *J. Exp. Bot.* 59, 1525–1541. doi: 10.1093/jxb/erm297

Bagheri, M., Marashi, S.-A., and Amoozegar, M. A. (2019). A Genome-Scale Metabolic Network Reconstruction of Extremely Halophilic Bacterium Salinibacter Ruber. *PloS One* 14, e0216336. doi: 10.1371/journal.pone.0216336

Bart, M. C., Hudspith, M., Rapp, H. T., Verdonschot, P. F. M., and de Goeij, J. M. (2021). A Deep-Sea Sponge Loop? Sponges Transfer Dissolved and Particulate

Organic Carbon and Nitrogen to Associated Fauna. *Front. Mar. Sci.* 8. doi: 10.3389/fmars.2021.604879

Bengtsson-Palme, J., Hartmann, M., Eriksson, K. M., Pal, C., Thorell, K., Larsson, D. G. J., et al. (2015). Metaxa 2: Improved Identification and Taxonomic Classification of Small and Large Subunit rRNA in Metagenomic Data. *Mol. Ecol. Resour.* 15, 1403–1414. doi: 10.1111/1755-0998.12399

Berg, I. A. (2011). Ecological Aspects of the Distribution of Different Autotrophic CO_2 Fixation Pathways. *Appl. Environ. Microbiol.* 77, 1925–1936. doi: 10.1128/AEM.02473-10

Blunt, J. W., Copp, B. R., Keyzers, R. A., Munro, M. H. G., and Prinsep, M. R. (2017). Marine Natural Products. *Nat. Prod. Rep.* 34, 235–294. doi: 10.1039/C6NP00124F

Bornemann, T. L. V., Adam, P. S., Turzynski, V., Schreiber, U., Figueroa-Gonzalez, P. A., Rahlff, J., et al. (2022). Genetic Diversity in Terrestrial Subsurface Ecosystems Impacted by Geological Degassing. *Nat. Commun.* 13, 284. doi: 10.1038/s41467-021-27783-7

Bornemann, T. L. V., Esser, S. P., Stach, T. L., Burg, T., and Probst, A. J. (2020). Ubin – A Manual Refining Tool for Metagenomic Bins Designed for Educational Purposes. *Genomics*. doi: 10.1101/2020.07.15.204776

Bowler, C., Vardi, A., and Allen, A. E. (2010). Oceanographic and Biogeochemical Insights From Diatom Genomes. *Annu. Rev. Mar. Sci.* 2, 333–365. doi: 10.1146/annurev-marine-120308-081051

Buckel, W., and Golding, B. T. (2006). Radical Enzymes in Anaerobes. *Annu. Rev. Microbiol.* 60, 27–49. doi: 10.1146/annurev.micro.60.080805.142216

Burt, J. A., Camp, E. F., Enochs, I. C., Johansen, J. L., Morgan, K. M., Riegl, B., et al. (2020). Insights From Extreme Coral Reefs in a Changing World. *Coral Reefs* 39, 495–507. doi: 10.1007/s00338-020-01966-y

Connell, J. H. (1978). Diversity in Tropical Rain Forests and Coral Reefs: High Diversity of Trees and Corals Is Maintained Only in a Nonequilibrium State. *Science* 199, 1302–1310. doi: 10.1126/science.199.4335.1302

Dai, A., and Trenberth, K. E. (2002). Estimates of Freshwater Discharge From Continents: Latitudinal and Seasonal Variations. *J. Hydrometeor.* 3, 660–687. doi: 10.1175/1525-7541(2002)003<0660:EOFDFC>2.0.CO;2

de Goeij, J. M., van Oevelen, D., Vermeij, M. J.A., Osinga, R., Middelburg, J. J., de Goeij, A. F.P.M., et al. (2013). Surviving in a Marine Desert: The Sponge Loop Retains Resources Within Coral Reefs. *Science* 342,108–110. doi: 10.1126/science.1241981

Drake, J. L., Mass, T., Stolarski, J., Von Euw, S., Schootbrugge, B., and Falkowski, P. G. (2020). How Corals Made Rocks Through the Ages. *Glob. Change Biol.* 26, 31–53. doi: 10.1111/gcb.14912

Engelberts, J. P., Robbins, S. J., de Goeij, J. M., Aranda, M., Bell, S. C., and Webster, N. S. (2020). Characterization of a Sponge Microbiome Using an Integrative Genome-Centric Approach. *Isme J.* 14, 1100–1110. doi: 10.1038/s41396-020-0591-9

Erb, T. J. (2011). Carboxylases in Natural and Synthetic Microbial Pathways. *Appl. Environ. Microbiol.* 77, 8466–8477. doi: 10.1128/AEM.05702-11

Fernandez, L., Peura, S., Eiler, A., Linz, A. M., McMahon, K. D., and Bertilsson, S. (2020). Diazotroph Genomes and Their Seasonal Dynamics in a Stratified Humic Bog Lake. *Front. Microbiol.* 11. doi: 10.3389/fmicb.2020.01500

Francini-Filho, R. B., Asp, N. E., Siegle, E., Hocevar, J., Lowyck, K., D'Avila, N., et al. (2018). Perspectives on the Great Amazon Reef: Extension, Biodiversity, and Threats. *Front. Mar. Sci.* 5. doi: 10.3389/fmars.2018.00142

Herter, S., Farfsing, J., Gad'On, N., Rieder, C., Eisenreich, W., Bacher, A., et al. (2001). Autotrophic CO_2 Fixation by *Chloroflexus Aurantiacus*: Study of Glyoxylate Formation and Assimilation *via* the 3-Hydroxypropionate Cycle. *J. Bacteriol.* 183, 4305–4316. doi: 10.1128/JB.183.14.4305-4316.2001

Hill, M. S., and Hill, A. L. (2009). "Porifera (Sponges)," in *Encyclopedia of Inland Waters* (Elsevier), 423–432. doi: 10.1016/B978-012370626-3.00186-1

Hügler, M., and Sievert, S. M. (2011). Beyond the Calvin Cycle: Autotrophic Carbon Fixation in the Ocean. *Annu. Rev. Mar. Sci.* 3, 261–289. doi: 10.1146/annurev-marine-120709-142712

Indraningrat, A., Micheller, S., Runderkamp, M., Sauerland, I., Becking, L., Smidt, H., et al. (2019). Cultivation of Sponge-Associated Bacteria From Agelas Sventres and Xestospongia Muta Collected From Different Depths. *Marine Drugs* 17, 578. doi: 10.3390/md17100578

Katoh, K. (2002). MAFFT: A Novel Method for Rapid Multiple Sequence Alignment Based on Fast Fourier Transform. *Nucleic Acids Res.* 30, 3059–3066. doi: 10.1093/nar/gkf436

Kazanidis, G., van Oevelen, D., Veuger, B., and Witte, U. F. M. (2018). Unravelling the Versatile Feeding and Metabolic Strategies of the Cold-Water Ecosystem Engineer Spongosorites Coralliophaga (Stephen). *Deep Sea Res. Part I: Oceanograph. Res. Papers* 141, 71–82. doi: 10.1016/j.dsr.2018.07.009

Knowlton, N., and Jackson, C. (2001). *The Ecology of Coral Reefs*.

Konneke, M., Schubert, D. M., Brown, P. C., Hugler, M., Standfest, S., Schwander, T., et al. (2014). Ammonia-Oxidizing Archaea Use the Most Energy-Efficient Aerobic Pathway for CO2 Fixation. *Proc. Natl. Acad. Sci.* 111, 8239–8244. doi: 10.1073/pnas.1402028111

Lewis, W. H., and Ettema, T. J. G. (2019). Culturing the Uncultured. *Nat. Biotechnol.* 37, 1278–1279. doi: 10.1038/s41587-019-0300-2

Medeiros, P. M., Seidel, M., Ward, N. D., Carpenter, E. J., Gomes, H. R., Niggemann, J., et al. (2015). Fate of the Amazon River Dissolved Organic Matter in the Tropical Atlantic Ocean: Dom in the Amazon River-Ocean Continuum. *Global Biogeochem. Cycles* 29, 677–690. doi: 10.1002/2015GB005115

Moura, R. L., Amado-Filho, G. M., Moraes, F. C., Brasileiro, P. S., Salomon, P. S., Mahiques, M. M., et al. (2016). An Extensive Reef System at the Amazon River Mouth. *Sci. Adv.* 2, e1501252. doi: 10.1126/sciadv.1501252

Nurk, S., Meleshko, D., Korobeynikov, A., and Pevzner, P. A. (2017). Metaspades: A New Versatile Metagenomic Assembler. *Genome Res.* 27, 824–834. doi: 10.1101/gr.213959.116

Oksanen, J., Blanchet, F. G., Kindt, R., Legendre, P., Minchin, P., O'Hara, R., et al. (2013). Vegan: Community Ecology Package. R Package Version. 2.0-10. *CRAN*.

Olm, M. R., Brown, C. T., Brooks, B., and Banfield, J. F. (2017). Drep: A Tool for Fast and Accurate Genomic Comparisons That Enables Improved Genome Recovery From Metagenomes Through De-Replication. *Isme J.* 11, 2864–2868. doi: 10.1038/ismej.2017.126

Omachi, C. Y., Asp, N. E., Siegle, E., Couceiro, M. A. A., Francini-Filho, R. B., and Thompson, F. L. (2019). Light Availability for Reef-Building Organisms in a Plume-Influenced Shelf. *Continent. Shelf Res.* 181, 25–33. doi: 10.1016/j.csr.2019.05.005

Parks, D. H., Chuvochina, M., Waite, D. W., Rinke, C., Skarshewski, A., Chaumeil, P.-A., et al. (2018). A Standardized Bacterial Taxonomy Based on Genome Phylogeny Substantially Revises the Tree of Life. *Nat. Biotechnol.* 36, 996–1004. doi: 10.1038/nbt.4229

Parks, D. H., Imelfort, M., Skennerton, C. T., Hugenholtz, P., and Tyson, G. W. (2015). CheckM: Assessing the Quality of Microbial Genomes Recovered From Isolates, Single Cells, and Metagenomes. *Genome Res.* 25, 1043–1055. doi: 10.1101/gr.186072.114

Parks, D. H., Rinke, C., Chuvochina, M., Chaumeil, P.-A., Woodcroft, B. J., Evans, P. N., et al. (2017). Recovery of Nearly 8,000 Metagenome-Assembled Genomes Substantially Expands the Tree of Life. *Nat. Microbiol.* 2, 1533–1542. doi: 10.1038/s41564-017-0012-7

Pester, M., Schleper, C., and Wagner, M. (2011). The Thaumarchaeota: An Emerging View of Their Phylogeny and Ecophysiology. *Curr. Opin. Microbiol.* 14, 300–306. doi: 10.1016/j.mib.2011.04.007

Pinto, O. H. B., Silva, T. F., Vizzotto, C. S., Santana, R. H., Lopes, F. A. C., Silva, B. S., et al. (2020). Genome-Resolved Metagenomics Analysis Provides Insights Into the Ecological Role of Thaumarchaeota in the Amazon River and Its Plume. *BMC Microbiol.* 20, 13. doi: 10.1186/s12866-020-1698-x

Pita, L., Rix, L., Slaby, B. M., Franke, A., and Hentschel, U. (2018). The Sponge Holobiont in a Changing Ocean: From Microbes to Ecosystems. *Microbiome* 6, 46. doi: 10.1186/s40168-018-0428-1

Price, M. N., Dehal, P. S., and Arkin, A. P. (2010). FastTree 2 – Approximately Maximum-Likelihood Trees for Large Alignments. *PloS One* 5, e9490. doi: 10.1371/journal.pone.0009490

R Core Team (2021). *R: A Language and Environment for Statistical Computing* (Vienna, Austria: R Version 4.1.2, R Foundation for Statistical Computing). Available at: https://www.r-project.org/.

Raven, J. (2009). Contributions of Anoxygenic and Oxygenic Phototrophy and Chemolithotrophy to Carbon and Oxygen Fluxes in Aquatic Environments. *Aquat. Microb. Ecol.* 56, 177–192. doi: 10.3354/ame01315

Reveillaud, J., Maignien, L., Eren, A. M., Huber, J. A., Apprill, A., Sogin, M. L., et al. (2014). Host-Specificity Among Abundant and Rare Taxa in the Sponge Microbiome. *Isme J.* 8, 1198–1209. doi: 10.1038/ismej.2013.227

Richey, J. E., Hedges, J. I., Devol, A. H., Quay, P. D., Victoria, R., Martinelli, L., et al. (1990). Biogeochemistry of Carbon in the Amazon River. *Limnol. Oceanogr.* 35, 352–371. doi: 10.4319/lo.1990.35.2.0352

Rix, L., Ribes, M., Coma, R., Jahn, M. T., de Goeij, J. M., van Oevelen, D., et al. (2020). Heterotrophy in the Earliest Gut: A Single-Cell View of Heterotrophic Carbon and Nitrogen Assimilation in Sponge-Microbe Symbioses. *Isme J.* 14, 2554–2567. doi: 10.1038/s41396-020-0706-3

Sieber, C. M. K., Probst, A. J., Sharrar, A., Thomas, B. C., Hess, M., Tringe, S. G., et al. (2018). Recovery of Genomes From Metagenomes *via* a Dereplication, Aggregation and Scoring Strategy. *Nat. Microbiol.* 3, 836–843. doi: 10.1038/s41564-018-0171-1

Silva, B. S., de, O., Coutinho, F. H., Gregoracci, G. B., Leomil, L., de Oliveira, L. S., et al. (2017). Virioplankton Assemblage Structure in the Lower River and Ocean Continuum of the Amazon. *mSphere* 2. doi: 10.1128/mSphere.00366-17

Stanley, G.D. Jr (2006). Photosymbiosis and the Evolution of Modern Coral Reefs. *Evolution* 1, 3. doi: 10.1126/science.1123701

Tabita, F. R., Hanson, T. E., Li, H., Satagopan, S., Singh, J., and Chan, S. (2007a). Function, Structure, and Evolution of the RubisCO-Like Proteins and Their RubisCO Homologs. *Microbiol. Mol. Biol. Rev.* 71, 576–599. doi: 10.1128/MMBR.00015-07

Tabita, F. R., Satagopan, S., Hanson, T. E., Kreel, N. E., and Scott, S. S. (2007b). Distinct Form I, II, III, and IV Rubisco Proteins From the Three Kingdoms of Life Provide Clues About Rubisco Evolution and Structure/Function Relationships. *J. Exp. Bot.* 59, 1515–1524. doi: 10.1093/jxb/erm361

Taylor, M. W., Radax, R., Steger, D., and Wagner, M. (2007). Sponge-Associated Microorganisms: Evolution, Ecology, and Biotechnological Potential. *Microbiol. Mol. Biol. Rev.* 71, 295–347. doi: 10.1128/MMBR.00040-06

Tomasch, J., Gohl, R., Bunk, B., Diez, M. S., and Wagner-Döbler, I. (2011). Transcriptional Response of the Photoheterotrophic Marine Bacterium Dinoroseobacter Shibae to Changing Light Regimes. *Isme J.* 5, 1957–1968. doi: 10.1038/ismej.2011.68

Trindade-Silva, A. E., Rua, C., Silva, G. G. Z., Dutilh, B. E., Moreira, A. P. B., Edwards, R. A., et al. (2012). Taxonomic and Functional Microbial Signatures of the Endemic Marine Sponge Arenosclera Brasiliensis. *PloS One* 7, e39905. doi: 10.1371/journal.pone.0039905

Turner, E. C. (2021). Possible Poriferan Body Fossils in Early Neoproterozoic Microbial Reefs. *Nature* 596, 87–91. doi: 10.1038/s41586-021-03773-z

Tyson, G. W., Chapman, J., Hugenholtz, P., Allen, E. E., Ram, R. J., Richardson, P. M., et al. (2004). Community Structure and Metabolism Through Reconstruction of Microbial Genomes From the Environment. *Nature* 428, 37–43. doi: 10.1038/nature02340

Vikram, S., Guerrero, L. D., Makhalanyane, T. P., Le, P. T., Seely, M., and Cowan, D. A. (2016). Metagenomic Analysis Provides Insights Into Functional Capacity in a Hyperarid Desert Soil Niche Community: Functional Capacity in Namib Hypoliths. *Environ. Microbiol.* 18, 1875–1888. doi: 10.1111/1462-2920.13088

Walker, C. B., de la Torre, J. R., Klotz, M. G., Urakawa, H., Pinel, N., Arp, D. J., et al. (2010). Nitrosopumilus Maritimus Genome Reveals Unique Mechanisms for Nitrification and Autotrophy in Globally Distributed Marine Crenarchaea. *Proc. Natl. Acad. Sci.* 107, 8818–8823. doi: 10.1073/pnas.0913533107

Webster, N. S., and Thomas, T. (2016). The Sponge Hologenome. *mBio* 7 (2), e00135–16. doi: 10.1128/mBio.00135-16

Wu, Y.-W., Simmons, B. A., and Singer, S. W. (2016). MaxBin 2.0: An Automated Binning Algorithm to Recover Genomes From Multiple Metagenomic Datasets. *Bioinformatics* 32, 605–607. doi: 10.1093/bioinformatics/btv638

Zarzycki, J., Brecht, V., Müller, M., and Fuchs, G. (2009). Identifying the Missing Steps of the Autotrophic 3-Hydroxypropionate CO_2 Fixation Cycle in *Chloroflexus Aurantiacus*. *Proc. Natl. Acad. Sci. U. S. A.* 106, 21317–21322. doi: 10.1073/pnas.0908356106

Zhou, Z., Tran, P. Q., Breister, A. M., Liu, Y., Kieft, K., Cowley, E. S., et al. (2022). METABOLIC: High-Throughput Profiling of Microbial Genomes for Functional Traits, Metabolism, Biogeochemistry, and Community-Scale Functional Networks. *Microbiome* 1, 10–33. doi: 10.1186/s40168-021-01213-8

Zweifler (Zvifler), A., O'Leary, M., Morgan, K., and Browne, N. K. (2021). Turbid Coral Reefs: Past, Present and Future—A Review. *Diversity* 13, 251. doi: 10.3390/d13060251

Conflict of Interest: The authors declare that the research was conducted in the absence of any commercial or financial relationships that could be construed as a potential conflict of interest.

Publisher's Note: All claims expressed in this article are solely those of the authors and do not necessarily represent those of their affiliated organizations, or those of the publisher, the editors and the reviewers. Any product that may be evaluated in this article, or claim that may be made by its manufacturer, is not guaranteed or endorsed by the publisher.

frontiers | Frontiers in Microbiology

TYPE Original Research
PUBLISHED 30 August 2022
DOI 10.3389/fmicb.2022.767334

OPEN ACCESS

EDITED BY
Yang Zhang,
South China Sea Institute
of Oceanology (CAS), China

REVIEWED BY
Christina Pavloudi,
George Washington University,
United States
Marco Fusi,
Edinburgh Napier University,
United Kingdom

*CORRESPONDENCE
Daniel P. R. Herlemann
daniel.herlemann@emu.ee

SPECIALTY SECTION
This article was submitted to
Microbial Symbioses,
a section of the journal
Frontiers in Microbiology

RECEIVED 30 August 2021
ACCEPTED 19 July 2022
PUBLISHED 30 August 2022

CITATION
Kivistik C, Käiro K, Tammert H,
Sokolova IM, Kisand V and
Herlemann DPR (2022) Distinct stages
of the intestinal bacterial community
of *Ampullaceana balthica* after
salinization.
Front. Microbiol. 13:767334.
doi: 10.3389/fmicb.2022.767334

Distinct stages of the intestinal bacterial community of *Ampullaceana balthica* after salinization

Carmen Kivistik[1], Kairi Käiro[1], Helen Tammert[1], Inna M. Sokolova[2,3], Veljo Kisand[1,4] and Daniel P. R. Herlemann[1]*

[1]Estonian University of Life Sciences, Center for Limnology, Tartu, Estonia, [2]Department of Marine Biology, Institute for Biological Sciences, University of Rostock, Rostock, Germany, [3]Department of Maritime Systems, Interdisciplinary Faculty, University of Rostock, Rostock, Germany, [4]Institute of Technology, University of Tartu, Tartu, Estonia

Environmental disturbances influence bacterial community structure and functioning. To investigate the effect of environmental disturbance caused by changes in salinity on host-protected bacterial communities, we analyzed the microbiome within the gastrointestinal tract of *Ampullaceana balthica* in different salinities. *A. balthica* is a benthic gastropod found in fresh- and mesohaline waters. Whereas the total energy reserves of *A. balthica* were unaffected by an increase of salinity to 3, a high mortality rate was detected after a shift from freshwater to salinity 6 suggesting a major disruption of energy homeostasis. The shift to salinity 6 also caused a change in the gastrointestinal bacterial community composition. At salinity 3, the bacterial community composition of different host individuals was related either to the freshwater or salinity 6 gastrointestinal bacterial community, indicating an ambivalent nature of salinity 3. Since salinity 3 represents the range where aquatic gastropods are able to regulate their osmolarity, this may be an important tipping point during salinization. The change in the intestinal microbiome was uncoupled from the change in the water bacterial community and unrelated to the food source microbiome. Our study shows that environmental disturbance caused by salinity acts also on the host-protected microbiome. In light of the sea-level rise, our findings indicate that salinization of the near-shore freshwater bodies will cause changes in organisms' intestinal microbiomes if a critical salinity threshold (presumably ~3) is exceeded.

KEYWORDS

salinity, aquatic snail, Baltic Sea, *Ampullaceana balthica*, osmolarity, gastrointestinal bacteria

Introduction

Disturbances caused by changes in resources or in the physical environment lead to changes in species richness, community structure (Mackey and Currie, 2001; Svensson et al., 2009), and ecosystem functioning (Naeem et al., 1994; Hooper et al., 2005). Communities respond differently to disturbances depending on the disturbance type, length, intensity, and frequency, as well as the species tolerance capacity (Sousa, 1984; Eckert et al., 2019; Miller et al., 2021). The intestinal tract has long been recognized as an important site for host-microbe interactions. In healthy animals, gut microbial communities benefit host development, growth, homeostasis (Strasdine and Whitaker, 1963; Levy et al., 2017; Sommer et al., 2017), and nutrition by detoxifying secondary compounds in the food (Bhat et al., 1998; Dillon and Dillon, 2004). Animals, which may experience periodic compositional changes in diet or environment, have variable microbiome structures (Hooks and O'malley, 2017). Microbiome community composition can shift when disturbances are stronger than forces driving stability (Levy et al., 2017). A healthy microbiome could be replaced by those associated with dysbiosis (Hamdi et al., 2011; Levy et al., 2017). When the new microbiome community is not anymore able to support resistance to disturbances (Lozupone et al., 2012; Clark et al., 2015; Sommer et al., 2017; Ma, 2020), it can lead to changes in host health and fitness (Marasco et al., 2022). Since bacteria in the gastrointestinal microbiome are key players in host-associated microbiomes, it is crucial to understand the effect of disturbances and how bacterial communities respond to them (Allison and Martiny, 2008; Shade et al., 2011).

Salinity is an important physiological stress factor and a key variable explaining the global distribution patterns of bacteria, causing shifts in composition and affecting the functional performance of bacterial communities (Del Giorgio and Bouvier, 2002; Langenheder et al., 2003; Lozupone and Knight, 2007; Herlemann et al., 2011). Differential distribution of bacterial taxa along a salinity gradient implies that certain taxa are vulnerable to altered salinity so pulse disturbance in salinity favors habitat generalists with ecological adaptability and broad salinity tolerance (Székely and Langenheder, 2014). Salinity has been frequently used to investigate a disturbance in planktonic bacterial communities (e.g., Székely and Langenheder, 2014; Berga et al., 2017; Herlemann et al., 2017) since salinity fluctuations cause severe stress for organisms (Shetty et al., 2019) by shifting the cellular and tissue osmotic balance and negatively impacting key cellular processes (Prosser, 1991; Berger and Kharazova, 1997). Animals react to changes in salinity either by actively regulating the osmotic pressure of extracellular fluids around the physiologically optimal set-point (osmoregulator) or by adjusting the intracellular osmolarity to match the external osmolarity (osmoconformers) (Truchot, 1993). Osmoregulators have high energy demand for water and solute transport (Sokolova et al., 2012). In osmoconformers, the extra- and intracellular environment is maintained isosmotic to the external environment to prevent cell volume changes. This strategy is less energy-demanding but the organisms must cope with the shifts in osmotic homeostasis (Sokolova et al., 2012). Typically, euryhaline fresh- and brackish-water gastropods can osmoregulate at low salinities (< 100 mOsm corresponding to salinity < 3) and become osmoconformers at higher salinities (Jordan and Deaton, 1999).

Several studies have investigated the effects of disturbances on bacterial community composition and functioning (e.g., Shade et al., 2012; Berga et al., 2017); however, little is known about disturbance effects on host-associated bacterial communities. A study of salinity manipulation on osmoregulating fish showed that on each salinity level a unique set of dominating bacteria exists that rarely overlap along salinity gradients (Schmidt et al., 2015). Schmidt et al. (2015) noted that the changes in host-protected microbiomes were not correlated with corresponding changes in surrounding water bacterial communities, which suggests host-specific effects shaping the intestinal microbiome. In this study, we used a common pond snail *Ampullaceana balthica* (Linnaeus, 1758) to investigate the impact of disturbances on bacterial communities in a host-protected environment. *A. balthica* is a Palaearctic species widely distributed in Eurasia (Mandahl-Barth, 1938; Økland, 1990;Kerney, 1999) and North Africa (Van Damme, 1984; Glöer and Diercking, 2010). The snail prefers low-altitude freshwater bodies such as lakes, ponds, drainage ditches, and lentic zones of rivers, rich in nutrients and submerged vegetation (Glöer and Diercking, 2010). *A. balthica* feeds on detritus, periphyton, diatoms, and filamentous algae (Gordon et al., 2018) and can selectively forage for high-quality food particles (Fink and Von Elert, 2006). It is typically found in freshwater but can tolerate salinity up to 15 (Zettler et al., 2006).

Current climate change and anthropogenic activities cause coastal freshwater areas and inland freshwater bodies to become more saline, affecting the organisms living in these areas (Horton et al., 2014; Jeppesen et al., 2020). Therefore, the effect of environmental disturbance and especially salinity on bacterial communities in host-protected systems requires better understanding. Salinization can occur suddenly as a short pulse by extreme weather events or slow by sea level rise. In this study, we investigated the effect of disturbance (salinity and antibiotics) on the host gastrointestinal microbiome of *A. balthica* during a sudden change in experimental conditions and *in situ* representing conditions that have adapted over long periods. By comparing a sudden manipulation of the gastrointestinal microbiome with holobionts that have had a long exposure to increased salinity *in situ* we also improve the understanding of the adaptation mechanism for salinity. We hypothesized that (I) disturbance (increase in salinity/antibiotics) influences the bacterial community composition in the host environment and in the surrounding water; and (II) a long-term adaptation is necessary for the

intestinal microbiome to cope with higher salinities. If salinity significantly influences the gastrointestinal microbiome, this would imply that the control of the host on its microbiome is weaker than the impact of salinity. If the response of the bacterial communities to the pulse manipulation has a negative effect compared to those observed in the holobionts adapted to different environmental salinity, we predict that a long adaptation to changes in salinity is necessary. Our alternative hypothesis was that salinity/antibiotics have no direct impact on the gastrointestinal microbiome. In this case, the host control over the microbiome is stronger than the effects of external disturbance.

Materials and methods

Sample collection and experimental setup

In vivo experiment

A. balthica snails (∼200 specimens) were collected from the freshwater Esna River (ER; **Figure 1A**) in Estonia on 3 September, 2018. After the collection, the snails were kept in two 50 L acclimation aquaria with freshly collected 85 μm pre-filtered lake (Võrtsjärv) water under constant air supply at a controlled temperature of 16–17°C for 24 h. After 24 h, snails were divided (15 snails to each aquarium) to reference (REF), antibiotic amended (AB), salinity 3 (SAL3), and salinity 6 (SAL6) aquaria; all aquarium groups had three parallels (**Figure 1B**). The reference (REF) aquaria contained freshly filtered (85 μm) lake water. In the salinity 3 (SAL3) and salinity 6 (SAL6) aquaria, the salinity of the water was increased using commercially available Reef Salt (AQUA MEDIC). In the antibiotics aquarium (AB), which was a disturbance control testing if the intestinal bacterial community responds to manipulation, freshwater was amended with ampicillin (5 mg/L) and streptomycin (5 mg/L). All aquaria contained a 2-cm layer of sandy sediment from Lake Võrtsjärv (sieved through a 0.5-mm mesh size plastic sieve) and stones and pebbles with natural biofilm as a food source. Aquaria were constantly supplied with air and held at 16.1–17.5°C for 8 days. Water conditions were monitored daily using a YSI ProDSS multisensor (**Supplementary Figure 1**).

At the beginning of the experiment, before any manipulation (day 0), water from each aquarium was sampled by filtering 3 × 100 mL through a 0.2-μm Durapore membrane filter (Millipore) and 14 *A. balthica* snails (day 0 snails - 8 for 16S rRNA gene analysis and 6 for energy reserve measurements) were shock frozen. In addition to the day 0 samples, water samples (3 × 100 mL from each aquarium) were taken on day 1 and day 8 of the experiment from each aquarium (n = 26). Snails from the aquaria were collected on day 8 for 16S rRNA gene analysis (n = 26) and energy reserve estimation measurements (n = 34). Snails for 16S rRNA gene analysis were starved for 24 h in sterile falcon tubes under conditions identical to the experiment aquaria to minimize the occurrence of transient bacteria (Van Horn et al., 2012). The feces were collected afterward from the tubes and stored at −80°C for further analysis.

In situ samples

A. balthica snails from Estonian coastal area sites with fresh- and brackish (salinity 3 and salinity 6) water conditions were collected on 17–18 June 2019 (**Figure 1A**). The *in situ* freshwater sampling sites were Selja pond (SP), Selja River (SR), and Kunda River (KR). The sampling site with salinity 3 included Selja Bay (SB) and sampling sites with salinity 6 were Nõva (NÕ), Ristna western site (RW), and Ristna eastern site (RE).

Snails collected from the freshwater and coastal brackish areas were starved for 24 h in their native water pre-filtered through 0.22 μm pore size Sterivex^{TM} filters, to reduce the number of food-derived microbes in the transient microbiome. The Sterivex^{TM} filters were used for water bacterial community analysis. Collected snails were divided for 16S rRNA gene analysis (n = 18) and energy reserve measurements (n = 21), shock frozen in liquid nitrogen and stored at −80°C for further analysis. Biofilm samples were collected from all studied sites by scraping the stones or pebbles, immediately shock frozen in liquid nitrogen, and stored at −80°C.

Lipid, carbohydrate, and protein measurements

To estimate the energy reserves, we measured lipid, carbohydrate, and protein content in snail tissues as described elsewhere (Haider et al., 2018). In brief, the frozen snails were thawed for 10 min at room temperature and removed from the shell with tweezers. The snails were frozen again in liquid nitrogen and powdered using a sterilized mortar. The tissue powder was placed in 2 mL microcentrifuge tubes. For lipid content analysis, approximately 30 mg of tissue powder was added to 3 mL of chloroform: methanol mixture (1:2, v:v) and incubated for 5 min with periodic vigorous mixing. The mixture was centrifuged at 3000 × g for 5 min at room temperature and the supernatants dried out at 100°C. Sunflower oil in acetone was used as a standard. The dry samples were solubilized with concentrated sulfuric acid (H_2SO_4) and mixed with a vanillin reagent. The absorbance of samples and standards was measured at 490 nm using a FLUOstar® Omega microplate reader. For the determination of the carbohydrate and protein content, ∼50 mg of tissue powder was mixed in 0.5 mL of distilled water with 0.1% Triton (1:10 tissue mass to volume). Cells were lysed by three rapid freeze-thaw cycles of 5 min at −80°C followed by 5 min in a 37°C water bath and centrifuged at 3000 × g for 3 min at room temperature. The supernatant was

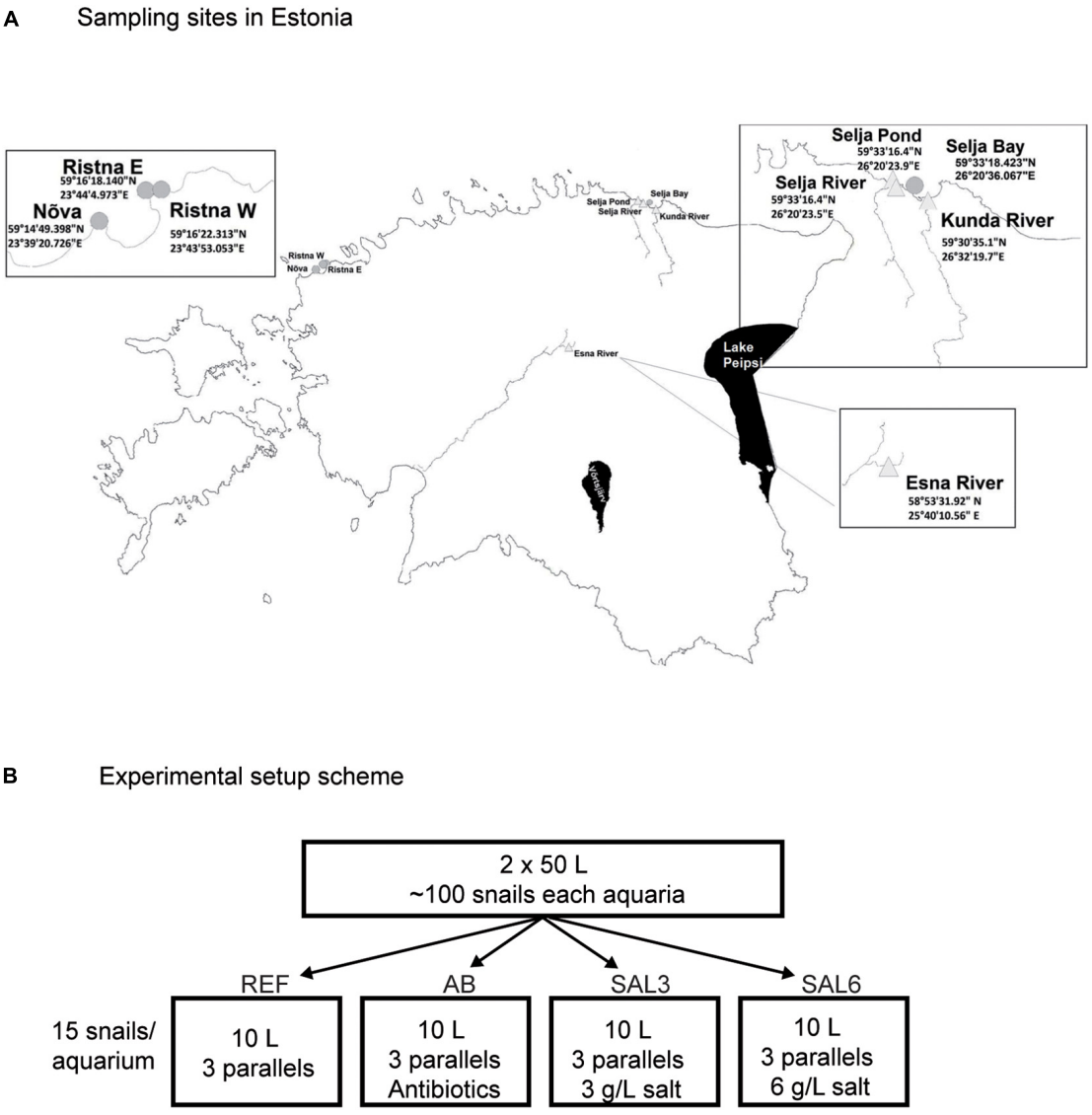

FIGURE 1
(A) Sampling sites in Estonia. Experiment snails were collected from the Esna River (ER). Coastal freshwater (*in situ* FW) sampling sites were: Selja pond (SP), Selja River (SR), and Kunda River (KR). Coastal brackish water sampling sites were: *in situ* SAL3 site was Selja Bay (SB), *in situ* SAL6 sites were Ristna western site (RW), Ristna eastern site (RE), and Nõva (NÕ). **(B)** Experimental setup scheme: REF, reference aquaria; AB, antibiotic manipulation aquaria; SAL3, salinity 3 manipulation aquaria; SAL6, salinity 6 manipulation aquaria.

used for carbohydrate and protein measurements. Carbohydrate concentrations were measured using the phenol-sulfuric acid method with glucose as a standard (Masuko et al., 2005). To calculate the carbohydrate content (in glucose equivalents), absorbance was measured at 492 nm using a FLUOstar® Omega microplate reader. The soluble protein content was determined using the Bradford assay with bovine serum albumin (BSA) as a standard by measuring absorbance at 595 nm using the FLUOstar® Omega microplate reader.

Total energy reserve was calculated by transforming the measured protein, lipid, and carbohydrate content into energy equivalents using their respective energy of combustion: 24 kJ g^{-1} for proteins, 39.5 kJ g^{-1} for lipids, and 17.5 kJ g^{-1} for carbohydrates (Gnaiger, 1983).

16S rRNA gene analysis

Snail preparation for 16S rRNA gene analysis

For the 16S rRNA gene analysis, the frozen snails were allowed to thaw for 10 min at room temperature and cleaned with 90% ethanol. The soft body of the snail was removed from the shell with tweezers on a sterile Petri dish without breaking the shell, avoiding contamination from bacteria living

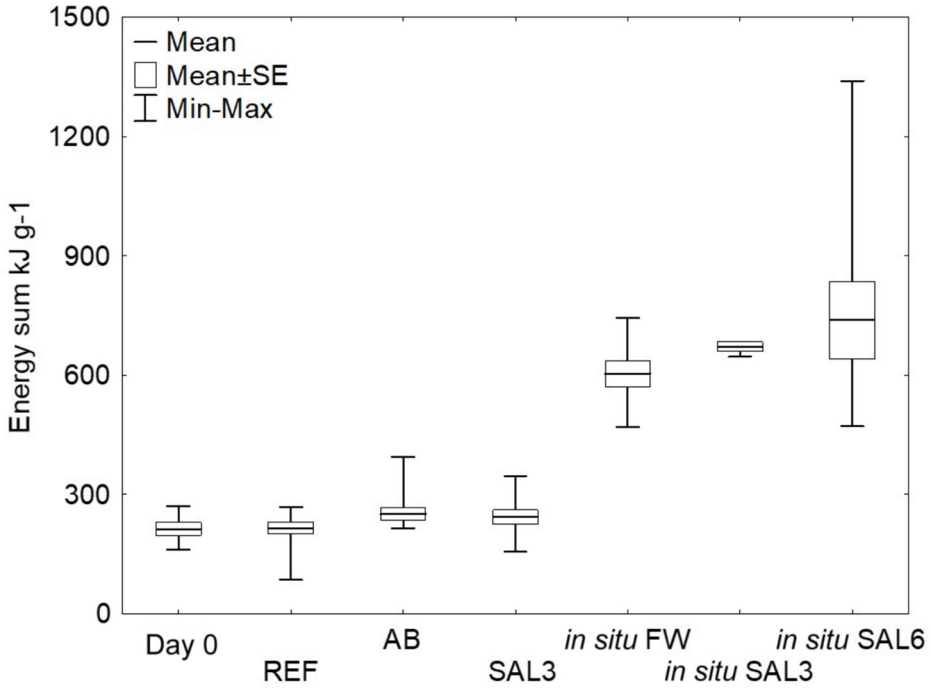

FIGURE 2
Total energy pool (kJ g^{-1}) of the snails from the experiment and *in situ* sampling sites. Total energy pool kJ g^{-1} calculated from the lipid, carbohydrate, and protein content of the snail tissues. Day 0: snails from freshwater Esna River on experiment's day 0 (n = 6); REF: reference snails from non-manipulated freshwater aquaria (n = 11); AB: snails from antibiotics manipulated aquaria (n = 11); SAL3: snails from aquaria with raised salinity to 3 (n = 12). *In situ* FW: snails collected from natural freshwater sites (SP, SR, KR; n = 9); *in situ* SAL3: snails collected from a natural site with salinity 3 (SB, n = 3); *in situ* SAL6: snails collected from natural sites with salinity 6 (RE, RW, NÕ; n = 9).

on the shell. The gastrointestinal tract of the snail was dissected, placed into the 2 mL Eppendorf tube and frozen at −80°C for further analysis.

DNA extraction process

DNA of the snails' gastrointestinal microbiome, biofilm, feces, and water filters was extracted using the phenol:chloroform method according to the modified protocols from Lueders et al. (2004) and (Weinbauer et al., 2002) as described in detail in Kivistik et al. (2020). In brief, to release the DNA, we used mechanical bead beating and thermal disruption (65°C for 1 h). For the precipitation, we used phenol:chloroform:isoamyl alcohol (25:24:1) at pH 8 and chloroform:isoamyl (24:1) to separate the DNA from the cell debris. The RNA was removed after chloroform/phenol extraction using RNase A (Qiagen). The subsequent purification steps included ice-cold isopropanol and 96% ethanol. The remaining pellet was resuspended in the 50 μL AE buffer (10 mM Tris-Cl, 0.5 mM EDTA; pH 9.0) (Qiagen). The amount and quality of the DNA were estimated using a NanoDrop™ UV-Vis spectrophotometer. The DNA sequences were amplified using the primers Bakt_341F and Bakt_805R according to a modified protocol of Herlemann et al. (2011) using 30 PCR cycles and processed as described in Kivistik et al. (2020).

Sequencing

Amplicons were purified using PCR Kleen (Bio-Rad). Illumina TrueSeq adapters and P5/P7primers tags were added to amplicons in the second PCR reaction and sequenced at FIMM, University of Helsinki, Finland. A total of 7,353,519 reads were generated for 66 samples by Illumina MiSeq sequencing using PE250 chemistry (MiSeq Reagent Kit v2). The resulting sequences were processed using Trimmomatic (V0.36) (Bolger et al., 2014) to remove Illumina-specific sequences and regions with low sequence quality (average quality score < Q20). PCR primers were removed using the default values in Cutadapt (V2.3) (Martin, 2011). The reads were paired (16 bp overlap, minimum length 300 bp) using the VSEARCH tool (Rognes et al., 2016). These were then taxonomically assigned using the SILVA next-generation sequencing (NGS) pipeline (Glöckner et al., 2017) using the SILVAngs analysis platform release version 138 (Pruesse et al., 2007). SILVAngs analysis platform performs additional quality checks according to SINA-based alignments (Pruesse et al., 2012) with a curated seed database in which PCR artifacts or non-SSU reads are excluded. The longest read serves as a reference for taxonomic classification using a BLAST

(version 2.2.30 +) search against the SILVA SSURef dataset. The classification of the reference sequence of each cluster (98% sequence identity) is mapped to all members of the respective cluster and to their replicates. Non-bacterial sequences such as chloroplasts, mitochondria, eukaryotes, and Archaea were excluded because the primer set employed in the analysis has only limited coverage. The raw reads of the 16S rRNA genes were deposited at the NCBI SRA under bioproject PRJNA724976, accession number SAMN18865776-SAMN18865895.

Host species taxonomic identification

To verify the species' taxonomic identification, an internal transcribed spacer 2 (ITS2) analysis of *A. balthica* was conducted. The DNA was amplified as described in (Kivistik et al., 2020) using the primers LT1 (Bargues et al., 2001) and ITS2-Rixo (Almeyda-Artigas et al., 2000). The PCR protocol was 94°C for 4 min for denaturation followed by 35 cycles of 94°C for 30 s, 56°C for 30 s, 72°C for 1 min, and the final extension at 72°C for 7 min. The amplicon was purified using PCR Kleen (Bio-Rad) and Sanger sequenced by the sequencing facility at Tartu University, Estonia. The sequences from the ITS2 region were quality-checked using the software Chromas (Technelysium Pty Ltd., Australia); forward and reverse reads were assembled after low-quality reads were discarded. All the sequences were imported into ARB (Ludwig et al., 2004) to calculate a maximum likelihood phylogenetic tree (PhyML). Bootstraps were calculated using the RAxML 7.0.3 (Stamatakis, 2006) rapid bootstrap analysis with 1000 runs as implemented in ARB and added to the PhyML tree. The ITS reads were deposited at EBI under accession number OA985092-OA985113.

Statistical analysis

The number of reads per sample varied between 1,004 and 86,933 reads, therefore, the data were normalized by cumulative sum scaling (CSS) using the R (Ihaka and Gentleman, 1996) package metagenomeSeq (Paulson et al., 2013). Bacterial α-diversity is represented by the Chao1 index calculated with R using the "phyloseq" package (Mcmurdie and Holmes, 2013). For testing the sample groups' homoscedasticity, we used Levene's test from calculated energy content and Chao1 means. A one-way ANOVA test with an additional *post hoc* Tukey's Honest Significant Differences (HSD) test was used to calculate significant differences between the number of OTUs in the samples and differences in total energy reserves. For the coastal snail samples' total energy reserve, we used Welch's ANOVA test with an additional Games-Howell *post hoc* test. The mean difference in community dissimilarity among the different treatments was determined by beta-dispersion analysis in PAST software, package version 4.07 (Hammer et al., 2001). Variations in bacterial community structure were characterized in a principal coordinate analysis (PCoA) using the Bray–Curtis dissimilarity in the "vegan" community ecology package of R (Oksanen et al., 2013) and PAST software package version 4.07 (Hammer et al., 2001) for visualization. The one-way permutational multivariate analysis of variance (PERMANOVA test) with Bray-Curtis dissimilarity was used to calculate differences between bacterial community compositions among analyzed sample groups. A linear discriminant analysis effect size (LEfSe) tool (Segata et al., 2011) was used to identify bacterial groups with multi-class analysis; the "One against all" was used with default settings (α = 0.05, N permutations = 1,000). OTUs identified in the LEfSe as significantly enriched were defined as indicator OTUs.

Results

Host body energy content

The snail mortality rate in salinity 6 aquaria was 95%; therefore, surviving snails from salinity 6 (n = 3) were excluded from the energy calculations and the rapid salinity rise from freshwater to salinity 6 was considered highly stressful for the snails. For testing the experimental sample groups' homoscedasticity, we used Levene's test from calculated energy content means, which was not significantly different ($p > 0.05$). Tukey's HSD test showed that the freshly collected (day 0) ER *A. balthica* samples had a lower lipid energy content (0.7 kJ g^{-1} SE ± 0.3, $p < 0.01$) compared to samples from REF (6.9 kJ g^{-1} SE ± 0.2), AB (6.6 kJ g^{-1} SE ± 0.2) and SAL3 (5.5 kJ g^{-1} SE ± 0.2) aquaria (**Supplementary Table 1**). The lipid concentration decreased in samples from manipulated SAL3 *A. balthica* compared to the reference samples. The protein-associated energy content was lower on day 0 *A. balthica* (162.6 kJ g^{-1} SE ± 1.3, $p < 0.01$, **Supplementary Table 1**) compared to REF (178.4 kJ g^{-1} SE ± 1), AB (178.4 kJ g^{-1} SE ± 0.9) and SAL3 snails (184 kJ g^{-1} SE ± 0.9). The calculated energy reserve stored in carbohydrate compounds did not show any significant difference between the studied groups of *A. balthica*. The average total energy reserve (calculated as the energy content of lipids, proteins, and carbohydrates per gram of tissue) was 213 kJ g^{-1} for day 0 *A. balthica*, 215 kJ g^{-1} for reference, 250 kJ g^{-1} for AB treated, and 242 kJ g^{-1} for salinity 3 treated samples (**Figure 2**). Tukey's HSD test did not show any significant difference in the total energy reserves between the studied groups of *A. balthica*.

The total energy reserves of the snail collected from the field sites with different salinities (SP, SR, KR, SB, NÕ, RW, and RE) were higher compared to ER snails on day 0 or those exposed to different experimental treatments in the laboratory ($p < 0.01$). The average energy content was 604 kJ g^{-1} for *in situ*

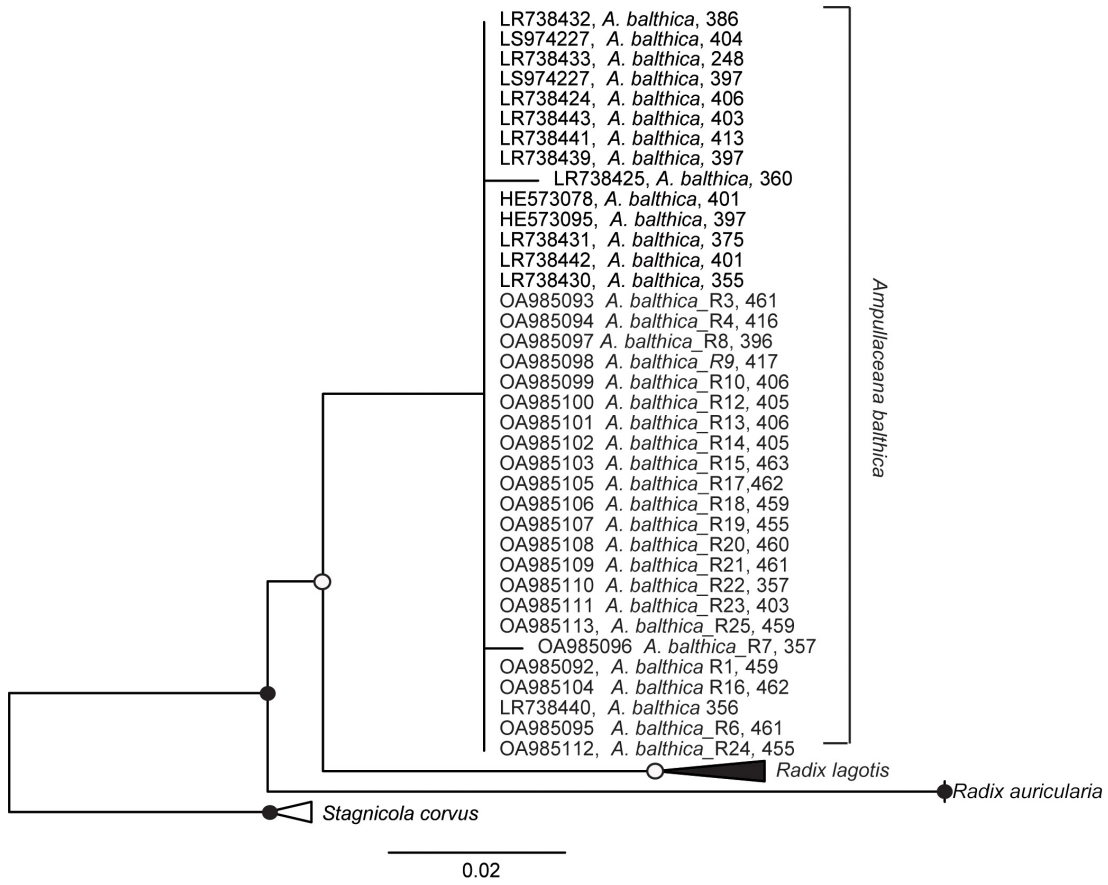

FIGURE 3
Maximum likelihood tree of nuclear marker internal transcribed spacer 2 (ITS2) sequence based on 398 sequence columns with ITS2 sequences using *Stagnicola corvus* as an outgroup. Sequences OA985092-OA985113 were derived in this study from *Ampullaceana balthica* sampled in the Esna River and the coastal sampling sites of Estonia. Filled dots represent a bootstrap value of 100% and empty dots of a bootstrap > 75%.

freshwater snails, 671 kJ g^{-1} for *in situ* salinity 3 samples, and 738 kJ g^{-1} for *in situ* salinity 6 samples (Figure 2). Welch's ANOVA test with an additional Games-Howell *post hoc* test did not show any significant difference for the total energy content between the field-collected snails from the freshwater, salinity 3 and salinity 6 sites.

Host species taxonomic identification

Since the total energy pools between *in situ* snails and experimental snails differed significantly, and snails from natural sites were tolerating higher salinity with no extra energy demand, we analyzed the internal transcribed spacer 2 (ITS2) biomarker regions to test whether this physiological variation might be due to the presence of cryptic species. Our analysis confirmed that the snails used in the experiments and from coastal regions (SP, SR, KR, SB, NÕ, RW, and RW) belong to *A. balthica* with almost identical ITS sequences (99% identity Figure 3).

Host gastrointestinal bacterial richness

Among laboratory experiments and *in situ* coastal site samples, SILVA NGS classified 3,435 operational taxonomic units (OTUs) from a total of 3,195,039 sequences in 75 different phyla. For testing the sample groups' homoscedasticity, we used Levene's test from bacterial Chao1 index means which was not significantly different ($p > 0.05$). Transferring snails collected from ER to the reference aquarium (REF) resulted in a decrease in the bacterial Chao1 mean (ER: 540 SE ± 48.3; REF: 290 SE ± 48.3, $p < 0.01$, Figure 4). Further treatment with antibiotics or elevated salinity in the laboratory caused no significant change in the Chao1 mean of the *A. balthica* intestinal microbiome (AB: 250 SE ± 51.6, SAL3: 323 SE ± 51.6 and SAL6: 161 SE ± 78.8; $p > 0.01$). Similar to the manipulation experiments, the bacterial Chao1 means of the field-collected freshwater snails (SP, SR, and KR: Chao1 = 569 SE ± 51.6), salinity 3 snails (SB: 476 SE ± 96.6), and salinity 6 snails (NÕ, RE, RW: 578 SE ± 39.4) (Figure 4) were not significantly different (Tukey's HSD test $p > 0.01$).

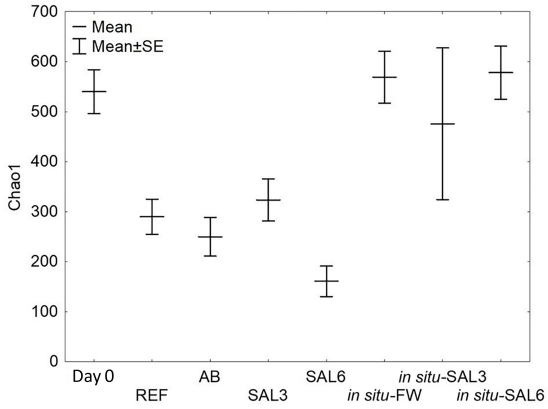

FIGURE 4
Bacterial α-diversity represented by the Chao1 index. Day 0: snails from freshwater Esna River on experiment's day 0; REF: reference snails from non-manipulated freshwater aquaria; AB: snails from antibiotics manipulated aquaria; SAL3: snails from aquaria with raised salinity to 3, SAL6: snails from aquaria with raised salinity to 6. *In situ* FW: snails collected from natural freshwater sites; *in situ* SAL3: snails collected from a natural site with salinity 3; *in situ* SAL6: snails collected from natural sites with salinity 6.

Interestingly, the detected bacterial diversity of the experiment's day 0 snails (Chao1 mean 540 SE ± 48.3) was comparable to the bacterial diversity of the snails collected from the freshwater coastal area *in situ* (569 SE ± 51.6, $p > 0.01$, Figure 4). Also, Chao1 mean of *in situ* SAL3 (578 SE ± 39.4) and experimental SAL3 aquaria snails bacterial diversity (323 SE ± 51.6) were not significantly different ($p > 0.05$). An exception was the Chao1 mean of *in situ* SAL6 snails bacterial diversity, which was higher (578 SE ± 39.4, $p < 0.01$) compared to laboratory experiment SAL6 aquaria snails bacterial diversity (161 SE ± 78.8).

Host gastrointestinal bacterial community composition

The bacterial community composition on phylum/class level was comparable among all analyzed samples (Figure 5A). Samples were dominated by *Proteobacteria* (34–71%) of which *Gammaproteobacteria* (69–73%) and *Alphaproteobacteria* (9–40%) were the dominant classes. Furthermore, *Planctomycetes* (2.4–28%), *Bacteroidetes* (3.4–15.8%), *Firmicutes* (1–15%), *Actinobacteria* (1–10%), and *Cyanobacteria* (1-9%) were found in high abundance.

At the genus level, the most abundant bacteria in all analyzed snail gastrointestinal samples were *Flavobacterium, Pirellula, Mycoplasma, Aeromonas, Pseudomonas,* uncultured Microscillaceae OTU, *Hydrogenophaga, Luteolibacter,* and unclassified Rhodobacteraceae OTU (Figure 5B). The most abundant OTUs in experiment's day 0 snail samples were *Flavobacterium* (0.5–1.0%), unclassified Rhizobiales (0.5–0.9%), and *Pirellula* (0.5–0.9%). After transferring snails to REF aquaria, the bacterial community was still dominated by *Flavobacterium* (1.0–2.9%), but *Acinetobacter* (1.0–2.3%), and *Aeromonas* (0.8–5.0%) became more abundant. The snails' microbiome from the SAL3 aquaria was dominated by similar bacteria (*Flavobacterium* 0.7–3.2%, *Acinetobacter* 0.7–3.6%, and *Aeromonas* 0.7–3.5%) as the REF aquaria snails' microbiome. Snails' microbiomes from SAL6 aquaria were dominated by *Aeromonas* (1.7–2.4%), and *Shewanella* (1.7–2.1%) along with *Pseudomonas* (1.4–2.0%). The antibiotic manipulation caused *Mycoplasma* (0.7–1.9%), *Pirellula* (0.8–1.8%), and *Chryseobacterium* (0.6–1.8%) to become more abundant. Genera that dominated the *in situ* freshwater snail samples (SP, SR, and KR) were *Mycoplasma* (0.3–1.0%), unclassified Microscillaceae (0.3–0.9%), and *Flavobacterium* (0.5–0.8%). The relative abundance of the dominant OTUs in *in situ* salinity 3 (SB) snail samples was *Rhodobacter* (0.5–0.9%), unclassified Rhodobacteraceae (3.8-9.9%), and *Hydrogenophaga* (0.4–0.8%). The relative abundance of the dominant OTUs in *in situ* salinity 6 (NŌ, RW, and RE) snail microbiome was *Mycoplasma* (0.5–2.2%), unclassified Rhizobiaceae OTU (0.4–1.7%), and *Pseudomonas* (0.5–1.3%). In addition to the abundant bacterial genera, we identified characteristic OTUs for snail sample groups using LEfSe (Table 1).

A multivariate dispersion analysis to determine the variability in species composition did not show any significant differences within the experimental snail samples nor within snails collected from *in situ* conditions ($p = 0.194$, $p = 0.020$, respectively, Supplementary Figure 2). To visualize the differences in the host-associated bacterial community composition between the experiment and snails collected from *in situ* conditions, we employed PCoA (Figure 6). The PCo analysis indicated the difference in the microbiome of the day 0 snails relative to the snails maintained in experimental aquaria (Figure 6A). PERMANOVA test confirmed the difference between microbiomes of experiment's day 0 snails and snails from aquaria ($R^2 = 85\%$, $p < 0.01$). The PCo2 separated antibiotic-treated snail microbiomes from the rest ($R^2 = 86\%$, $p < 0.01$; Figure 6A). Furthermore, the gastrointestinal bacterial community of salinity 6 treated snails was significantly different ($R^2 = 89\%$, $p < 0.01$) from the rest of the experiment snails (Figure 6A). Interestingly, five SAL3 aquaria snails' microbiomes (Figure 6A) grouped with the snails from REF (Figure 6A) and two – with SAL6 samples (Figure 6A). Similar to the experiment, the *in situ* SAL6 samples differed significantly from the *in situ* freshwater (SP, SR, and KR) and *in situ* SAL3 (SB) snails microbiomes ($R^2 = 76\%$, $p < 0.01$, Figure 6B). The difference between *in situ* freshwater and *in situ* SAL3 snails' microbiome was minor ($p > 0.01$). Comparison between the *in situ* snail's and laboratory experiment snail's

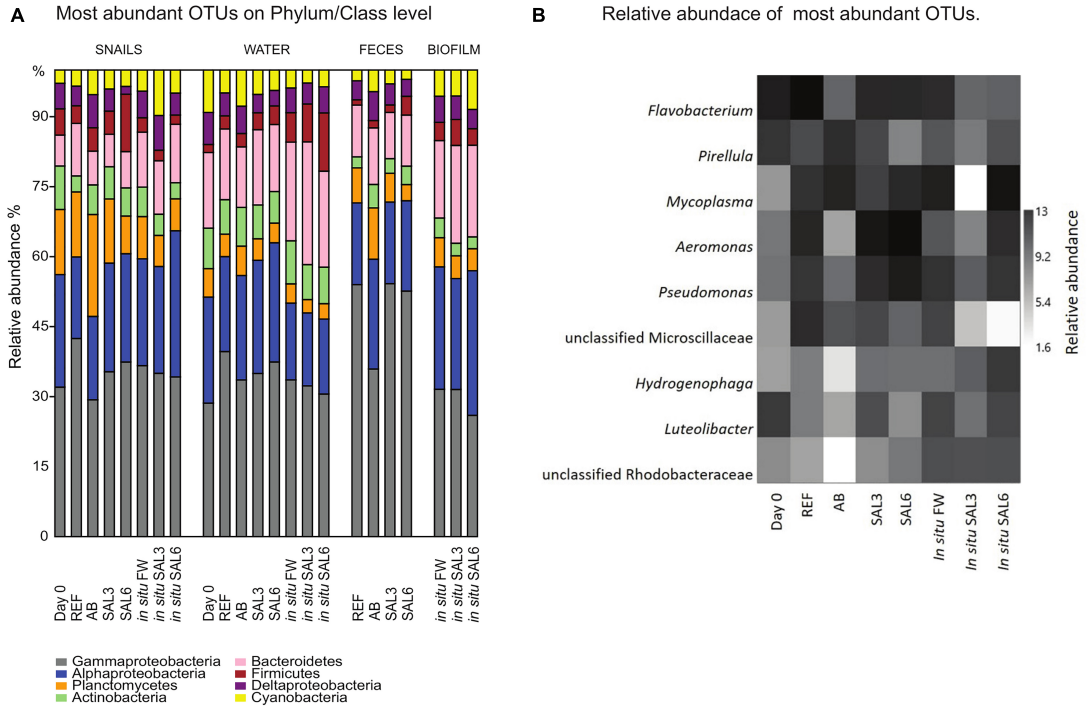

FIGURE 5

(A) Relative abundance (%) of most abundant operational taxonomic units (OTUs) on Phylum/Class level in all analyzed samples. **(B)** Relative abundance of most abundant OTUs of laboratory experiment snail samples and *in situ* coastal area snail samples. Day 0: snails from freshwater Esna River on experiment's day 0; REF, reference snails from non-manipulated freshwater aquaria; AB, snails from antibiotics manipulated aquaria; SAL3, snails from aquaria with raised salinity to 3, SAL6, snails from aquaria with raised salinity to 6. *In situ* FW, snails collected from natural freshwater sites; *in situ* SAL3, snails collected from natural site with salinity 3; *in situ* SAL6, snails collected from natural sites with salinity 6.

TABLE 1 Characteristic operational taxonomic units (OTUs) for snail sample groups using linear discriminant analysis effect size (LEfSe) tool.

Day 0 snail	REF	AB	SAL3	SAL6	*In situ* freshwater	*In situ* SAL3	*In situ* SAL6
Tabrizicola	*Acinetobacter*	*Chryseobacterium*	*Acinetobacter*	*Shewanella*	*Neochlamydia*	Candidatus Competibacter	*Spiroplasma*
Rhodobacter	*Aeromonas*	*Ensifer*	*Aeromonas*	*Aeromonas*	Candidatus Competibacter	Phormidium ETS-05	
	Mycoplasma		*Tabrizicola*	*Mycoplasma*			
			Shewanella				

gastrointestinal bacterial communities revealed a separation on the PCo1 (PERMANOVA R^2 = 79%, $p < 0.01$, Figure 6C). The experiment day 0 and *in situ* freshwater bacterial communities (Figure 6C) clustered together. However, the microbiome of *in situ* fresh- and brackish site snails differed from experiments REF, AB, SAL3, and SAL6 aquaria snails (R^2 = 60%, $p < 0.01$).

Bacterioplankton community composition

The aquarium water bacterial α-diversity, represented by Chao1 mean, was 906 (SE ± 45.7) on experiment day 1 and 705 (SE ± 52.1) on day 8 and did not show significant difference across all aquaria (REF, AB, SAL3, and SAL6). The Chao1 mean of day 0 water samples 865 (SE ± 33.1) did not differ from day 1 and day 8 water samples' bacterial diversity. The Chao1 mean was 1,055 (SE ± 45.6) for *in situ* freshwater water samples, 993 (SE ± 69.6) for *in situ* SAL3 samples, and 1,143 (SE ± 69.6) for *in situ* SAL6 samples. According to Tukey's HSD test, the bacterial richness of water samples was not significantly different between the coastal area sampling sites (Supplementary Figure 3).

The most abundant bacterioplankton species in aquaria water samples and in *in situ* water samples were *Flavobacterium* and *Limnohabitans*. However, the aquarium water was also enriched with LD29, *Methylocystis,* and *Cyanobium* PCC-6307, and water from the coastal sites was enriched with *Fluviicola, Sporichthyaceae* hgcI clade, and *Pseudomonas*. Surprisingly,

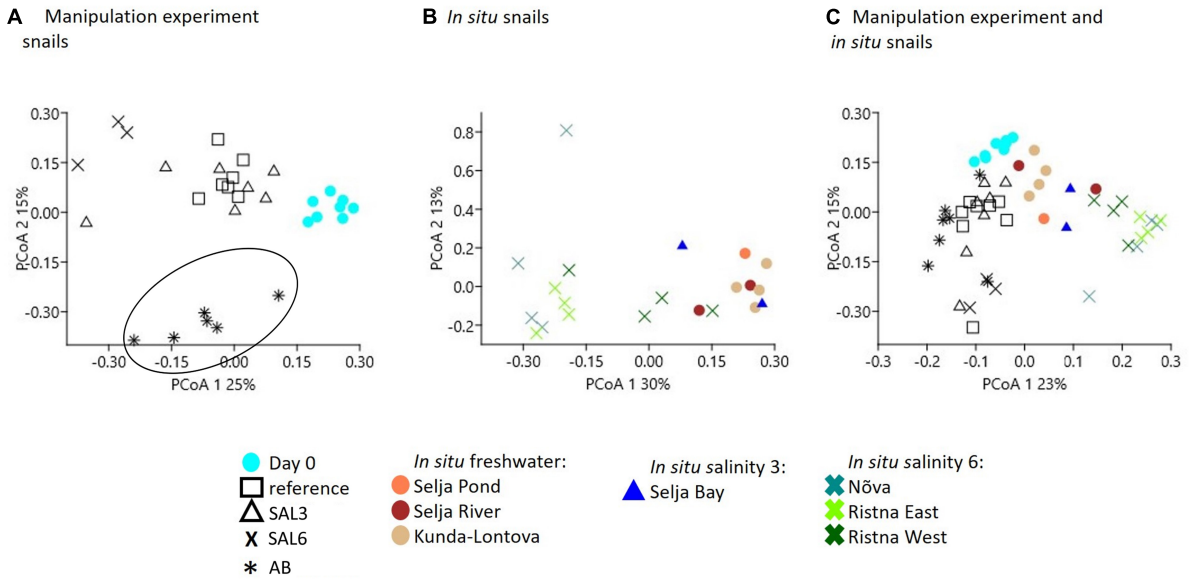

FIGURE 6
Principal coordinate analysis based on the Bray-Curtis dissimilarity of bacterial community composition on operational taxonomic unit (OTU) level. **(A)** Experiment snail samples (AB samples are surrounded with the circle to illustrate the clustering from the other samples), **(B)** *in situ* coastal area snail samples, **(C)** experiment, and *in situ* coastal area snail samples.

even though the PCo1 separated the day 1 and day 8 water samples, the bacterial community composition was similar according to PERMANOVA test (REF: R^2 = 54%, p = 0.09, n = 5; AB: R^2 = 23%, p = 0.2, n = 4; SAL3: R^2 = 43%, p = 0.1, n = 6), except for SAL6 aquaria day 1 and day 8 samples (R^2 = 51%, $p < 0.01$, n = 8) (**Supplementary Figure 4A**). However, a larger sample size might have shown a clearer result. Water bacterial communities from the *in situ* fresh- and brackish sites differed from each other showing site-specific bacterial community compositions (**Supplementary Figure 4B**).

Impact of water and food sources on the gastrointestinal bacterial community composition

The most abundantly found bacteria in biofilm samples differed from those in the water and the snail microbiome and included uncultured *Rhodobacteraceae*, *Flavobacterium*, uncultured *Saprospiraceae*, *Hydrogenophaga*, and *Porphyrobacter*. The most abundant bacteria found in the snail feces were *Pseudomonas*, *Acinetobacter*, *Flavobacterium*, *Simplicispira*, and *Acidovorax*. PCoA (**Figures 7A,B**) indicated a clear difference between gastrointestinal tract microbiome and water samples for both experiments and *in situ* samples with no similarity between water–microbiome pairings from the same aquarium or *in situ* sampling site. The PERMANOVA test with the Bray–Curtis dissimilarity confirmed that the bacterial communities of snail microbiome samples were different from water samples (R^2 = 70%; $p < 0.01$; **Figures 7A,B**), biofilm (R^2 = 54%; $p < 0.01$), and feces (R^2 = 5%; $p < 0.01$) (**Figures 7C,D**).

Discussion

Communities respond differently to disturbances depending on the disturbance type, length, intensity, and frequency, as well as the species tolerance capacity (Sousa, 1984). We investigated the impact of the disturbance caused by salinity upshift on the gastrointestinal microbiome of *A. balthica* to understand the capacity of the host to protect its microbiome. Although this investigation is based only on one species, it improves our understanding of host-microbiome interactions in a changing environment especially in view of further sea level rise, change in land use, and extreme weather events affecting coastal and inland freshwater communities.

Impact of the salinity manipulation on the hosts' total energy pool

In this study, we used lipid, carbohydrate, and protein compound measurements from the snail tissue to estimate the total energy pool of the specimens. The experimental shift from freshwater to salinity 6 caused high mortality

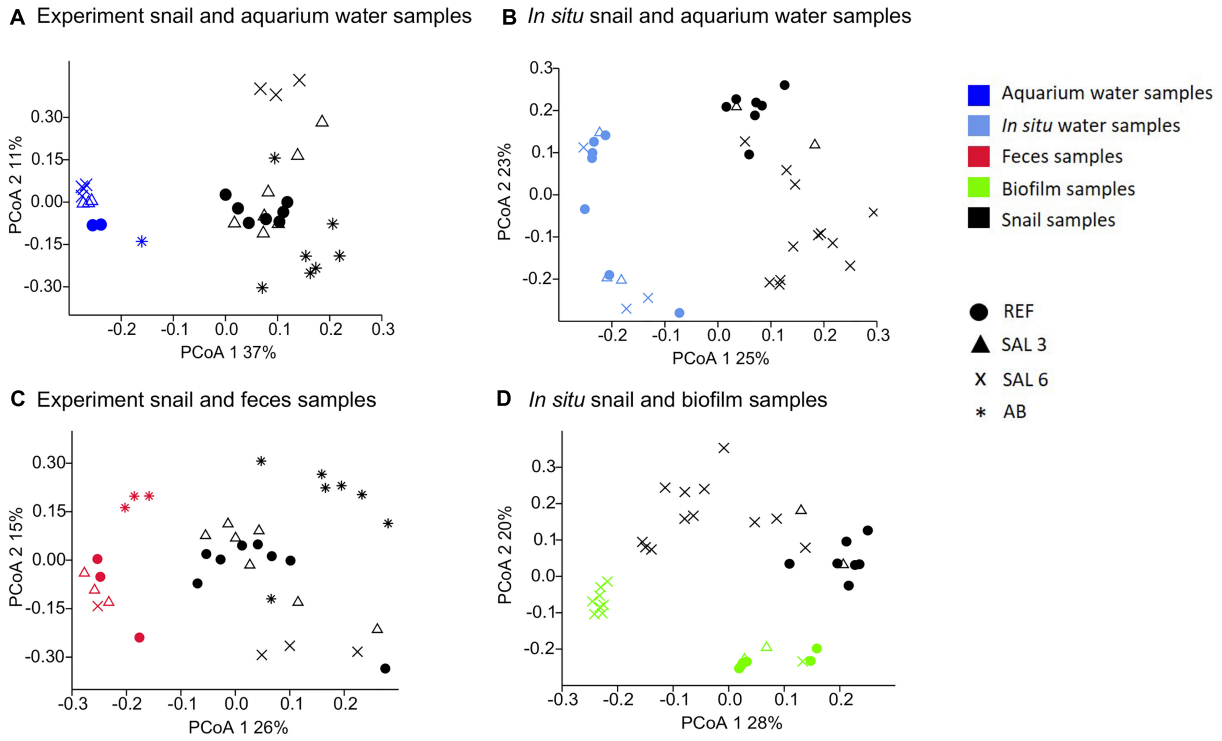

FIGURE 7
Principal coordinate analysis of bacterial community composition based on the Bray-Curtis dissimilarity on operational taxonomic unit (OTU) level. **(A)** Experiment snail and aquarium water samples, **(B)** *in situ* coastal area snail and water samples, **(C)** experiment snail and fecal samples, **(D)** *in situ* coastal area snail and biofilm samples.

(95%) after 8 days of saline stress. The high mortality indicated that the freshwater population of *A. balthica* used for the laboratory experiments has limited capacities to osmoregulate during a sudden salinity increase. However, *A. balthica* can be found at a salinity of >15 in coastal areas, demonstrating its general capability to adapt to elevated salinity (Zettler et al., 2006). The high levels of energy reserves of the snails taken at salinity 6 on the coastal sites indicated that the long-term adaptation to elevated salinity is not associated with the impaired energy status (**Figure 2**). However, lower energy availability (such as has been observed in the laboratory-maintained snails in our present study) might impair the ability of snails to survive an acute increase of salinity to 6. Although we could not assess the energy status of the snails during the laboratory experiments with salinity 6, high mortality in this experimental group suggests a major disruption of metabolism and energy homeostasis (Sokolova, 2021). The sudden shift from freshwater to salinity 3 showed no change in the total energy reserves. Differences in the response to salinity 6 and salinity 3 may be connected with the different osmoregulation strategies employed by the snails at these salinities (Jordan and Deaton, 1999). Many euryhaline gastropods osmoregulate in the lower part of their salinity tolerance range (typically < 100 mOsm corresponding to salinity < 3) and osmoconform at higher salinities (Jordan and Deaton, 1999). Thus, the transition to the osmoconforming strategy combined with the low levels of energy reserves in the laboratory-maintained *A. balthica* might have overstressed the organism's capacity to maintain intracellular homeostasis at salinity 6.

The body energy content of the snails maintained for 8 days in the aquaria was higher than in those collected from the freshwater ER (day 0 snails, **Figure 2**). Furthermore, the energy reserves of the day 0 snail samples were lower than in the snails collected from *in situ* coastal sampling sites. This suggests a stressful situation in the freshwater ER during sampling. Data from the Estonian Weather Service (www.ilmateenistus.ee) indicate that the summer of 2018 was unusually warm and dry in Estonia. This could explain the lower total energy pool measurements of day 0 snails compared to the total energy pool of the samples collected from the Estonian coastline from 2019. *A. balthica* has a low tolerance to increasing water temperatures (Cordellier and Pfenninger, 2009) and their optimal temperature is 16-20°C with elevated mortality and reproductive failure above 24°C (Johansson and Laurila, 2017). Therefore, a temperature rise of >20°C for an unusually

long period in rivers, observed in the summer of 2018, could cause high-stress levels and may be responsible for the impaired energy status of the experiment's day 0 snails. In the laboratory experiments, eight days of recovery under optimal temperature conditions (∼17°C) restored the energy balance and increased the deposition of energy reserves in *A. balthica*.

Impact of disturbance on the host gastrointestinal bacterial community

Impact of salinity on host gastrointestinal bacterial richness

Changes in salinity (freshwater or marine water becoming brackish) cause a reduction in invertebrate richness (Remane, 1934) and phytoplankton diversity (Olli et al., 2019). However, in certain cases, a peak of microbial species occurring in intermediate salinities has been described (Telesh et al., 2011; Pavloudi et al., 2017). Our results showed evidence for a similar Chao1 mean of the experiment's day 0 snails and the field-collected snails from the coastal freshwater sites (SP, SR, and KR) (**Figure 4**). Furthermore, Chao1 means did not differ between the samples from different experimental conditions or between different *in situ* samples (**Figure 4**). This is consistent with the earlier findings showing that the pelagic and benthic bacterial richness is rather constant along environmental salinity gradients (Herlemann et al., 2011, 2016; Berga et al., 2017; Klier et al., 2018). Previous research in host-associated systems has shown that the freshwater-saltwater change did not affect the bacterial α-diversity in *Salmo salar L.* (Dehler et al., 2017) or *Theodoxus fluviatilis* (Kivistik et al., 2020) even with the salinity change from 0.5 to 28.

However, a reduction of Chao1 was observed by transferring day 0 snails to the REF aquarium for 8 days (Tukey's HSD test, $p < 0.01$) and the Chao1 index of the aquarium snails was lower than the Chao1 mean of coastal area samples. This may indicate an experimental-driven response. A decline in bacterial richness and changes in the bacterial community composition due to an organism's transfer from natural conditions to aquaria settings has been observed previously (Pratte et al., 2015; Kivistik et al., 2020). The changes in bacterial communities due to the transfer to closed systems have been ascribed to grazing (Jürgens and Güde, 1994), changes in the carbon quality (Herlemann et al., 2014), missing replacement of bacteria (Ionescu et al., 2015), alternative strategies to acquire carbon (Herlemann et al., 2019), and accumulation of toxic metabolites. In addition, the change in the conditions of the host due to the shift from a river environment to a pond-like environment in the aquarium could influence the bacterial richness. Overall, our results suggest that the number of bacteria observed in a host-protected environment is influenced by other factors than by the changes in salinity.

Impact of the salinity on host gastrointestinal bacterial community composition

The bacterial 16S rRNA gene profiling revealed a diverse community predominantly derived from *Gammaproteobacteria, Alphaproteobacteria, Bacteroidetes, Firmicutes, Actinobacteria, Planctomycetes,* and *Cyanobacteria*. The high abundance of *Gammaproteobacteria* and *Alphaproteobacteria* has been previously found in invertebrate gastrointestinal microbiomes including *Achatina fulica* (Pawar et al., 2012), Diplopoda, *Cylindroiulus fulviceps* (Knapp et al., 2009), and oysters (King et al., 2012). However, the analysis at a finer taxonomic resolution (OTUs) indicates that the composition of the gastrointestinal bacterial community of *A. balthica* changes in response to elevated salinity. A clear difference between freshwater and salinity 6 treated snails was found, but interestingly, the bacterial community composition of snails from salinity 3 seems to have the ability to develop in opposite ways to resemble either the freshwater or salinity 6 samples. This pattern was apparent in the snails from the experimental aquarium SAL3 as well as in those collected *in situ* at the salinity 3 (SAL3) site. In pelagic environments, gradual changes in the bacterial community composition at increasing salinities have been previously observed (Herlemann et al., 2011) similar to the changes found in the water samples in our present experiment. Our results suggest that in a host-protected environment of *A. balthica*, the gastrointestinal bacterial communities show distinct salinity-associated profiles, either freshwater-like or salinity 6-like. This may be due to the gastropods' ability to maintain stable internal osmolarity below salinity 3 and transition to osmoconformity at higher salinities (Jordan and Deaton, 1999). The presence of both types of gastrointestinal bacterial communities in the snails acclimated or adapted to salinity 3 might be due to the individual variability of the hosts' osmoregulatory capacities, so that some individuals maintain the internal osmolarity similar to that found in the freshwater, while others switch to osmoconformity. This hypothesis requires further investigation. Overall, our bacterial community composition analysis partially contradicts the first hypothesis of our present study that snails collected from freshwater habitats change their bacterial community composition in response to the salinity pulse. The response and scope of the change in the host-associated bacterial community depend strongly on the disturbance strength since only a strong change (freshwater to salinity 6) affected the bacterial community composition. Therefore, in a host-protected environment, the strength of the disturbance determines its effect. Previous studies in other environments also identified intensity as a key feature that determines

how communities respond to the disturbance (Sousa, 1984; Mccabe and Gotelli, 2000; Berga et al., 2012; Shade et al., 2012; Gibbons et al., 2016).

In this study, we also used antibiotic amended aquaria for the control manipulation since the antibiotics are known to be a very strong disturbance to bacterial communities. A clear effect on the bacterial community composition of AB-treated samples was recognized, indicating that the antibiotics treatment influenced the bacterial community strongly and differently than salinity. Antibiotics have been previously shown to change the gastrointestinal bacterial community of humans (Nogueira et al., 2019) and aquatic invertebrates (Holt et al., 2021). Our experiment shows that different stressors cause distinct reactions in the bacterial community in a host-protected environment.

Our results indicate also that the water bacterial community are disconnected from the host-protected microbiome and have little influence on its composition (**Figure 7**). Similar to our results, Schmidt et al. (2015) found that changes in the microbiome of a euryhaline fish are not correlated with the changes in the surrounding water bacterial communities. Therefore, deterministic processes may play a main role in composing the host-associated microbiome and leave little room for stochastic impacts (Tilman, 2004). Schmidt et al. (2015) also concluded that niche-appropriation with the best competitors at each salinity level is likely driving host-associated microbiome assembly; this mechanism might also partially explain our present findings.

Permanent members of the host gastrointestinal bacterial community composition

Regardless of the manipulation with different salinity levels, specific bacteria were present in all samples, suggesting an important role of these in the symbiotic relationship with the host. For example, *Mycoplasma* was one of the most abundant bacterial genera found in the snails' gastrointestinal tract regardless of the origin (aquarium or field sites). As permanent residents of the *A. balthica* gastrointestinal tract, *Mycoplasma* may support the digestion of the algal (cellulose-based) food (Fraune and Zimmer, 2008). Genome studies of *Mycoplasma* revealed a high number of genes involved in the degradation of glycans, proteins, and complex oligosaccharides, suggesting that *Mycoplasma* supplies amino sugars and simple carbohydrates to the host (Wang et al., 2016). *Mycoplasma* has been shown to play an important ecological role for gastropods (Cicala et al., 2018) by protecting the hosts against microbial pathogen infections through sialic acid lyases that can break down the sialic acid cell-wall "coat" used by many bacterial pathogens (Severi et al., 2007; Wang et al., 2016). *Mycoplasma* has been found in various host-microbe systems including Atlantic salmon (Llewellyn et al., 2016), abalone (Cicala et al., 2018), oysters (Arfken et al., 2021), and the freshwater snail *Radix auricularia* (Hu et al., 2018).

In addition to *Mycoplasma*, *Flavobacterium*, and *Pseudomonas* were very abundant in all our snail samples. These genera are among the most commonly detected bacteria in the gastrointestinal systems of aquatic animals such as fish and aquatic invertebrates (Harris, 1993; Huber et al., 2004). Several *Flavobacteria* play a role in the mineralization of carbohydrates, amino acids, proteins, and polysaccharides in aquatic ecosystems. *Flavobacterium* as well as *Pseudomonas* are generalists and their abundant presence may reflect their broad environmental tolerance ranges and the important role of dispersal-related mechanisms in their community assembly (Yasuda and Kitao, 1980; Dempsey et al., 1989; Liu et al., 2011; Székely and Langenheder, 2014).

Adaptation to higher salinity of the host gastrointestinal bacterial community

The studied organism, *A. balthica*, can tolerate a salinity level of >6 in its natural environment. However, the experimental pulse salinity increase resulted in a high mortality rate. The bacterial community composition at salinity 6 in aquaria and *in situ* salinity 6 sites showed significant differences. Therefore, our results support the second hypothesis that the intestinal microbiome needs a long-term adaptation to higher salinity. Unlike the changes induced by salinity 6, the gastrointestinal microbiome responses to salinity 3 were less distinct and tended to converge on the community profiles similar to either those found in the freshwater or salinity 6. Salinity 3 is near the salinity threshold where *A. balthica* is able to regulate the osmolarity of extracellular fluids (Jordan and Deaton, 1999) and may therefore represent a critical tipping point for the host-microbiome relationship in gastropods.

Our study shows that within a host-protected environment the salinity disturbance causes the development of distinct states that depend on the strength of the disturbance. For sea level rise scenarios this indicates that an increase in salinity will also influence the host-protected microbiome if specific thresholds (in the case of gastropods, salinity ~3) are exceeded. However, our study also showed that long-term adaptation influences the response of the host and its bacterial communities. The influence of other factors including food source, gastrointestinal physiology, and morphology, as well as the host's gastrointestinal unique environment are expected to have a strong influence and may be subject to further studies.

Data availability statement

The datasets presented in this study can be found in online repository: NCBI, BioProject PRJNA724976, accession OA985092–OA985113.

Author contributions

KK and CK sampled snails, dissected the gastrointestinal tract. KK, CK, DH, and HT performed the experiments. CK did DNA extraction. CK and VK did preparation for sequencing. CK, VK, and DH did statistical and bioinformatics analysis. DH and VK did ITS sequencing and phylogenetic analysis. HT submitted sequences. IS introduced energy measurements. DH planned experiments. All authors contributed to the writing of the manuscript.

Funding

DH, CK, VK, KK, and HT were supported by the European Regional Development Fund/Estonian Research Council funded "Mobilitas Plus Top Researcher grant MOBTT24". VK was additionally supported by the Estonian Research Council grant PUT1389. This work was in part supported by the Research Training Group "Baltic TRANSCOAST" funded by the DFG (Deutsche Forschungsgemeinschaft, award number GRK 2000) to IMS.

Conflict of interest

The authors declare that the research was conducted in the absence of any commercial or financial relationships that could be construed as a potential conflict of interest.

Publisher's note

All claims expressed in this article are solely those of the authors and do not necessarily represent those of their affiliated organizations, or those of the publisher, the editors and the reviewers. Any product that may be evaluated in this article, or claim that may be made by its manufacturer, is not guaranteed or endorsed by the publisher.

Supplementary material

The Supplementary Material for this article can be found online at: https://www.frontiersin.org/articles/10.3389/fmicb.2022.767334/full#supplementary-material

References

Allison, S. D., and Martiny, J. B. (2008). Colloquium paper: resistance, resilience, and redundancy in microbial communities. *Proc. Natl. Acad. Sci. U S A* 105(Suppl. 1), 11512–11519. doi: 10.1073/pnas.0801925105

Almeyda-Artigas, R. J., Bargues, M. D., and Mas-Coma, S. (2000). ITS-2 rDNA sequencing of Gnathostoma species (Nematoda) and elucidation of the species causing human gnathostomiasis in the Americas. *J. Parasitol.* 86, 537–544. doi: 10.1645/0022-3395(2000)086[0537:IRSOGS]2.0.CO;2

Arfken, A., Song, B., Allen, S. K. Jr., and Carnegie, R. B. (2021). Comparing larval microbiomes of the eastern oyster (*Crassostrea virginica*) raised in different hatcheries. *Aquaculture* 531:735955. doi: 10.1016/j.aquaculture.2020.735955

Bargues, M. D., Vigo, M., Horak, P., Dvorak, J., Patzner, R. A., Pointier, J. P., et al. (2001). European Lymnaeidae (Mollusca: Gastropoda), intermediate hosts of trematodiases, based on nuclear ribosomal DNA ITS-2 sequences. *Infect. Genet. Evol.* 1, 85–107. doi: 10.1016/S1567-1348(01)00019-3

Berga, M., Szekely, A. J., and Langenheder, S. (2012). Effects of disturbance intensity and frequency on bacterial community composition and function. *PLoS One* 7:e36959. doi: 10.1371/journal.pone.0036959

Berga, M., Zha, Y., Szekely, A. J., and Langenheder, S. (2017). Functional and Compositional Stability of Bacterial Metacommunities in Response to Salinity Changes. *Front. Microbiol.* 8:948. doi: 10.3389/fmicb.2017.00948

Berger, V. J., and Kharazova, A. (1997). *Mechanisms of salinity adaptations in marine molluscs in Interactions and adaptation strategies of marine organisms*. New York, NY: Springer, 115–126. doi: 10.1007/978-94-017-1907-0_12

Bhat, T. K., Singh, B., and Sharma, O. P. (1998). Microbial degradation of tannins–a current perspective. *Biodegradation* 9, 343–357. doi: 10.1023/A:1008397506963

Bolger, A. M., Lohse, M., and Usadel, B. (2014). Trimmomatic: a flexible trimmer for Illumina sequence data. *Bioinformatics* 30, 2114–2120. doi: 10.1093/bioinformatics/btu170

Cicala, F., Cisterna-Celiz, J. A., Moore, J. D., and Rocha-Olivares, A. (2018). Structure, dynamics and predicted functional role of the gut microbiota of the blue (*Haliotis fulgens*) and yellow (*H. corrugata*) abalone from Baja California Sur, Mexico. *PeerJ* 6:e5830. doi: 10.7717/peerj.5830

Clark, R. I., Salazar, A., Yamada, R., Fitz-Gibbon, S., Morselli, M., Alcaraz, J., et al. (2015). Distinct shifts in microbiota composition during Drosophila aging impair intestinal function and drive mortality. *Cell Rep.* 12, 1656–1667. doi: 10.1016/j.celrep.2015.08.004

Cordellier, M., and Pfenninger, M. (2009). Inferring the past to predict the future: climate modelling predictions and phylogeography for the freshwater gastropod *Radix balthica* (Pulmonata, Basommatophora). *Mol. Ecol.* 18, 534–544. doi: 10.1111/j.1365-294X.2008.04042.x

Dehler, C. E., Secombes, C. J., and Martin, S. A. (2017). Environmental and physiological factors shape the gut microbiota of Atlantic salmon parr (*Salmo salar* L.). *Aquaculture* 467, 149–157. doi: 10.1016/j.aquaculture.2016.07.017

Del Giorgio, P. A., and Bouvier, T. C. (2002). Linking the physiologic and phylogenetic successions in free-living bacterial communities along an estuarine salinity gradient. *Limnol. Oceanogr.* 47, 471–486. doi: 10.4319/lo.2002.47.2.0471

Dempsey, A. C., Kitting, C. L., and Rosson, R. A. (1989). Bacterial Variability Among Individual Penaeid Shrimp Digestive Tracts. *Crustaceana* 56, 267–278. doi: 10.1163/156854089X00248

Dillon, R. J., and Dillon, V. M. (2004). The gut bacteria of insects: nonpathogenic interactions. *Annu. Rev. Entomol.* 49, 71–92. doi: 10.1146/annurev.ento.49.061802.123416

Eckert, E. M., Quero, G. M., Di Cesare, A., Manfredini, G., Mapelli, F., Borin, S., et al. (2019). Antibiotic disturbance affects aquatic microbial community composition and food web interactions but not community resilience. *Mol. Ecol.* 28, 1170–1182. doi: 10.1111/mec.15033

Fink, P., and Von Elert, E. (2006). Physiological responses to stoichiometric constraints: nutrient limitation and compensatory feeding in a freshwater snail. *Oikos* 115, 484–494. doi: 10.1111/j.2006.0030-1299.14951.x

Fraune, S., and Zimmer, M. (2008). Host-specificity of environmentally transmitted Mycoplasma-like isopod symbionts. *Environ. Microbiol.* 10, 2497–2504. doi: 10.1111/j.1462-2920.2008.01672.x

Gibbons, S. M., Scholz, M., Hutchison, A. L., Dinner, A. R., Gilbert, J. A., and Coleman, M. L. (2016). Disturbance regimes predictably alter diversity in an ecologically complex bacterial system. *mBio* 2016:7. doi: 10.1128/mBio.01372-16

Glöckner, F. O., Yilmaz, P., Quast, C., Gerken, J., Beccati, A., Ciuprina, A., et al. (2017). 25 years of serving the community with ribosomal RNA gene reference databases and tools. *J. Biotechnol.* 261, 169–176. doi: 10.1016/j.jbiotec.2017.06.1198

Glöer, P., and Diercking, R. (2010). Atlas und Rote Liste der Süßwassermollusken in Hamburg. *Behörde für Stadtentwicklung und Umwelt, Freie und Hansestadt Hamburg* 2010:31768.

Gnaiger, E. (1983). *Calculation of energetic and biochemical equivalents of respiratory oxygen consumption in Polarographic oxygen sensors*. New York, NY: Springer, 337–345. doi: 10.1007/978-3-642-81863-9_30

Gordon, T. A. C., Neto-Cerejeira, J., Furey, P. C., and O'gorman, E. J. (2018). Changes in feeding selectivity of freshwater invertebrates across a natural thermal gradient. *Curr. Zool.* 64, 231–242. doi: 10.1093/cz/zoy011

Haider, F., Sokolov, E. P., and Sokolova, I. M. (2018). Effects of mechanical disturbance and salinity stress on bioenergetics and burrowing behavior of the soft-shell clam *Mya arenaria*. *J. Exp. Biol.* 2018:221. doi: 10.1242/jeb.172643

Hamdi, C., Balloi, A., Essanaa, J., Crotti, E., Gonella, E., Raddadi, N., et al. (2011). Gut microbiome dysbiosis and honeybee health. *J. Appl. Entomol.* 135, 524–533. doi: 10.1111/j.1439-0418.2010.01609.x

Hammer, O., Harper, D. A., and Ryan, P. D. (2001). PAST: paleontological statistics software package for education and data analysis. *Palaeontol. Electron.* 4:9.

Harris, J. M. (1993). The presence, nature, and role of gut microflora in aquatic invertebrates: a synthesis. *Microb. Ecol.* 25, 195–231. doi: 10.1007/BF00171889

Herlemann, D. P. R., Manecki, M., Meeske, C., Pollehne, F., Labrenz, M., Schulz-Bull, D., et al. (2014). Uncoupling of bacterial and terrigenous dissolved organic matter dynamics in decomposition experiments. *PLoS One* 9:e93945. doi: 10.1371/journal.pone.0093945

Herlemann, D. P. R., Labrenz, M., Jürgens, K., Bertilsson, S., Waniek, J. J., and Andersson, A. F. (2011). Transitions in bacterial communities along the 2000 km salinity gradient of the Baltic Sea. *ISME J.* 5, 1571–1579. doi: 10.1038/ismej.2011.41

Herlemann, D. P. R., Lundin, D., Andersson, A. F., Labrenz, M., and Jürgens, K. (2016). Phylogenetic signals of salinity and season in bacterial community composition across the salinity gradient of the baltic sea. *Front. Microbiol.* 7:1883. doi: 10.3389/fmicb.2016.01883

Herlemann, D. P. R., Manecki, M., Dittmar, T., and Jürgens, K. (2017). Differential responses of marine, mesohaline and oligohaline bacterial communities to the addition of terrigenous carbon. *Environ. Microbiol.* 19, 3098–3117. doi: 10.1111/1462-2920.13784

Herlemann, D. P. R., Markert, S., Meeske, C., Andersson, A. F., De Bruijn, I., Hentschker, C., et al. (2019). Individual physiological adaptations enable selected bacterial taxa to prevail during long-term incubations. *Appl. Environ. Microbiol.* 2019:85. doi: 10.1128/AEM.00825-19

Holt, C. C., Bass, D., Stentiford, G. D., and Van Der Giezen, M. (2021). Understanding the role of the shrimp gut microbiome in health and disease. *J. Invertebr. Pathol.* 186:107387. doi: 10.1016/j.jip.2020.107387

Hooks, K. B., and O'malley, M. A. (2017). Dysbiosis and its discontents. *MBio* 8, e1492–e1417. doi: 10.1128/mBio.01492-17

Hooper, D. U., Chapin Iii, F., Ewel, J., Hector, A., Inchausti, P., Lavorel, S., et al. (2005). Effects of biodiversity on ecosystem functioning: a consensus of current knowledge. *Ecol. Monogr.* 75, 3–35. doi: 10.1890/04-0922

Horton, B. P., Rahmstorf, S., Engelhart, S. E., and Kemp, A. C. (2014). Expert assessment of sea-level rise by AD 2100 and AD 2300. *Quat. Sci. Rev.* 84, 1–6. doi: 10.1016/j.quascirev.2013.11.002

Hu, Z., Chen, X., Chang, J., Yu, J., Tong, Q., Li, S., et al. (2018). Compositional and predicted functional analysis of the gut microbiota of *Radix auricularia* (Linnaeus) *via* high-throughput Illumina sequencing. *PeerJ* 6:e5537. doi: 10.7717/peerj.5537

Huber, I., Spanggaard, B., Appel, K. F., Rossen, L., Nielsen, T., and Gram, L. (2004). Phylogenetic analysis and *in situ* identification of the intestinal microbial community of rainbow trout (*Oncorhynchus mykiss*, Walbaum). *J. Appl. Microbiol.* 96, 117–132. doi: 10.1046/j.1365-2672.2003.02109.x

Ihaka, R., and Gentleman, R. (1996). R: a language for data analysis and graphics. *J. Comput. Graph. Stat.* 5, 299–314. doi: 10.1080/10618600.1996.10474713

Ionescu, D., Bizic-Ionescu, M., Khalili, A., Malekmohammadi, R., Morad, M. R., De Beer, D., et al. (2015). A new tool for long-term studies of POM-bacteria interactions: overcoming the century-old Bottle Effect. *Sci. Rep.* 5:14706. doi: 10.1038/srep14706

Jeppesen, E., Beklioğlu, M., Özkan, K., and Akyürek, Z. (2020). Salinization increase due to climate change will have substantial negative effects on inland waters: a call for multifaceted research at the local and global scale. *Innov. J.* 2020:1. doi: 10.1016/j.xinn.2020.100030

Johansson, M. P., and Laurila, A. (2017). Maximum thermal tolerance trades off with chronic tolerance of high temperature in contrasting thermal populations of radix balthica. *Ecol. Evol.* 7, 3149–3156. doi: 10.1002/ece3.2923

Jordan, P. J., and Deaton, L. E. (1999). Osmotic regulation and salinity tolerance in the freshwater snail *Pomacea bridgesi* and the freshwater clam *Lampsilis teres*. *Comp. Biochem. Physiol.* 122, 199–205. doi: 10.1016/S1095-6433(98)10167-8

Jürgens, K., and Güde, H. (1994). The potential importance of grazing-resistant bacteria in planktonic systems. *Mar. Ecol. Prog. Ser.* 1994, 169–188. doi: 10.3354/meps112169

Kerney, M. P. (1999). *Atlas of land and freshwater molluscs of Britain and Ireland*. Leiden: Brill.

King, G. M., Judd, C., Kuske, C. R., and Smith, C. (2012). Analysis of stomach and gut microbiomes of the eastern oyster (*Crassostrea virginica*) from coastal Louisiana, USA. *PLoS One* 7:e51475. doi: 10.1371/journal.pone.0051475

Kivistik, C., Knobloch, J., Kairo, K., Tammert, H., Kisand, V., Hildebrandt, J. P., et al. (2020). Impact of Salinity on the Gastrointestinal Bacterial Community of *Theodoxus fluviatilis*. *Front. Microbiol.* 11:683. doi: 10.3389/fmicb.2020.00683

Klier, J., Dellwig, O., Leipe, T., Jürgens, K., and Herlemann, D. P. R. (2018). Benthic bacterial community composition in the oligohaline-marine transition of surface sediments in the baltic sea based on rRNA analysis. *Front. Microbiol.* 9:236. doi: 10.3389/fmicb.2018.00236

Knapp, B. A., Seeber, J., Podmirseg, S. M., Rief, A., Meyer, E., and Insam, H. (2009). Molecular fingerprinting analysis of the gut microbiota of *Cylindroiulus fulviceps* (Diplopoda). *Pedobiologia* 52, 325–336. doi: 10.1016/j.pedobi.2008.11.005

Langenheder, S., Kisand, V., Wikner, J., and Tranvik, L. J. (2003). Salinity as a structuring factor for the composition and performance of bacterioplankton degrading riverine DOC. *FEMS Microbiol. Ecol.* 45, 189–202. doi: 10.1016/S0168-6496(03)00149-1

Levy, M., Kolodziejczyk, A. A., Thaiss, C. A., and Elinav, E. (2017). Dysbiosis and the immune system. *Nat. Rev. Immunol.* 17, 219–232. doi: 10.1038/nri.2017.7

Liu, H., Wang, L., Liu, M., Wang, B., Jiang, K., Ma, S., et al. (2011). The intestinal microbial diversity in Chinese shrimp (*Fenneropenaeus chinensis*) as determined by PCR–DGGE and clone library analyses. *Aquaculture* 317, 32–36. doi: 10.1016/j.aquaculture.2011.04.008

Llewellyn, M. S., Mcginnity, P., Dionne, M., Letourneau, J., Thonier, F., Carvalho, G. R., et al. (2016). The biogeography of the atlantic salmon (*Salmo salar*) gut microbiome. *ISME J.* 10, 1280–1284. doi: 10.1038/ismej.2015.189

Lozupone, C. A., and Knight, R. (2007). Global patterns in bacterial diversity. *Proc. Natl. Acad. Sci. U S A* 104, 11436–11440. doi: 10.1073/pnas.0611525104

Lozupone, C. A., Stombaugh, J. I., Gordon, J. I., Jansson, J. K., and Knight, R. (2012). Diversity, stability and resilience of the human gut microbiota. *Nature* 489, 220–230. doi: 10.1038/nature11550

Ludwig, W., Strunk, O., Westram, R., Richter, L., Meier, H., Buchner, A., et al. (2004). ARB: a software environment for sequence data. *Nucleic. Acids. Res.* 32, 1363–1371. doi: 10.1093/nar/gkh293

Lueders, T., Manefield, M., and Friedrich, M. W. (2004). Enhanced sensitivity of DNA- and rRNA-based stable isotope probing by fractionation and quantitative analysis of isopycnic centrifugation gradients. *Environ. Microbiol.* 6, 73–78. doi: 10.1046/j.1462-2920.2003.00536.x

Ma, Z. S. (2020). Testing the Anna Karenina principle in human microbiome-associated diseases. *Iscience* 23:101007. doi: 10.1016/j.isci.2020.101007

Mackey, R. L., and Currie, D. J. (2001). The diversity–disturbance relationship: is it generally strong and peaked? *Ecology* 82, 3479–3492. doi: 10.1890/0012-9658(2001)082[3479:TDDRII]2.0.CO;2

Mandahl-Barth, G. (1938). *Land and Freshwater Mollusca*. Munksgaard: Levin and Munksgaard.

Marasco, R., Fusi, M., Callegari, M., Jucker, C., Mapelli, F., Borin, S., et al. (2022). Destabilization of the bacterial interactome identifies nutrient restriction-induced dysbiosis in insect guts. *Microbiol. Spectr.* 10, e1580–e1521. doi: 10.1128/spectrum.01580-21

Martin, M. (2011). Cutadapt removes adapter sequences from high-throughput sequencing reads. *EMBnet j.* 17, 10–12. doi: 10.14806/ej.17.1.200

Masuko, T., Minami, A., Iwasaki, N., Majima, T., Nishimura, S.-I., and Lee, Y. C. (2005). Carbohydrate analysis by a phenol–sulfuric acid method in microplate format. *Anal. Biochem.* 339, 69–72. doi: 10.1016/j.ab.2004.12.001

Mccabe, D. J., and Gotelli, N. J. (2000). Effects of disturbance frequency, intensity, and area on assemblages of stream macroinvertebrates. *Oecologia* 124, 270–279. doi: 10.1007/s004420000369

Mcmurdie, P. J., and Holmes, S. (2013). phyloseq: an R package for reproducible interactive analysis and graphics of microbiome census data. *PLoS One* 8:e61217. doi: 10.1371/journal.pone.0061217

Miller, A. D., Inamine, H., Buckling, A., Roxburgh, S. H., and Shea, K. (2021). How disturbance history alters invasion success: biotic legacies and regime change. *Ecol. Lett.* 24, 687–697. doi: 10.1111/ele.13685

Naeem, S., Thompson, L. J., Lawler, S. P., Lawton, J. H., and Woodfin, R. M. (1994). Declining biodiversity can alter the performance of ecosystems. *Nature* 368, 734–737. doi: 10.1038/368734a0

Nogueira, T., David, P. H., and Pothier, J. (2019). Antibiotics as both friends and foes of the human gut microbiome: the microbial community approach. *Drug Dev. Res.* 80, 86–97. doi: 10.1002/ddr.21466

Økland, J. (1990). *Lakes and snails: Environment and Gastropoda in 1,500 Norwegian lakes, ponds and rivers*. Backhuys: Balogh Scientific Books.

Oksanen, J., Blanchet, F. G., Kindt, R., Legendre, P., Minchin, P. R., O'hara, R., et al. (2013). *Package 'vegan'. Community ecology package, version* 2, 1–295.

Olli, K., Ptacnik, R., Klais, R., and Tamminen, T. (2019). Phytoplankton Species Richness along Coastal and Estuarine Salinity Continua. *Am. Nat.* 194, E41–E51. doi: 10.1086/703657

Paulson, J. N., Stine, O. C., Bravo, H. C., and Pop, M. (2013). Differential abundance analysis for microbial marker-gene surveys. *Nat. Methods* 10, 1200–1202. doi: 10.1038/nmeth.2658

Pavloudi, C., Kristoffersen, J. B., Oulas, A., De Troch, M., and Arvanitidis, C. (2017). Sediment microbial taxonomic and functional diversity in a natural salinity gradient challenge Remane's "species minimum" concept. *PeerJ.* 5:e3687. doi: 10.7717/peerj.3687

Pawar, K. D., Banskar, S., Rane, S. D., Charan, S. S., Kulkarni, G. J., Sawant, S. S., et al. (2012). Bacterial diversity in different regions of gastrointestinal tract of giant african snail (*Achatina fulica*). *Microbiologyopen* 1, 415–426. doi: 10.1002/mbo3.38

Pratte, Z. A., Richardson, L. L., and Mills, D. K. (2015). Microbiota shifts in the surface mucopolysaccharide layer of corals transferred from natural to aquaria settings. *J. Invertebr. Pathol.* 125, 42–44. doi: 10.1016/j.jip.2014.12.009

Prosser, C. L. (1991). *Comparative animal physiology, environmental and metabolic animal physiology*. Hoboken, NJ: John Wiley & Sons.

Pruesse, E., Peplies, J., and Glöckner, F. O. (2012). SINA: accurate high-throughput multiple sequence alignment of ribosomal RNA genes. *Bioinformatics* 28, 1823–1829. doi: 10.1093/bioinformatics/bts252

Pruesse, E., Quast, C., Knittel, K., Fuchs, B. M., Ludwig, W., Peplies, J., et al. (2007). SILVA: a comprehensive online resource for quality checked and aligned ribosomal RNA sequence data compatible with ARB. *Nucleic Acids Res.* 35, 7188–7196. doi: 10.1093/nar/gkm864

Remane, A. (1934). Die Brackwasserfauna: Mit besonderer Berücksichtigung der Ostsee. *Zool. Anz.*

Rognes, T., Flouri, T., Nichols, B., Quince, C., and Mahé, F. (2016). VSEARCH: a versatile open source tool for metagenomics. *PeerJ.* 4:e2584. doi: 10.7717/peerj.2584

Schmidt, V. T., Smith, K. F., Melvin, D. W., and Amaral-Zettler, L. A. (2015). Community assembly of a euryhaline fish microbiome during salinity acclimation. *Mol. Ecol.* 24, 2537–2550. doi: 10.1111/mec.13177

Segata, N., Izard, J., Waldron, L., Gevers, D., Miropolsky, L., Garrett, W. S., et al. (2011). Metagenomic biomarker discovery and explanation. *Genome Biol.* 12:R60. doi: 10.1186/gb-2011-12-6-r60

Severi, E., Hood, D. W., and Thomas, G. H. (2007). Sialic acid utilization by bacterial pathogens. *Microbiology* 153, 2817–2822. doi: 10.1099/mic.0.2007/009480-0

Shade, A., Peter, H., Allison, S. D., Baho, D. L., Berga, M., Burgmann, H., et al. (2012). Fundamentals of microbial community resistance and resilience. *Front. Microbiol.* 3:417. doi: 10.3389/fmicb.2012.00417

Shade, A., Read, J. S., Welkie, D. G., Kratz, T. K., Wu, C. H., and Mcmahon, K. D. (2011). Resistance, resilience and recovery: aquatic bacterial dynamics after water column disturbance. *Environ. Microbiol.* 13, 2752–2767. doi: 10.1111/j.1462-2920.2011.02546.x

Shetty, P., Gitau, M. M., and Maroti, G. (2019). Salinity stress responses and adaptation mechanisms in eukaryotic green microalgae. *Cells* 8:1657. doi: 10.3390/cells8121657

Sokolova, I. (2021). Bioenergetics in environmental adaptation and stress tolerance of aquatic ectotherms: linking physiology and ecology in a multi-stressor landscape. *J. Exp. Biol.* 224:jeb236802. doi: 10.1242/jeb.236802

Sokolova, I. M., Frederich, M., Bagwe, R., Lannig, G., and Sukhotin, A. A. (2012). Energy homeostasis as an integrative tool for assessing limits of environmental stress tolerance in aquatic invertebrates. *Mar. Environ. Res.* 79, 1–15. doi: 10.1016/j.marenvres.2012.04.003

Sommer, F., Anderson, J. M., Bharti, R., Raes, J., and Rosenstiel, P. (2017). The resilience of the intestinal microbiota influences health and disease. *Nat. Rev. Microbiol.* 15, 630–638. doi: 10.1038/nrmicro.2017.58

Sousa, W. P. (1984). The role of disturbance in natural communities. *Annu. Rev. Ecol. Evol. Syst.* 15, 353–391. doi: 10.1146/annurev.es.15.110184.002033

Stamatakis, A. (2006). RAxML-VI-HPC: maximum likelihood-based phylogenetic analyses with thousands of taxa and mixed models. *Bioinformatics* 22, 2688–2690. doi: 10.1093/bioinformatics/btl446

Strasdine, G., and Whitaker, D. (1963). On the origin of the cellulase and chitinase of *Helix pomatia*. *Can. J. Biochem. Physiol.* 41, 1621–1626. doi: 10.1139/y63-185

Svensson, J. R., Lindegarth, M., and Pavia, H. (2009). Equal rates of disturbance cause different patterns of diversity. *Ecology* 90, 496–505. doi: 10.1890/07-1628.1

Székely, A. J., and Langenheder, S. (2014). The importance of species sorting differs between habitat generalists and specialists in bacterial communities. *FEMS Microbiol. Ecol.* 87, 102–112. doi: 10.1111/1574-6941.12195

Telesh, I. V., Schubert, H., and Skarlato, S. O. (2011). Revisiting Remane's concept: evidence for high plankton diversity and a protistan species maximum in the horohalinicum of the Baltic Sea. *Mar. Ecol. Prog. Ser.* 421, 1–11. doi: 10.3354/meps08928

Tilman, D. (2004). Niche tradeoffs, neutrality, and community structure: a stochastic theory of resource competition, invasion, and community assembly. *Proc. Natl. Acad. Sci. U S A* 101, 10854–10861. doi: 10.1073/pnas.0403458101

Truchot, J. (1993). Acid-base balance in aquatic invertebrates: the effects of environmental factors. *Aquaculture* 43, 1–14. doi: 10.1029/CE043p0001

van Damme, D. (1984). *The freshwater Mollusca of Northern Africa. Distribution, biogeography and paleoecology: Developments in hydrobiology*. Dordrecht: Dr. W. Junk Publishers, 25.

Van Horn, D., Garcia, J., Loker, E., Mitchell, K., Mkoji, G., Adema, C., et al. (2012). Complex intestinal bacterial communities in three species of planorbid snails. *J. Molluscan Stud.* 78, 74–80. doi: 10.1093/mollus/eyr038

Wang, Y., Huang, J. M., Wang, S. L., Gao, Z. M., Zhang, A. Q., Danchin, A., et al. (2016). Genomic characterization of symbiotic mycoplasmas from the stomach of deep-sea isopod bathynomus sp. *Environ. Microbiol.* 18, 2646–2659. doi: 10.1111/1462-2920.13411

Weinbauer, M. G., Fritz, I., Wenderoth, D. F., and Hofle, M. G. (2002). Simultaneous extraction from bacterioplankton of total RNA and DNA suitable for quantitative structure and function analyses. *Appl. Environ. Microbiol.* 68, 1082–1087. doi: 10.1128/AEM.68.3.1082-1087.2002

Yasuda, K., and Kitao, T. (1980). Bacterial flora in the digestive tract of prawns, *Penaeus japonicus* Bate. *Aquaculture* 19, 229–234. doi: 10.1016/0044-8486(80)90046-0

Zettler, M. L., Jueg, U., Menzel-Harloff, H., Göllnitz, U., Petrick, S., Weber, E., et al. (2006). *Die Land- und Süßwassermollusken Mecklenburg-Vorpommerns*. Schwerin: Obotritendruck, 318.

Frontiers in Marine Science

Explores ocean-based solutions for emerging global challenges

The third most-cited marine and freshwater biology journal, advancing our understanding of marine systems and addressing global challenges including overfishing, pollution, and climate change.

Discover the latest Research Topics

See more →

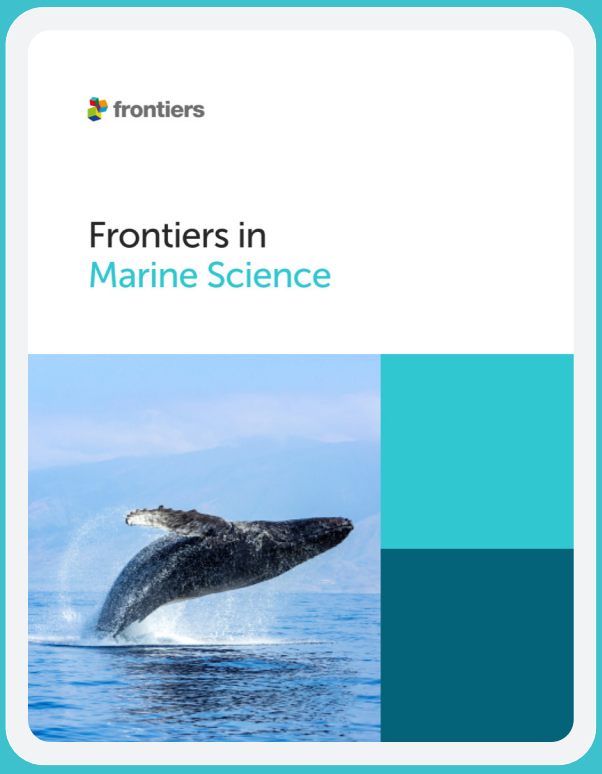

Frontiers

Avenue du Tribunal-Fédéral 34
1005 Lausanne, Switzerland
frontiersin.org

Contact us

+41 (0)21 510 17 00
frontiersin.org/about/contact